Practical Electronics

The UK's premier electronics, computing and maker magazine

Max's Cool Beans
Making test fixtures & building the VFD clock

Teach-In 12
Part 10: short-range RF devices, including LoRa

Audio Out
Linear-phase crossovers

Circuit Surgery
Anti-aliasing and reconstruction filters

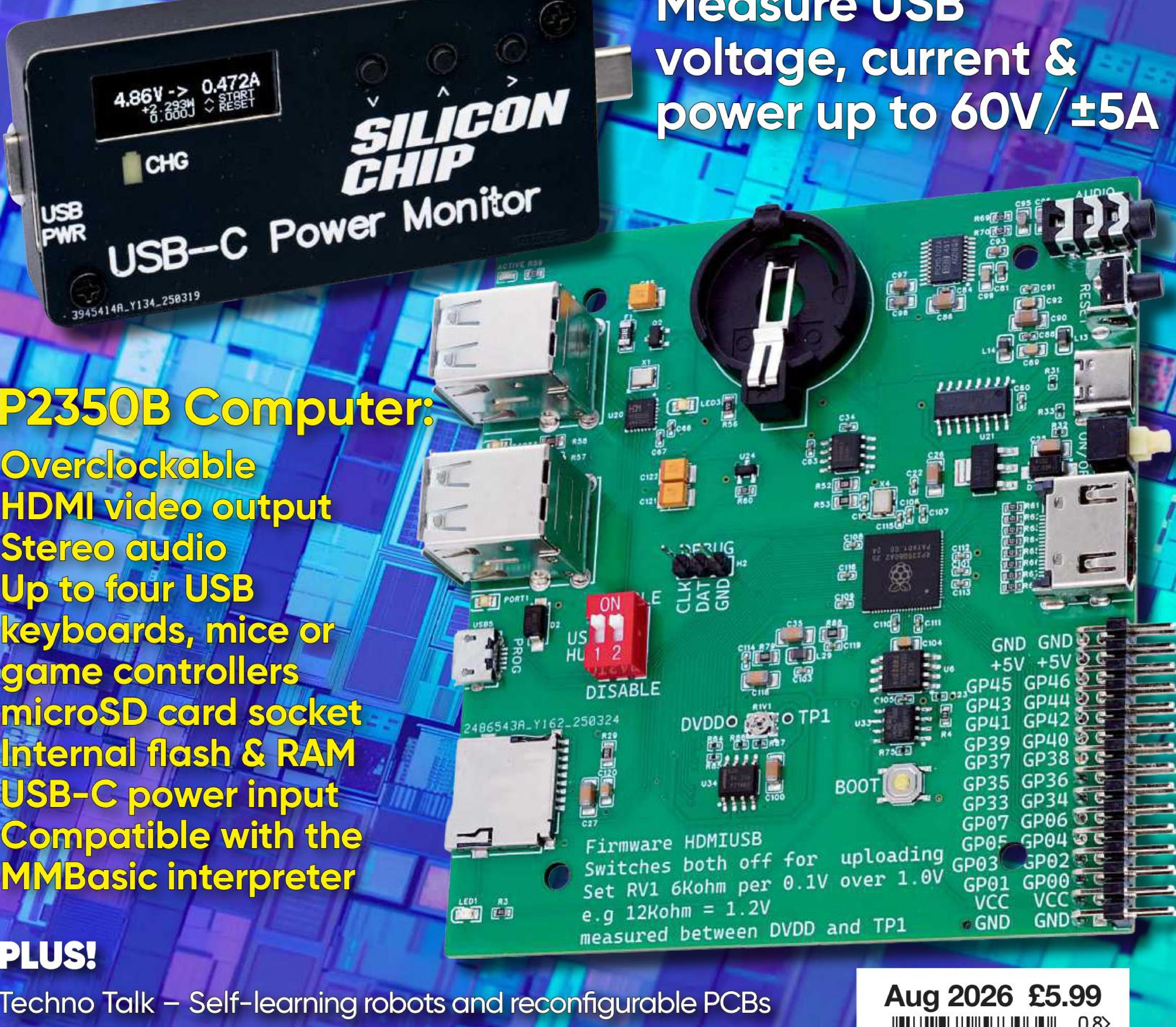

4.86V -> 0.472A
+2.293W ^ START
0.000J ^ RESET
CHG
SILICON CHIP
USB PWR
USB-C Power Monitor
3945414A_Y134_250319
DEBUG
CLK DAT GND
ON
1 2
DISABLE
PROG
DVDD
TP1
BOOT
2486543A_Y162_250324
Firmware HDMIUSB
Switches both off for uploading
Set RV1 6Kohm per 0.1V over 1.0V
e.g 12Kohm = 1.2V
measured between DVDD and TP1
GND GND
+5V +5V
GP45 GP46
GP43 GP44
GP41 GP42
GP39 GP40
GP37 GP38
GP35 GP36
GP33 GP34
GP07 GP06
GP05 GP04
GP03 GP02
GP01 GP00
VCC VCC
GND GND
AUDIO
RESET
ON/OFF

Measure USB voltage, current & power up to 60V/±5A

RP2350B Computer:

- Overclockable
- HDMI video output
- Stereo audio
- Up to four USB keyboards, mice or game controllers
- microSD card socket
- Internal flash & RAM
- USB-C power input
- Compatible with the MMBasic interpreter

PLUS!

Techno Talk – Self-learning robots and reconfigurable PCBs

The Fox Report – Manhattan's new Freeview receiver box

Feature – How USB-C Power Delivery works

Aug 2026 £5.99

Beyond Standard —

Discover PCBWay's

Advanced PCB Lineup

About PCBWay:

With dedicated workshops for advanced PCBs, PCBWay offers full-spec, high-precision, and large-scale production. We ensure customers are supplied with PCBs that meet stringent quality standards at the lowest cost.

HDI PCB //

- 4-60 layers
- FR-4, High Tg, Halogen-free, PTFE
- Finished Copper: 1/3OZ–8OZ
- Min Track/Spacing (inner): 2/2mil (H/HOZ base copper)
- Min BGA Pitch: 0.35mm

High Frequency PCB //

- RO4003C, RO4350B, Ro3003, Ro3010, RT5880
- Min. Track/Spacing: 2mil
- Min. Hole Size: 0.15mm
- Finished Cooper: 1-2oz
- Board Thickness: 0.2–3.2mm

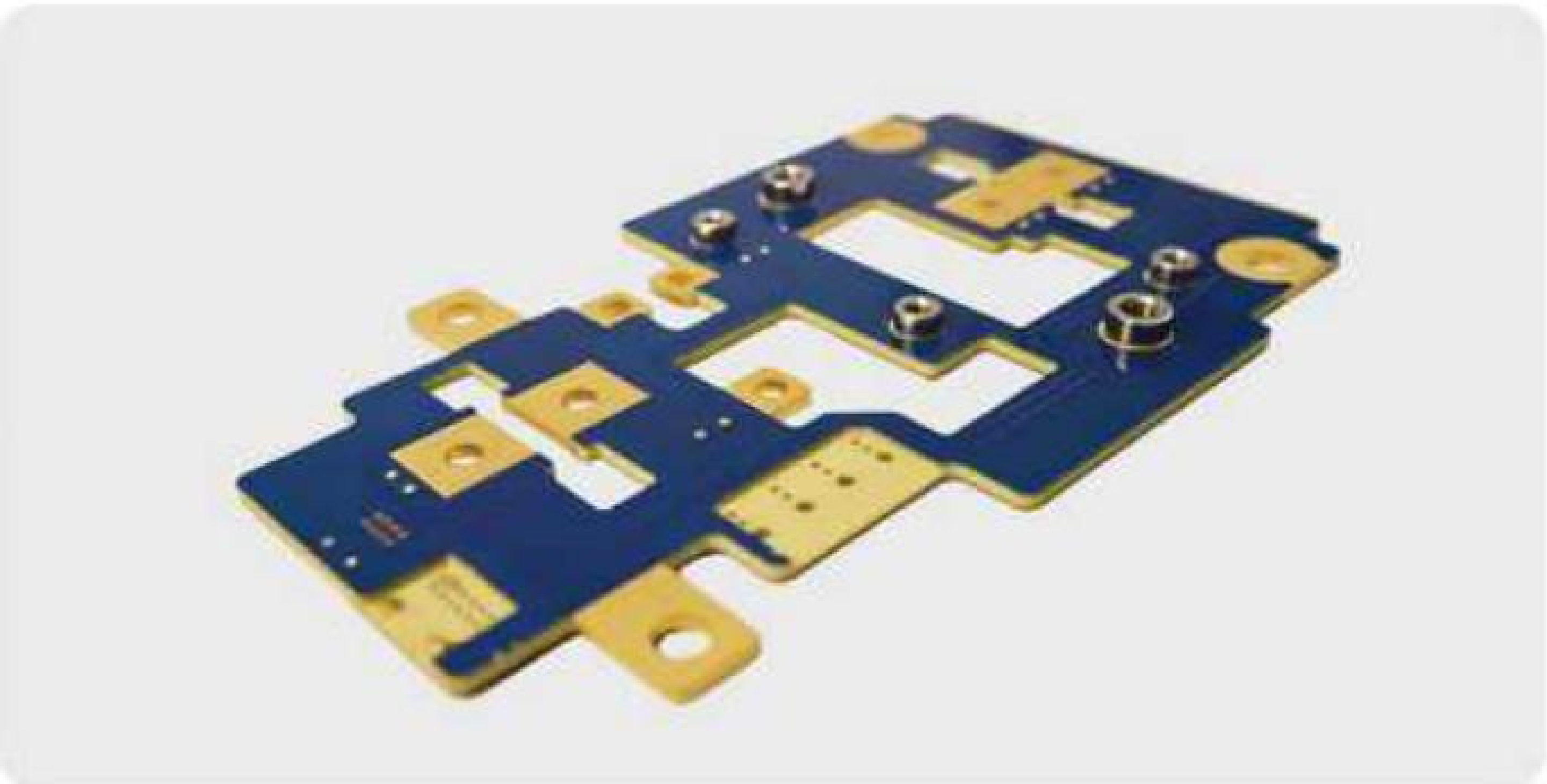

Other PCBs with Special Process //

- Embedded Copper PCB
- Backplane PCB
- Cavity PCB
- White/Partially Hybrid PCB
- Black Core PCB (After-dark)

www.pcbway.com service@pcbway.com

Practical
Electronics

Volume 55. No. 08
August 2026
ISSN 2632 573X

Contents

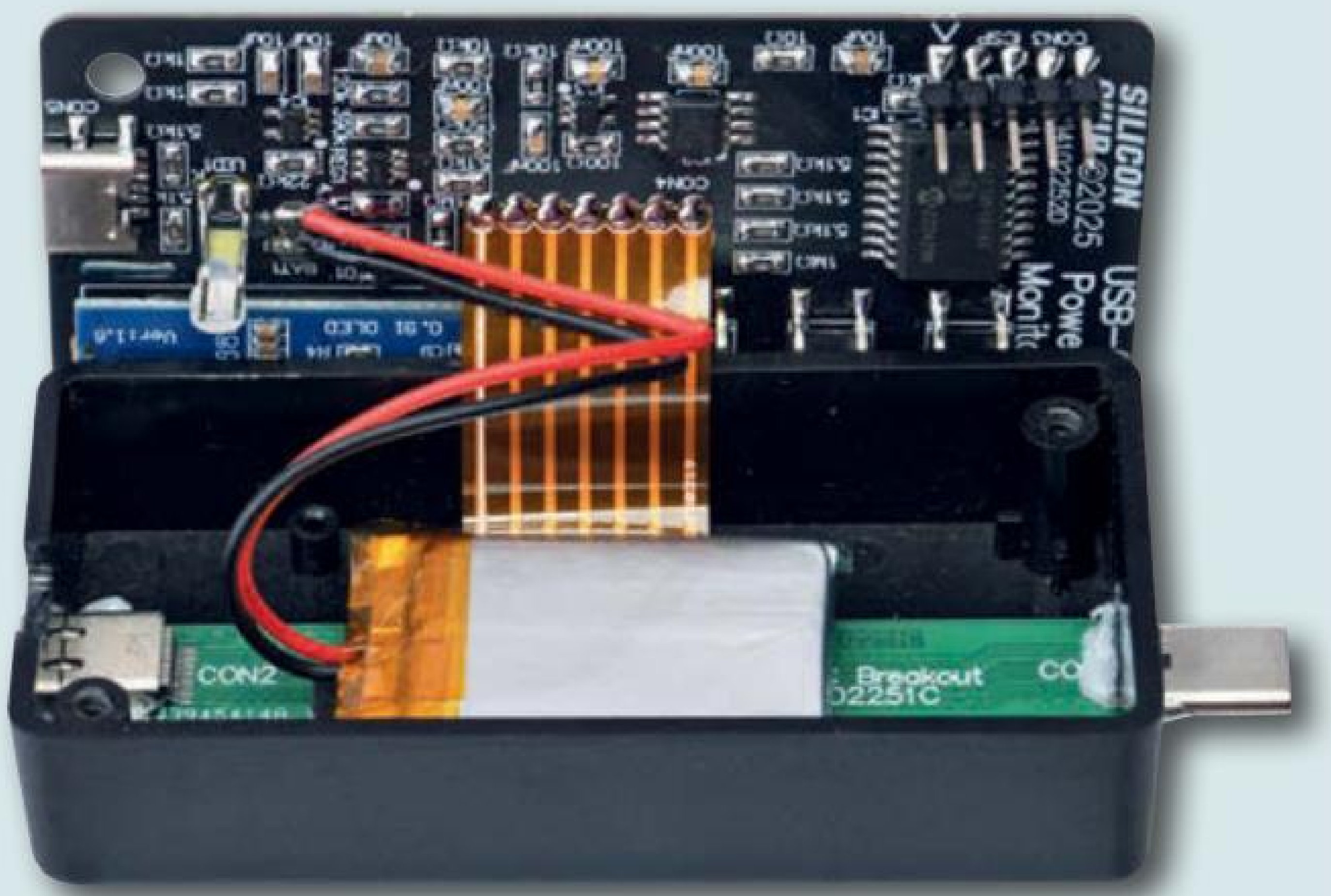

4.86V -> 0.472A
+2.293M START
0.000J RESET
CHG
USB
PWR
SILICON CHIP
USB-C Power Monitor

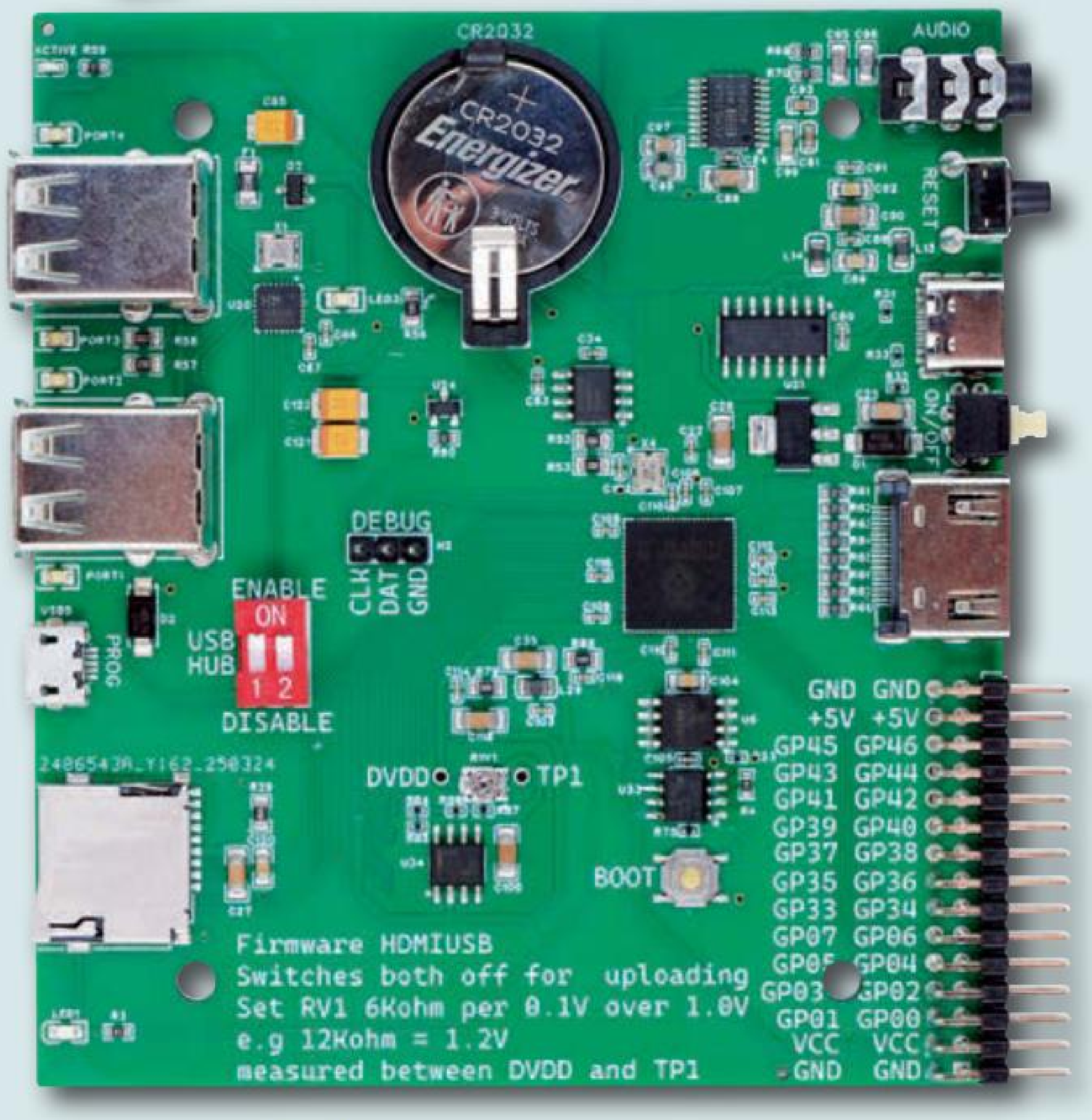
CR2032
AUDIO
DEBUG
CLK
DAT
GND
ENABLE
ON
USB HUB
DISABLE
DVDD
TP1
BOOT
Firmware HDMIUSB
Switches both off for uploading
Set RV1 6Kohm per 0.1V over 1.0V
e.g 12Kohm = 1.2V
measured between DVDD and TP1

Made in Australia & the UK.

Written in Britain, Australia, the USA and Ireland.

Read everywhere.

© Silicon Chip Publications Pty Ltd 2026

Copyright in all drawings, photographs, articles, technical designs, software and intellectual property published in *Practical Electronics* is fully protected, and reproduction or imitation in whole or in part are expressly forbidden.

The September 2026 issue of *Practical Electronics* will be published on Wednesday, 5th of August, 2026 (see p80).

Projects and Circuits

USB-C Power Monitor, part one by Tim Blythman 10
It is always handy to know what voltage and current a USB device is using. Now that USB-C is prevalent, it's time for a USB-C Power Monitor. It can be used for all modern USB-C devices, as well as legacy USB devices, with the right adaptor.

The RP2350B Computer by Geoff Graham & Peter Mather 28
This small computer board can be purchased pre-assembled and comes with a dual-core RP2350B processor, HDMI video output, stereo audio, four USB ports, a microSD card socket, 14MiB of integrated storage, and RAM that's expandable to over 6MiB.

Series, Features and Columns

How USB-C Power Delivery Works by Andrew Levido 4
The widespread adoption of USB 3.2 introduced the Type-C connector, plus a new Power Delivery (PD) capability that allows up to 100W (20V @ 5A) to be delivered. It is quite a bit more complicated than previous USB power schemes.

Teach-In 12.10: the World of Wireless by Mike Tooley 18
This month, our focus shifts to short-range wireless devices (SRD). These versatile chips and modules enable data transmission and reception between remote devices without requiring a wired connection.

The Fox Report by Barry Fox 39
A review of the new Manhattan Freesat receiver.

Circuit Surgery by Ian Bell 40
Measuring circuit frequency response using a PC sound card, part 11: anti-aliasing & reconstruction filter circuits. We look at multi-pole active filters using op amps. These filters are handy for reconstruction filters but have many other uses too.

Max's Cool Beans by Max The Magnificent 48
Weird & Wonderful Arduino Projects, part 20: pogo pins and pixel grins. We get busy creating some test jigs and then start assembling our VFD-based countdown clock, piece by piece.

Power Electronics, part five by Andrew Levido 56
Power factor correction & EMI filtering – we look at circuit design rules to meet EMI regulations. We also describe how conducted EMI can be measured and investigate an example power-factor correction (PFC) evaluation board and circuit.

Audio Out by Jake Rothman 66
A phase-linear crossover board, plus all-pass filters, part five and final notes. We present a circuit and PCB for this special kind of active crossover for loudspeakers. We also have some more information on the NE5532 fiasco mentioned last month.

Techno Talk by Max the Magnificent 74
Scan me! – CynLr's robots learn by interacting with their environment, Brilliant Labs is making smart glasses and Itera's circuit boards can rewire themselves!

Regulars and Services

Editorial 2
Europe needs a proactive policy on local tech & manufacturing

Reader services – Editorial and Advertising Departments 2

Subscribe to Practical Electronics and save money 3

Practical Electronics PCB Service 76-78
PCBs for Practical Electronics projects

Classified ads and Advertiser index 79

Next month! – highlights of our next issue of *Practical Electronics* 80

Renewals paid by PayPal, Visa and Mastercard are now handled via our website:
www.electronpublishing.com

Practical Electronics

Volume 55. No. 08
August 2026
ISSN 2632 573X

Editorial

Editorial offices

Electron Publishing (Australia)
Tel +61 2 9939 3295
Email pe@pemag.au
Web www.electronpublishing.com

Address mail to:

Electron Publishing (Australia)
PO Box 194, Matraville NSW 2036
Australia

Advertising enquiries

+61 2 9939 3295 pe@pemag.au

Editor	Nicholas Vinen		
Publisher	Nicholas Vinen		
Digital subscriptions	Stewart Kearn	**Tel**	**07918 614662**
Online Editor	Alan Winstanley		
Web Systems	Kris Thain		
Production	Bao Smith		
Technical staff	Tim Blythman, John Clarke		

Print subscriptions

Practical Electronics Subscriptions
PO Box 6337
Bournemouth BH1 9EH
United Kingdom
Tel 01202 087631
Email pesubs@selectps.com

Technical enquiries

We regret that technical enquiries cannot be answered over the telephone. We are unable to offer any advice on the use, purchase, repair or modification of commercial equipment or the incorporation or modification of designs published in the magazine.

Questions about articles or projects should be sent to the editor by email: pe@pemag.au

Projects and circuits

All reasonable precautions are taken to ensure that the advice and data given to readers is reliable. We cannot, however, guarantee it and we cannot accept legal responsibility for it.

Some projects and circuits published in *Practical Electronics* employ voltages that can be lethal. Do not build, test, modify or fix any mains-powered equipment unless you fully understand the safety aspects involved and you use an RCD (GFCI) adaptor.

Component supplies

Silicon Chip Publications may offer kits or other parts for making our projects, but not in all cases. When kits are not available, readers will need to find and source parts themselves. We advise readers to check that all parts are still available before commencing any project in a back-dated issue.

Advertisements

Although the proprietors and staff of *Practical Electronics* take reasonable precautions to protect the interests of readers by ensuring as far as practicable that advertisements are bona fide, the magazine and its publishers cannot give any undertakings in respect of statements or claims made by advertisers, whether these advertisements are printed as part of the magazine, or in inserts. The Publishers regret that under no circumstances will the magazine accept liability for non-receipt of goods ordered, or for late delivery, or for faults in manufacture.

Transmitters/bugs/telephone equipment

We advise readers that certain items of radio transmitting and telephone equipment which may be advertised in our pages cannot be legally used in the UK. Readers should check the law before buying any transmitting or telephone equipment, as a fine, confiscation of equipment and/or imprisonment can result from illegal use or ownership. The laws vary from country to country; readers should check local laws.

Europe needs a proactive policy on local tech & manufacturing

Last November, the Dutch government took the practical step of suspending its intervention in Nexperia, the semiconductor supplier with roots in Philips and NXP. Wingtech, a Chinese company, completed its controlling acquisition of Nexperia in December 2019. Six years later, the Dutch government attempted to regain control using emergency powers, then had to step back.

That episode is interesting, but this is not really a post mortem. The more important question is simpler: if Nexperia is critical European infrastructure, why was it allowed to pass into overseas control in the first place? The time to act was before the sale, not years later, after the ownership structure had become a diplomatic and industrial mess.

Philips' history is full of two things: innovation and disappointment. It created or helped to develop an extraordinary amount of technology, yet so much of that value was spun off, sold or squandered. Philips was often a better innovator than custodian. The lesson for Europe, and the West more broadly, is that we need to use the carrot rather than the stick if we want to create and keep serious technology companies. We also need a clear, consistent policy.

Global trade is inevitable and often beneficial. It gives us lower prices, more choice and efficient supply chains. However, efficiency is not the same thing as resilience. If a conflict, blockade or sanctions clash between the USA and China disrupted trade, Europe would not want to discover that its industries could no longer obtain critical parts.

In a free market, it is almost impossible for local manufacturers to compete with the scale, state support and supply-chain depth of Chinese industry. If we want local technology and manufacturing capacity to survive, we have to accept that some form of support will be needed.

That support has to be disciplined. Subsidies can distort markets, reward poor management and create bizarre incentives. They can also become corporate welfare if governments spend public money building strategic industries, then allow them to be sold off once they become valuable.

So the policy needs to be proactive: encourage local design and manufacturing and support industries that genuinely matter, while placing sensible limits on foreign takeovers where national resilience is at stake. That does not mean retreating from global trade and it should not mean starting a trade war. It means recognising that some capabilities are too important to rebuild in a panic.

I don't pretend to have a complete solution. But Nexperia is a useful warning. Let's not sell more critical businesses, then realise too late that we needed them.

Nicholas Vinen, Electron Publishing (Australia)*

* a division of SILICON CHIP Publications Pty Ltd.

Practical Electronics

UK readers SAVE £1 on every issue

SUBSCRIBE NOW!

01202 087631

Take out a one-year subscription and save more than £10 over the year.
Even better – save over £1 per issue if you subscribe for two years – a total saving of £26.

Overseas rates represent exceptional value

You also:
- **Avoid any cover price increase for the duration of your subscription**
- **Get your magazine delivered to your door each month**
- **Guarantee a copy, even if your local newsagent sells out**

Order by:
- **Phone or post with a cheque, postal order or credit card**
- **Or order online at: www.electronpublishing.com**

Practical Electronics

SUBSCRIPTION PRICES

Subscriptions for delivery direct to any address in:

UK: 6-months £33.99, 12-months £59.99, 24-months £114.99

Europe Airmail: 6-months £38.99, 12-months £69.99, 24-months £129.99

Rest Of The World Airmail: 6-months £46.99, 12-months £84.99, 24-months £164.99

Cheques (in **£ sterling only**) payable to ***Select Publisher Services Ltd*** and sent to: Practical Electronics Subscriptions, PO Box 6337, Bournemouth BH1 9EH, United Kingdom

Tel: 01202 087631
Email: pesubs@selectps.com

Also via our online shop at**: www.electronpublishing.com**

Subscriptions start with the next available issue. We accept MasterCard or Visa.
(For past issues see the Back Issues page.)

DIGITAL SUBSCRIPTIONS

Electronic subscriptions are available from £29.99 for 12 months, more details at: **www.electronpublishing.com**

SUBSCRIPTION ORDER FORM

☐ **6 Months: UK £33.99, Europe £38.99 (Airmail), Rest of the World £46.99 (Airmail)**
☐ **1 Year: UK £59.99, Europe £69.99 (Airmail), Rest of the World £84.99 (Airmail)**
☐ **2 Years: UK £114.99, Europe £129.99 (Airmail), Rest of the World £164.99 (Airmail)**

To: **Practical Electronics Subscriptions**
PO Box 6337
Bournemouth BH1 9EH
United Kingdom

Tel: 01202 087631
Email: pesubs@selectps.com

I enclose payment of £ ....
(cheque/PO in £ sterling only)
payable to ***Select Publisher Services Ltd***

☐ Please charge my Visa/Mastercard

My card number is: ....
Please print clearly, and check that you have the number correct

Card Security Code .... Valid From Date........................
(The last 3 digits on or just under the signature strip)

Card Ex. Date ....

Name ....

Address ....

Post code .... Tel. ....

Email ....

Subscriptions start with the next available issue.

How USB-C Power Delivery Works

By Andrew Levido

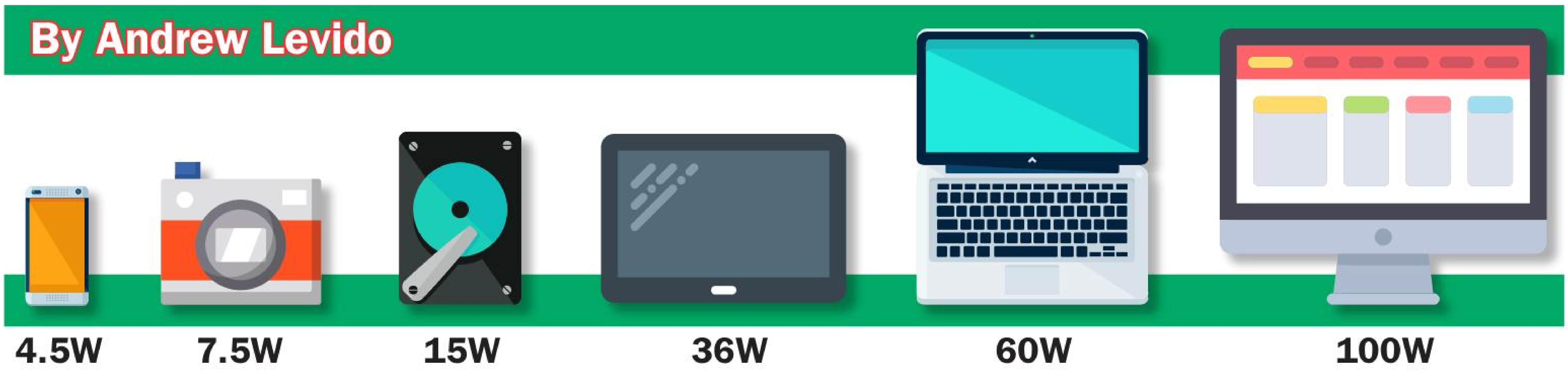

USB has come a long way from when it was introduced in the mid-1990s. The widespread adoption of USB 3.2 introduced the Type-C connector, plus a new Power Delivery (PD) capability that allows up to 100W (20V @ 5A) to be delivered. It is quite a bit more complicated than previous USB power schemes, but well worth a look.

When the USB standard was first introduced, it was only designed to supply 5V at up to 500mA (or less under some circumstances), the idea being that this would form the power supply for the USB device itself.

Nobody had really considered the USB power supply being a way to charge devices or do anything else back then. That 2.5W was more than enough for most devices; larger ones, like printers or scanners, were expected to have their own mains-based power supply.

Of course, a lot has changed since 1996, when USB 1.0 was introduced. 2.5W is nowhere near enough to fast-charge a smartphone, tablet or even laptop/notebook computer. Even the 5W limit introduced later (5V @ 1A) is far too low for charging devices.

The USB 3.2 standard is the first that officially allows power sources and sinks (and the cable!) to negotiate the voltage and current supplied.

But before we get into the details for how all this works, we need to get a few terms straight. Things have gotten more complicated since the days when there were only two possible things you could plug a USB cable into: a host, which sourced power and controlled communication, and a device, which consumed power and responded to host communication.

Now USB ports can have three possible data roles and three possible power roles. Data roles include:

- Downstream-facing ports (DFPs) – typically a host or hub
- Upstream-facing ports (UFPs) – typically a device
- Dual-role ports (DRPs), which can switch between device and host roles

USB-C ports also have a power role:

- Source role, supplying power
- Sink role, consuming power
- Dual-role power port

Dual-role power ports can switch between source and sink roles. A good example of this is the USB-C port on a laptop, which can be a sink when connected to a power brick (or a monitor which can supply power) to power or charge the device, or a source when connected to a peripheral such as a USB hard disk.

On attach, DFPs are source ports and UFPs are sink ports; however, this can be changed later by mutual agreement.

The USB-C connector

USB 3.2 introduced the new Type-C connector, which is used on both ends of a USB-C cable. This connector can be inserted either way around, and the connectors can optionally contain electronics that allows the system to identify specific cable capabilities.

The USB-C connection includes a dedicated Configuration Channel (CC), used to detect cable attachment, plug orientation, cable capability, and to negotiate 'Power Contracts' between source and sink.

In addition, USB-C has two super speed full-duplex differential channels for high-speed data communication, and two sideband use lines. We will focus on the CC for this discussion.

The two rows of contacts in the receptacle are shown in the middle of Fig.1, with the two possible plug orientations (un-flipped and flipped) shown above and below respectively.

The GND and VBUS pins are

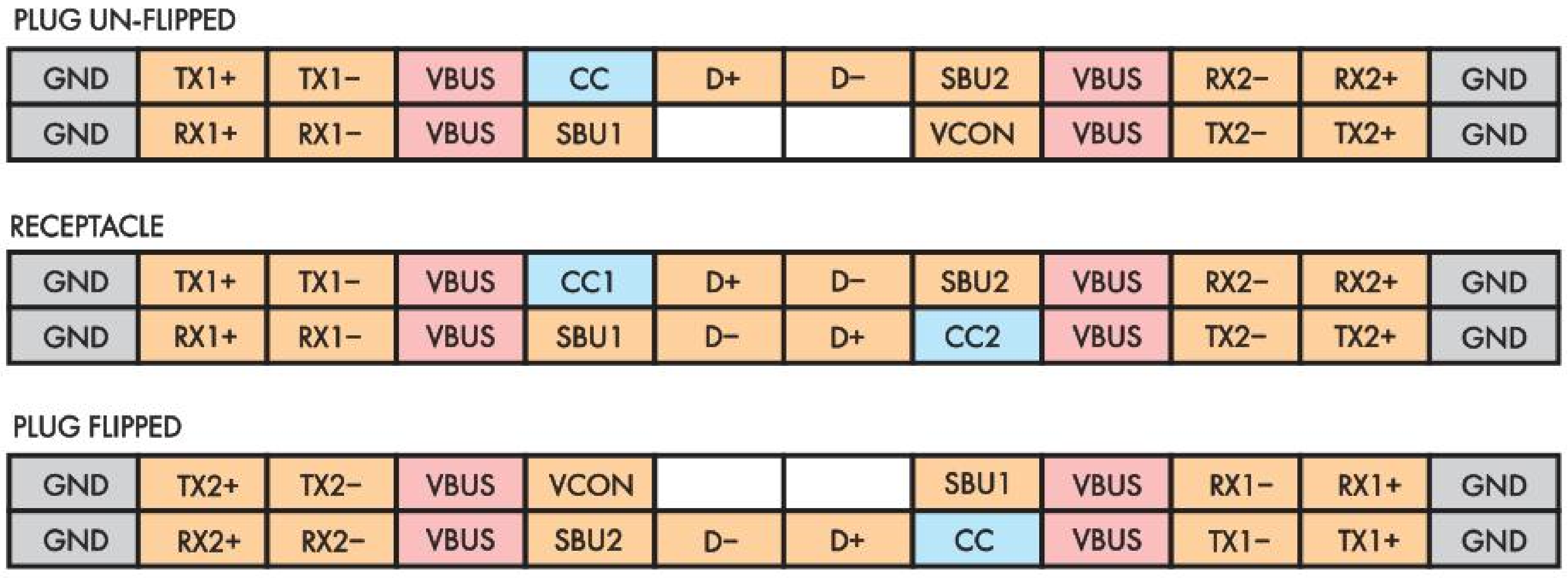

PLUG UN-FLIPPED

GND	TX1+	TX1−	VBUS	CC	D+	D−	SBU2	VBUS	RX2−	RX2+	GND
GND	RX1+	RX1−	VBUS	SBU1			VCON	VBUS	TX2−	TX2+	GND

RECEPTACLE

GND	TX1+	TX1−	VBUS	CC1	D+	D−	SBU2	VBUS	RX2−	RX2+	GND
GND	RX1+	RX1−	VBUS	SBU1	D−	D+	CC2	VBUS	TX2−	TX2+	GND

PLUG FLIPPED

GND	TX2+	TX2−	VBUS	VCON			SBU1	VBUS	RX1−	RX1+	GND
GND	RX2+	RX2−	VBUS	SBU2	D−	D+	CC	VBUS	TX1−	TX1+	GND

Fig.1: the pin assignment of the USB Type-C receptacle is shown in the centre. Above and below are two possible plug orientations. The CC1 and CC2 pins on the receptacle connect to the CC and VCON pins on the plug; it can tell which way the plug is inserted by monitoring which of CC1 or CC2 connect to CC.

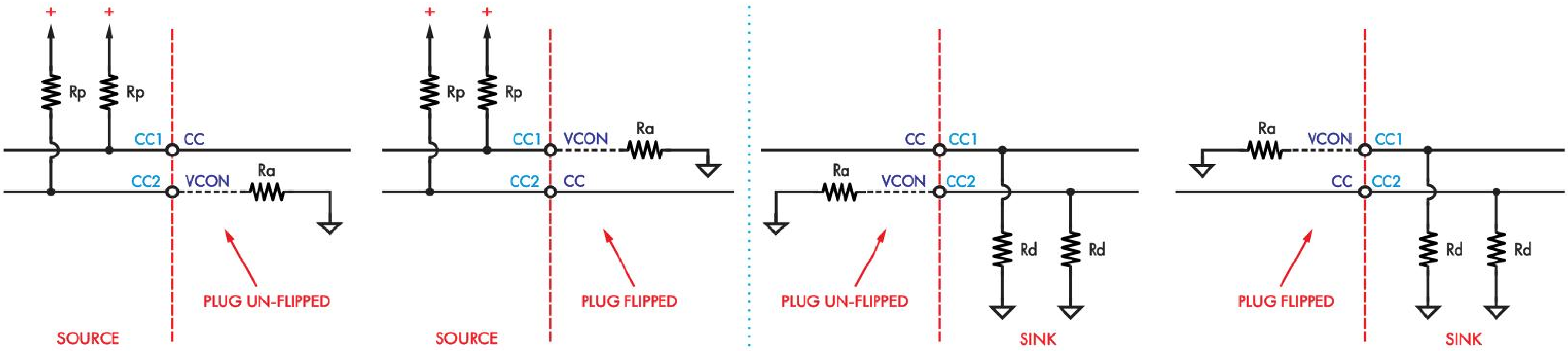

Fig.2: on attach, the source pulls up CC1 and CC2 via Rp, and the sink pulls them down via Rd. There is only one CC line in the cable, so both the source and sink can detect whether or not the plug is flipped at their end. An active cable pulls the VCON pin down via Ra to signal its presence. Passive cables leave VCON open.

symmetrical, so these pins connect correctly regardless of the plug orientation. The classic USB D+ and D- also work correctly, as the two D+ pins and the two D- pins on the receptacle are connected together internally.

The two super-speed twisted pairs will be swapped depending on the plug orientation, so the device must use a high-speed mux to un-swap these if the plug is flipped. Similarly, the sideband use (SBU) pins are swapped, and must be sorted out depending on the plug orientation.

The pins we are interested in for Power Delivery are the two Configuration Channel (CC) pins on the receptacle, and the CC and VCON pins on the plug. These allow the ports at each end of the cable to work out the plug orientation, detect attachment, and determine the other end's capabilities.

Detecting attachment and cable orientation

Refer now to Fig.2. When two USB Type-C ports are connected, the DFP will default to a source and pull the two CC lines high with resistors Rp, and the sink end will pull the CC lines down via resistors Rd. The source detects attachment when one of the two CC pins is pulled low by Rd, and the sink detects attachment when one of its CC pins is pulled high by Rp.

On attachment, the source voltage defaults to 5V for compatibility and safety. The sink can determine what current the source can provide at 5V by measuring Rp's value (or, more accurately, the current sourced). Table 1 shows how this works (overleaf).

The source and sink can determine the plug orientation by noting whether their CC1 or CC2 pin is pulled up by Rp or down by Rd.

Electronically marked cable assembly (EMCA)

The connectors on a USB Type-C cable can optionally contain a microchip, allowing the cable to report its capabilities to the source and sink devices. For example, a standard USB Type-C cable can support power delivery at up to 3A.

To take advantage of the maximum 5A capability, you need to use an active cable that can tell the source that it is rated to that level. The source will not allow the sink to draw more than 3A if the cable does not report that it can handle it.

On attach, a cable indicates it is electronically marked by pulling the VCON pin down via resistor Ra, which is between 800Ω and 1.2kΩ. Non-marked cables leave VCON open. If a Marked cable is detected, the source device is responsible for supplying a voltage at the appropriate CC pin to VCON to power the microchip in the cable, as shown in Fig.3.

Other modes

Type-C connectors support additional modes that use the sideband use (SBU) channels. These are the audio accessory mode (for headphones, for example) and a debug accessory mode, where the SBU channels can be used for transmitting debugging signals.

Table 2 summarises the various combinations of pull-up and pull-down on the CC pins and what they signify.

Power Delivery

When attached, a USB Power Delivery source is configured to supply 5V for compatibility with legacy devices. It will be capable of supplying up to 1.5A for a maximum power of 7W, or 3A/15W, depending on Rp's value as described above. If this is all the sink requires, it does not need to

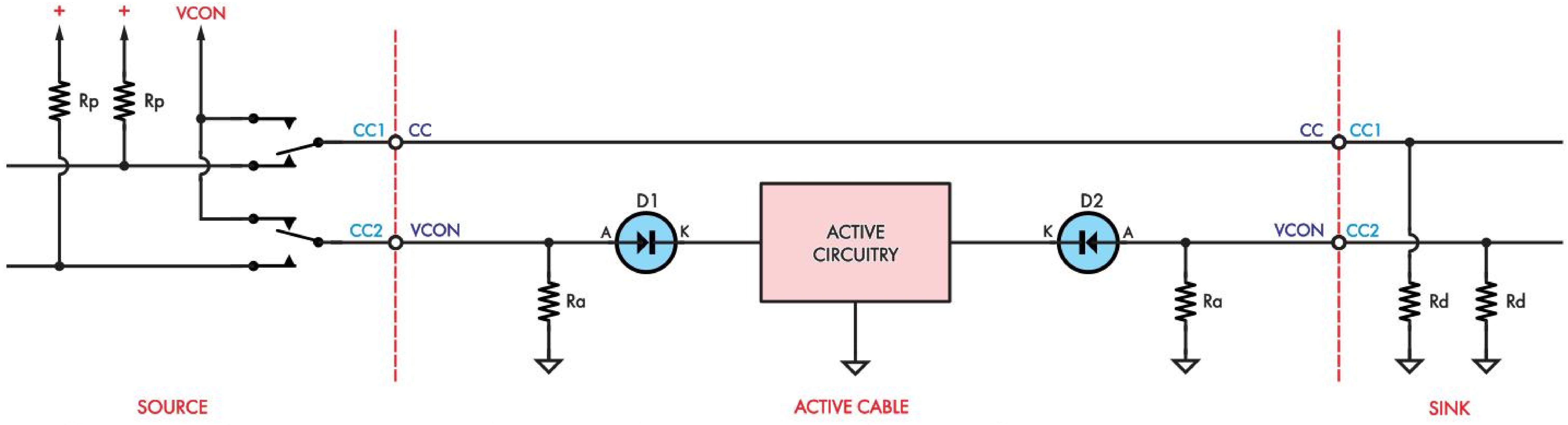

Fig.3: if the source detects an active cable, it switches a power supply on to the VCON pin to power up the microchip in the connector. The cable must be capable of being powered from either end, as a USB Type-C cable can be connected either way around.

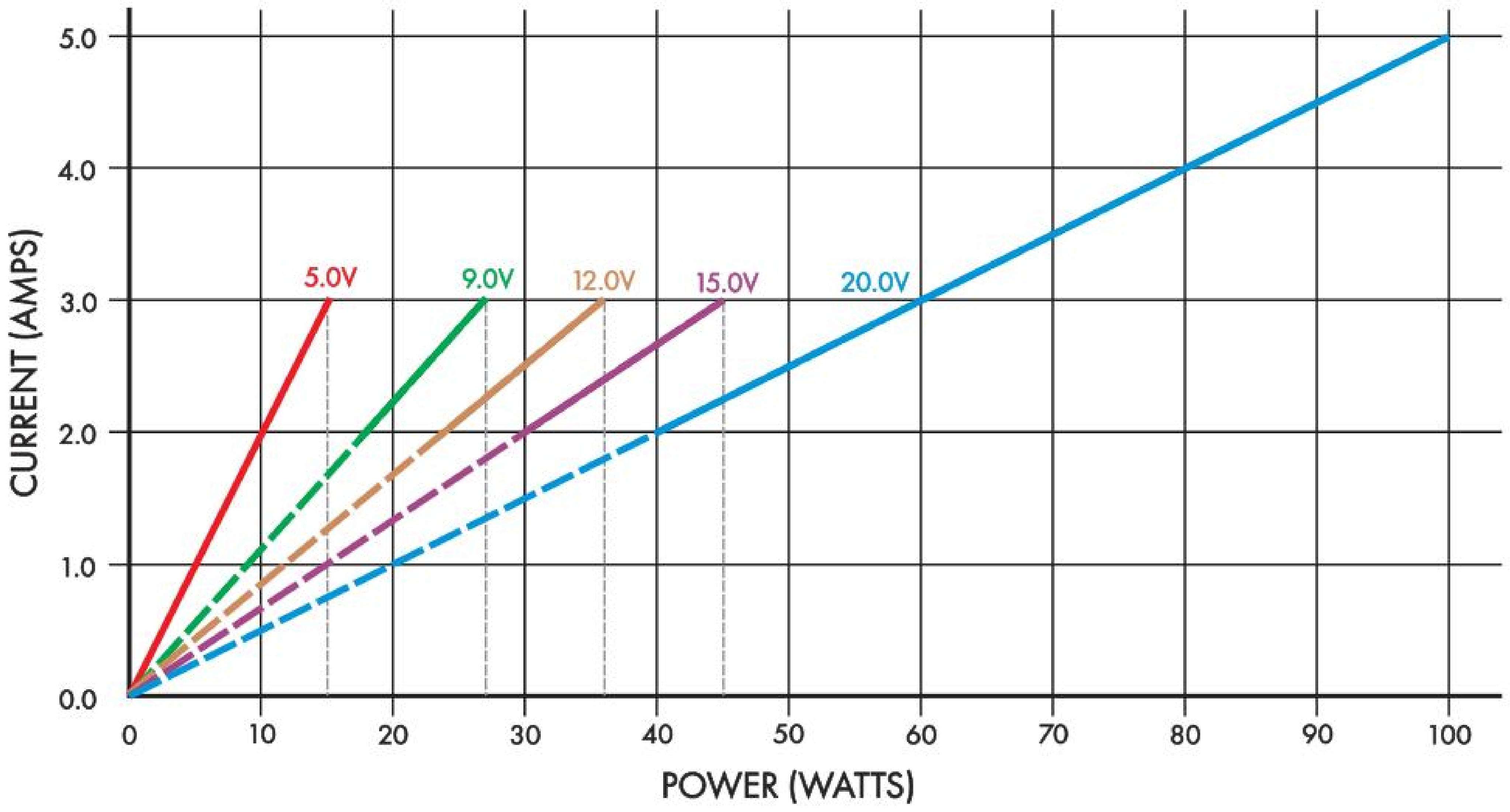

Fig.4: the power rating of a USB Power Delivery source generally indicates the range of voltages it can provide. This is not always the case (I’m looking at you, Apple), so it pays to check before buying.

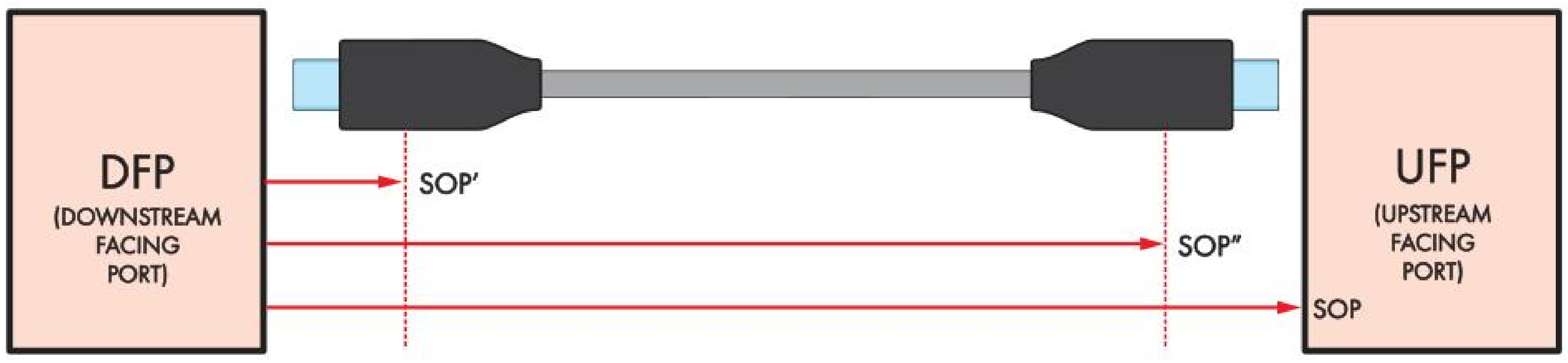
DFP
(DOWNSTREAM
FACING
PORT)
SOP’
SOP”
SOP
UFP
(UPSTREAM
FACING
PORT)

Fig.5: the “start-of-packet” (SOP) header indicates whether the message is intended for the UFP, or a particular connector of an active cable. These are confusingly called SOP, SOP’ and SOP” packets respectively.

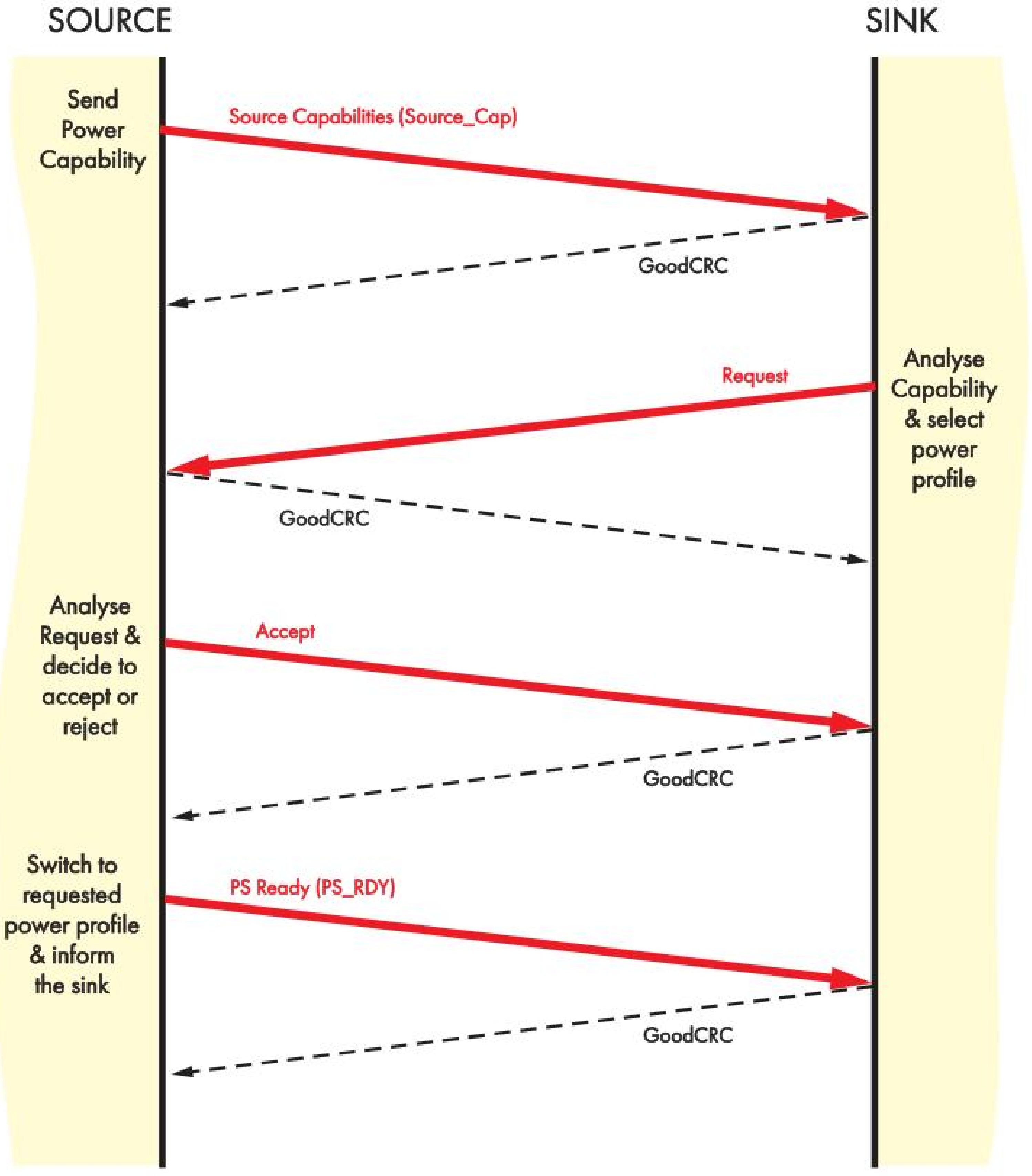
SOURCE
SINK
Send Power Capability
Source Capabilities (Source_Cap)
GoodCRC
Request
Analyse Capability & select power profile
GoodCRC
Analyse Request & decide to accept or reject
Accept
GoodCRC
Switch to requested power profile & inform the sink
PS Ready (PS_RDY)
GoodCRC

Fig.6: a successful power contract negotiation starts with the source advertising its capabilities. The sink then requests one of these capabilities. If the request is accepted, the source sends an “Accept” message, changes its output, and then sends a “PS_RDY” message. All messages are acknowledged with a “GoodCRC” message if they are received correctly.

do anything more. This is known as an implicit contract.

If the sink requires more power or a higher voltage, it can request more by negotiating an explicit contract over the Configuration Channel.

Before we get into details of how this is done, we should look at the voltages and currents typical USB Type-C sources can supply.

Fig.4 shows that USB Power Delivery sources are generally rated by the power they can source. Up to 15W, they typically only supply 5V. Those rated above 15W generally supply 5V or 9V; those rated above 27W should offer 5V, 9V and 12V, while those above 36W should offer 5V, 9V, 12V and 15V. Those rated above 45W add 20V to the list.

Note that while this is generally the case, some vendors have gone their own way and offer some oddball combinations.

Negotiating a Power Contract

Data across the Configuration Channel is encoded into 32-bit packets using bi-phase mark coding (BMC) at 300 kilobaud, with CRC error correction. Communication is initiated by the DFP (usually a source).

Messages start with a ‘start-of-packet’ (SOP) packet, which describes where the message is intended to go. Confusingly, these are designated SOP, SOP’ and SOP’’ packets.

As shown in Fig.5, messages headed by SOP packets are intended for the UFP; those with SOP’ packets are intended for the connector at the source end of an electronically marked cable (ie, that receiving VCON); and those with SOP” packets are for the connector at the sink end of the cable.

It is important to keep in mind that, while the SOP signalling means the Configuration Channel uses a multidrop protocol, overall USB remains a point-to-point connection. The D+, D– signalling is unchanged from previous generations of USB, and the superspeed channels also operate point-to-point. You can still only connect one DFP to one UFP, and have one source and one sink in a given connection.

The basic process for negotiating an explicit Power Contract is shown in Fig.6. Until an explicit Contract has been negotiated, the source will periodically send a “Source_Cap” message to advertise its voltage and current capacity. If this is received

Table 1: RP values and source current vs current capability

Maximum source current	Rp (pulled to 5V)	Rp (pulled to 3.3V)	Current sourced
Default (0.5A or 0.9A)	56kΩ	36kΩ	80μA
1.5A	22kΩ	12kΩ	180μA
3.0A	10kΩ	4.7kΩ	330μA

Table 2: decoding CC1 & CC2 states (from the source perspective)

CC1	CC2	Attach?	Active Cable?	Flipped?
open	open	no	–	–
Rd	open	yes	no	no
open	Rd	yes	no	yes
open	Ra	no	yes	no
Ra	open	no	yes	yes
Rd	Ra	yes	yes	no
Ra	Rd	yes	yes	yes
Rd	Rd	debug accessory mode		
Ra	Ra	audio adaptor mode		

successfully by the sink, it will respond with a "GoodCRC" message.

The "Source_Cap" message includes a list of the possible voltages and maximum currents it can source. The sink may then request the source provide a specific voltage identified in one of the source capabilities, and specify the maximum current required (up to the advertised capacity) by sending a 'Request' message to the source. This is also acknowledged by the source with a "GoodCRC" message.

The source will analyse the request and determine if it can accommodate it. If it can, it sends an 'Accept' message to the sink. Assuming it received a "GoodCRC" message acknowledging receipt by the sink, the source will change its output to the agreed level and send "PS_RDY" message to the sink. If that message is acknowledged, then the Contract is considered complete.

Fig.7 shows a screen capture of this process, using a Total Phase USB Power Delivery analyser. At the top of the screen are the messages passing between the source and sink as a contract is negotiated. The bottom half of the screen shows an expansion of the highlighted "Source_Cap" message.

You can see that this particular source (a 45W Targus unit labelled APA95AU) can supply 5V, 9V, 12V, 15V and 20V, as described in the five "Power Objects" contained in the "Source_Cap" Message.

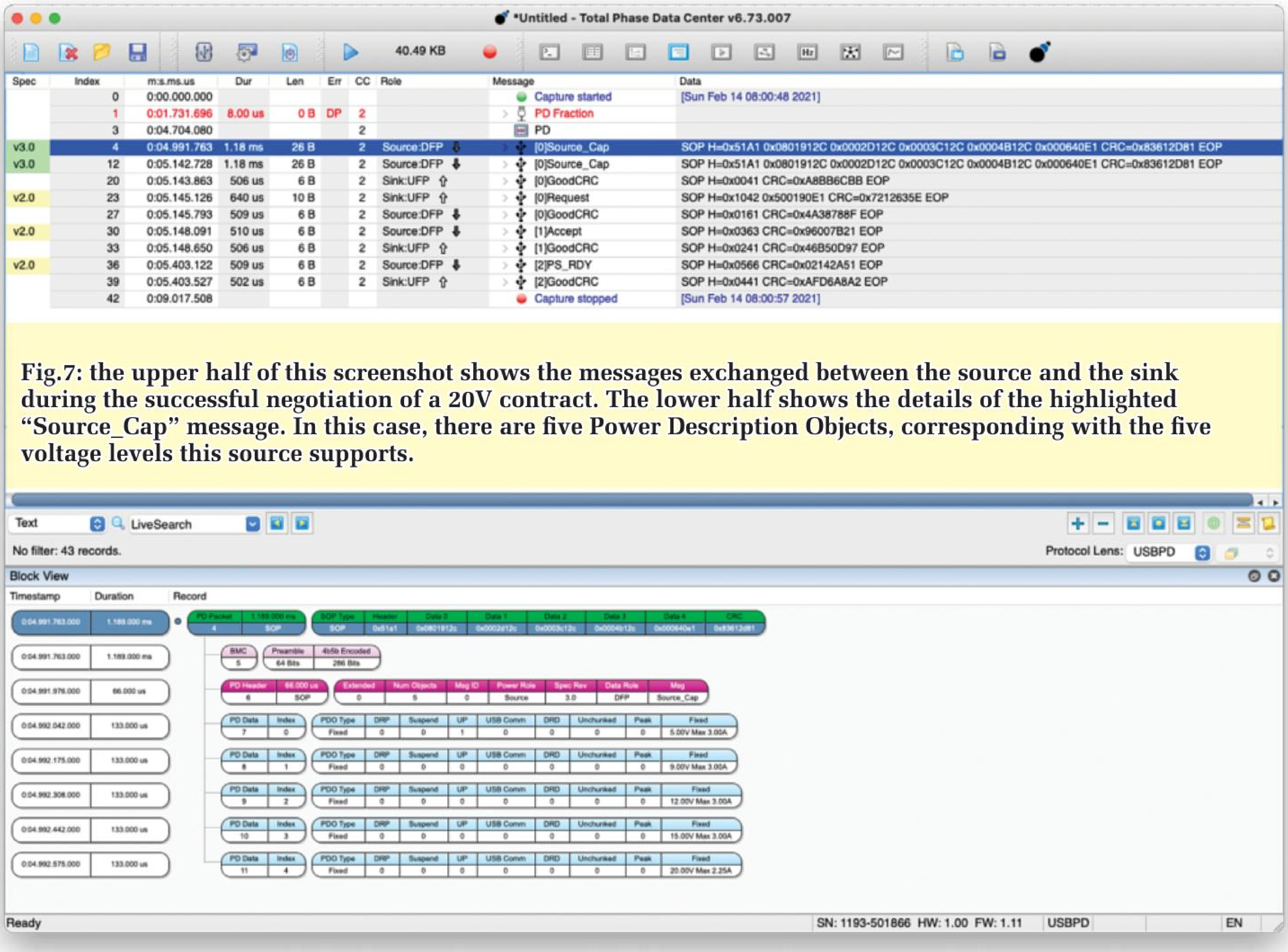

Spec	Index	m:s.ms.us	Dur	Len	Err	CC	Role	Message	Data
	0	0:00.000.000						Capture started	[Sun Feb 14 08:00:48 2021]
	1	0:01.731.696	8.00 us	0 B	DP	2		PD Fraction	
	3	0:04.704.080				2		PD	
v3.0	4	0:04.991.763	1.18 ms	26 B		2	Source:DFP ⇩	[0]Source_Cap	SOP H=0x51A1 0x0801912C 0x0002D12C 0x0003C12C 0x0004B12C 0x000640E1 CRC=0x83612D81 EOP
v3.0	12	0:05.142.728	1.18 ms	26 B		2	Source:DFP ⇩	[0]Source_Cap	SOP H=0x51A1 0x0801912C 0x0002D12C 0x0003C12C 0x0004B12C 0x000640E1 CRC=0x83612D81 EOP
	20	0:05.143.863	506 us	6 B		2	Sink:UFP ⇧	[0]GoodCRC	SOP H=0x0041 CRC=0xA8BB6CBB EOP
v2.0	23	0:05.145.126	640 us	10 B		2	Sink:UFP ⇧	[0]Request	SOP H=0x1042 0x500190E1 CRC=0x7212635E EOP
	27	0:05.145.793	509 us	6 B		2	Source:DFP ⇩	[0]GoodCRC	SOP H=0x0161 CRC=0x4A38788F EOP
v2.0	30	0:05.148.091	510 us	6 B		2	Source:DFP ⇩	[1]Accept	SOP H=0x0363 CRC=0x96007B21 EOP
	33	0:05.148.650	506 us	6 B		2	Sink:UFP ⇧	[1]GoodCRC	SOP H=0x0241 CRC=0x46B50D97 EOP
v2.0	36	0:05.403.122	509 us	6 B		2	Source:DFP ⇩	[2]PS_RDY	SOP H=0x0566 CRC=0x02142A51 EOP
	39	0:05.403.527	502 us	6 B		2	Sink:UFP ⇧	[2]GoodCRC	SOP H=0x0441 CRC=0xAFD6A8A2 EOP
	42	0:09.017.508						Capture stopped	[Sun Feb 14 08:00:57 2021]

Fig.7: the upper half of this screenshot shows the messages exchanged between the source and the sink during the successful negotiation of a 20V contract. The lower half shows the details of the highlighted "Source_Cap" message. In this case, there are five Power Description Objects, corresponding with the five voltage levels this source supports.

No filter: 43 records.

Timestamp	Duration	Record
0:04.991.763.000	1.189.000 ms	PD Packet 4, 1.189.000 ms SOP; SOP Type SOP, Header 0x51a1, Data 0 0x0801912c, Data 1 0x0002d12c, Data 2 0x0003c12c, Data 3 0x0004b12c, Data 4 0x000640e1, CRC 0x83612d81
0:04.991.763.000	1.189.000 ms	BMC 5; Preamble 64 Bits, 4b5b Encoded 286 Bits
0:04.991.976.000	66.000 us	PD Header 6, 66.000 us SOP; Extended 0, Num Objects 5, Msg ID 0, Power Role Source, Spec Rev 3.0, Data Role DFP, Msg Source_Cap
0:04.992.042.000	133.000 us	PD Data 7, Index 0; PDO Type Fixed, DRP 0, Suspend 0, UP 1, USB Comm 0, DRD 0, Unchunked 0, Peak 0, Fixed 5.00V Max 3.00A
0:04.992.175.000	133.000 us	PD Data 8, Index 1; PDO Type Fixed, DRP 0, Suspend 0, UP 0, USB Comm 0, DRD 0, Unchunked 0, Peak 0, Fixed 9.00V Max 3.00A
0:04.992.308.000	133.000 us	PD Data 9, Index 2; PDO Type Fixed, DRP 0, Suspend 0, UP 0, USB Comm 0, DRD 0, Unchunked 0, Peak 0, Fixed 12.00V Max 3.00A
0:04.992.442.000	133.000 us	PD Data 10, Index 3; PDO Type Fixed, DRP 0, Suspend 0, UP 0, USB Comm 0, DRD 0, Unchunked 0, Peak 0, Fixed 15.00V Max 3.00A
0:04.992.575.000	133.000 us	PD Data 11, Index 4; PDO Type Fixed, DRP 0, Suspend 0, UP 0, USB Comm 0, DRD 0, Unchunked 0, Peak 0, Fixed 20.00V Max 2.25A

Ready

SN: 1193-501866 HW: 1.00 FW: 1.11 USBPD EN

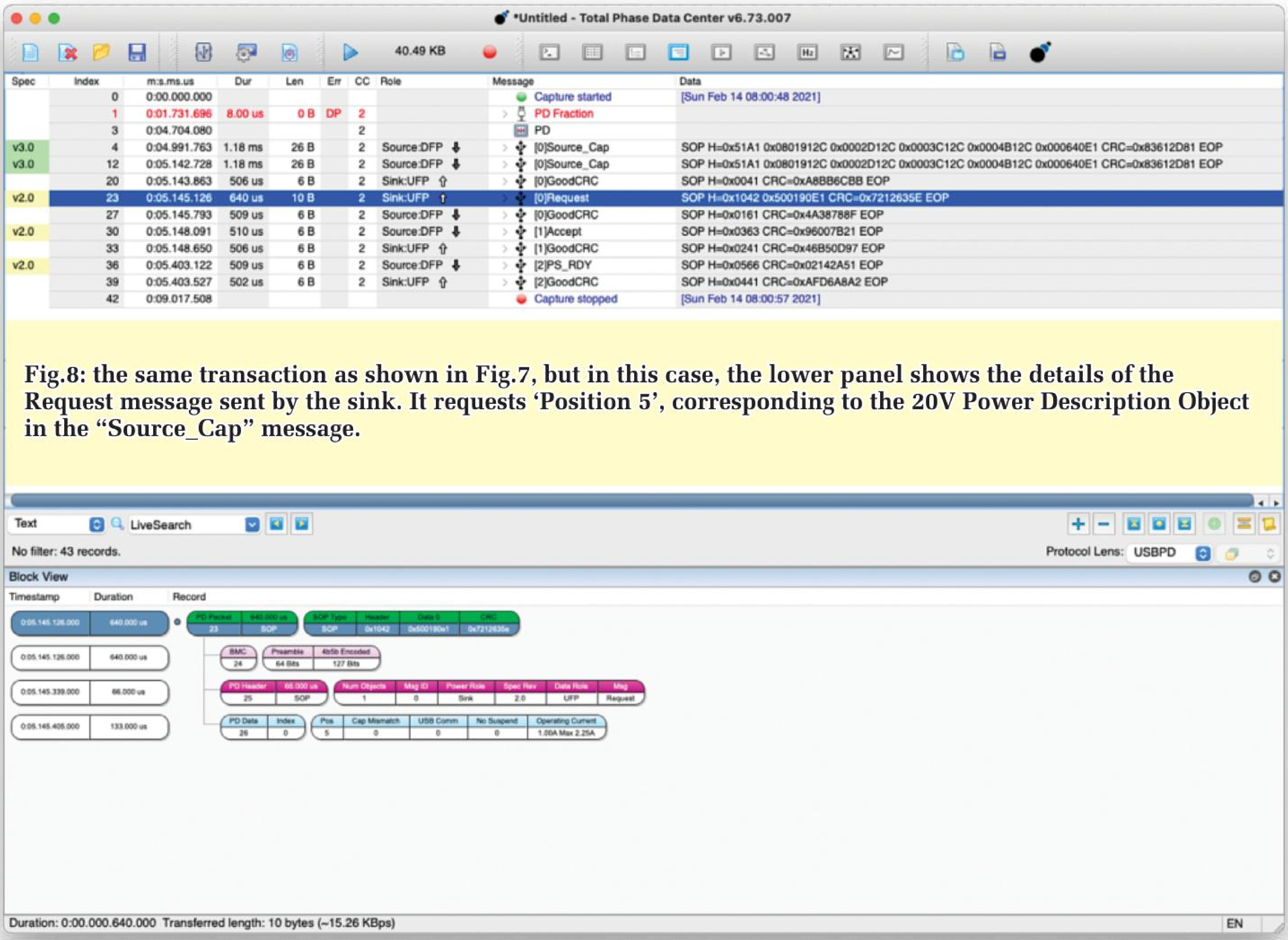
*Untitled - Total Phase Data Center v6.73.007
40.49 KB
Text
LiveSearch
No filter: 43 records.
Protocol Lens: USBPD
Block View
Timestamp
Duration
Record
0:05.145.126.000
640.000 us
0:05.145.126.000
640.000 us
0:05.145.339.000
66.000 us
0:05.145.405.000
133.000 us
PD Packet
640.000 us
23
SOP
SOP Type
Header
Data 0
CRC
SOP
0x1042
0x500190e1
0x7212635e
BMC
24
Preamble
64 Bits
4b5b Encoded
127 Bits
PD Header
66.000 us
25
SOP
Num Objects
1
Msg ID
0
Power Role
Sink
Spec Rev
2.0
Data Role
UFP
Msg
Request
PD Data
26
Index
0
Pos
5
Cap Mismatch
0
USB Comm
0
No Suspend
0
Operating Current
1.00A Max 2.25A
Duration: 0:00.000.640.000 Transferred length: 10 bytes (~15.26 KBps)
EN

Spec	Index	m:s.ms.us	Dur	Len	Err	CC	Role	Message	Data
	0	0:00.000.000						Capture started	[Sun Feb 14 08:00:48 2021]
	1	0:01.731.696	8.00 us	0 B	DP	2		PD Fraction	
	3	0:04.704.080				2		PD	
v3.0	4	0:04.991.763	1.18 ms	26 B		2	Source:DFP ⇩	[0]Source_Cap	SOP H=0x51A1 0x0801912C 0x0002D12C 0x0003C12C 0x0004B12C 0x000640E1 CRC=0x83612D81 EOP
v3.0	12	0:05.142.728	1.18 ms	26 B		2	Source:DFP ⇩	[0]Source_Cap	SOP H=0x51A1 0x0801912C 0x0002D12C 0x0003C12C 0x0004B12C 0x000640E1 CRC=0x83612D81 EOP
	20	0:05.143.863	506 us	6 B		2	Sink:UFP ⇧	[0]GoodCRC	SOP H=0x0041 CRC=0xA8BB6CBB EOP
v2.0	23	0:05.145.126	640 us	10 B		2	Sink:UFP ⇧	[0]Request	SOP H=0x1042 0x500190E1 CRC=0x7212635E EOP
	27	0:05.145.793	509 us	6 B		2	Source:DFP ⇩	[0]GoodCRC	SOP H=0x0161 CRC=0x4A38788F EOP
v2.0	30	0:05.148.091	510 us	6 B		2	Source:DFP ⇩	[1]Accept	SOP H=0x0363 CRC=0x96007B21 EOP
	33	0:05.148.650	506 us	6 B		2	Sink:UFP ⇧	[1]GoodCRC	SOP H=0x0241 CRC=0x46B50D97 EOP
v2.0	36	0:05.403.122	509 us	6 B		2	Source:DFP ⇩	[2]PS_RDY	SOP H=0x0566 CRC=0x02142A51 EOP
	39	0:05.403.527	502 us	6 B		2	Sink:UFP ⇧	[2]GoodCRC	SOP H=0x0441 CRC=0xAFD6A8A2 EOP
	42	0:09.017.508						Capture stopped	[Sun Feb 14 08:00:57 2021]

Fig.8: the same transaction as shown in Fig.7, but in this case, the lower panel shows the details of the Request message sent by the sink. It requests 'Position 5', corresponding to the 20V Power Description Object in the "Source_Cap" message.

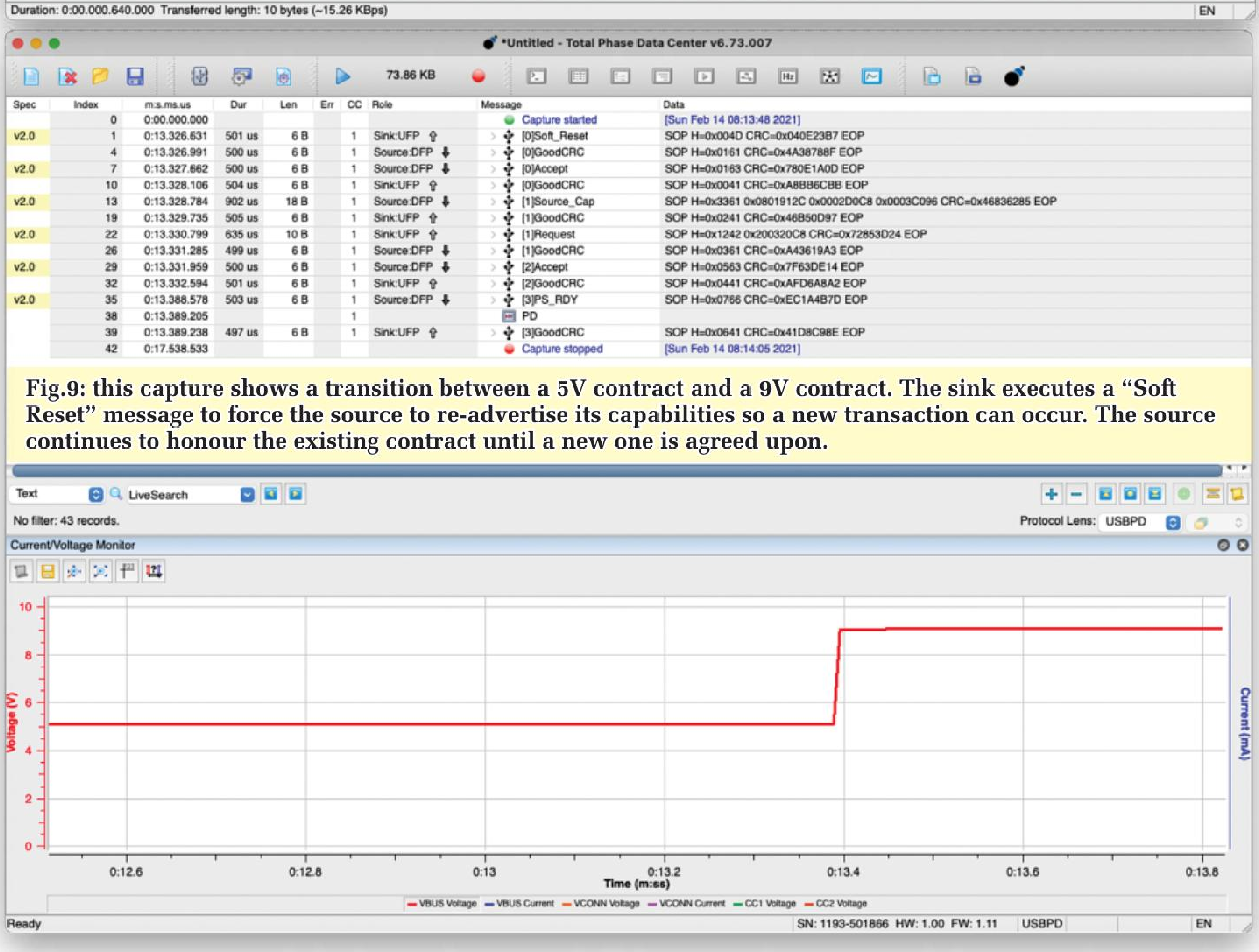
*Untitled - Total Phase Data Center v6.73.007
73.86 KB
Text
LiveSearch
No filter: 43 records.
Protocol Lens: USBPD
Current/Voltage Monitor
10
8
6
4
2
0
Voltage (V)
Current (mA)
0:12.6
0:12.8
0:13
0:13.2
0:13.4
0:13.6
0:13.8
Time (m:ss)
VBUS Voltage
VBUS Current
VCONN Voltage
VCONN Current
CC1 Voltage
CC2 Voltage
Ready
SN: 1193-501866 HW: 1.00 FW: 1.11
USBPD
EN

Spec	Index	m:s.ms.us	Dur	Len	Err	CC	Role	Message	Data
	0	0:00.000.000						Capture started	[Sun Feb 14 08:13:48 2021]
v2.0	1	0:13.326.631	501 us	6 B		1	Sink:UFP ⇧	[0]Soft_Reset	SOP H=0x004D CRC=0x040E23B7 EOP
	4	0:13.326.991	500 us	6 B		1	Source:DFP ⇩	[0]GoodCRC	SOP H=0x0161 CRC=0x4A38788F EOP
v2.0	7	0:13.327.662	500 us	6 B		1	Source:DFP ⇩	[0]Accept	SOP H=0x0163 CRC=0x780E1A0D EOP
	10	0:13.328.106	504 us	6 B		1	Sink:UFP ⇧	[0]GoodCRC	SOP H=0x0041 CRC=0xA8BB6CBB EOP
v2.0	13	0:13.328.784	902 us	18 B		1	Source:DFP ⇩	[1]Source_Cap	SOP H=0x3361 0x0801912C 0x0002D0C8 0x0003C096 CRC=0x46836285 EOP
	19	0:13.329.735	505 us	6 B		1	Sink:UFP ⇧	[1]GoodCRC	SOP H=0x0241 CRC=0x46B50D97 EOP
v2.0	22	0:13.330.799	635 us	10 B		1	Sink:UFP ⇧	[1]Request	SOP H=0x1242 0x200320C8 CRC=0x72853D24 EOP
	26	0:13.331.285	499 us	6 B		1	Source:DFP ⇩	[1]GoodCRC	SOP H=0x0361 CRC=0xA43619A3 EOP
v2.0	29	0:13.331.959	500 us	6 B		1	Source:DFP ⇩	[2]Accept	SOP H=0x0563 CRC=0x7F63DE14 EOP
	32	0:13.332.594	501 us	6 B		1	Sink:UFP ⇧	[2]GoodCRC	SOP H=0x0441 CRC=0xAFD6A8A2 EOP
v2.0	35	0:13.388.578	503 us	6 B		1	Source:DFP ⇩	[3]PS_RDY	SOP H=0x0766 CRC=0xEC1A4B7D EOP
	38	0:13.389.205				1		PD	
	39	0:13.389.238	497 us	6 B		1	Sink:UFP ⇧	[3]GoodCRC	SOP H=0x0641 CRC=0x41D8C98E EOP
	42	0:17.538.533						Capture stopped	[Sun Feb 14 08:14:05 2021]

Fig.9: this capture shows a transition between a 5V contract and a 9V contract. The sink executes a "Soft Reset" message to force the source to re-advertise its capabilities so a new transaction can occur. The source continues to honour the existing contract until a new one is agreed upon.

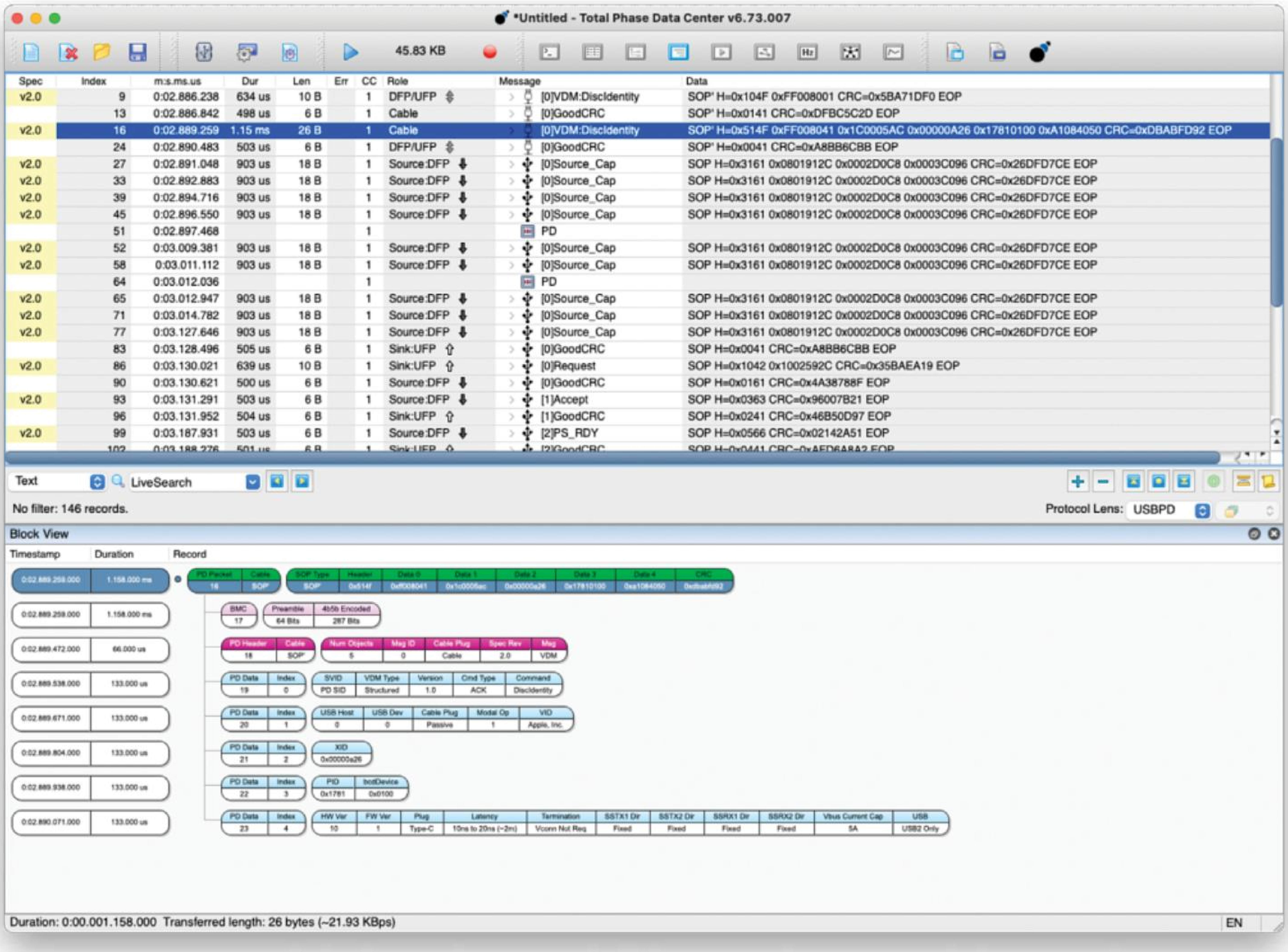

Spec	Index	m:s.ms.us	Dur	Len	Err	CC	Role	Message	Data
v2.0	9	0:02.886.238	634 us	10 B		1	DFP/UFP	[0]VDM:DiscIdentity	SOP' H=0x104F 0xFF008001 CRC=0x5BA71DF0 EOP
	13	0:02.886.842	498 us	6 B		1	Cable	[0]GoodCRC	SOP' H=0x0141 CRC=0xDFBC5C2D EOP
v2.0	16	0:02.889.259	1.15 ms	26 B		1	Cable	[0]VDM:DiscIdentity	SOP' H=0x514F 0xFF008041 0x1C0005AC 0x00000A26 0x17810100 0xA1084050 CRC=0xDBABFD92 EOP
	24	0:02.890.483	503 us	6 B		1	DFP/UFP	[0]GoodCRC	SOP' H=0x0041 CRC=0xA8BB6CBB EOP
v2.0	27	0:02.891.048	903 us	18 B		1	Source:DFP	[0]Source_Cap	SOP H=0x3161 0x0801912C 0x0002D0C8 0x0003C096 CRC=0x26DFD7CE EOP
v2.0	33	0:02.892.883	903 us	18 B		1	Source:DFP	[0]Source_Cap	SOP H=0x3161 0x0801912C 0x0002D0C8 0x0003C096 CRC=0x26DFD7CE EOP
v2.0	39	0:02.894.716	903 us	18 B		1	Source:DFP	[0]Source_Cap	SOP H=0x3161 0x0801912C 0x0002D0C8 0x0003C096 CRC=0x26DFD7CE EOP
v2.0	45	0:02.896.550	903 us	18 B		1	Source:DFP	[0]Source_Cap	SOP H=0x3161 0x0801912C 0x0002D0C8 0x0003C096 CRC=0x26DFD7CE EOP
	51	0:02.897.468				1		PD	
v2.0	52	0:03.009.381	903 us	18 B		1	Source:DFP	[0]Source_Cap	SOP H=0x3161 0x0801912C 0x0002D0C8 0x0003C096 CRC=0x26DFD7CE EOP
v2.0	58	0:03.011.112	903 us	18 B		1	Source:DFP	[0]Source_Cap	SOP H=0x3161 0x0801912C 0x0002D0C8 0x0003C096 CRC=0x26DFD7CE EOP
	64	0:03.012.036				1		PD	
v2.0	65	0:03.012.947	903 us	18 B		1	Source:DFP	[0]Source_Cap	SOP H=0x3161 0x0801912C 0x0002D0C8 0x0003C096 CRC=0x26DFD7CE EOP
v2.0	71	0:03.014.782	903 us	18 B		1	Source:DFP	[0]Source_Cap	SOP H=0x3161 0x0801912C 0x0002D0C8 0x0003C096 CRC=0x26DFD7CE EOP
v2.0	77	0:03.127.646	903 us	18 B		1	Source:DFP	[0]Source_Cap	SOP H=0x3161 0x0801912C 0x0002D0C8 0x0003C096 CRC=0x26DFD7CE EOP
	83	0:03.128.496	505 us	6 B		1	Sink:UFP	[0]GoodCRC	SOP H=0x0041 CRC=0xA8BB6CBB EOP
v2.0	86	0:03.130.021	639 us	10 B		1	Sink:UFP	[0]Request	SOP H=0x1042 0x1002592C CRC=0x35BAEA19 EOP
	90	0:03.130.621	500 us	6 B		1	Source:DFP	[0]GoodCRC	SOP H=0x0161 CRC=0x4A38788F EOP
v2.0	93	0:03.131.291	503 us	6 B		1	Source:DFP	[1]Accept	SOP H=0x0363 CRC=0x96007B21 EOP
	96	0:03.131.952	504 us	6 B		1	Sink:UFP	[1]GoodCRC	SOP H=0x0241 CRC=0x46B50D97 EOP
v2.0	99	0:03.187.931	503 us	6 B		1	Source:DFP	[2]PS_RDY	SOP H=0x0566 CRC=0x02142A51 EOP
	102	0:03.188.276	501 us	6 B		1	Sink:UFP	[2]GoodCRC	SOP H=0x0441 CRC=0xAFD6A8A2 EOP

No filter: 146 records.

Block View

Timestamp	Duration	PD Packet	Cable	SOP Type	Header	Data 0	Data 1	Data 2	Data 3	Data 4	CRC
0:02.889.259.000	1.158.000 ms	16	SOP	SOP	0x514f	0xff008041	0x1c0005ac	0x00000a26	0x17810100	0xa1084050	0xdbabfd92

Timestamp	Duration	BMC	Preamble	4b5b Encoded
0:02.889.259.000	1.158.000 ms	17	64 Bits	287 Bits

Timestamp	Duration	PD Header	Cable	Num Objects	Msg ID	Cable Plug	Spec Rev	Msg
0:02.889.472.000	66.000 us	18	SOP'	5	0	Cable	2.0	VDM

Timestamp	Duration	PD Data	Index	SVID	VDM Type	Version	Cmd Type	Command
0:02.889.538.000	133.000 us	19	0	PD SID	Structured	1.0	ACK	DiscIdentity

Timestamp	Duration	PD Data	Index	USB Host	USB Dev	Cable Plug	Modal Op	VID
0:02.889.671.000	133.000 us	20	1	0	0	Passive	1	Apple, Inc.

Timestamp	Duration	PD Data	Index	XID
0:02.889.804.000	133.000 us	21	2	0x00000a26

Timestamp	Duration	PD Data	Index	PID	bcdDevice
0:02.889.938.000	133.000 us	22	3	0x1781	0x0100

Timestamp	Duration	PD Data	Index	HW Ver	FW Ver	Plug	Latency	Termination	SSTX1 Dir	SSTX2 Dir	SSRX1 Dir	SSRX2 Dir	Vbus Current Cap	USB
0:02.890.071.000	133.000 us	23	4	10	1	Type-C	10ns to 20ns (~2m)	Vconn Not Req	Fixed	Fixed	Fixed	Fixed	5A	USB2 Only

Duration: 0:00.001.158.000 Transferred length: 26 bytes (~21.93 KBps)

Fig.10: this transaction shows what happens on attach if an electronically marked cable is detected. The source first queries the cable with a "DiscIdentity" message. The lower panel shows the cable's response. We can see, among other things, that this is an Apple cable and it can handle up to 5A.

Fig.8 shows precisely the same negotiation, but highlights the sink's Request message in response to the "Source_Cap" message. In this case, the sink requests 20V by asking for "Position 5", corresponding to the fifth Power Object in the "Source_Cap" message. It also requests an operating current of 1A and a peak current of 2.25A, the maximum available at that voltage.

Renegotiation

If the sink wishes to negotiate a new Contract with the source, it can send a 'Soft Reset' message, which will result in the sink re-sending the "Source_Cap" messages. The sink can then request a different Contract. The current Contract remains in force until a new one is successfully negotiated.

Fig.9 shows this in action. In this case, the sink requests a change from 5V to 9V. The bottom half of the screen capture shows the VBUS change corresponding with the "PS_RDY" message, just before the 13.4 second mark.

All of the transactions shown so far have involved a passive cable, so no SOP' or SOP" packets were issued.

Fig.10 shows the messaging after attach when an active cable is used. Initially, the source sends a "DiscIdentity" packet to the cable, which responds with a similarly labelled message containing details about the cable. This response is expanded in the bottom half of the screen. In the bottom row, you can see the cable is reporting its latency and indicates that it has a 5A capacity.

Practical considerations

If you want to build a project using USB Type-C power, you have a few options. By far, the simplest is to live with just 5V; ie, do nothing and accept the implicit 5V contract. This is identical to powering your device from a USB Type-B connector such as Mini-B or Micro-B.

If you want to negotiate an explicit contract, you can use one of the off-the-shelf chips which provide various degrees of integration. Assuming you are building a sink-only device, a good option I have used is the ST Microelectronics STUSB4500.

This can be used as a standalone controller (once programmed, if the default does not suit you), or it can be used with a microcontroller, to give you full control over the negotiation process.

I used this chip to build a simple power supply. This uses a linear regulator for low noise, and manages its input voltage via USB Power Delivery to minimise internal power dissipation.

References

- "STUSB4500 – Standalone USB PD Controller for Power Sinking Devices – STMicroelectronics" – https://pemag.au/link/ab73
- Microchip "AN1953 Introduction to USB Type-C" – https://pemag.au/link/ab74
- Texas Instruments "USB PD Power Negotiations," 2016, 21 – https://pemag.au/link/ab75

PE

Part 1 by Tim Blythman

USB-C Power Monitor

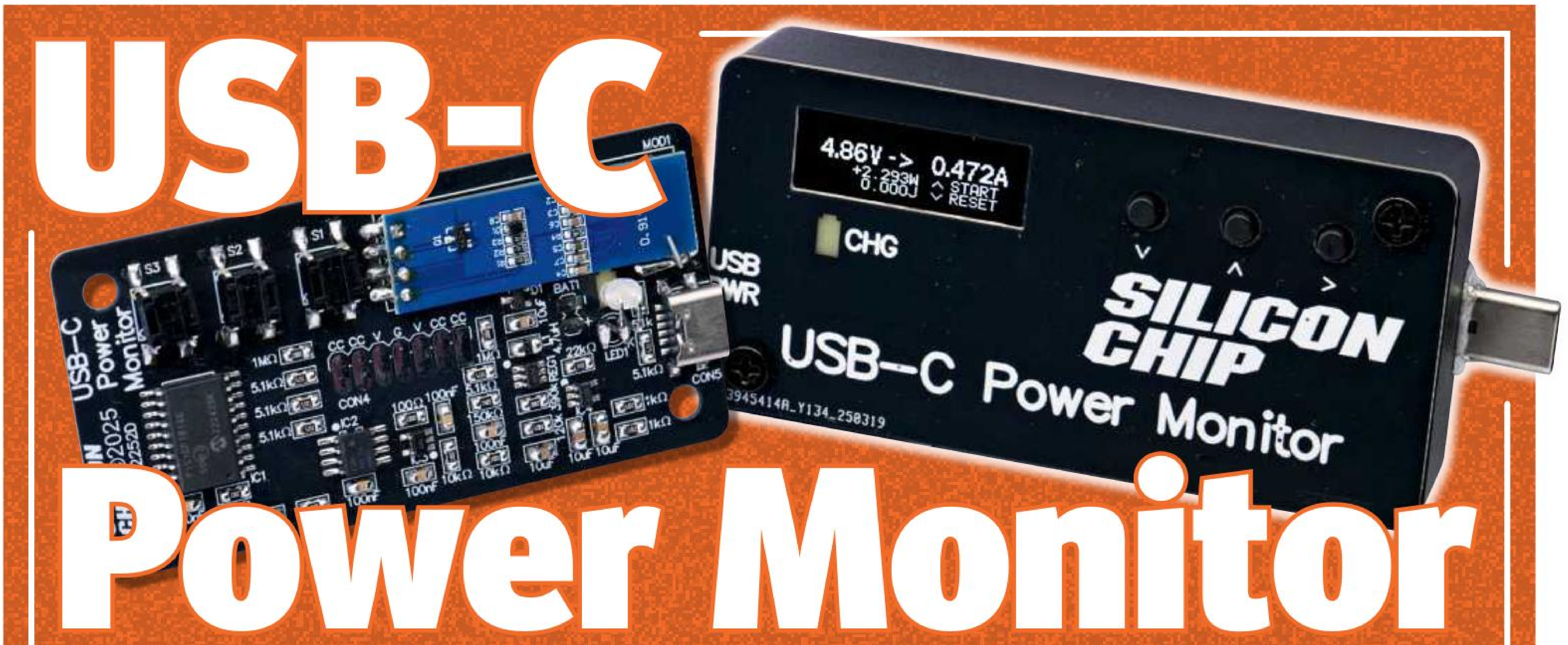

It is always handy to know what voltage and current a USB device is using. Now that USB-C is prevalent, it's time for a USB-C Power Monitor. It can be used for all modern USB-C devices, as well as legacy USB devices, with the right adaptor.

There are many situations where it's helpful to see how much power or current a USB device is drawing, or what voltage is being applied to it. This design makes that very easy, and it works with virtually all modern USB-C devices.

Say you have a fast charger and a smartphone or tablet that's capable of fast charging. While the situation is getting better, there are cases where they are incompatible and will not actually fast charge, or will, but only at a modest rate. With this device, you can see exactly how much power is being transferred.

Another situation is if you are developing a USB device and you want to see how much power it draws when performing certain functions, or whether it's correctly signalling the power supply to give it a certain voltage or amount of power.

Ideally, you want a compact device that can just be plugged between two devices, with a screen to show the voltage, current, power, energy and more. That's exactly what this device is.

It doesn't even matter which way around you connect it – it can monitor current and thus power flow in either direction! It doesn't need an external power supply, either. Its controls are simple yet intuitive; it uses just three pushbuttons and an OLED screen.

A bit of history

Low-cost USB power monitoring devices are available but many of them will not work with the latest USB standards and devices.

Many of them simply insert a shunt resistor in series with the V_{BUS} pin and monitor the voltage across it to determine the device's current draw. They will also measure the V_{BUS} voltage itself. By multiplying those two values, they can calculate the power draw.

More advanced devices can also accumulate the power figure over time to derive a total energy figure. We published a design along those lines in the August 2016 issue, which used an LCD screen to show the USB voltage, current draw, power and more.

Critically, though, many of these devices (like the one just mentioned) are based around the assumption (that was true until recently) that V_{BUS} will always be in the range of 4.75-5.25V. They also usually only have USB Type-A plugs and sockets.

While such devices can be useful, their legacy Type-A connectors rule out the option of working with newer USB 3.x features, such as Power Delivery (PD) or SuperSpeed USB data transfer. If USB Power Delivery were somehow to be used with these devices connected, and V_{BUS} rose to 12V or higher, they may well break, possibly in spectacular fashion!

Also, keep in mind that with USB 3.x, power can flow in either direction as the cables now have the same USB-C connector at either end. Those earlier monitors usually also assumed power conuld only flow in one direction.

USB-C is now very widespread. We have recently switched to using USB-C sockets on practically all projects that need a USB connection. In 2024, USB-C was legislated in the European Union as the standard charging port for mobile phones and similar gadgets.

The demand for higher currents, higher voltages and the consequent higher power levels means that a USB-C Power Monitor is necessary for some scenarios. USB-PD (power delivery) is currently rated to provide up to 48V at 5A, well beyond what the older USB power monitors can tolerate or measure.

Of course, legacy USB 2.0 devices with the older USB-A and USB-B connectors can work with our new USB

Silicon Chip Short-form Kit (SC7489, ~£38 + P&P): *this kit includes all the non-optional parts listed except the case, lithium-ion cell and glue. It also includes the FFC (flat flexible cable PCB) for joining the two PCBs.*

USB-C Power Monitor, part one

Features & Specifications

- Main screen reports current, voltage, power, energy (in J or Wh) & time
- Configuration channel (CC) status screen
- All 24 USB data lines pass through
- Self-contained with 400mAh rechargeable lithium battery
- Internal battery means no extra load on the USB circuit under test
- Compact case is only 80 × 40mm
- Automatic offset trimming
- Voltage measurements: up to 60V with 10mV resolution
- Current measurements: up to ±5A with 1mA resolution; 10μA resolution below ~25mA
- Power: up to 300W with 1mW resolution (limited by V and I)
- Energy: up to 999999J (1mJ resolution) or up to 999Wh (10μWh resolution)
- Battery consumption: <20mA, giving 20 hours of usage per charge
- Sleep mode: <10μA drawn from battery, less than typical self-discharge

Power Monitor with simple adaptors. However, there is a lot more to the USB-C Power Monitor than just adding USB-C connectors to an older design!

We'll describe some of the technical features that apply to USB-C and how they have affected our design. If you want more background on USB Power Delivery technology, see our article on "How USB Power Delivery works", starting on page 4 of this issue.

Early USB was simple

The original USB 1.0 specification dates back to 1996, and uses much the same hardware and electrical arrangement as the later USB 1.1 and USB 2.0 standards.

Two conductors (V_{BUS} and GND) are provided for a nominal 5V power supply. Another two conductors (D+ and D–) providing a bi-directional differential signalling pair. A separate shield connection is also present.

These connections are carried through the original USB Power Monitor, with only the V_{BUS} line interrupted by a current measuring shunt. All these earlier specifications have been carried forward into the newer versions of the USB specifications, although many aspects are now considered 'legacy'.

The design of the plugs and sockets enforced upstream and downstream ends. Assuming the standards have been followed, this means that current can only flow one way, and thus the USB Power Monitor's simple design only needed to handle current flowing in one direction.

The supply voltage was fixed at a nominal 5V, meaning that it could directly power a 5V microcontroller without even needing a regulator. In fact, all the ICs on the original USB Power Monitor run directly from the USB 5V supply.

Given USB's broad usage as a power supply and for charging, it was also useful when no USB communication takes place. For example, you could use it to check how much current a mobile phone used while charging.

The USB-C standard

USB-C is a 2014 design that allows all USB protocols, so far up to USB4, to be transmitted. Importantly, USB-C only specifies things like the connectors and cables; it permits many other protocols aside from USB.

Some other communication technologies that can be carried over USB-C include Thunderbolt, PCIe, HDMI and DisplayPort (including digital video & audio).

The USB-C connector is symmetrical and can be inserted in two ways (no more fumbling to figure out the right way!). It can also be used at both ends of a cable, so the cable itself does not enforce an upstream or downstream end; current and data can flow either way in a USB-C cable. In fact, USB-C allows the power source or sink role to be separate from the USB host or device function.

USB-PD (USB power delivery) provides a means to negotiate voltages up to 48V and currents up to 5A. So clearly, there are many factors that need to be considered in designing a USB-C capable power monitor.

Because of all these features, a USB-C receptacle can have up to 24 conductors, plus a shield. Some of these are symmetrically arranged duplicates. For example, there are four ground pins and four V_{BUS} pins to share the current load, as shown in Fig.1. The plug is mirrored relative to the socket.

In the receptacle, there are two each of the D+ and D– legacy USB data pins. There are four more differential pairs, two in each direction. These are the same pairs that were introduced with USB 3.0, and the blue-coloured connectors that marked the new SuperSpeed transfer rate.

The four remaining conductors are for signalling related to USB-C's features. The two CC (configuration channel) lines are the channel over which USB-PD communication takes place. The aforementioned article on how USB Power Delivery works gets into the details of the power delivery protocol.

There are now chips specifically designed to handle USB-PD communications, and these are often found in the so-called 'trigger' or 'decoy' modules that can request a specific voltage

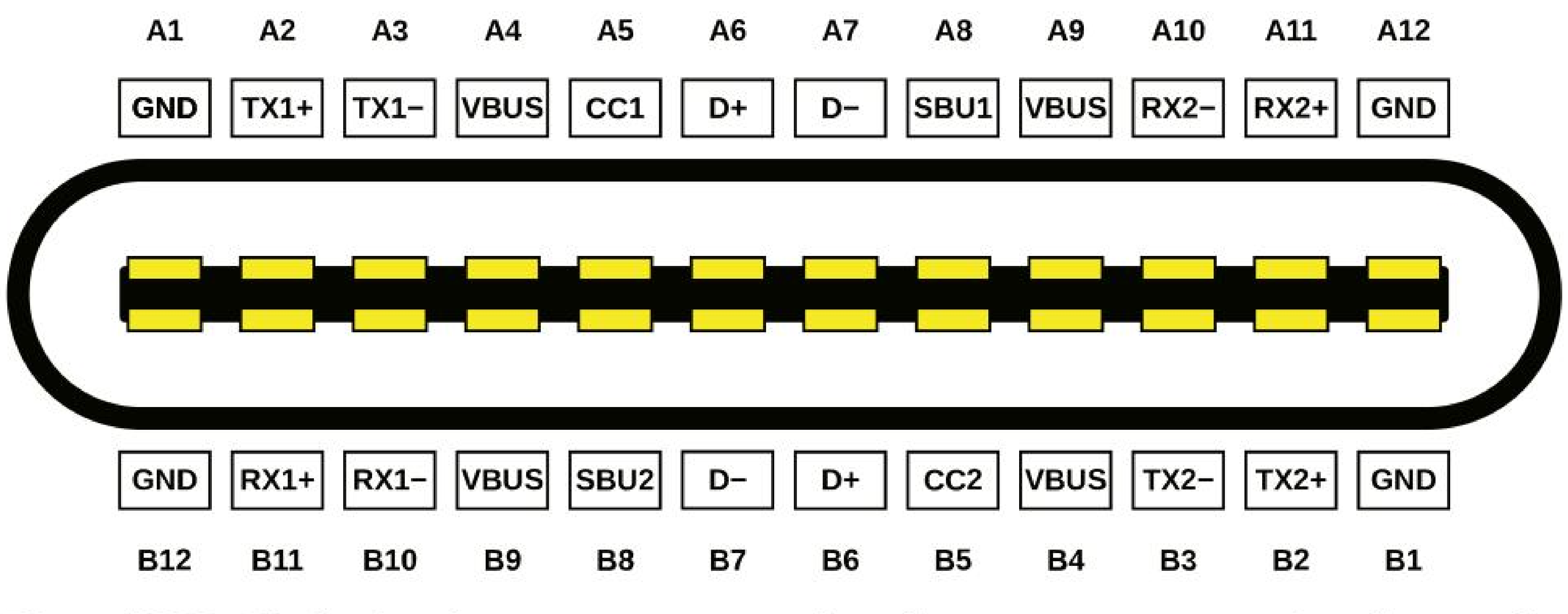

Fig.1: USB-C's design incorporates rotational symmetry, removing the need to flip the connector like earlier USB plugs/sockets. This requires extra conductors, with many being duplicated. The configuration channel lines provide cable rotation detection for correct operation.

The main PCB of the Power Monitor connects to the USB Breakout board using a flexible PCB (FFC).

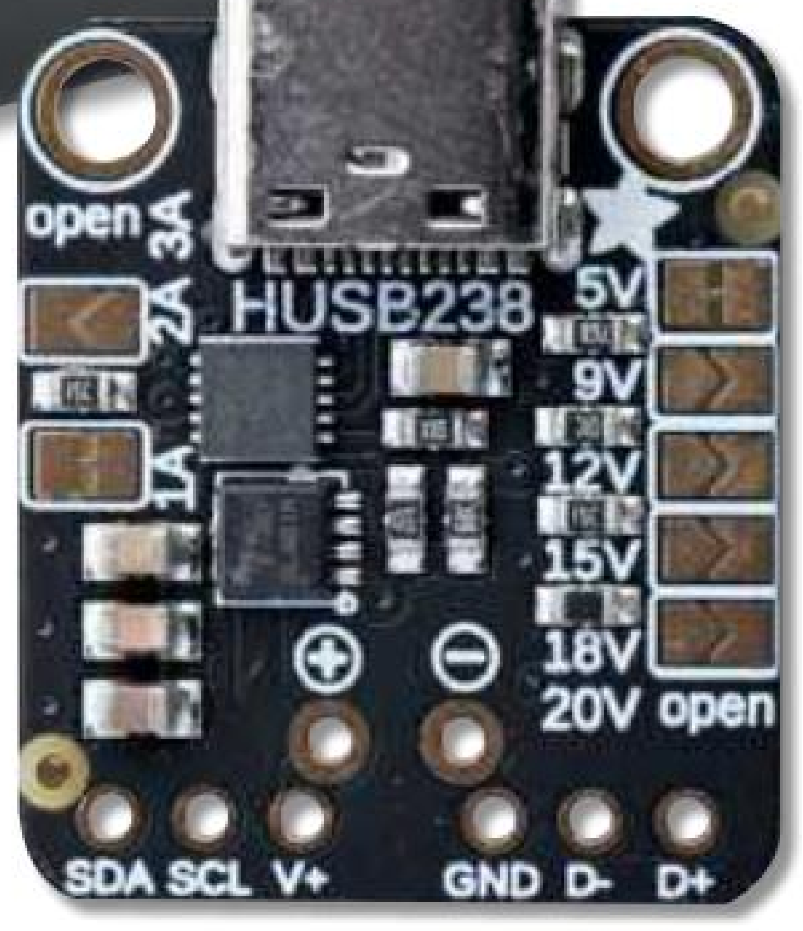

A typical USB-PD trigger board has a USB-C socket, a USB-PD interface IC and an output connector. This example sets the requested PD voltage by solder jumpers; some can be controlled digitally, with an I^2C serial interface or similar.

using USB-PD's digital signalling. The photo above shows an example of such a module.

Early versions of USB-PD supported up to six power profiles at various currents and voltages of 5V, 12V or 20V. Subsequent revisions added support for 9V, 15V, 28V, 36V and 48V. A more recent protocol, known as PPS (Programmable Power Supply), allows voltages to be requested up to 21V in 20mV steps and current limits in 50mA steps.

The simplest signalling is done via pullups and pulldowns on the CC lines with specific resistor values; this can be used to offer or request the legacy 5V supply voltage. We have used this arrangement in our projects using USB-C sockets for 5V power.

Fig.2 shows the basic arrangement using the resistor-based signalling, which is quite simple and elegant. Only one CC line is typically connected through in a cable; this allows both devices to determine the orientation of the conductors if the cable has been flipped.

The source will only apply V_{BUS} if it sees that a sink has connected with the correct pulldown resistance. The pulldown can be applied by a simple resistor to ground, so the signalling will work even on a device that has no power to begin with.

Cleverly, V_{BUS} switching can be achieved by not much more than a logic-level P-channel Mosfet. The Mosfet's gate is pulled up until a sink is connected, switching the Mosfet off. The sink's R_D resistor pulls the gate low and turns the Mosfet on, allowing the source to provide current to the sink.

The current that the source applies to the CC line also encodes a V_{BUS} current capacity, and the sink can detect this by the voltage across the R_D resistor on the CC line. This allows sink devices to limit their current draw to what the source can provide.

The second CC conductor can also supply power to the electronics embedded in an 'e-marked' cable. In this role, it is known as V_{CONN}, indicated by the resistors labelled R_A in Fig.2.

E-marking involves embedding a chip inside the cable. One use of such a chip is to indicate to the source that the cable can handle 5A. Any cable that is not identified as such is limited to 3A. The CC lines are also used to communicate other USB-C features, such as support for alternative modes.

Finally, there are the two SBU (sideband use) lines, which are used by an audio adaptor accessory mode and the USB4 protocol. It's also possible to use them for a specific custom purpose through USB-PD negotiation.

In summary, USB-C offers a lot more variety in voltages, currents and protocols than the legacy standards and connectors. So the USB-C Power Monitor has more to do than just measure the current and voltage.

We need to be able to measure voltages up to 48V and monitor currents up to 5A in either direction. There are signals, such as those on the CC lines, that we can monitor for connectivity and possibly take control of.

We considered including a USB-PD chip to allow monitoring of the power delivery communications, but ultimately decided against doing so. Most of these chips are in leadless packages (eg, QFN) that are difficult to solder.

We also thought it would be best to avoid a situation where multiple chips are trying to communicate over the same configuration channel bus, lest that lead to improper voltages being requested, potentially causing damage to equipment connected to the Monitor.

USB-C specifications

It is an unfortunate fact that the USB-C Power Monitor (or any design like it) cannot meet the USB-C specifications. As you can see from the photos, it has a USB-C socket at one end and a USB-C plug at the other. As such, it is effectively a USB-C extension cable.

Such cables are simply forbidden by

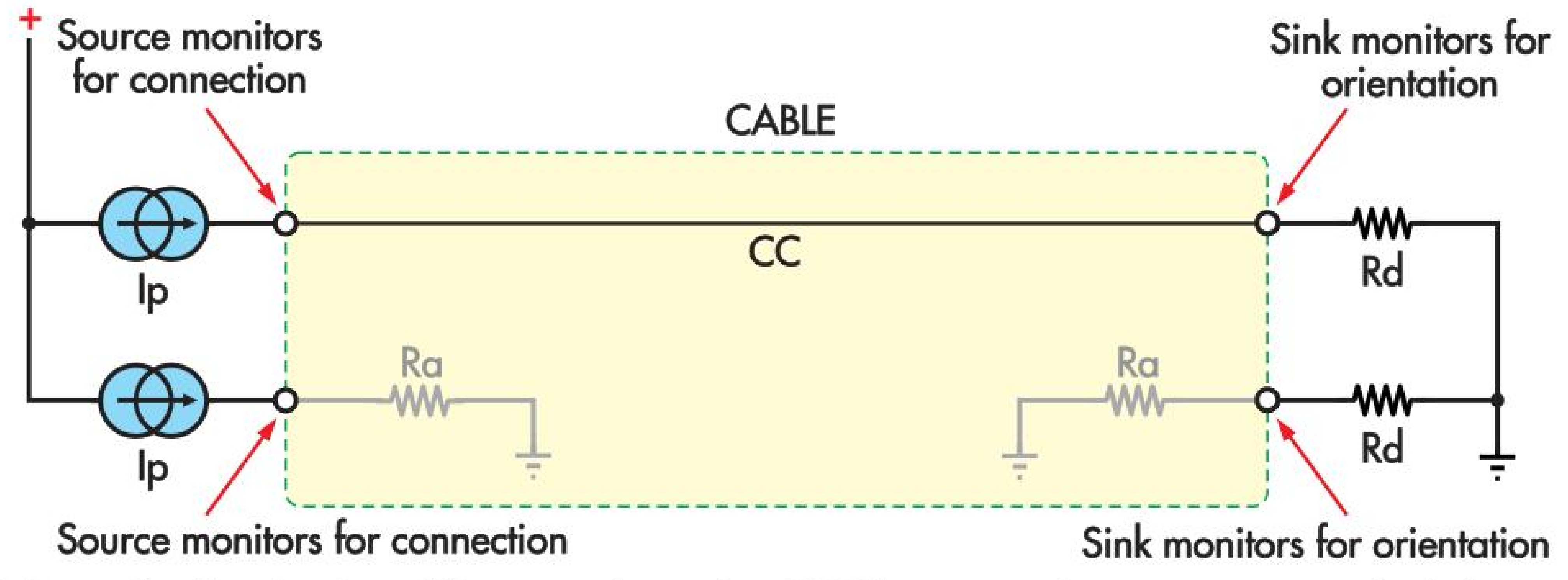
+
Source monitors for connection
CABLE
Sink monitors for orientation
CC
Ip
Rd
Ra
Ra
Ip
Rd
Source monitors for connection
Sink monitors for orientation

Fig.2: the basic signalling used on the CC lines requires sources and sinks to use specific resistor values (or current sources/sinks) to determine rotation and the current required. Before a source can apply power on V_{BUS}, it must detect that a sink is correctly connected.

Parts List – USB-C Power Monitor

1 double-sided green PCB coded 04102251, 78 × 11 × 0.8mm
1 double-sided black PCB coded 04102252, 80 × 40 × 0.8mm
1 flat flexible PCB (FFC) coded 04102253, 18 × 40mm
  OR 5cm of 7-way ribbon cable
  OR 30cm of light-duty flexible cable
1 Hammond 1551KBK 80 × 40 × 20mm enclosure
1 small lithium-ion rechargeable pouch cell with protection circuitry
1 Amphenol 12401981E412A straddle-mount 24-pin USB-C plug (CON1) **[DigiKey, Mouser]**
1 Würth 632723100011 24-pin SMT+through-hole USB-C socket (CON2) ◆ **[DigiKey, Mouser]**
1 5-pin header, 2.54mm pitch (CON3; **optional**, for ICSP)
1 USB-C SMD power-only socket (CON5) **[GCT USB4135 or equivalent]**
1 M2016/0806 size 4.7μH 1A inductor (L1) **[Murata LQM2MPN4R7NG0L]**
1 128×32 pixel 0.91-inch I^2C OLED module (MOD1)
3 Adafruit 5410 reverse-mount SMD tactile switches (S1-S3) **[DigiKey, Mouser]**
1 tube of neutral-cure silicone sealant or similar flexible adhesive
1 piece of foam-cored double-sided tape (to secure BAT1)
◆ *Würth 632723300011 is an alternative but it might be harder to solder*

Semiconductors
1 PIC16F18146-I/SO 8-bit micro programmed with 0410225A.HEX, SOIC-20 (IC1)
1 INA296A3 or INA282 current monitor, SOIC-8 (IC2)
1 AD8541A or NCS325 rail-to-rail CMOS op amp, SOT-23-5 or SC-70-5 (IC3)
1 MCP73831T-2ACI/OT Li-ion charge regulator, SOT23-5 (IC4)
1 MCP16252T-I/CH boost regulator, SOT-23-6 (REG1)
1 3mm bi-colour red/green LED (LED1)
1 BAT54C common-cathode schottky diode, SOT-23 (D1)

Capacitors *(all SMD M2012/0805 size X7R ceramic)*
5 10μF 16V
5 100nF 50V

Resistors *(all SMD M2012/0805 size ⅛W, 1% unless noted)*
2 1MΩ
1 390kΩ
1 150kΩ
1 120kΩ
1 22kΩ
3 10kΩ
6 5.1kΩ
2 1kΩ
2 220Ω
1 100Ω
1 10Ω
1 15mΩ M6331/2512 size 3W

Articles on USB technology

If you wish to delve into the technical details of USB, the following *Practical Electronics* articles may be of interest:

- USB Power Injector for External Hard Drives by John Clarke (April 2010)
- USB Port Voltage Checker by Nicholas Vinen (August 2014)
- USB Power Monitor by Nicholas Vinen (August 2016)
- USB Port Protector by Nicholas Vinen (May 2019)
- USB Power Delivery Chargers by Jim Rowe (August 2022)
- USB-PD Triggers, Decoys and Testers by Jim Rowe (September 2022)
- USB Cable Tester by Tim Blythman (November & December 2022)
- USB-C Serial Adaptor by Tim Blythman (May 2025)

the specification. Consider what would happen if a 5A e-marked cable were connected to a 3A extension cable. The signalling for the 5A cable would be passed through the 3A cable, and the source would behave as though both cables are capable of 5A when they might not be.

Extension cables also diminish the signal integrity due to the extra junctions between the plugs and sockets and the cable length. This means that the higher speed communications are more likely to be compromised.

Providing two USB-C sockets on the Monitor (effectively turning it into a cable joiner) would be possible, but would result in much the same concerns.

The specification also allows cables to omit some internal conductors, since the cable orientation sensing can deal with that scenario. Connecting two such cables with a joiner could result in some signals not being passed through at all.

We performed several speed tests with different devices through our Power Monitor, comparing the performance between having the Monitor inline or not. We did not find a device for which it made a difference. It takes some powerful gear to run the high-speed (many GHz) tests needed to validate USB 3.2 communication, and we do not have access to such test equipment.

However, by making the USB-C Power Monitor as short as practically possible, we minimise the possibility of introducing signal integrity problems. Still, we cannot guarantee they can't happen.

So, while the USB-C Power Monitor can't comply with the USB-C specifications, we have worked hard and performed some thorough testing to ensure that it works with as many devices as possible.

Circuit details

The circuit shown in Fig.3 is split over two PCBs joined by a 7-pin header (CON4) at each end. The smaller PCB (inside the dashed box) has a USB-C plug (CON1) and a USB-C socket (CON2). All the V_{BUS} and GND connections are joined at each end to simplify routing; this is actually required in the USB-C specification.

Apart from a few, all the other lines are connected straight through, forming the forbidden USB-C extension lead. The V_{BUS}, CC1 and CC2 lines each have a resistor between CON1 and CON2. The 15mΩ shunt resistor in series with V_{BUS} is for measuring the current flow.

The resistors inline with CC1 and CC2 allow us to determine the source and sink nature of whatever is connected to CON1 and CON2. The extra resistance is about the smallest we could use to reliably detect that difference, while being low enough to not affect the CC detection thresholds according to the specifications.

Typical currents in the CC lines are in the hundreds of microamps (from source current I_P to sink resistor R_D), so the drop across the 220Ω resistors is in the tens of millivolts. This is the precision of the voltage thresholds in the specifications.

When a CC line is allocated to a V_{CONN} role, it can supply 5V power at up to 200mA to electronics in an e-marked cable. Clearly, 220Ω is too high to allow 200mA to be passed successfully, although our testing didn't find any cables that had problems with this.

A typical e-marked cable will try to source V_{CONN} from both ends of the cable using diodes or similar to prevent V_{CONN} being carried through the cable. So if you run into problems, try reversing the Monitor; that should allow V_{CONN} to be sourced from the other end.

CON4 breaks out the important signals back to the main PCB for monitoring. There is a ground connection, and two wires for V_{BUS}, CC1 and CC2, fed from each side of their respective resistors. CON4's connections are arranged symmetrically so that the entire PCB can be rotated 180°.

This means that if you prefer the USB-C plug on the left and the USB-C socket on the right, you can wire the boards in this fashion during the construction phase.

Main circuit

A microcontroller is required to make measurements and drive the display to report them. We're using an 8-bit PIC16F18146 (IC1), since it has some useful internal peripherals, including a 4.096V reference, an 8-bit buffered digital-to-analog converter (DAC) and a 12-bit analog-to-digital converter (ADC).

IC1 has the usual 100nF bypass capacitor on its power and ground pins (1 and 20 respectively). A 10kΩ resistor pulls up the $\overline{\text{MCLR}}$ pin (pin 4) to allow normal operation, unless a programmer is connected at ICSP header CON3. Pins 1, 4, 18, 19 and 20 are taken to CON3 for programming and debugging.

Pins 11, 12 and 13 connect to tactile switches S1, S2 and S3. They are configured with internal pullups, and the micro detects the pin level changing to low when the switch is pressed, closing the circuit to ground. A pin-change interrupt allows the micro to be woken up from deep sleep by pressing any of the switches.

These 8-bit PICs have a good output pin drive strength and so can directly power other circuit elements, allowing them to be switched off when the Monitor needs to be in low-power sleep mode.

Pin 16 powers OLED module MOD1, a 128×32 pixel monochrome display, so it can show a few lines of text or similar. IC1's pins 14 and 15 provide a bit-banged I²C serial interface to control the OLED. IC1's pin 2 is used to provide power to IC2 and IC3, as well as to control the ENABLE pin on REG1.

With both pin 2 and pin 16 low and the microcontroller in low-power sleep, only IC1 and REG1 draw power from BAT1. The nominal 5V rail falls slightly below the cell voltage (because of the diode and resistor). The greatest current draw is the 6μA flowing through REG1's feedback divider, with IC1 and REG1 drawing less than 1μA each, for a total under 8μA.

Analog circuitry

IC2 is a current shunt monitor that amplifies the voltage across the 15mΩ current measuring shunt connected via CON4. It has a gain of 50, so its output voltage is 0.75V for every amp through the shunt.

IC2 is equipped with two reference inputs (REF1 and REF2); the output voltage is offset against the average of the voltage at these two pins. The two-pin reference feature makes it easy to set up a mid-rail reference for bidirectional current sensing, although we don't use that here.

Instead, we feed both reference pins with a voltage supplied from pin 17 of IC1. This is derived from an 8-bit DAC connected to a 4.096V internal reference. By setting the DAC, we can change the IC2 reference to be anywhere between 0V and 4.096V.

This allows us to nearly double the span available for readings. For currents in one direction, we set the reference to near (but not quite) 0V and we have almost 4V of range, allowing up to 5A to be measured. If the current reverses direction, the reference is taken near 4V, allowing similar magnitudes to be measured in the opposite direction.

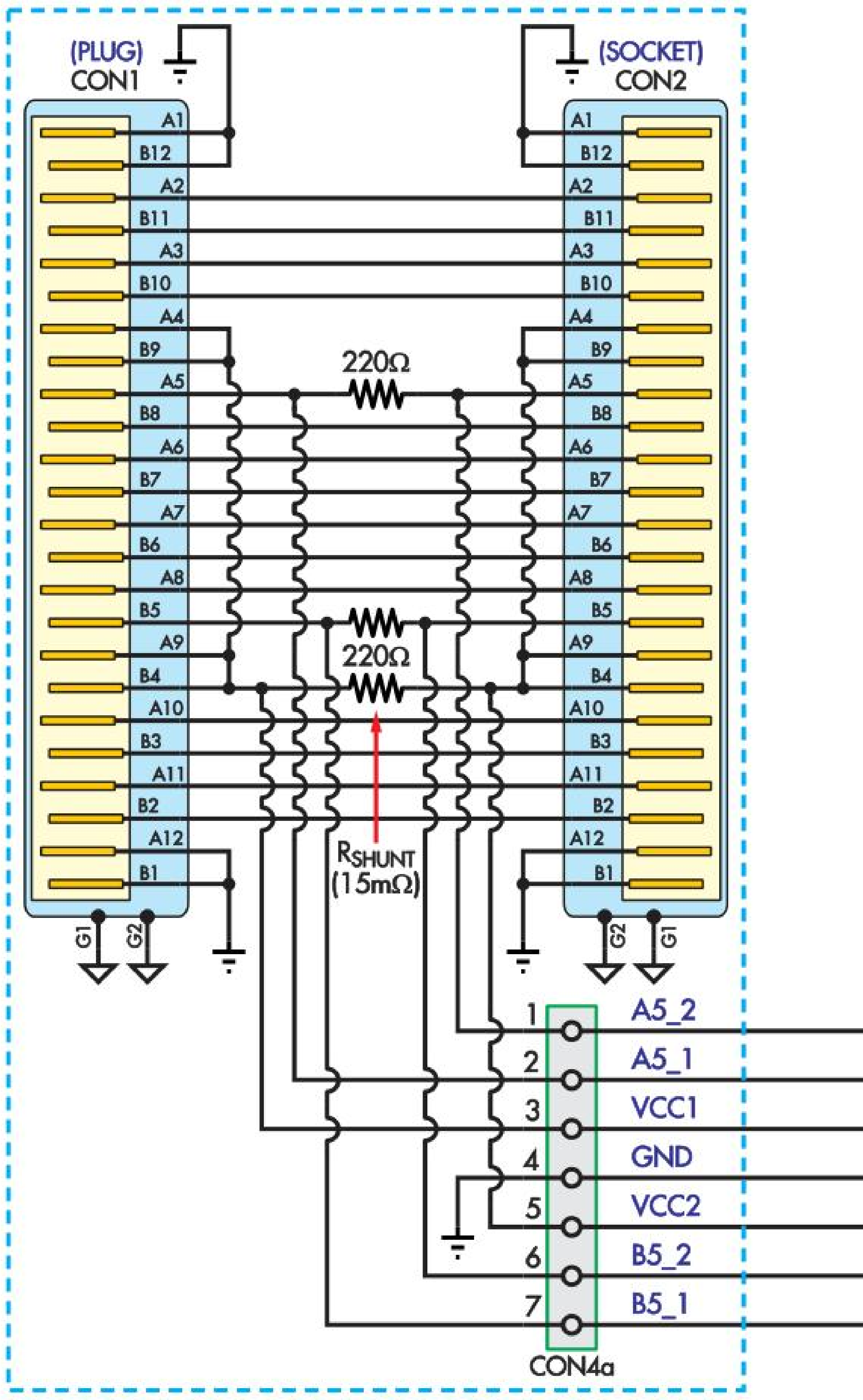

Fig.3: the circuit is split into two sections connected by CON4s; one section has a USB-C plug (CON1) and a USB receptacle (CON2), wired straight through apart from some resistors. The other section has microcontroller IC1, which measure voltages, currents and so forth and displays them on the OLED module.

IC3 is a single op amp configured to amplify the output from IC2 (relative to the same reference) by a factor of 100. The 100nF capacitor across the feedback resistor provides low-pass filtering of the amplified signal. IC1's pin 9 is used for ADC readings of the low range (amplified) voltages from IC3, while pin 3 samples the higher range voltages directly from IC2.

The ADC peripheral can perform differential readings, so the reference is simply used as the second channel for these readings. This scheme gives us more dynamic range to accurately read currents in both directions over the two ranges.

The 150kΩ/10kΩ divider connected to one of the V_{CC} pins of CON4 is used for measuring the V_{BUS} voltage. The 100nF capacitor on its lower leg provides a lower source impedance to charge up pin 10's ADC sampling capacitor. With a 4.096V reference, the divider allows up to 65V to be measured, comfortably above the 48V currently allowed by the USB-C specification.

USB-C Power Monitor, part one

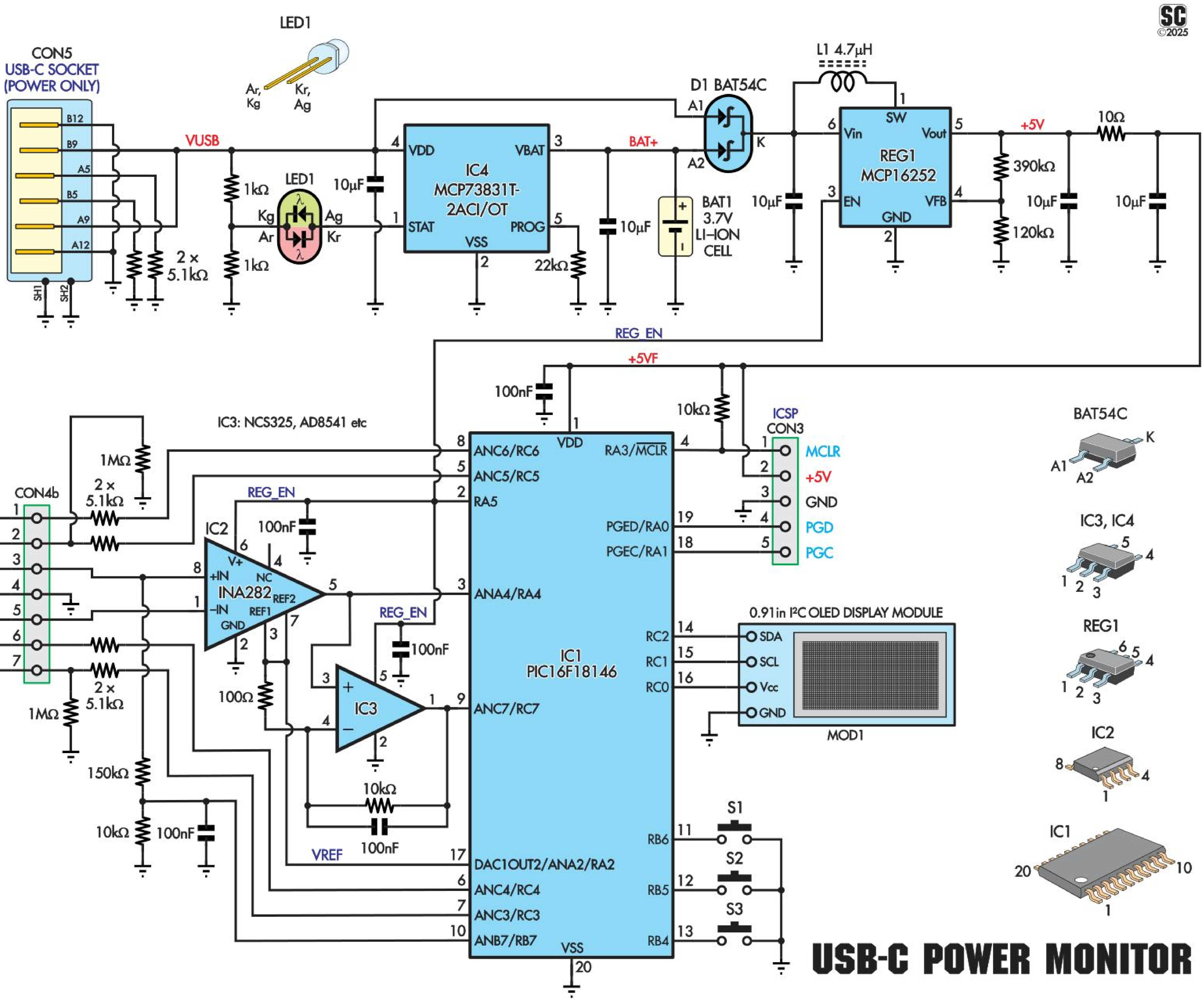
SC ©2025
CON5
USB-C SOCKET (POWER ONLY)
B12
B9
A5
B5
A9
A12
SH1
SH2
2 × 5.1kΩ
VUSB
LED1
Ar, Kg
Kr, Ag
1kΩ
1kΩ
Kg
Ar
Ag
Kr
10μF
IC4
MCP73831T-2ACI/OT
VDD
VBAT
STAT
PROG
VSS
22kΩ
BAT+
10μF
BAT1
3.7V
LI-ION CELL
D1 BAT54C
A1
A2
K
L1 4.7μH
10μF
REG1
MCP16252
SW
Vin
Vout
EN
VFB
GND
+5V
390kΩ
120kΩ
10μF
10Ω
10μF
REG_EN
+5VF
100nF
10kΩ
ICSP
CON3
MCLR
+5V
GND
PGD
PGC
IC3: NCS325, AD8541 etc
1MΩ
2 × 5.1kΩ
CON4b
IC2
INA282
V+
+IN
–IN
NC
REF2
REF1
GND
100nF
100Ω
IC3
10kΩ
100nF
VREF
150kΩ
10kΩ
100nF
IC1
PIC16F18146
VDD
ANC6/RC6
ANC5/RC5
RA5
ANA4/RA4
ANC7/RC7
DAC1OUT2/ANA2/RA2
ANC4/RC4
ANC3/RC3
ANB7/RB7
VSS
RA3/MCLR
PGED/RA0
PGEC/RA1
RC2
RC1
RC0
RB6
RB5
RB4
0.91in I²C OLED DISPLAY MODULE
SDA
SCL
Vcc
GND
MOD1
S1
S2
S3
BAT54C
IC3, IC4
REG1
IC2
IC1
USB-C POWER MONITOR

CC sensing

The remaining resistors are used to drive and sample the two CC lines. Normally, pins 5, 6, 7 and 8 are set as analog inputs to monitor the state of the CC lines. The series 5.1kΩ resistors do not noticeably affect the sensed voltage when these pins are inputs.

The state of the pins can determine what current the source can provide. By monitoring for the slight voltage difference across the 220Ω resistors, it can also determine which end is the source and which end is the sink.

The 5.1kΩ resistors also allow the USB-C Power Monitor to behave as a power sink by driving one or more of these pins to a low logic level (0V). This allows you to check the capabilities of a source, even if a sink is not connected.

It is only a very limited use of the CC signalling. But USB-C now allows scenarios which seem improbable; for example, a mobile phone attempting to charge a laptop computer. So we think the ability to identify such situations could be helpful.

Power supply

One interesting problem is that we realised a USB-C cable does not always provide power, even if it is connected to a suitable source such as a computer or power supply. Thus, we needed a way to power the USB-C Power Monitor independently.

We chose to use a lithium-ion rechargeable battery (BAT1). This has the advantage that the power supply is decoupled from the USB-C circuitry, and the USB-C Power Monitor does not load the circuit under test, apart from a voltage divider totalling 160kΩ, which draws about 31μA at 5V.

We used similar circuitry to our other recent projects that include a Li-ion cell. The most recent was the Compact OLED Clock and Timer, in the July 2025 issue.

In this case, 5V power for charging comes in via CON5, a power-only USB-C socket with the 5.1kΩ resistors necessary to identify it as a power sink. The MCP73831 charger, IC4, has a 10μF smoothing capacitor on its input pin and another on its output to the battery.

The MCP73831 monitors the charging current and voltage of BAT1 and provides a multi-stage charging regime. It has a status output and the charging current can be programmed. All in a tiny 5-pin SOT-23 package!

The charge current is set to 45mA by the 22kΩ resistor connected to IC4's pin 5 (PROG). The STAT pin drives one side of bicolour LED1; it is low during charging and is high when it finishes.

SILICON CHIP ©2024
CC CC V G V CC CC
15mΩ
R015
220Ω
220Ω

The Breakout PCB is used to provide the USB connections and will be described in more detail in next month's issue.

The arrangement of 1kΩ resistors allows the LED to light up red during charging and green when charging is complete.

Dual diode D1 is a common-cathode schottky type. Power from the battery and CON5 are connected to its anodes, so there is no load on the battery when power is available at CON5.

The remainder of the circuitry is powered from D1's cathode, and because there is no draw on the battery while charging, IC4 can charge it fully. This arrangement also means that the USB-C Power Monitor can be powered directly from CON5 even if a battery is not fitted.

The cathode of D1 is connected to MCP16252 boost regulator REG1, which also has 10μF bypass capacitors at its input (pin 6) and output (pin 5). This part has an ENABLE input at its pin 3. When this pin is low, the REG1's input is connected directly to its output, providing a low-quiescent-current mode with no voltage boost.

When ENABLE is taken high, the boost regulator operates. It has internal N-channel and P-channel Mosfets. The SW pin (pin 1) is pulled low by the N-channel Mosfet, drawing current through inductor L1. When this Mosfet switches off, the P-channel Mosfet switches on, dumping current from the inductor into the output and boosting the voltage.

Using a Mosfet as an active switch is more efficient than using a diode, since there is negligible voltage drop across the switch when it is on. The 390kΩ/120kΩ divider at the output provides feedback for the regulator and sets the output to a nominal 5.2V.

After the 10μF capacitor on REG1's output is a 10Ω resistor and a further 10μF capacitor to provide a degree of filtering for the rest of the circuit. At the circuit's nominal 20mA draw, the 10Ω resistor drops about 0.2V, leaving close to 5V.

Software

As we noted, the PIC16F18146 has a handy set of peripherals, so we'll describe those next, along with some aspects of the software operation. The capabilities of the ADC are critical to this project.

The PIC provides an internal reference that can be set to a nominal 1.024V, 2.048V or 4.096V, and can be used to set the ADC scale. The 4.096V reference is used for most of the analog readings and its measured value (in millivolts) is stored in non-volatile memory at the time of manufacture.

Being able to use the 4.096V range is the main reason for the boost converter (REG1). The 4.096V reference will not be functional if the supply is only 3.7V, as might be the case for a Li-ion cell that is nearly flat without this boosting.

The analog peripheral is actually described as an 'Analog-to-Digital Converter with Computation' (ADCC) module. It can produce a 12-bit result and can also accumulate multiple results. The accumulator has 18 bits, so the software configures it to accumulate 64 12-bit results, giving a notional 18-bit result.

Since the total ADCC error is around two bits, the lower two bits are discarded, and the software works with convenient 16-bit numbers. It takes about two milliseconds to perform the 64 samples, so the processor sets it running and uses an interrupt routine to store the readings, then commence the next sample while it continues with other tasks.

A set of 13 samples is taken in round-robin fashion; the two current readings are taken in differential mode using the pin 17 VREF voltage as the second channel. The voltages across the 220Ω resistors in the CC lines are also measured in differential mode; this allows us to note the sign and determine the direction that the current is flowing in those lines.

All these differential readings are also validated by taking corresponding single-ended (absolute) readings. For example, this allows us to detect when the low-range current reading approaches the rails, an indication that we should shift the reference (by setting the DAC) to allow more headroom or use the high-current range instead.

A second 8-bit DAC is internally connected to IC1's supply. The DAC is set to code 32, or ⅛ of the supply. The ADCC sample of this channel uses the 1.024V reference, meaning that we can accurately check that the supply voltage is high enough for the 4.096V reference to work and that the other readings are correct.

A timer peripheral is also used to provide an internal clock. This is set to count at an integer fraction of a second and make the calculations easy (for an 8-bit processor) without using computationally complex floating-point values. The time each sample set takes to complete is also recorded.

This is necessary because the most accurate ADCC results can be achieved when the ADCC is run from its own internal oscillator and completely decoupled from the micro's other internal clocks.

v
^
>
CHG
USB
PWR
SILICON CHIP
USB-C Power Monitor
3945414A_Y134_250319

The ">" button cycles through various screens, while the up/down buttons are used to adjust values and modes.

USB-C Power Monitor, part one

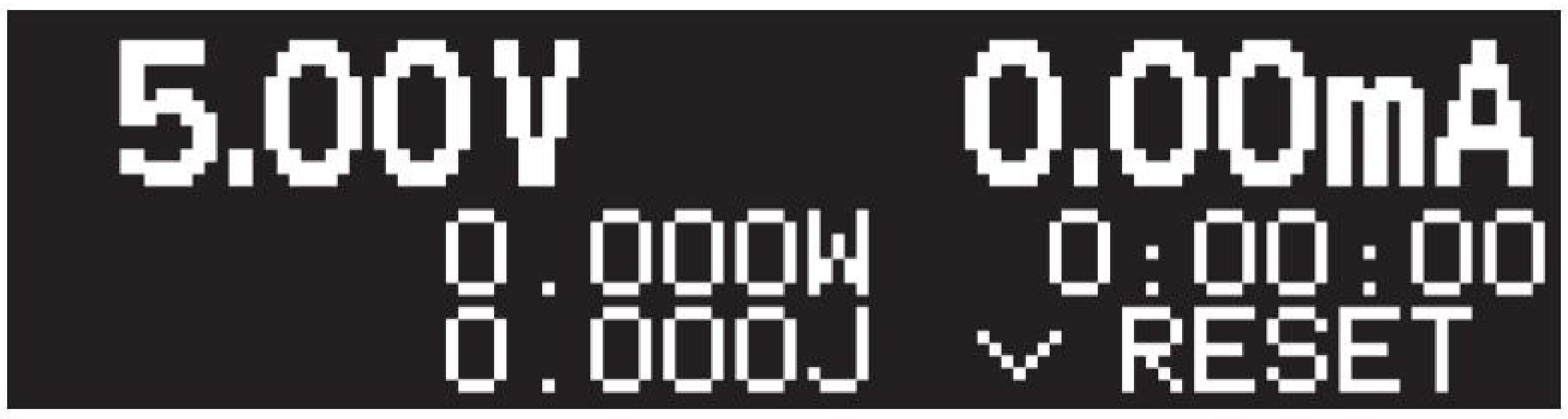

```
5.00V     0.00mA
  0.000W  0:00:00
  0.000J  ✓ RESET
```

Screen 1: the main screen reports the V_{BUS} voltage and current (including direction). Power and accumulated energy are also calculated; a timer is available too. Another screen can be used to monitor and test the condition of the configuration channel lines.

The appropriate scaling factors are applied to provide the numerical values that are needed. Derived values like power (current multiplied by voltage) and energy (power multiplied by time) are also calculated. This part of the software also sets flags indicating which of the low or high current ranges is valid and should be used.

These measurements continue to run any time the micro is active and not sleeping; the results are displayed according to the screen that the user has selected. The main screen, for example, reports the same basic statistics as the older Monitor: voltage, current (now including direction), power and total energy.

The energy totaliser is paired with a timer; both can be started, paused and reset together. The totaliser also runs in the background if other screens are selected, providing seamless operation.

Another screen allows monitoring and control of the CC lines, while a third can be used to put the Monitor into low-power sleep mode or check the battery voltage. You can also access the configuration screens by a long press of S3.

Most of the configuration is involved with trimming the calibration factors to suit the components used in a specific build, although there are also the options to adjust the screen brightness and choose between watt-hours (Wh) or Joules (J) for the units displayed for energy. We'll look more at the user interface later.

Hardware

The two PCBs fit into a compact 80 × 40 × 20mm enclosure; we used a Hammond 1551KBK, which is available from Farnell (3536439). One PCB replaces the lid, so the final unit is only 18mm high, but is slightly longer than 80mm because of the plug protruding at one end.

Both PCBs require reasonably good soldering skills to build. Fully featured USB-C plugs and sockets are only available with very tight pin spacings of around 0.5mm. When the Breakout PCB is completed, it can be tested in isolation by using it as an extension for a USB-C cable. Thus, it is possible to detect problems early in the process.

The PCB hosting CON1 and CON2 must be 0.8mm thick because the plug (CON1) is a so-called 'straddle-mount' that clips over the edge of the PCB. It sounds fussy, but the mounting style allows the part to be precisely placed before soldering begins, and we actually found it easier to work with than the socket (CON2).

The upper PCB is populated with M2012 (imperial 0805) sized passives, which are 2mm long. This is about the minimum size we consider easy to handle. There are a couple of SOIC chips and a few SOT-23 variants with three, five and six pins.

Since the top PCB is also the lid, there are a couple of unusual constructions steps. If you have built the likes of the Compact Clock and Timer (or read its article), these will be familiar.

The two PCBs must be joined with wires. Our early prototypes used pluggable headers, but we found that these had enough variation in resistance to interfere with the performance of the current-measuring shunt.

We designed a flat flexible cable (FFC) that can be soldered to the PCBs to give a simple and elegant connection. You can also use hookup wire for this, or a section of 7-way ribbon cable, if you find the FFC is too expensive or difficult to source (we'll supply the FFC with our kits – see the panel).

We had originally planned to use a 10440-sized lithium-ion cell as the battery. These are the same physical size as a AAA cell, and there is just enough room to fit a AAA cell holder to allow simple and safe connection of the cell.

However, we think that our final design, using a small, rectangular pouch cell like Altronics' Cat S4723, works better. The slim shape is a better fit for the available space, and the nominal 400mAh capacity is higher than we have seen in 10440 lithium cells. This cell measures 38 × 25 × 6mm and includes protection circuitry.

Many small pouch cells are available from various online sellers. So you might find an alternative with slightly different dimensions that still fits.

Until next month

This is a very detailed project, and we have run out of room to describe it in this issue. The second part next month will include the construction, setup, calibration and use of the USB-C Power Monitor.

ENIGMA
COMPONENT SHOP
www.enigma-shop.com

Electronic Components for the Hobbyist!

Cable & Wire • Capacitors • Connectors • Filters
Kits & Modules • Hardware & Cooling
and much more...

READY TO BE REWARDED? Join our loyalty scheme and **earn points** on every purchase you make which can be **used for discounts** in the future.

Read our reviews on Trustpilot

Teach-In 2026

by Mike Tooley

World of Wireless – An Introduction to Radio and Wireless Technology, part 12.10

Short-range RF devices

Last month, we took a deep dive into RF sources, explaining the architecture and operation of some typical low-cost phase-locked loop (PLL) and direct digital synthesis (DDS) devices.

This month, our focus shifts to short-range wireless devices (SRD). These versatile chips and modules enable data transmission and reception between remote devices without requiring a wired connection.

For good measure, our *Hands-On* constructional project features a simple RF field strength indicator that can be used for relative measurements up to 450MHz.

Short-range wireless applications

A growing number of electronic applications are now using wireless technology to transmit data from remote sensors or between distributed sites. These inexpensive wireless systems eliminate the need for physical wiring, providing fast and reliable communication between distant devices.

Establishing data connections requires only a pair of wireless transceivers placed at each end. Depending on factors that include device configuration, data rate, antenna type and transmission path, wireless systems can easily achieve working ranges of several kilometres. Fig.10.1 shows a selection of low-cost wireless modules suitable for short-range applications.

SRD devices operate with low radiated power and consequently have limited range, so they are unlikely to interfere with other radio services using the same frequency. Because of this, they're generally subject to less strict regulations compared with most radio communications equipment.

Many SRDs operate licence-free, but developers must ensure compliance with rules from national authorities like Ofcom (UK), ACMA (Australia) and the FCC (USA).

Typical applications for wireless-connected SRDs include:

- access control (including door and gate openers)
- control and regulatory systems
- cordless audio devices
- intruder and other alarms
- local area networks (LANs)
- lighting control
- medical devices and implants
- metering devices
- motion detectors
- radio-frequency identification (RFID)
- remote control systems
- telematics
- wireless microphones

Typical frequency ranges for SRD include the 'sub-GHz' bands at 433MHz, 868MHz and 917MHz, as well as the popular 2.4GHz band already used extensively for Wi-Fi and Bluetooth devices. Frequency ranges and effective radiated power (ERP) limits in the UK as well as most of Europe are:

- 433.05-434.79MHz: +10dBm
- 868-870MHz: +10dBm
- 2400-2483.5MHz: +20dBm

It's important to recognise that frequency allocations are subject to the policies established by individual national regulatory authorities. The bands listed are further subdivided and allocated to designated services, including 'non-specific' categories. Limits apply to individual applications, modes of operation, duty cycles and maximum permitted ERP.

The industrial, scientific and medical (ISM) bands, particularly at 2.4GHz, are used for purposes other than telecommunications and broadcasting. These bands permit high-power emissions that can potentially disrupt other low-power services.

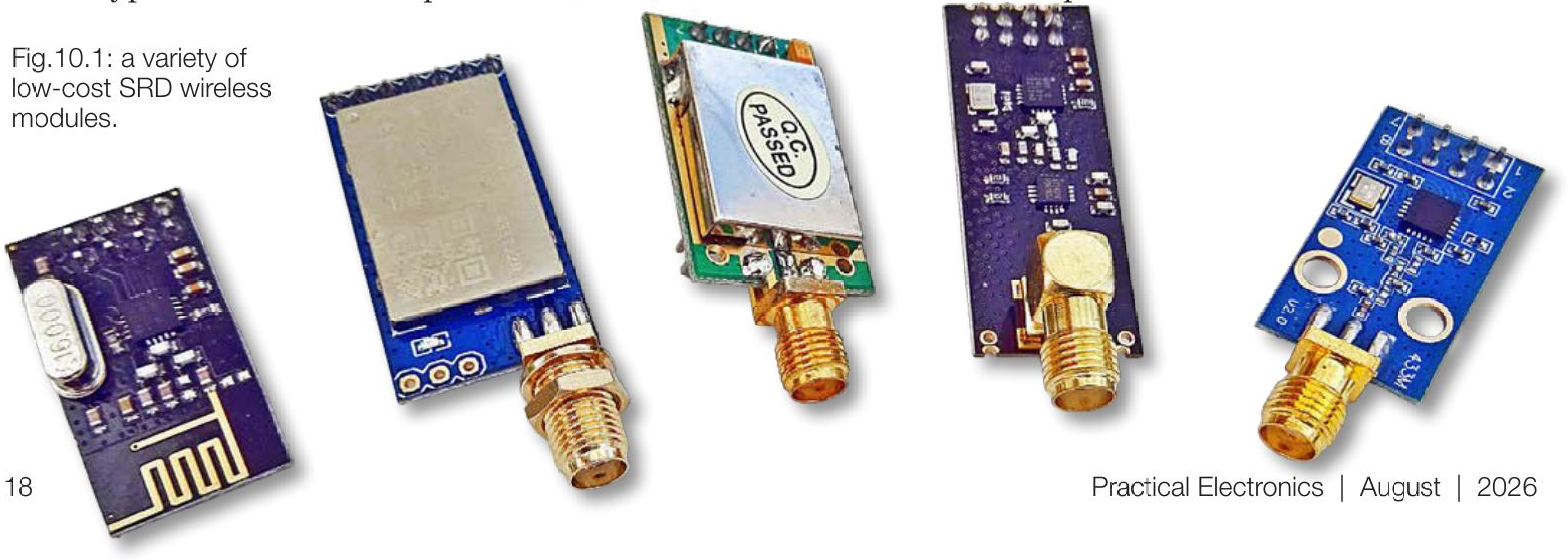

Fig.10.1: a variety of low-cost SRD wireless modules.

Table 10.1: 2.4GHz Wi-Fi channels

Channel	Frequency
1	2.412GHz
2	2.417GHz
3	2.422GHz
4	2.427GHz
5	2.432GHz
6	2.437GHz
7	2.442GHz
8	2.447GHz
9	2.452GHz
10	2.457GHz
11	2.462GHz
12	2.467GHz*
13	2.472GHz*
14	2.484GHz**

* channels 12 & 13 restricted in the USA
** channel 14 is only currently available in Japan and is the only band not 5MHz from the previous band

Such applications include RF heating and microwave ovens, so the use of the ISM bands is made conditional on users being willing to tolerate interference generated by such equipment.

The 2.4GHz frequency band

The 2.4GHz band extends from 2.400GHz to 2.4835GHz (sometimes higher) and it has become immensely popular in a wide variety of domestic and commercial short-range license-free applications. The band is used worldwide for services such as Bluetooth and limited-range wireless networks that provide local internet access. The various Wi-Fi channels are listed in Table 10.1.

While most of the world has access to channels 1-11 (2.42-2.462GHz), restrictions can apply to the use of bands 12, 13 and 14 in some countries.

The increased popularity of Wi-Fi, Bluetooth and other services has led to a significant amount of congestion and interference, especially in densely populated areas.

Many readers will already be aware of the need to find unoccupied channels when configuring their own Wi-Fi networks but despite potential interference, the licence-free 2.4GHz ISM band can be a great place to start experimenting with SRD. The technology is well understood and the hardware is cheap!

The nRF24 wireless module

The nRF24L01 from Nordic Semiconductor is a single-chip 2.4GHz transceiver that incorporates an embedded protocol engine to handle the transfer of data to/from a microcontroller. It is ideal for a wide range of low-cost, low-power wireless applications. It is designed for operation in the globally available 2.4GHz ISM band.

There are several members of the NRF24 family. The latest device (nRF24L01+) is pin-compatible with the nRF24L01 and on-air compatible with the nRF2401A, nRF2402, nRF24E1 and nRF24E2.

The nRF24L01+ offers significantly better performance than its predecessor (notably intermodulation and wideband blocking). The addition of internal filtering in the latest version of the chip has improved the margins for meeting national and international RF regulatory standards.

The simplified internal schematic of the nRF24L01 is shown in Fig.10.2. We've divided it into six functional blocks:

1. Low-power 2.4GHz RF transmitter
2. Sensitive 2.4GHz RF receiver
3. RF synthesiser, to generate the required 2.4GHz channels from a stable quartz crystal-controlled reference oscillator
4. First-in, first-out (FIFO) registers for storing transmitted and received data (which is sent serially) together with a protocol engine, general-purpose registers and a serial peripheral interface (SPI) linked via an internal data bus
5. Radio control logic for the RF section
6. Power management logic that provides several power-saving modes

The chip's SPI interface makes it easy to interface with a microcontroller. This interface provides access to the chip's internal registers so it can be configured to operate in various ways.

The RF front end uses Gaussian frequency-shift keying (GFSK). This is more efficient than conventional frequency-shift keying (FSK) and is the same method of digital modulation that's used by Bluetooth devices.

The chip's operating parameters, such as channel/frequency, output power and transmitted data rate, are all user-programmable. Its embedded baseband protocol engine is based on conventional packet communication techniques.

The nRF24L01 can be programmed for operation in 125 channels within the 2.4GHz ISM band. These channels extend from 2.400GHz to 2.525GHz with a channel spacing of 1MHz. The selected channel needs to comply with the regulations in your country.

For example, in the USA, the Federal Communications Commission (FCC) permits operation from 2.400GHz to 2.4835GHz, which is equivalent to the first 84 channels (numbers 0 to 83) for the nRF24L01. For best performance, it's important to avoid heavily used and adjacent Wi-Fi channels in your locality (see Table 10.1).

The range that can be achieved using typical low-power 2.4GHz wireless modules is usually between 10m (inside a building) up to about 100m on a line-of-sight path. With higher power output and an external

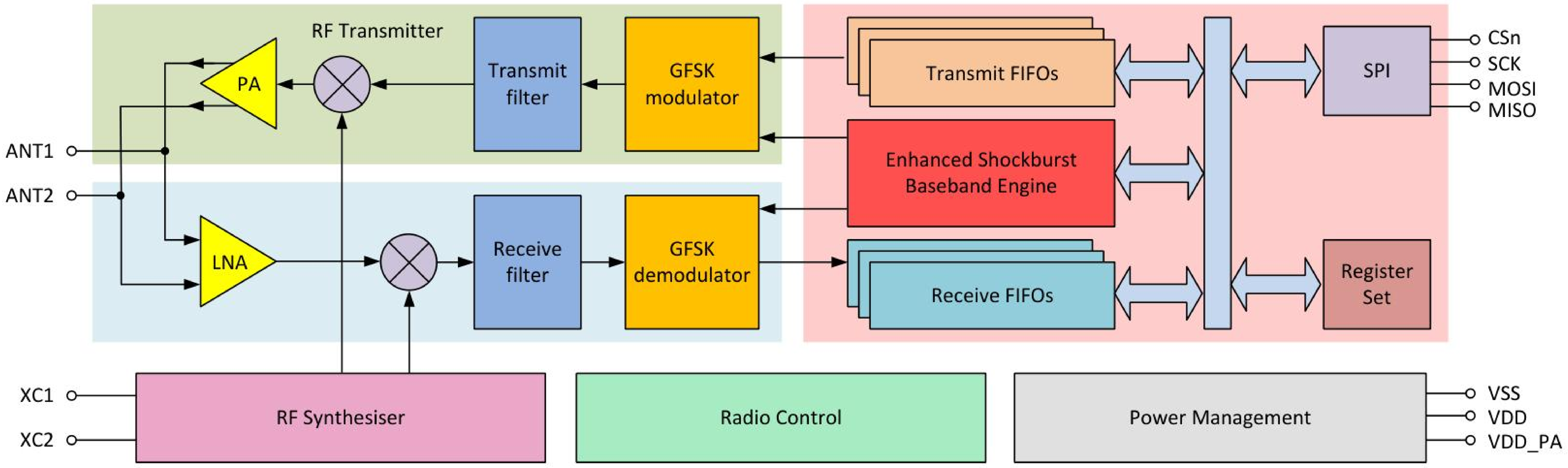

Fig.10.2: the simplified internal schematic of an nRF24L01 wireless transceiver chip.

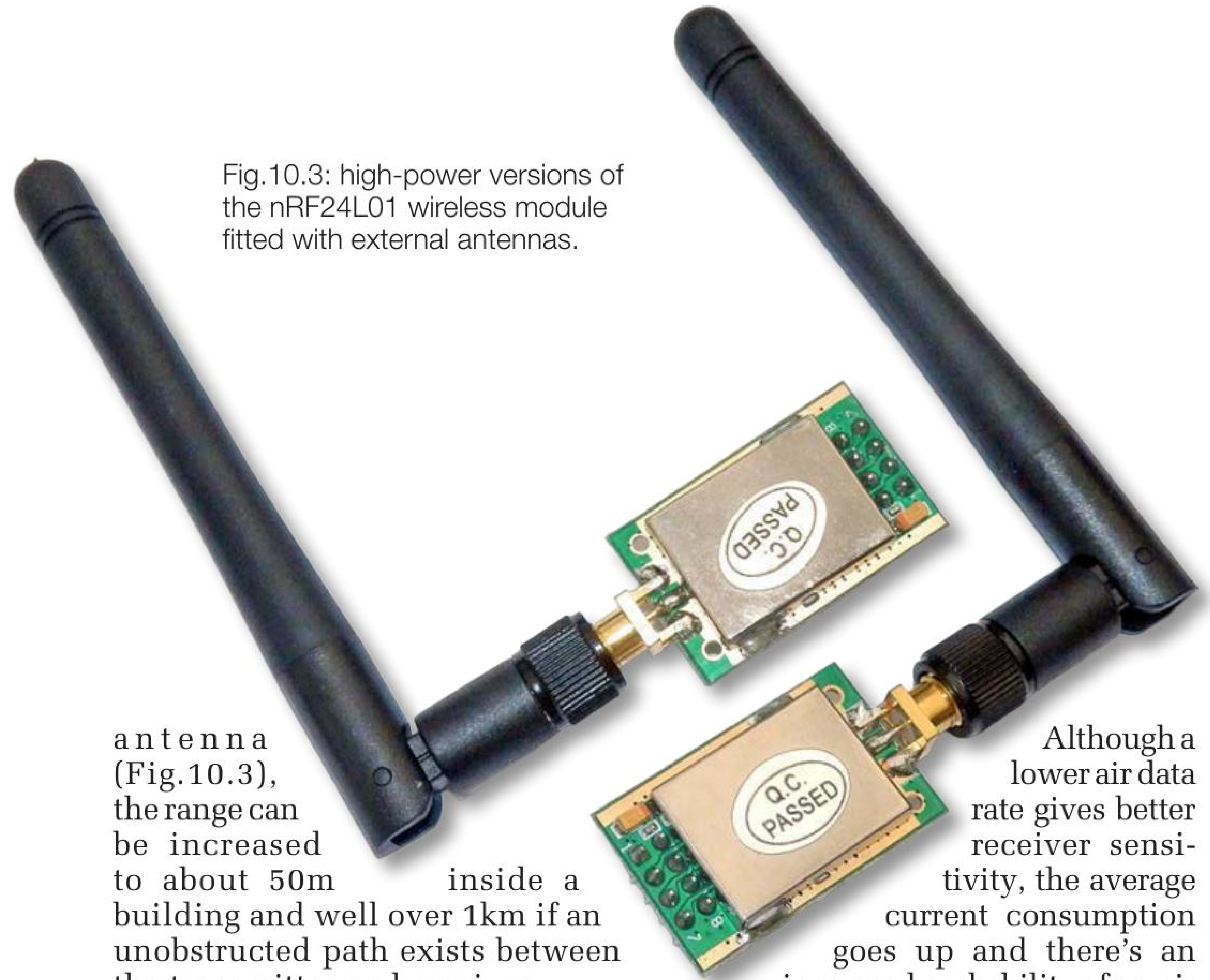

Fig.10.3: high-power versions of the nRF24L01 wireless module fitted with external antennas.

antenna (Fig.10.3), the range can be increased to about 50m inside a building and well over 1km if an unobstructed path exists between the transmitter and receiver.

The nRF24L01 transmitter output power is programmable to 0dBm, -6dBm, -12dBm or -18dBm. dBm means decibels relative to 1mW so 0dBm corresponds to 1mW, -6dBm to about 250µW, -12dBm to about 62.5mW and -18dBm to about 16mW. When the output power is configured to its maximum (0dBm), the chip needs a supply current of about 11mA; lower at reduced output levels.

The transmission data rate (sometimes referred to as the 'air data rate') is the modulated signalling rate the nRF24L01 uses when the RF front end is transmitting or receiving data. It can be 250kbps, 1Mbps or 2Mbps.

Fig.10.5: an inexpensive DHT22 temperature and humidity sensor.

Although a lower air data rate gives better receiver sensitivity, the average current consumption goes up and there's an increased probability of on-air collisions.

The channel, data rate and power can be easily set by writing values to the chip's internal registers. The transmitter and a receiver must be programmed with the same data rate and channel to be able to communicate with each other!

When implementing a data link between two microcontrollers, one needs to be configured as a server whilst the other must be configured as a client. Fig.10.4 shows how this can be done using two nRF24L01 modules and two Arduino microcontrollers.

Interfacing remote sensors

Let's look at an application that uses nRF24L01 modules to send data from a remote sensor, receiving it using another nRF24L01 wireless module. We've used compact and inexpensive Arduino Nano microcontrollers.

At the transmitter, we've included an inexpensive DHT22 temperature and humidity sensor (Fig.10.5). It uses a simple three-wire interface to the Arduino Nano. For the receiver, we've used a second nRF24L01 module and Nano with the data displayed on a host computer (this can be the same computer used for programming the two Nano microcontrollers).

The circuits for the transmitter and receiver are shown in Figs.10.6 & 10.7, respectively.

In both the transmitter and receiver, the nRF24L01 wireless modules are interfaced to their respective controllers using the Nano's serial peripheral interface (SPI). The pin connections for the nRF24L01 are shown in Fig.10.8, while the signals are listed together with their function in Table 10.2. The pin connections for an Arduino Nano are shown in Fig.10.9.

We've used the microcontroller's USB port for programming and also as the 5V power source.

Using the NRF library

An NRF24 library can be used to simplify interfacing with the wireless module. While several are available, we've used the RadioHead library from **www.airspayce.com/mikem/arduino/RadioHead/**

This library consists of two main classes: Drivers and Managers. Drivers provide low-level access to a range of different packet radio chips (and other devices designed for transporting data in packet form), while Managers provide high-level message sending and receiving facilities.

The code will have an instance of a Driver to provide access to the radio and a Manager that uses the specified driver to send and receive messages for your application. Your code needs to instantiate the Driver and Manager; it also needs to initialise the Manager. The Manager can then be used to send and receive messages.

The NRF24 libraries are easy to use. For example, to set the RF channel, you could use a statement of the form:

`nrf24.setChannel(9);`

The channel parameter should be a value between 0 and 83. Values outside this range will be outside the approved ISM band in most countries (including the UK); 66 should be the highest channel used in the USA.

To set the data rate and transmit

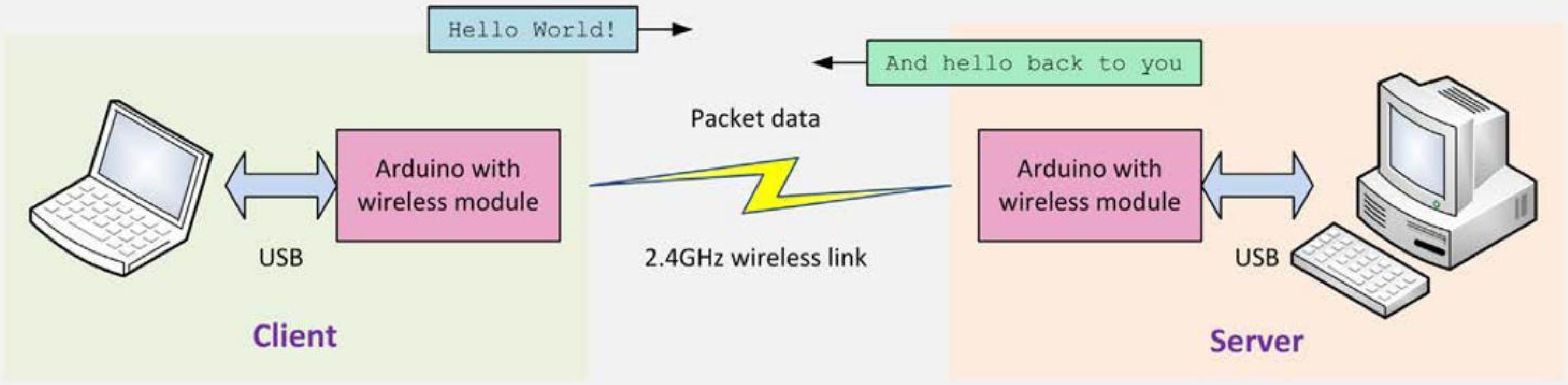

Fig.10.4: a simple wireless data link based on the nRF24L01.

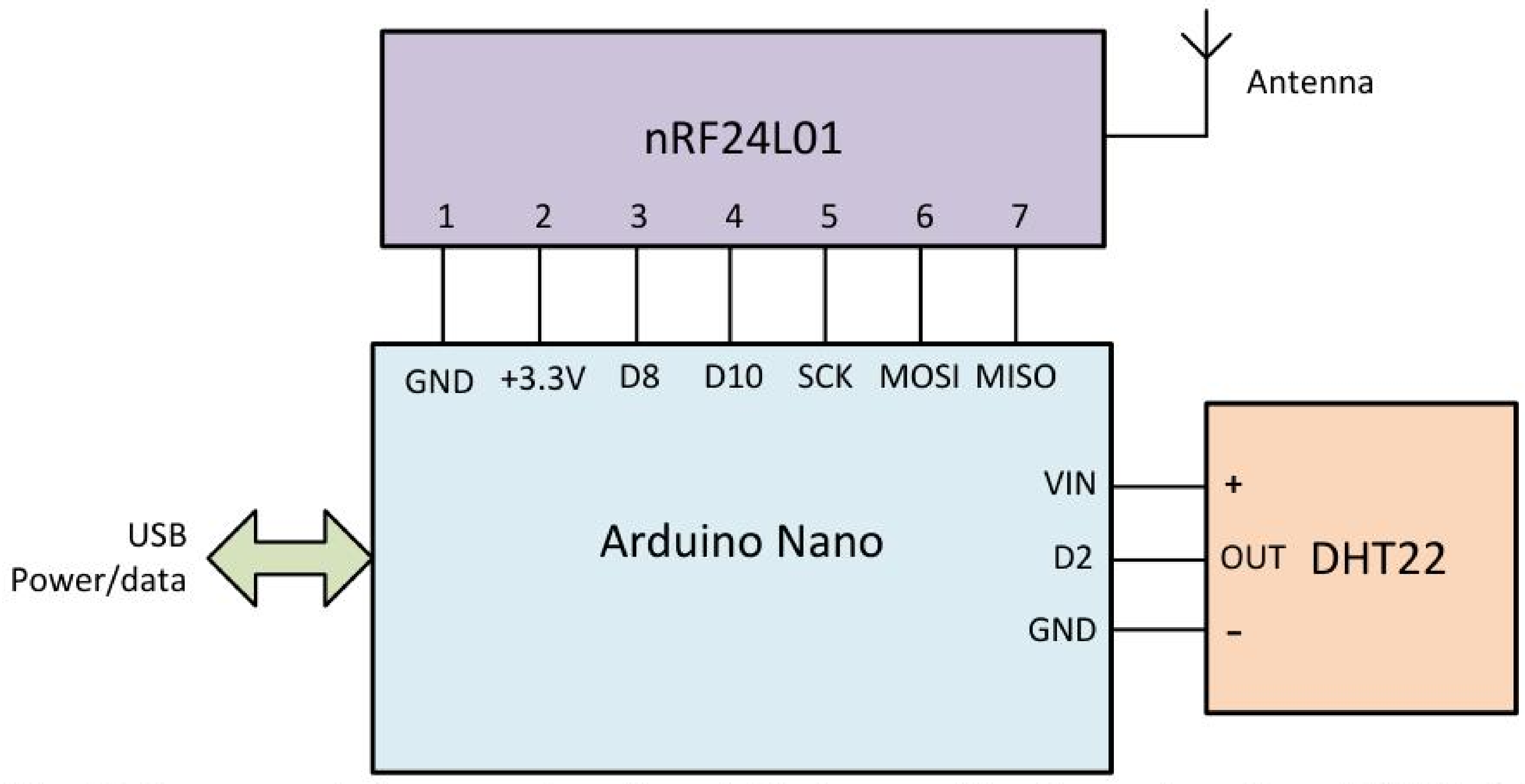
nRF24L01
Antenna
1 2 3 4 5 6 7
GND +3.3V D8 D10 SCK MOSI MISO
Arduino Nano
USB
Power/data
VIN
D2
GND
+
OUT DHT22
-

Fig.10.6: a remote temperature/humidity transmitter based on the nRF24L01.

power, you can use a statement like:

```
nrf24.setRF(
  RH_NRF24::DataRate2Mbps,
  RH_NRF24::TransmitPower0dBm);
```

There are two parameters here: one sets the data rate, while the other sets the transmission power. The data rate can take values of 2Mbps, 1Mbps and 250kbps whilst the transmit power can take values of 18mBm (-18dBm), m12dBm (-12dBm), m6dBm (-6dBm) or 0dBm.

As a further example, to set the data rate to 1Mbps and a transmit power of -6dBm, you would use:

```
nrf24.setRF(
 RH_NRF24::DataRate1Mbps,
 RH_NRF24::TransmitPowerm6dBm);
```

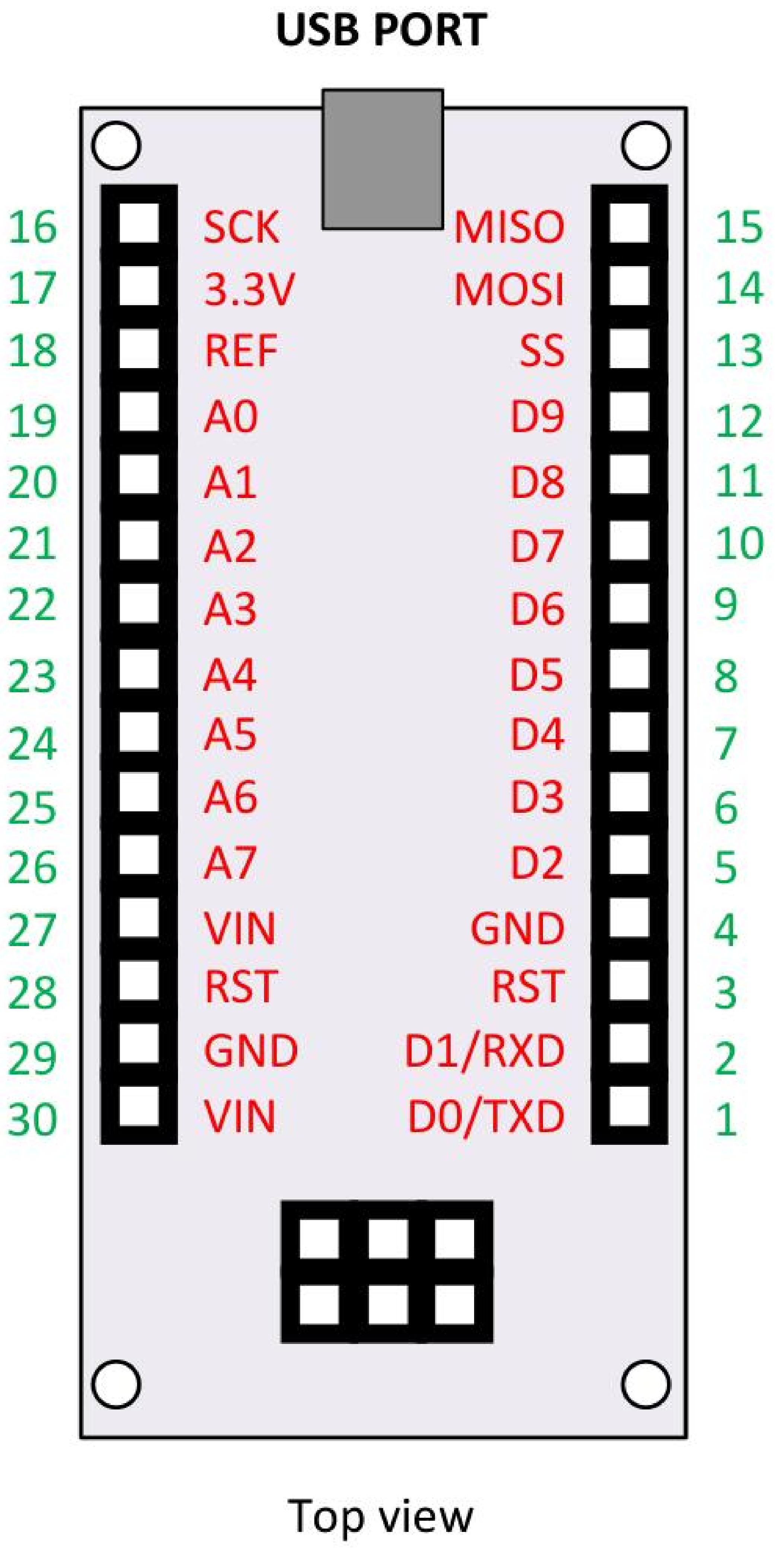
USB PORT
16 SCK MISO 15
17 3.3V MOSI 14
18 REF SS 13
19 A0 D9 12
20 A1 D8 11
21 A2 D7 10
22 A3 D6 9
23 A4 D5 8
24 A5 D4 7
25 A6 D3 6
26 A7 D2 5
27 VIN GND 4
28 RST RST 3
29 GND D1/RXD 2
30 VIN D0/TXD 1
Top view

Fig.10.9: the pinout of the Arduino Nano.

The chip can be set to transmit or receive mode using statements like:

```
nrf24.setRF(
  RH_NRF24::setModeRx());
nrf24.setRF(
  RH_NRF24::setModeTx());
```

Transmitter code

The remote temperature/humidity transmitter code is shown in Listing 10.1. This requires including four library header files: Arduino.h, DHT_Async.h, SPI.h and RH_NRF24.h.

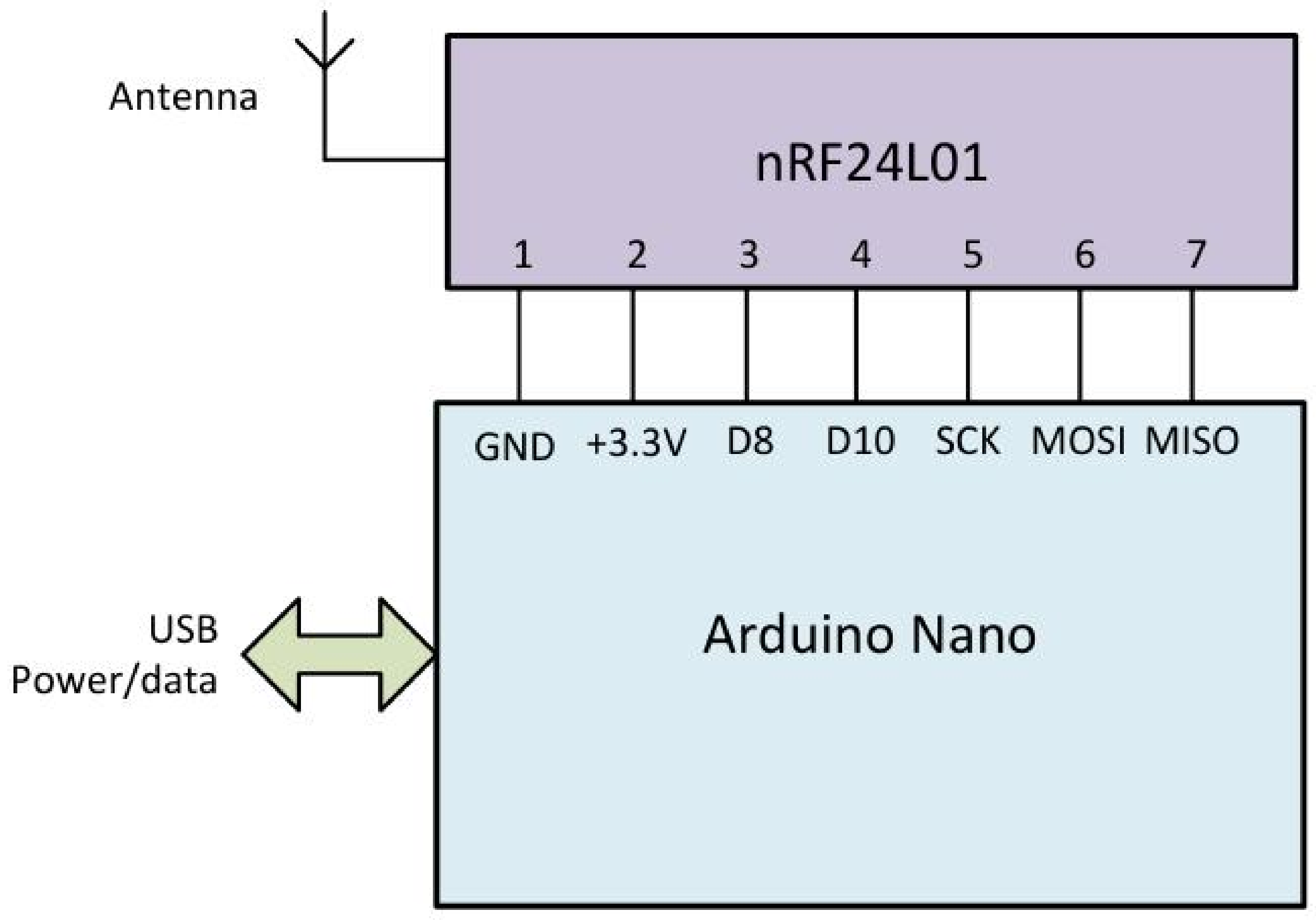
Antenna
nRF24L01
1 2 3 4 5 6 7
GND +3.3V D8 D10 SCK MOSI MISO
Arduino Nano
USB
Power/data

Fig.10.7: a receiver for the remote temperature/humidity sensor.

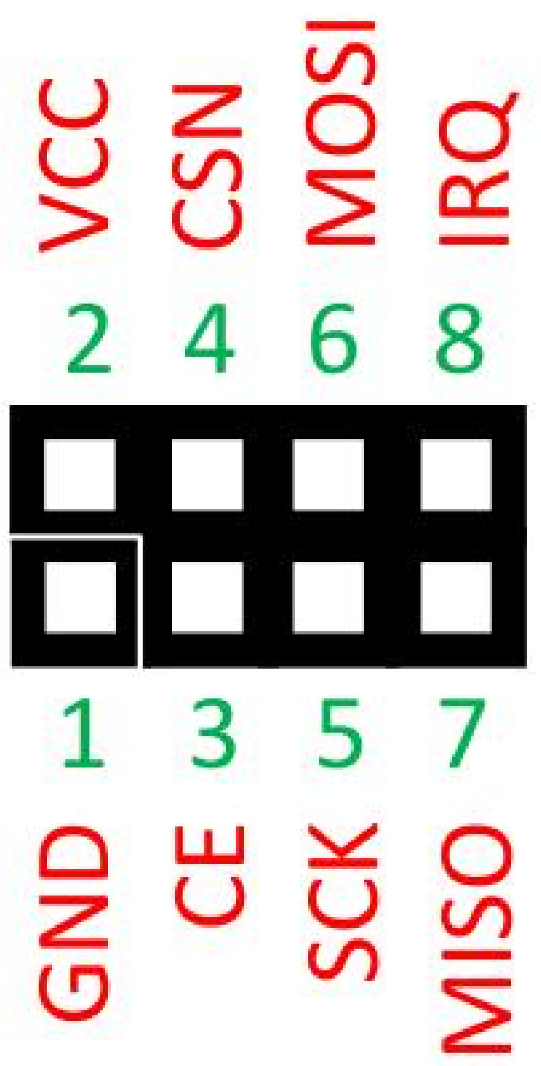
VCC
CSN
MOSI
IRQ
2 4 6 8
1 3 5 7
GND
CE
SCK
MISO

Fig.10.8: the pinout of the nRF24L01.

Listing 10.1: the code for the remote temperature/humidity transmitter. The listings and libraries in this article can be downloaded from https://pemag.au/link/acby

```
#include <Arduino.h>
#include "DHT_Async.h"
#include <SPI.h>
#include <RH_NRF24.h>

RH_NRF24 nrf24;

/* Uncomment for different sensors */
//#define DHT_SENSOR_TYPE DHT_TYPE_11
//#define DHT_SENSOR_TYPE DHT_TYPE_21
#define DHT_SENSOR_TYPE DHT_TYPE_22

static const int DHT_SENSOR_PIN = 2;
DHT_Async dht_sensor(DHT_SENSOR_PIN, DHT_SENSOR_TYPE);

/* Initialize the serial port and wireless module */
void setup() {
  nrf24.init();
  nrf24.setChannel(1);
  nrf24.setRF(RH_NRF24::DataRate2Mbps, RH_NRF24::TransmitPower0dBm);
}

/* Obtain a reading from the DHT sensor */
static bool measure_environment(float *temperature, float *humidity) {
  static unsigned long measurement_timestamp = millis();
  /* Get readings at five second intervals */
  if (millis() - measurement_timestamp > 5000ul) {
    if (dht_sensor.measure(temperature, humidity)) {
      measurement_timestamp = millis();
      return (true);
    }
  }
  return (false);
}

/* Main program loop */
void loop() {
  float temperature;
  float humidity;
  if (measure_environment(&temperature, &humidity)) {
    // Send data via the NRF24
    byte data[4];  // Four bytes of data
    data[0] = ((int(temperature) >> 8) & 0xFF);
    data[1] = (int(temperature) & 0xFF);
    data[2] = ((int(humidity) >> 8) & 0xFF);
    data[3] = (int(humidity) & 0xFF);
    nrf24.send(data, sizeof(data));
  }
}
```

Table 10.2: nRF24L01 signals

Pin	Signal	Function
1	GND	0V common
2	VCC	+3.3V supply
3	CE	Active-high chip enable
4	CSN	Active-low chip select
5	SCK	Serial clock
6	MOSI	Serial data to the module
7	MISO	Serial data from the module
8	IRQ	Interrupt request (not used here)

```
#include <Arduino.h>
#include <SPI.h>
#include <RH_NRF24.h>

int tempdataReceived;  // Temperature data received
int humidataReceived;  // Humidity data received

RH_NRF24 nrf24;

static const int DHT_SENSOR_PIN = 2;

/* Initialize the serial port and radio */
void setup() {
  Serial.begin(115200);
  nrf24.init();
  nrf24.setChannel(1);
  nrf24.setRF(RH_NRF24::DataRate2Mbps, RH_NRF24::TransmitPower0dBm);
}

/* Main program loop */
void loop() {
  byte buf[RH_NRF24_MAX_MESSAGE_LEN];
  byte len = sizeof(buf);
  if (nrf24.waitAvailableTimeout(500)) {
    Serial.println("Checking for received data ...");
    // Check for message data
    if (nrf24.recv(buf, &len)) {
      tempdataReceived = (buf[0] << 0) + buf[1];
      humidataReceived = (buf[2] << 0) + buf[3];
    }

    delay(400);
    Serial.print("Temperature = ");
    Serial.print(tempdataReceived, 1);
    Serial.println(" deg. C");
    Serial.print("Humidity = ");
    Serial.print(humidataReceived, 1);
    Serial.println("%");
  }
}
```

Listing 10.2: the code for the temperature/humidity receiver.

These library files can be downloaded and installed in the usual way; if you experience problems, a web search for the named file will usually help.

We've used a DHT22 sensor for this application (and the wireless frost alarm that follows) because it has an extended low-temperature range. If desired, alternative DHT-series temperature sensors can be selected by simply uncommenting the corresponding code.

The nRF24L01 is initialised using just three lines of code. We've selected channel 1, a data rate of 2Mbps and a transmission power of 0dBm (1mW). Readings of temperature and humidity are taken at intervals of five seconds (5000ms) and two float variables are used to store the temperature and humidity data.

The data is sent over the wireless link as a packet of four bytes (two bytes for the temperature data and two bytes for the humidity data). The code has been liberally commented and is given here as a basis for further experimentation.

Receiver code

The code for the remote temperature/humidity receiver is shown in Listing 10.2. This requires three library headers: Arduino.h, SPI.h and RH_NRF24.h (DHT_Async.h is not needed). The nRF24L01 must be initialised with the same parameters used for the transmitter. If you make any changes to the RH_NRF24 parameters in the transmitter code, make identical changes in the receiver code.

The receiver waits for data from the transmitter (arriving every five seconds) before sending it via the Nano's serial interface for display using the Arduino IDE running on the host computer. The temperature and humidity data received (tempdataReceived and humidataReceived) are both defined as integers.

Testing

The receiver and transmitter should work well at distances of up to about 15m with an unobstructed path. In a building, coverage will be reduced by factors like walls, wiring and interference from other 2.4GHz devices. The antenna type and positioning can be crucial for good performance, so it's worth experimenting with the orientation and position.

Received signals may suffer from multiple reflections, with direct and reflected waves arriving simultaneously at the receiver via different paths. It's therefore extremely difficult to predict the performance of low-power wireless systems; some on-site experimentation will invariably be required to yield the best results.

A wireless frost alarm system

Having demonstrated a simple communication system using wireless modules, we shall move on to describe a simple stand-alone application in which wireless is used to implement a remote frost alarm. We shall use the same transmitter arrangement as before, but here the sensor must be a DHT22 to work properly below 0°C.

The receiver arrangement incorporates three LEDs to indicate the sensed temperature ranges, together with a piezoelectric sounder to provide an audible frost warning. The receiver circuit diagram is shown in Fig.10.10.

The code for the wireless frost alarm receiver is in Listing 10.3. Once again, we need to include three library headers: Arduino.h, SPI.h and RH_NRF24.h. In this application, we are only concerned with temperature data, so we have only declared the tempdataReceived variable. Next, we have defined constants for the upper and lower temperature thresholds, ut and lt respectively.

In Listing 10.3, we've set these to 5°C (above which the green LED will light) and 2°C (below which the red LED will be illuminated and the alarm will sound). Between the two thresholds, the amber LED is illuminated.

For testing purposes, you might like to replace the values shown in Listing 10.3 with values closer to those found in your environment (we used 25 for ut and 23 for lt, corresponding to 25°C and 23°C, respectively).

The sub-GHz bands

Frequencies below 1GHz offer superior performance at reduced power levels and are generally less congested than the 2.4GHz band, where Wi-Fi and Bluetooth links proliferate.

Therefore there has been an increasing interest in modules that use the sub-GHz ISM/SRD bands at 315MHz, 433MHz, 868MHz and 915MHz. As not all of these may be legally used in your country, it's essential to check with your national regulator.

The proliferation of devices available from global online sources and 'grey imports' makes it essential to check specifications before purchase, particularly to ensure the frequency coverage is correct for your location.

The CC1101 from Texas Instruments is a good example of a low-cost sub-GHz wireless transceiver. It is primarily intended for use within the ISM and SRD frequency bands at 315MHz, 433MHz, 868MHz and 915MHz, but it can also be programmed for operation within several additional frequency ranges, including 300-348MHz, 387-464MHz and 779-928MHz.

The transceiver incorporates a configurable baseband modem supporting various modulation formats at data rates up to 600kbps. The chip incorporates packet management, data buffering, burst transmission, clear channel assessment, link quality indication and wake-on-radio functions. Like the nRF24L01, it has a conventional SPI microcontroller interface (see Fig.10.11).

Its receiving sensitivity is -116dBm at 0.6kbaud when operating at 433MHz and -112dBm at 1.2kbaud for 868MHz operation. Current consumption is typically less than 15mA, varying with the selected transmission power level. The maximum transmission power is +12dBm, while the maximum data rate is 600kbps.

Its normal working range is similar to that which can be achieved with similar devices in the 2.4GHz band operating at higher power levels. Distances of 10-100m are typical with lower data rates, but over 1km can be achieved with suitable antennas and a clear, line-of-sight path.

Where extended range is essential, for long-range (LoRa) applications,

Listing 10.3: the NRF24 wireless frost alarm code.

```
#include <Arduino.h>
#include <SPI.h>
#include <RH_NRF24.h>

int tempdataReceived;  // Temperature data received
int ut = 5;           // upper threshold
int lt = 2;           // lower threshold
int green = 2;         // Green LED
int amber = 3;         // Amber LED
int red = 4;           // Red LED
int alarm = 5;         // Sounder

RH_NRF24 nrf24;

static const int DHT_SENSOR_PIN = 2;

/* Initialize the serial port, radio and I/O */
void setup() {
  Serial.begin(115200);
  nrf24.init();
  nrf24.setChannel(1);
  nrf24.setRF(RH_NRF24::DataRate2Mbps, RH_NRF24::TransmitPower0dBm);
  // Setup digital outputs
  pinMode(green, OUTPUT);
  pinMode(amber, OUTPUT);
  pinMode(red, OUTPUT);
  pinMode(alarm, OUTPUT);
}

/* Main program loop */
void loop() {
  byte buf[RH_NRF24_MAX_MESSAGE_LEN];
  byte len = sizeof(buf);
  if (nrf24.waitAvailableTimeout(500)) {
    Serial.println("Checking for received data ...");
    // Check for message data
    if (nrf24.recv(buf, &len)) {
      tempdataReceived = (buf[0] << 0) + buf[1];
    }

    delay(400);
    Serial.print("Temperature = ");
    Serial.print(tempdataReceived, 1);
    Serial.println(" deg. C");

    if (tempdataReceived > ut)  // Green ON
    {
      digitalWrite(green, HIGH);
      digitalWrite(amber, LOW);
      digitalWrite(red, LOW);
      digitalWrite(alarm, LOW);
    } else if (tempdataReceived <= lt)  // Red and alarm ON
    {
      digitalWrite(green, LOW);
      digitalWrite(amber, LOW);
      digitalWrite(red, HIGH);
      digitalWrite(alarm, HIGH);
    } else  // Amber ON
    {
      digitalWrite(green, LOW);
      digitalWrite(amber, HIGH);
      digitalWrite(red, LOW);
      digitalWrite(alarm, LOW);
    }
  }
}
```

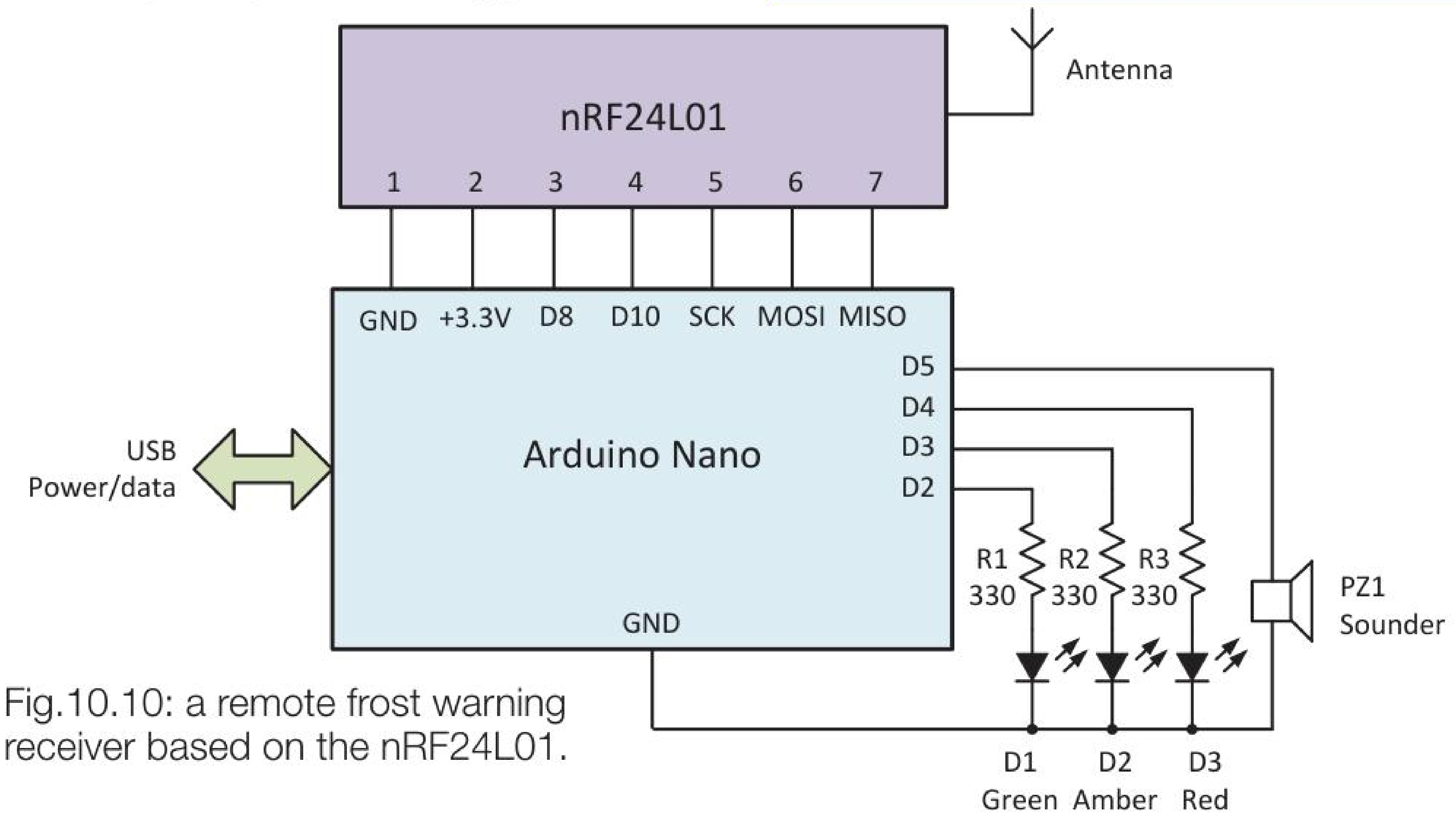

Fig.10.10: a remote frost warning receiver based on the nRF24L01.

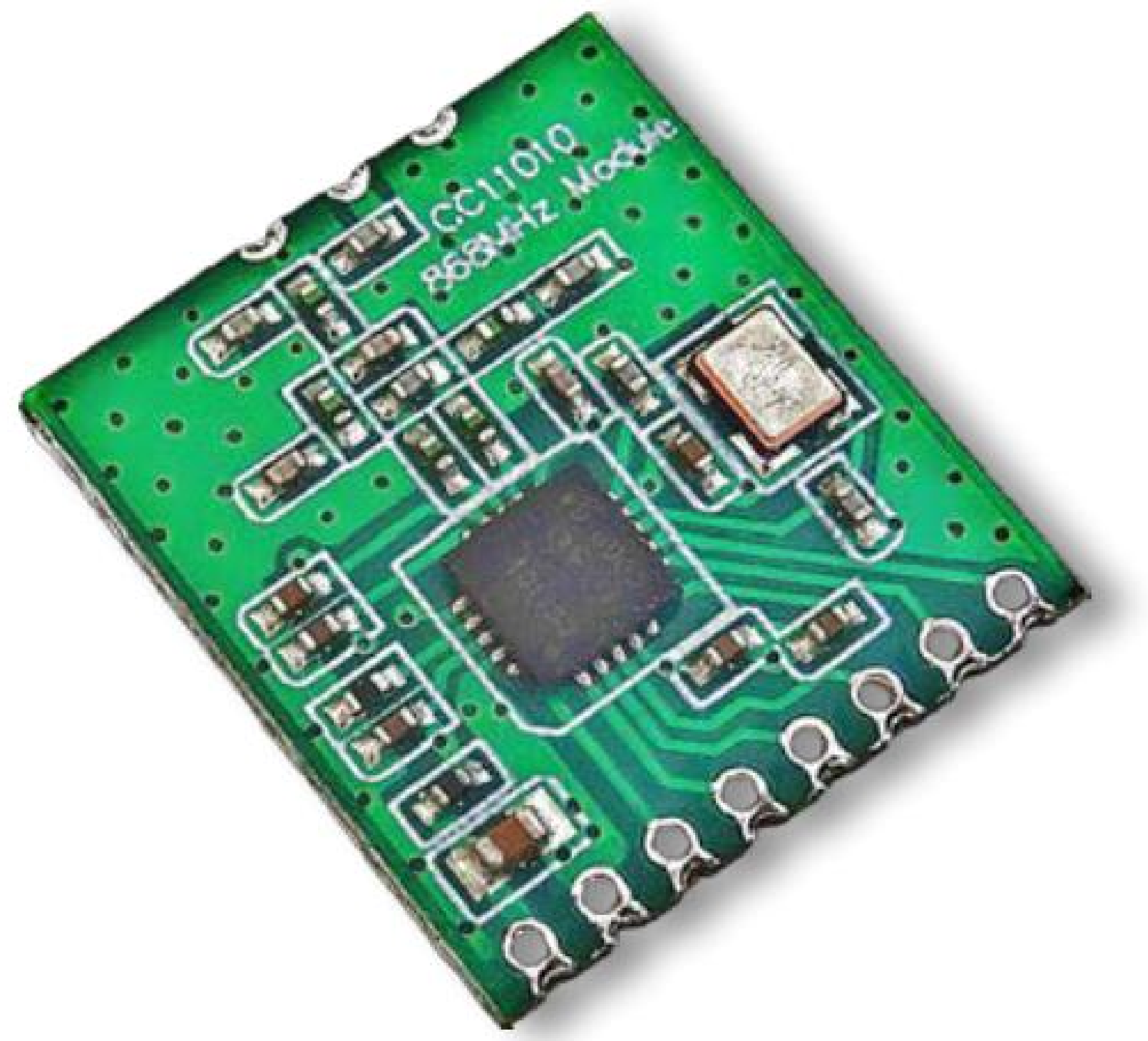

Fig.10.11: a tiny (17 × 19mm) CC1101 module designed for use at 868MHz.

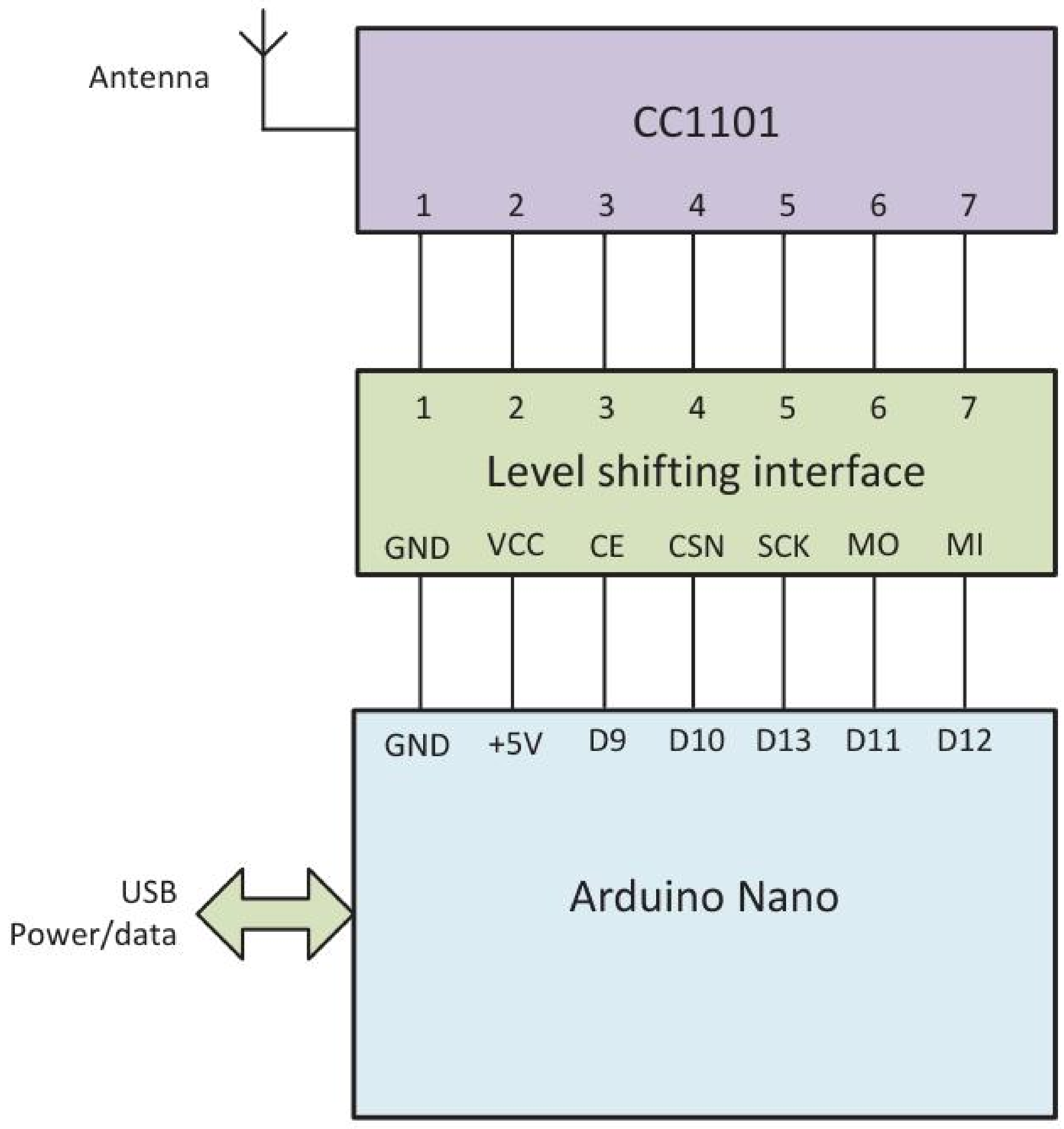
Antenna
CC1101
1 2 3 4 5 6 7
1 2 3 4 5 6 7
Level shifting interface
GND VCC CE CSN SCK MO MI
GND +5V D9 D10 D13 D11 D12
USB
Power/data
Arduino Nano

Fig.10.12: the 433MHz multi-mode beacon circuit.

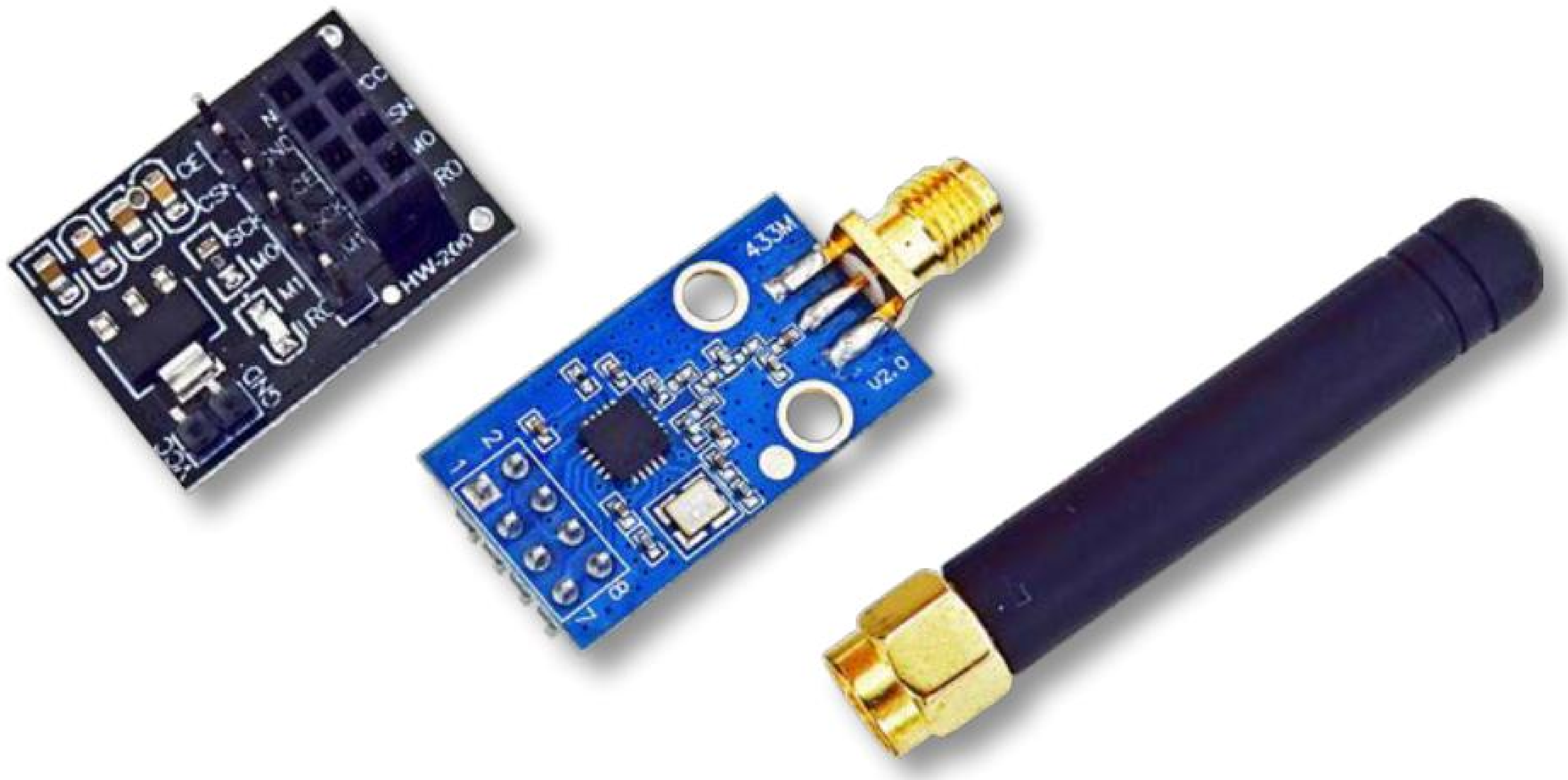

Fig.10.13: the wireless components for the 433MHz multi-mode beacon. From left to right, a low-cost interface board, 433MHz CC1101 wireless module and SMA antenna.

the chip can be paired with its CC1109 matching range extender. This add-on provides up to +20dBm output at 868MHz and up to +27dBm at 915MHz. This also improves the receiving sensitivity by about 6dB.

An interesting feature of the CC1101 is that it caters for several different forms of modulation, including two- and four-level frequency-shift keying (2-FSK and 4-FSK), Gaussian frequency-shift keying (GFSK) and minimum frequency-shift keying (MSK).

GFSK is an extension of the FSK modulation scheme where the frequency of the modulated signal doesn't change instantaneously at the start of each change of data bit. Abrupt changes in frequency are thus avoided. Consequently, the transition from one logic state to another becomes smoother.

In MSK, the frequency difference between logical 0 and 1 is minimised to half the data rate, resulting in a spectrally efficient constant-envelope waveform. The CC11010 also offers amplitude-shift keying (ASK), which is the same as on/off keying (OOK) when a binary signal is applied.

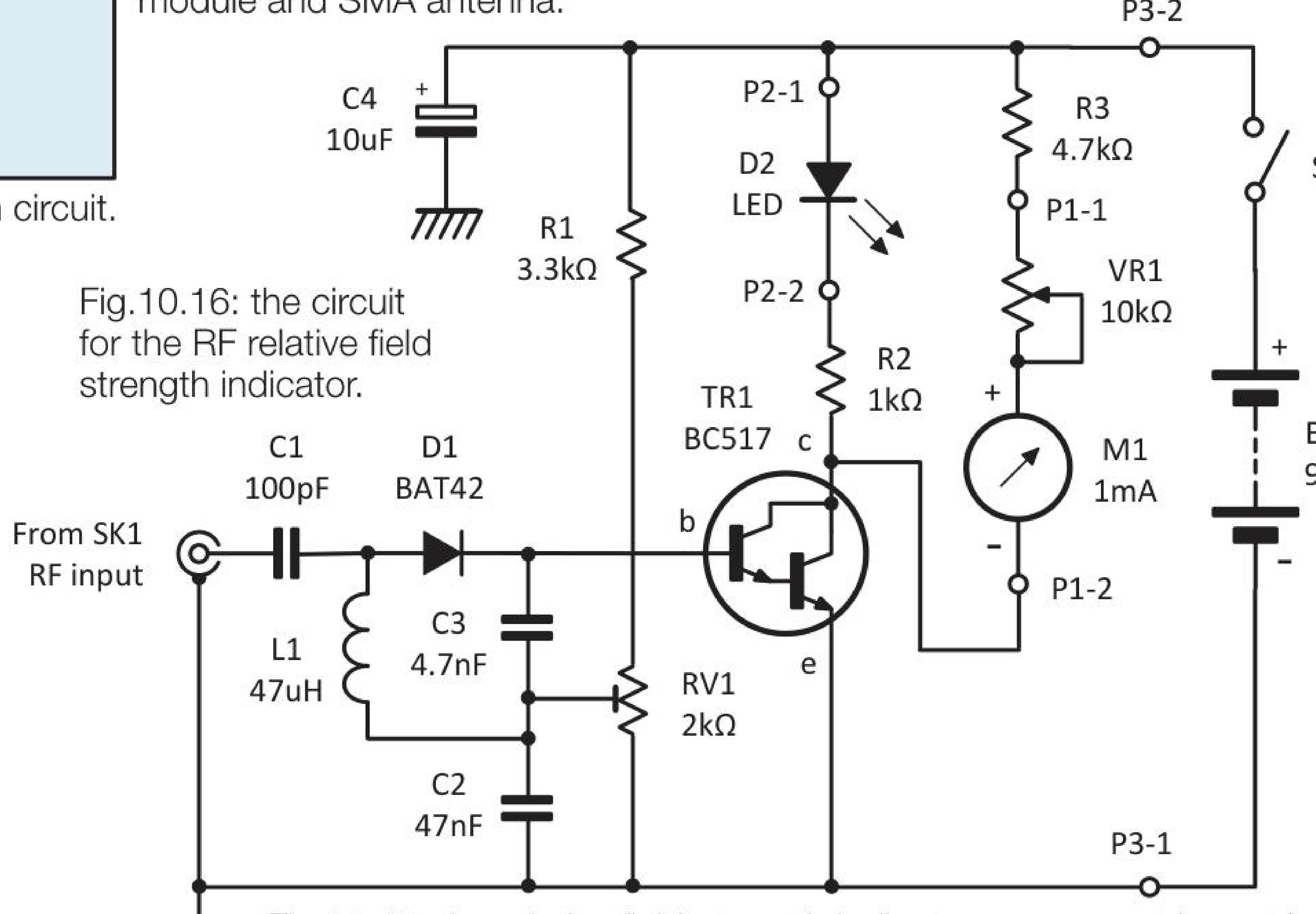
P3-2
C4
10uF
+
P2-1
R3
4.7kΩ
S1
D2
LED
P1-1
R1
3.3kΩ
P2-2
VR1
10kΩ
+
R2
1kΩ
+
TR1
BC517
c
M1
1mA
B1
9V
-
C1
100pF
D1
BAT42
From SK1
RF input
b
L1
47uH
C3
4.7nF
-
P1-2
e
RV1
2kΩ
C2
47nF
P3-1

Fig.10.16: the circuit for the RF relative field strength indicator.

Fig.10.17: the relative field strength indicator component layout (top).

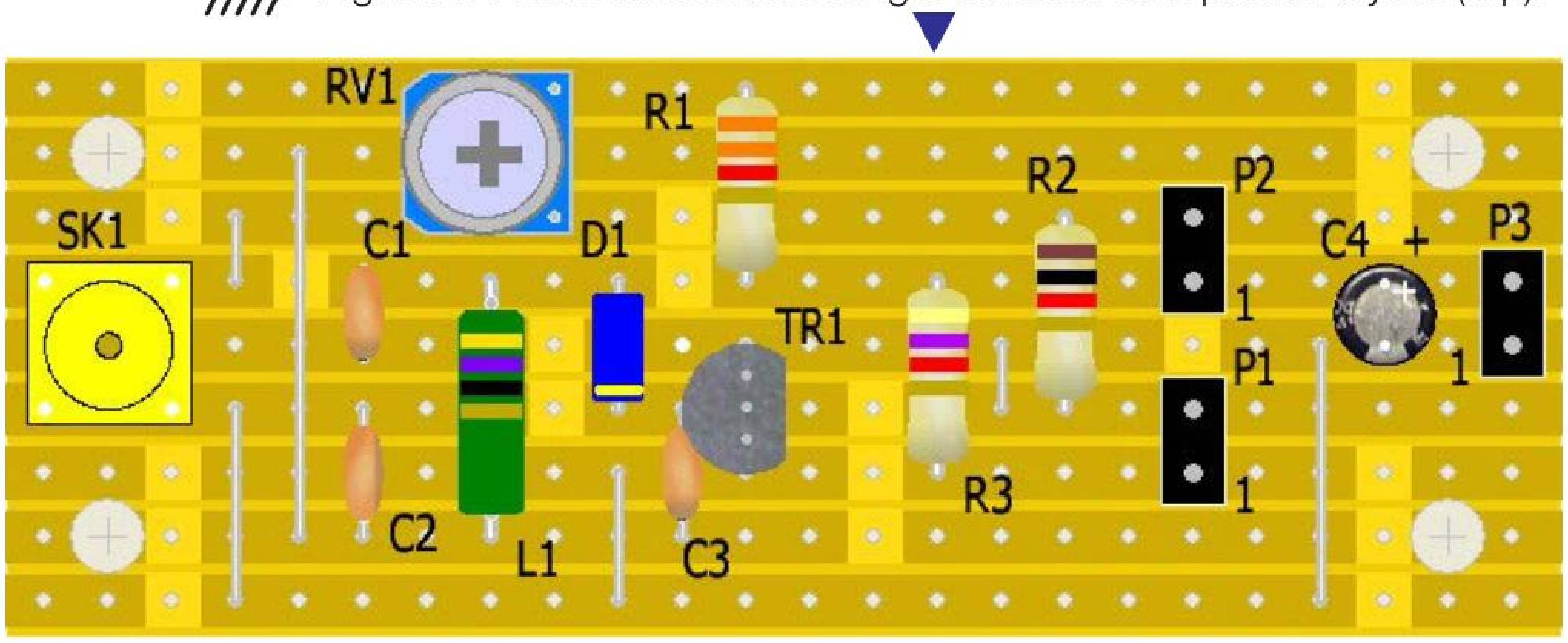
RV1
R1
SK1
C1
D1
R2
P2
C4
+
P3
TR1
1
P1
1
C2
L1
C3
R3
1

A sub-GHz multi-mode beacon

To provide you with an example of using the sub-GHz bands, we've made a simple CC1101 multi-mode beacon for experimental operation. The beacon operates on the SRD frequency of 433.92 MHz, which is shared with part of the 70cm amateur band.

Our example generates successive identification messages (including the author's callsign and location) at five-second intervals using four different modulation methods: 2-FSK, GFSK, ASK/OOK, and 4-FSK.

The circuit of the 433MHz multi-mode beacon is shown in Fig.10.12. Connections to the Arduino Nano microcontroller via SPI are like those used for the nRF24L01, but we've added an interface to cope with the level-shifting necessary required to interface the 3.3V world of the

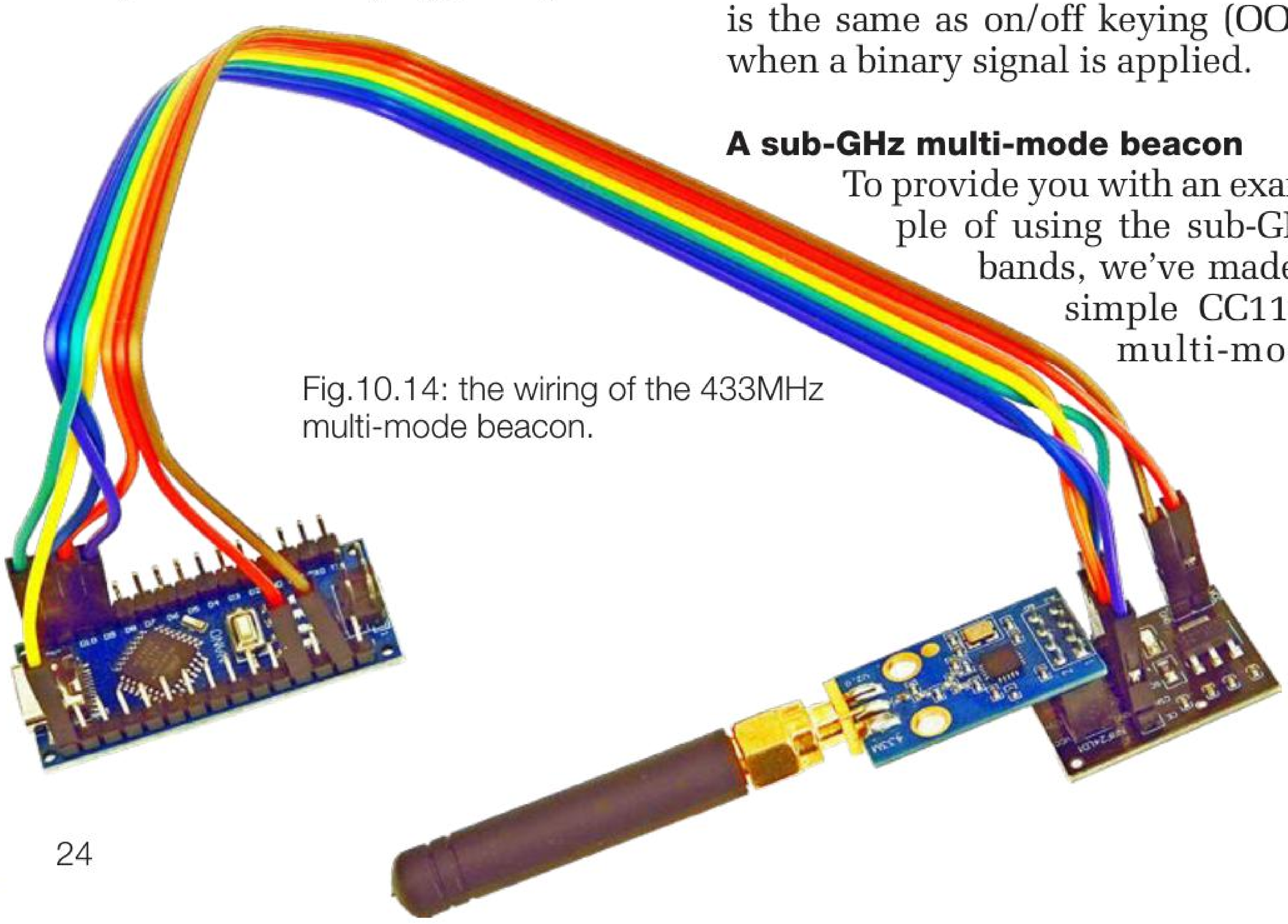

Fig.10.14: the wiring of the 433MHz multi-mode beacon.

CC1101 with the 5V levels used by the Nano.

The level-shifting can be accomplished using an inexpensive module that's compatible with SRD devices like the CC1101 and nRF24 (available from several online suppliers, eg, **https://pemag.au/link/acck**). Fig.10.13 shows the three wireless components required.

The interconnection between the interface board and Nano microcontroller can be conveniently made using a short ribbon cable, as shown in Fig.10.14. Incoming power is supplied via the Nano's type-C USB connector.

The code for the 433MHz multi-mode beacon is shown in Listing 10.4. We've used the excellent ELECHOUSE_cc1101 library that provides a huge range of configuration options. In Listing 10.4, we configure the device for operation at 433.92MHz with a frequency deviation of 2.5kHz, a data rate of 125bps and an RF output of 10mW (10dBm).

Fig.10.15 shows the frequency spectrum of the output of the 433MHz multi-mode beacon. This was obtained using an inexpensive spectrum analyser (see part 7 in the May 2026 issue) together with a 10dB SMA attenuator connected in the RF output.

Hands-On: A simple RF relative field strength indicator

This month's *Hands-On* project is another useful item of RF test equipment: a simple RF relative field strength meter. It is designed primarily for operation over 3.5-150MHz but provides indications from below 1MHz to over 400MHz with reduced sensitivity.

The circuit is shown in Fig.10.16; it comprises a Schottky diode detector (D1) followed by a high-gain Darlington transistor amplifier (TR1). The instrument provides indications using a 1mA moving coil meter (M1) and one LED, which becomes illuminated when strong signals are detected.

Sensitivity is varied by means of a preset control, RV1. The instrument is self-contained and operates from an internal 9V PP3 battery.

As with our previous *Hands-On* projects, it is built on a 25 × 64mm piece of perforated copper stripboard, arranged as nine strips each of 24 rows. The component layout (viewed from the top) is shown in Fig.10.17, while the corresponding track layout (viewed from below) is in Fig.10.18.

Listing 10.4: CC1101 433MHz beacon code demonstrating different modulation methods.

```
#include <ELECHOUSE_CC1101_SRC_DRV.h>

int gdo0;

void setup() {
  gdo0 = 9;  // for Arduino Nano
  Serial.begin(9600);
  if (ELECHOUSE_cc1101.getCC1101()) {  // Check the CC1101 SPI
    Serial.println("Connected to the wireless module");
  } else {
    Serial.println("Not connected to the radio module!");
  }
  ELECHOUSE_cc1101.Init();
  ELECHOUSE_cc1101.setGDO0(gdo0);
  ELECHOUSE_cc1101.setCCMode(2);
  ELECHOUSE_cc1101.setMHZ(433.92);     // Frequency = 433.92MHz
  ELECHOUSE_cc1101.setDeviation(2.50); // Deviation = 2.5kHz
  ELECHOUSE_cc1101.setDRate(0.125);    // Data rate = 125bps
  ELECHOUSE_cc1101.setPA(10);          // RF output = 10mW
  ELECHOUSE_cc1101.setPktFormat(0);
  ELECHOUSE_cc1101.setLengthConfig(1);
  Serial.println("Tx Mode");
}

void loop() {
  // Beacon message generated every five seconds
  Serial.println("Sending 2-FSK");
  ELECHOUSE_cc1101.setModulation(0);  // set modulation mode to 2-FSK
  ELECHOUSE_cc1101.SendData("2-FSK de G8CKT Billingshurst West Sussex");
  delay(5000);
  Serial.println("Sending GFSK");
  ELECHOUSE_cc1101.setModulation(1);  // set modulation mode to GFSK
  ELECHOUSE_cc1101.SendData("GFSK de G8CKT Billingshurst West Sussex");
  delay(5000);
  Serial.println("Sending ASK/OOK");
  ELECHOUSE_cc1101.setModulation(2);  // set modulation mode to ASK/OOK
  ELECHOUSE_cc1101.SendData("ASK/OOK de G8CKT Billingshurst West Sussex");
  delay(5000);
  Serial.println("Sending 4-FSK");
  ELECHOUSE_cc1101.setModulation(3);  // set modulation mode to 4-FSK
  ELECHOUSE_cc1101.SendData("FSK de G8CKT Billingshurst West Sussex");
  delay(5000);
  Serial.println("Sending MSK");
  ELECHOUSE_cc1101.setModulation(4);  // set modulation mode to MSK
  ELECHOUSE_cc1101.SendData("MSK de G8CKT Billingshurst West Sussex");
  delay(5000);
}
```

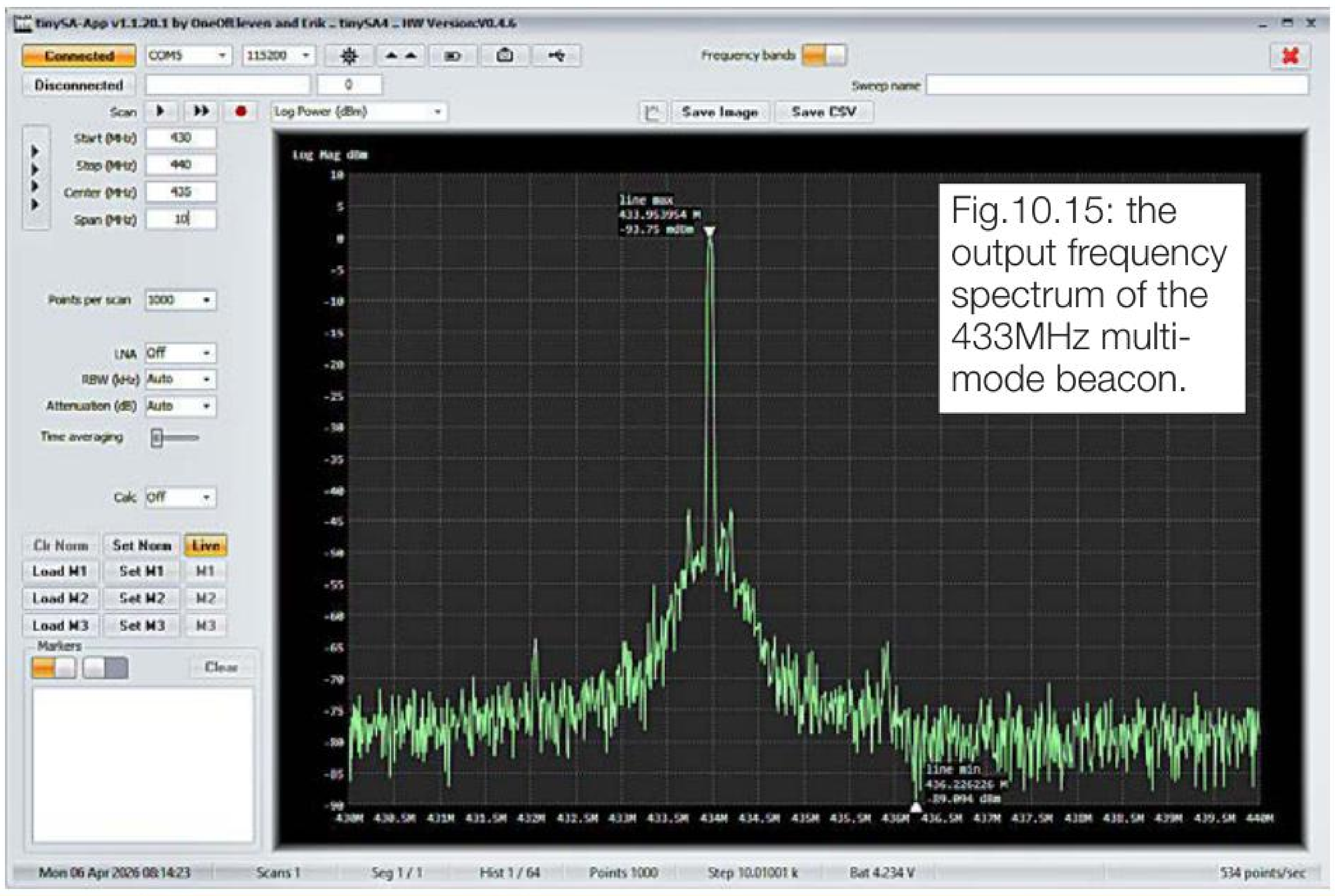
tinySA-App v1.1.20.1 by OneOfEleven and Erik _ tinySA4 _ HW Version:V0.4.6
Connected
Disconnected
Frequency bands
Sweep name
Scan
Save Image
Save CSV
Clr Norm
Set Norm
Live
Load M1
Set M1
M1
Load M2
Set M2
M2
Load M3
Set M3
M3
Markers
Clear
Log Mag dBm
10
5
0
-5
-10
-15
-20
-25
-30
-35
-40
-45
-50
-55
-60
-65
-70
-75
-80
-85
-90
430M 430.5M 431M 431.5M 432M 432.5M 433M 433.5M 434M 434.5M 435M 435.5M 436M 436.5M 437M 437.5M 438M 438.5M 439M 439.5M 440M
line max
433.953954 M
-93.75 mdBm
line min
436.226226 M
-89.094 dBm

COM5 115200

Log Power (dBm)

Start (MHz) 430
Stop (MHz) 440
Center (MHz) 435
Span (MHz) 10
Points per scan 1000
LNA Off
RBW (kHz) Auto
Attenuation (dB) Auto
Time averaging
Cal Off

Mon 06 Apr 2026 08:14:23 | Scans 1 | Seg 1 / 1 | Hist 1 / 64 | Points 1000 | Step 10.01001 k | Bat 4.234 V | 534 points/sec

Fig.10.15: the output frequency spectrum of the 433MHz multi-mode beacon.

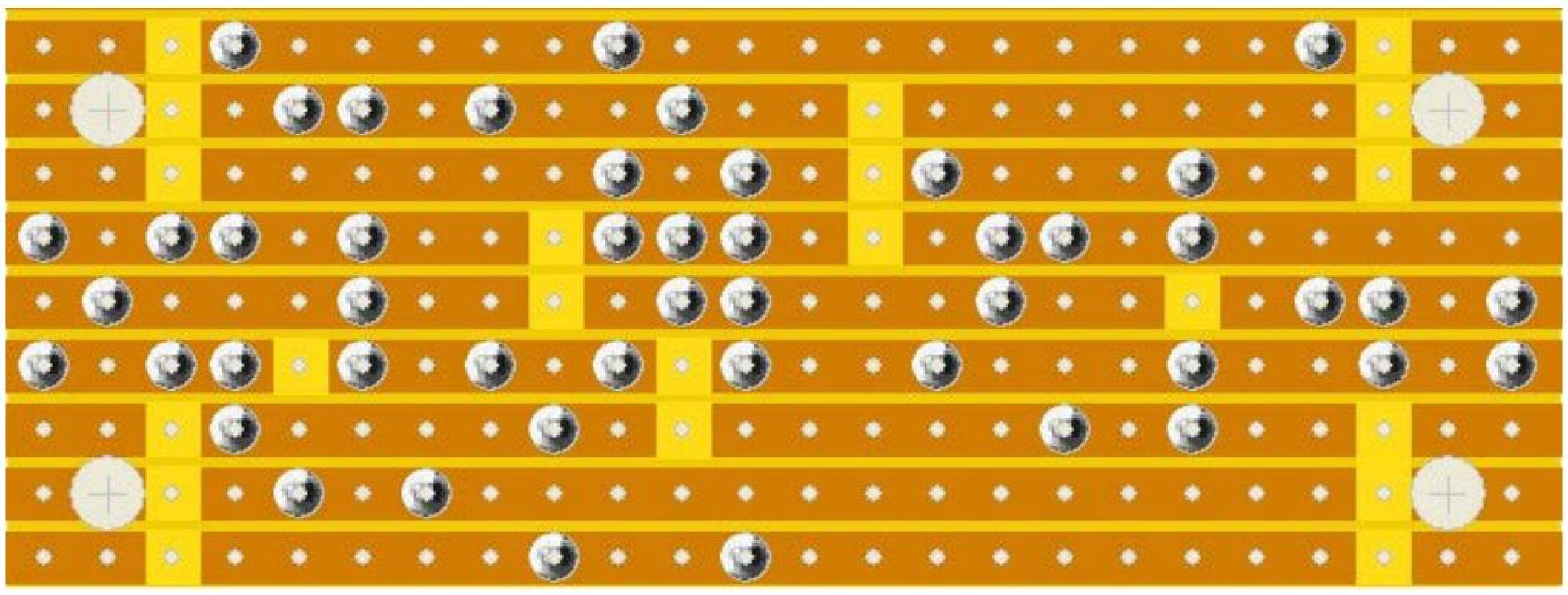

Fig.10.18: the RF relative field strength indicator track layout (underside view). ▶

HAMMOND®

1591 ABS flame-retardant enclosures

Learn more:
hammondmfg.com/1591

uksales@hammfg.com • 01256 812812

The required 21 track breaks can be made using a spot-face cutter or a small drill bit, while the six links on the upper side of the board can be made using short lengths of tinned copper wire or component lead off-cuts.

Take care to observe the correct polarity of Darlington transistor TR1 and diode D1 (the stripe on the package of D1 indicates the cathode).

The completed stripboard is mounted, together with the combined VR1/S1, inside a small ABS enclosure.

Suitable cases are available from several online suppliers at a reasonable cost. When purchasing, it's important to check that the dimensions of the case are sufficient to accommodate the board (25 × 64mm) and 9V battery, while also having sufficient depth to accept the meter movement.

The enclosure used for the prototype measured 100 × 68 × 50mm.

Fig.10.19 shows the internal wiring of the RF relative field strength meter. The circuit board is mounted in the base of the enclosure alongside the battery. The variable sensitivity control (VR1), on/off switch (S1), LED indicator (D2) and meter (M1) are mounted on the lid.

Point-to-point wiring is used to link the lid-mounted components to the board and battery in the main part of the case.

The RF input connector (SK1) is mounted on the top of the enclosure.

To avoid the need to solder the coaxial connector, we've used a ready-made panel-mounting BNC socket with a 15cm pigtail cable and SMA connector (see Fig.10.20).

Adjustment

The RF voltmeter probe requires initial adjustment of trimpot RV1 for maximum sensitivity. This is accomplished by disconnecting the RF input (remove any antenna) and setting RV1 to its fully anticlockwise position.

Next, switch the unit on and advance VR1 to its maximum

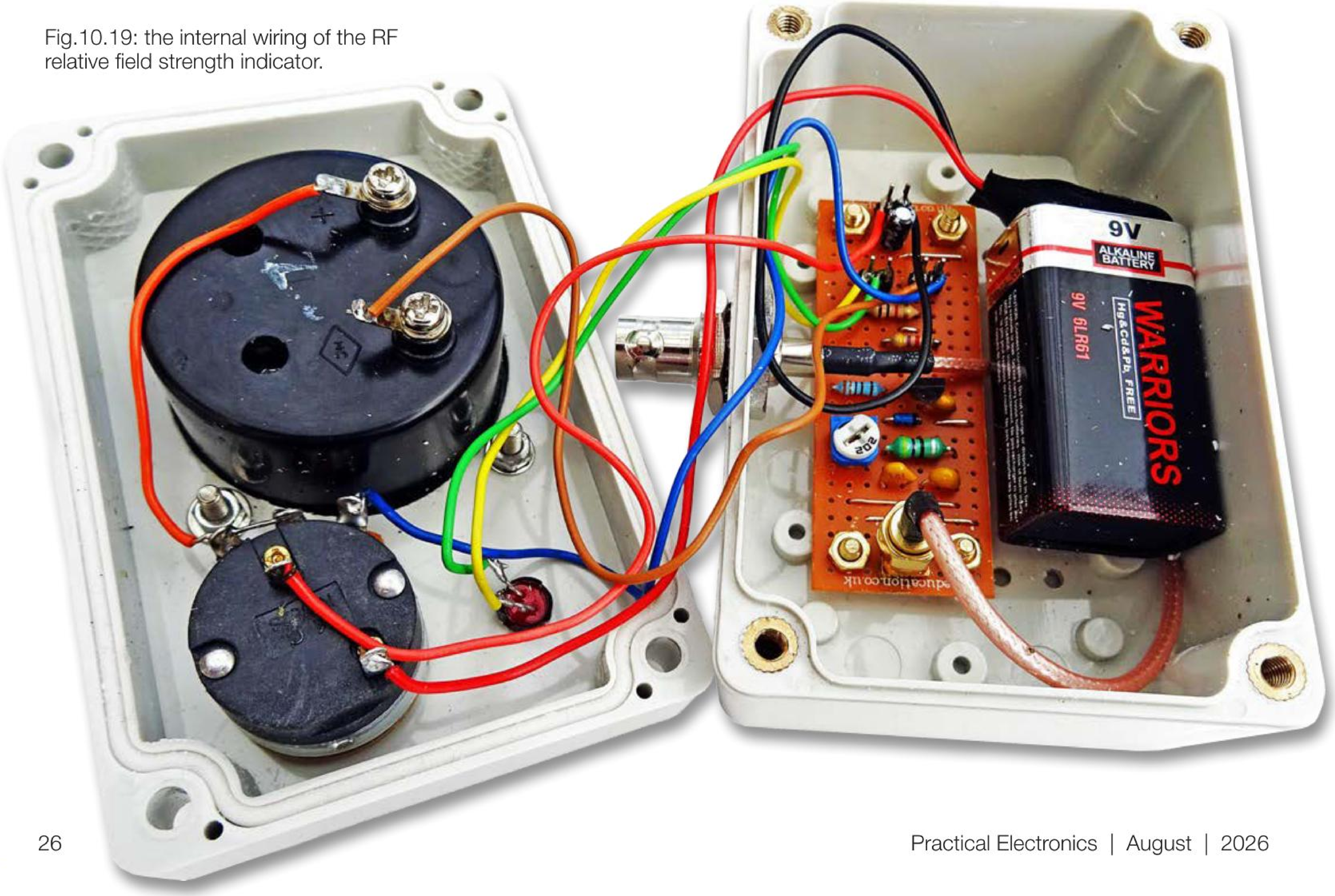

Fig.10.19: the internal wiring of the RF relative field strength indicator.

clockwise setting (corresponding to maximum sensitivity).

Now carefully adjust RV1, turning it clockwise until the meter pointer just lifts off the zero position.

This completes the adjustment and the meter is ready for use by placing the antenna in the RF field to be measured, eg, near a transmitting antenna. A short telescopic antenna fitted with a male BNC connector will work well for most measurements from 3.5MHz to 450MHz, but care should be taken to avoid overloading the detector.

Coming up...

Next month, our final Teach-In 12 instalment will provide a host of ideas for further exploration.

We will supply some information to get you started with shortwave listening, amateur radio and aircraft radio, as well as LoRa and LoRa WAN technology.

Our *Hands-On* constructional project will be a handy RF preamplifier for use with an SDR or conventional HF receiver. See you next time! **PE**

Parts list – RF relative field strength meter

- 1 47µH axial RF inductor (L1)
- 1 1mA moving coil meter (M1)
- 3 2-way 0.1-inch/2.54mm pitch headers (P1-P3)
- 1 2k miniature horizontal preset (RV1)
- 1 panel-mount female BNC socket with male SMA 15cm pigtail connector (SK1)
- 1 10kΩ linear variable resistor with integral switch (VR1/S1)
- 1 small plastic pointer knob to suit VR1/S1
- 1 9V PP3 battery and connecting clip

Hardware

- 1 ABS enclosure, at least 100 × 68 × 50mm
- 4 brass or nylon M3 × 5mm tapped hex standoffs/spacers
- 4 M3 × 5mm panhead machine screws
- 4 M3 × 5mm countersunk head machine screws

Semiconductors

- 1 BAT42 Schottky diode (D1)
- 1 5mm LED (D2)
- 1 BC517 NPN Darlington transistor, TO-92 (TR1)

Capacitors

- 1 10µF 16V radial electrolytic (C4)
- 1 47nF 50V ceramic (C2)
- 1 4.7nF 50V ceramic (C3)
- 1 100pF 50V ceramic (C1)

Resistors (all ¼W axial, ±5% or better)

1 4.7kΩ (R3)　1 3.3kΩ (R1)　1 1kΩ (R2)

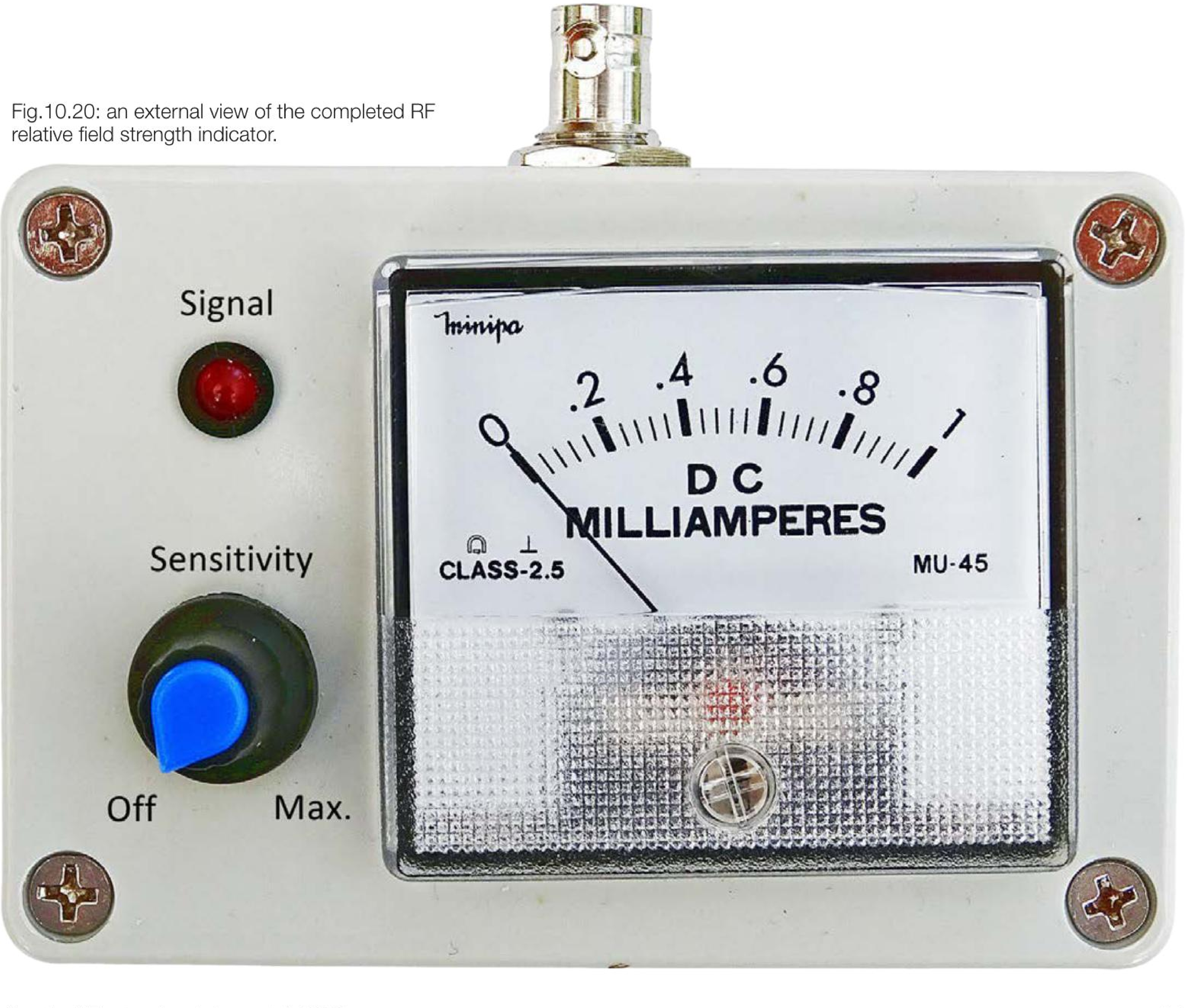

Fig.10.20: an external view of the completed RF relative field strength indicator.

RP2350B COMPUTER

WORDS & MMBASIC BY GEOFF GRAHAM | DESIGN & FIRMWARE BY PETER MATHER

RP2350B
HDMI
USB
Pico 2 Computer
Version 2

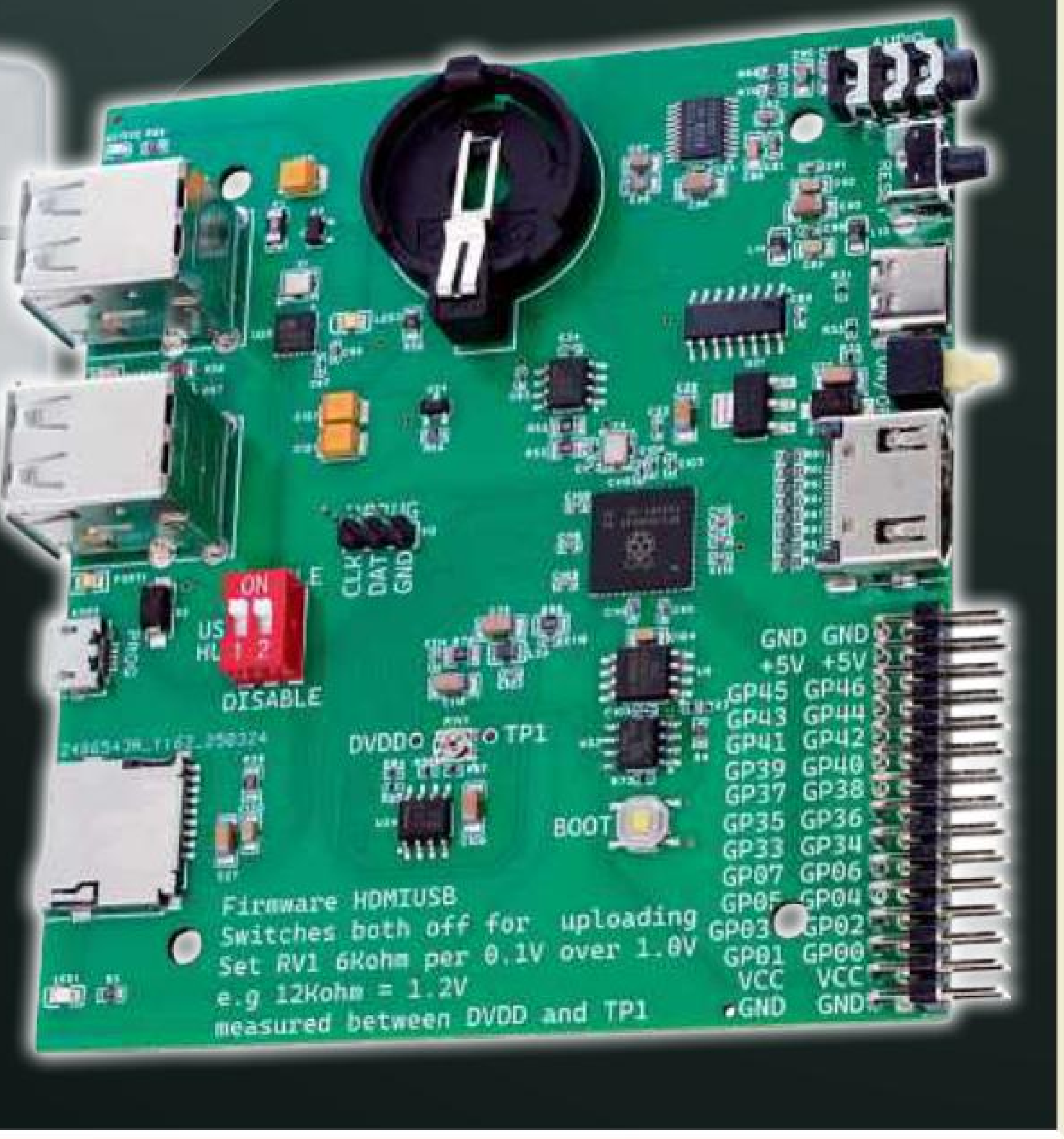

This board is an improved version of the Pico 2 Computer that requires almost no soldering, has more I/O pins available, a much improved stereo audio output and a few other nice tweaks.

- › **RP2350B Computer Assembled Module (SC7531, $90)** includes a fully-assembled PCB, except for the optional components
- › **RP2350B Computer Front & Rear Panels (SC7532, $7.50)** pre-cut panels with white silkscreen printing on a black solder mask

This new low-cost computer can run BASIC programs and is excellent for creating applications, games, controlling external circuits and generally messing around with an easy-to-use but capable computer.

It is based on the RP2350B chip, which is similar to the RP2350A used in the Raspberry Pi Pico 2 module. Using this expanded version of this chip, with extra pins, allows us to provide many very useful and powerful features.

Some of the features of this design include:

- A low-cost boot-to-BASIC computer with keyboard support and video output.
- DVI/HDMI video output with resolutions up to 1280 × 720 pixels.
- An accurate internal clock that is battery backed.
- Support for up to four USB devices, including keyboards, mice and game controllers.
- A microSD card socket supports cards formatted in FAT16 or FAT32 with capacities up to 32GB.
- A built-in full-featured BASIC interpreter that includes its own full-screen editor, support for programs up to 184kiB and general purpose RAM of 220kiB.

PWM	Serial	I^{2}C	SPI	Function	I/O Pin		Function	SPI	I^{2}C	Serial	PWM
				GND	1	2	GND				
				3.3V	3	4	3.3V				
PWM0B	COM1 RX	I^{2}C SCL		GP01	5	6	GP00	SPI RX	I^{2}C SDA	COM1 TX	PWM0A
PWM1B		I^{2}C2 SCL	SPI TX	GP03	7	8	GP02	SPI CLK	I^{2}C2 SDA		PWM1A
PWM2B	COM2 RX	I^{2}C SCL		GP05	9	10	GP04	SPI RX	I^{2}C SDA	COM2 TX	PWM2A
PWM3B		I^{2}C2 SCL	SPI TX	GP07	11	12	GP06	SPI CLK	I^{2}C2 SDA		PWM3A
PWM8B	COM1 RX	I^{2}C SCL		GP33	13	14	GP34	SPI CLK	I^{2}C2 SDA		PWM9A
PWM9B		I^{2}C2 SCL	SPI TX	GP35	15	16	GP36	SPI RX	I^{2}C SDA	COM2 TX	PWM10A
PWM10B	COM2 RX	I^{2}C SCL		GP37	17	18	GP38	SPI CLK	I^{2}C2 SDA		PWM11A
PWM11B		I^{2}C2 SCL	SPI TX	GP39	19	20	GP40	SPI2 RX	I^{2}C SDA	COM2 TX	PWM8A
PWM8B	COM2 RX	I^{2}C SCL		GP41	21	22	GP42	SPI2 CLK	I^{2}C2 SDA		PWM9A
PWM9B		I^{2}C2 SCL	SPI2 TX	GP43	23	24	GP44	SPI2 RX	I^{2}C SDA	COM1 TX	PWM10A
PWM10B	COM1 RX	I^{2}C SCL		GP45	25	26	GP46	SPI2 CLK	I^{2}C2 SDA		PWM11A
				5V	27	28	5V				
ANALOG PINS				GND	29	30	GND				

Table 1 – GPIO Pin Capabilities
note that pin 1 is at the bottom right of the PCB

- It uses an RP2350B processor soldered directly to the PCB with supporting components that make overclocking of the processor (to support HDMI video) easier. That means you don't need to obtain and solder a Pico 2 module to the board; it's available fully pre-assembled and ready to use. All you have to do is load the firmware into it (which is easy with a computer and a USB cable) and away you go.
- It includes a proper audio output with a built-in digital-to-analog converter (DAC) to deliver high-fidelity, noise-free stereo audio.
- It provides many general purpose I/O (GPIO) pins for connecting to external circuits. This includes seven that are analog-capable (they can measure voltages).
- It has support for a PSRAM chip that can add 6MiB of additional RAM for MMBasic.
- It uses a larger flash memory chip that provides a 14MiB internal "A:" drive.

With this self-contained, low-cost computer, you can have fun creating your own programs, learning or teaching programming, or simply have fun exploring an easy-to-use computer with a lot of potential. It also makes a capable embedded controller.

Video output

The video output is DVI/HDMI in six resolutions: 640 × 480, 720 × 400, 800 × 600, 848 × 480, 1280 × 720 and 1024 × 768 pixels. The firmware generates a DVI signal, but HDMI monitors automatically support DVI, so this is transparent.

That means we can use an HDMI connector for video output, which is the standard for modern monitors. However, you cannot use other HDMI features, such as audio, over the HDMI cable.

Using the MODE command, you can select a variety of colours and resolutions, with lower resolutions supporting more colours.

The built-in BASIC program editor uses the full resolution and, by using the TILE functionality, colours characters for you. Keywords are cyan, comments are green etc. This makes for a colourful and intuitive program editing experience.

Four Type-A USB sockets are provided, supporting USB keyboards, mice and game controllers. The keyboard input includes support for the function keys, arrow keys, etc and can handle wireless keyboards with a USB dongle, so you do not need to be restricted by a cable.

A USB mouse is very useful with the built in MMBasic program editor, where it gives you the ability to position the insert point and copy and paste using the mouse.

Within a BASIC program, you can query the mouse position and the state of the buttons and, as with the keyboard, you can also use a wireless mouse.

One or two USB game controllers can also be used. Within the BASIC program, you can get the current position of the joystick and discover what buttons are pressed. This is most useful if you are creating games for the computer.

Digital audio

One excellent feature of this Computer is that it has an I^{2}S interface to a separate DAC (digital-to-analog converter) chip for the audio output. I^{2}S was developed by Philips Semiconductor (now NXP Semiconductors) as an interface for transferring digital audio between a microcontroller and a DAC in an appliance.

Many Pico-based computers use a pulse-width modulation (PWM) scheme for generating their audio output, which requires a low-pass filter to remove the carrier frequency. This is a simple method for generating the audio but, even with advanced filter designs, some of the carrier frequency still reaches the output, and the filter reduces the high-frequency range of the audio signal.

In this design, the I^{2}S signal is processed by a dedicated 32-bit audio DAC chip. The I^{2}S protocol transfers data as numbers, so the audio frequency response is perfectly flat from 20Hz to 20kHz. Purists with good audio systems will appreciate this feature as MMBasic can play files in high-quality stereo WAV, FLAC, MP3 or MOD formats.

External storage is provided by a microSD card slot, which can accept cards up to 32GiB formatted in FAT16 or FAT32. The files created can be read/written on personal computers running Windows, Linux or macOS. The PicoMite firmware uses the SPI protocol to communicate with the card, with all types (Class 4, 10, UHS-1 etc) being supported.

Processor: Raspberry Pi RP2350B (dual-core ARM Cortex-M33 & dual Hazard3 RISC-V)

Clock Speed: 252-375MHz (depending on the video resolution)

Firmware: PicoMite/MMBasic V6.00.03 or greater

Non-volatile program memory: 184kiB

General usage RAM: 220kiB (expandable to over 6MiB)

Internal File Storage: 14MiB

Removable file storage: microSD Card, FAT16/FAT32, up to 32GiB

Video output: DVI via an HDMI connector @ 640 × 480, 720 × 400, 800 × 600, 848 × 480, 1280 × 720 or 1024 × 768 pixels

Audio output: 5.5V peak-to-peak (2V RMS), response flat from 20Hz to 20kHz

Audio formats supported: single-frequency tones, stereo WAV, FLAC, MP3 & MOD

USB ports: four Type-A for peripherals, one Type-C for power/console and one micro Type-B for firmware loading

Keyboard support: standard or wireless USB keyboard (without a built-in mouse)

Mouse input: standard or wireless USB mouse

Gamepads: up to two SNES controllers with USB Type-A connectors

Clock: battery-backed real-time clock & calendar (typical accuracy ±3sec/month)

External console: serial over USB @ 115200 baud via the USB Type-C socket

External I/O connector: 30 pins with 22 GPIOs, including 7 with analog input ability, plus ground, 3.3V and 5V outputs

Power supply: 5V @ 220mA via the rear USB Type-C socket

PCB size: 100 × 90mm

Optional case size: 130 × 100 × 30mm

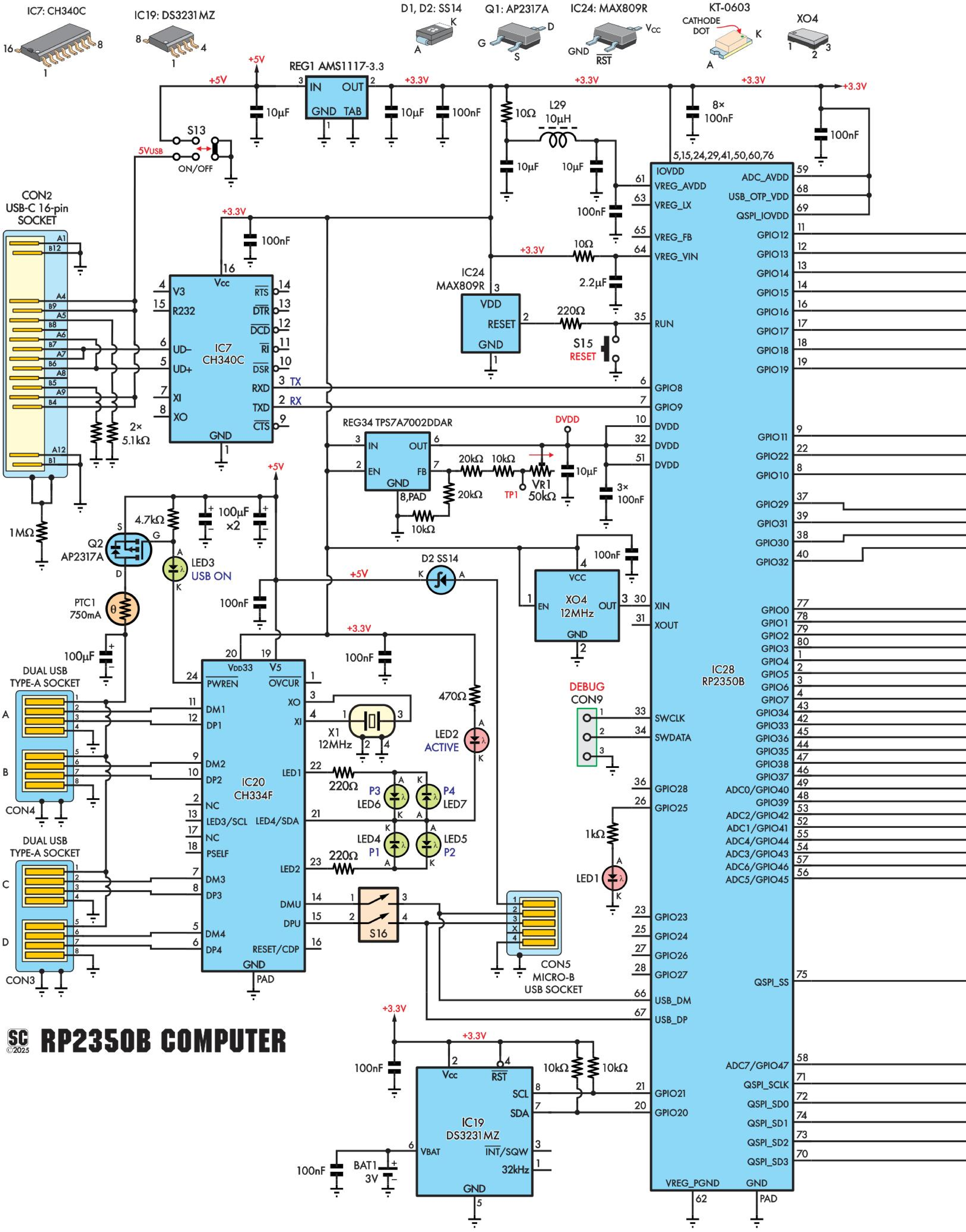
IC7: CH340C
IC19: DS3231MZ
D1, D2: SS14
Q1: AP2317A
IC24: MAX809R
KT-0603
CATHODE DOT
XO4
+5V
REG1 AMS1117-3.3
IN OUT
GND TAB
+3.3V
10μF
100nF
10Ω
L29 10μH
8× 100nF
S13
ON/OFF
5VUSB
CON2 USB-C 16-pin SOCKET
A1 B12 A4 B9 A5 B8 A6 B7 A7 B6 A8 B5 A9 B4 A12 B1
2× 5.1kΩ
1MΩ
IC7 CH340C
V3 R232 UD– UD+ XI XO Vcc GND
RTS DTR DCD RI DSR RXD TXD CTS
TX RX
IC24 MAX809R
VDD RESET GND
220Ω
2.2μF
S15 RESET
REG34 TPS7A7002DDAR
IN OUT EN FB GND 8,PAD
20kΩ 10kΩ 20kΩ 10kΩ
DVDD
TP1
VR1 50kΩ
3× 100nF
Q2 AP2317A
4.7kΩ
100μF ×2
LED3 USB ON
PTC1 750mA
D2 SS14
XO4 12MHz
VCC EN OUT GND
DUAL USB TYPE-A SOCKET
CON4
CON3
IC20 CH334F
VDD33 V5 PWREN OVCUR DM1 DP1 DM2 DP2 NC LED3/SCL LED4/SDA NC PSELF DM3 DP3 DM4 DP4 XO XI LED1 LED2 DMU DPU RESET/CDP GND PAD
X1 12MHz
470Ω
LED2 ACTIVE
LED6 P3 LED7 P4 LED4 P1 LED5 P2
S16
CON5 MICRO-B USB SOCKET
DEBUG CON9
1kΩ
LED1
IC28 RP2350B
IOVDD VREG_AVDD VREG_LX VREG_FB VREG_VIN RUN GPIO8 GPIO9 DVDD XIN XOUT SWCLK SWDATA GPIO28 GPIO25 GPIO23 GPIO24 GPIO26 GPIO27 USB_DM USB_DP GPIO21 GPIO20 VREG_PGND GND PAD
ADC_AVDD USB_OTP_VDD QSPI_IOVDD GPIO12 GPIO13 GPIO14 GPIO15 GPIO16 GPIO17 GPIO18 GPIO19 GPIO11 GPIO22 GPIO10 GPIO29 GPIO31 GPIO30 GPIO32 GPIO0 GPIO1 GPIO2 GPIO3 GPIO4 GPIO5 GPIO6 GPIO7 GPIO34 GPIO33 GPIO36 GPIO35 GPIO38 GPIO37 ADC0/GPIO40 GPIO39 ADC2/GPIO42 ADC1/GPIO41 ADC4/GPIO44 ADC3/GPIO43 ADC6/GPIO46 ADC5/GPIO45 QSPI_SS ADC7/GPIO47 QSPI_SCLK QSPI_SD0 QSPI_SD1 QSPI_SD2 QSPI_SD3
5,15,24,29,41,50,60,76
IC19 DS3231MZ
Vcc RST SCL SDA VBAT INT/SQW 32kHz GND
10kΩ 10kΩ
BAT1 3V
SC ©2025

RP2350B COMPUTER

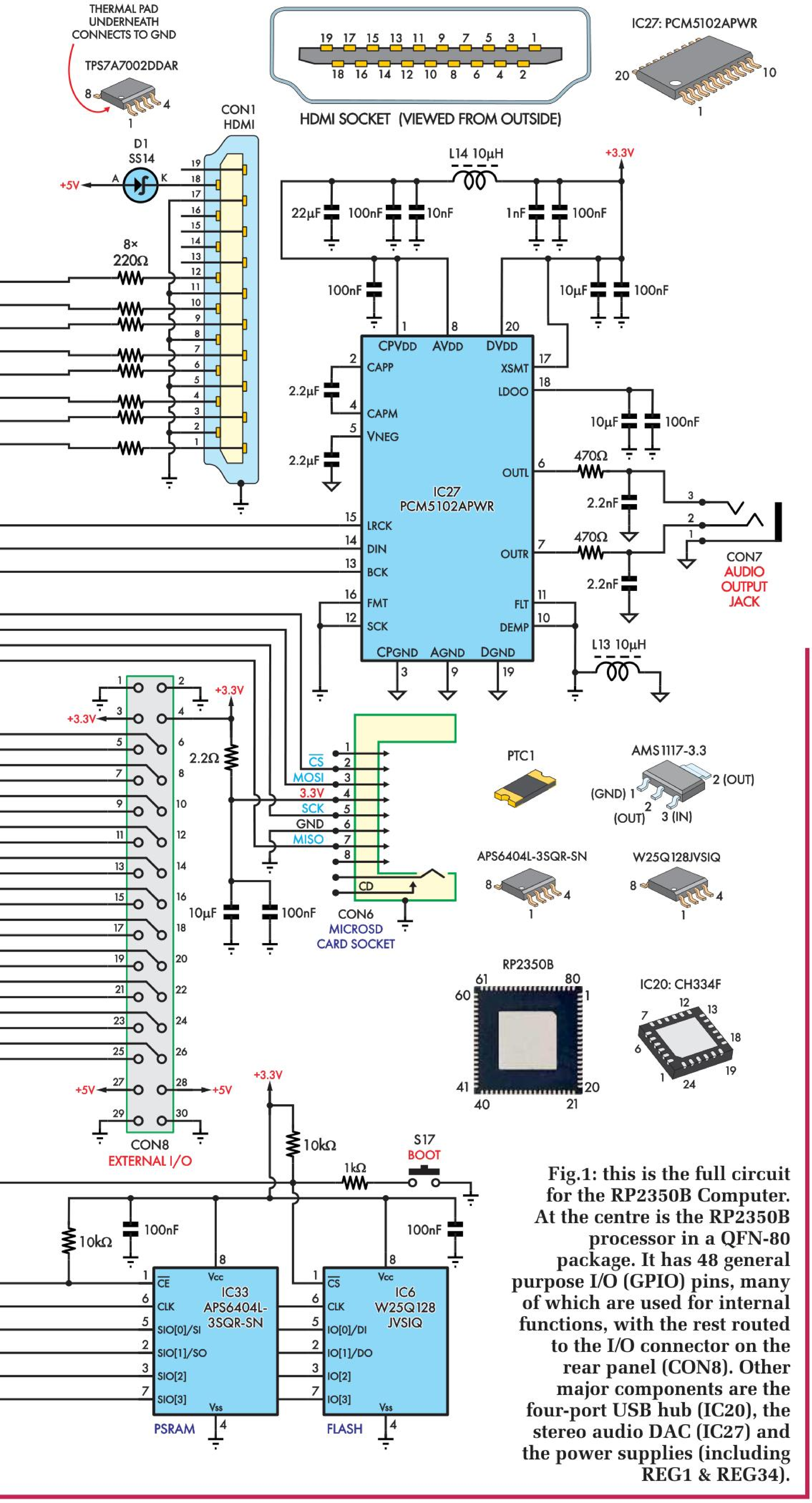
THERMAL PAD UNDERNEATH CONNECTS TO GND
TPS7A7002DDAR
HDMI SOCKET (VIEWED FROM OUTSIDE)
IC27: PCM5102APWR
CON1 HDMI
D1 SS14
+5V
A
K
8× 220Ω
L14 10µH
+3.3V
22µF
100nF
10nF
1nF
10µF
CPVDD
AVDD
DVDD
CAPP
XSMT
LDOO
2.2µF
CAPM
VNEG
OUTL
470Ω
2.2nF
IC27 PCM5102APWR
LRCK
DIN
BCK
OUTR
FMT
FLT
SCK
DEMP
CPGND
AGND
DGND
CON7 AUDIO OUTPUT JACK
L13 10µH
2.2Ω
CS
MOSI
3.3V
SCK
GND
MISO
CD
CON6 MICROSD CARD SOCKET
PTC1
AMS1117-3.3
(GND) 1
2 (OUT)
(OUT) 2
3 (IN)
APS6404L-3SQR-SN
W25Q128JVSIQ
RP2350B
IC20: CH334F
CON8 EXTERNAL I/O
+5V
10kΩ
1kΩ
S17 BOOT
CE
CLK
Vcc
IC33 APS6404L-3SQR-SN
SIO[0]/SI
SIO[1]/SO
SIO[2]
SIO[3]
Vss
PSRAM
IC6 W25Q128 JVSIQ
IO[0]/DI
IO[1]/DO
IO[2]
IO[3]
FLASH

Fig.1: this is the full circuit for the RP2350B Computer. At the centre is the RP2350B processor in a QFN-80 package. It has 48 general purpose I/O (GPIO) pins, many of which are used for internal functions, with the rest routed to the I/O connector on the rear panel (CON8). Other major components are the four-port USB hub (IC20), the stereo audio DAC (IC27) and the power supplies (including REG1 & REG34).

A battery-backed real-time clock and calendar (RTCC) keeps track of the correct time, which can be accessed from within a BASIC program. It is also used to stamp files with the correct creation time. This clock is very accurate (within a few seconds per month), and is supported by a battery when the power is removed, so you will rarely need to set the time.

For controlling external devices and circuits, 22 GPIO pins are brought out to a 30-pin connector on the rear panel. All of these can be set as a digital input, digital output or a mixture of serial I/O, I²C, SPI, PWM and analog inputs. Also provided on this connector are the ground pins, +5V and +3.3V power supply outputs. Table 1 lists the pins on this connector and their functions.

Circuit details

Fig.1 shows the full circuit for the RP2350B Computer, which is based around the RP2350B processor (IC28) in an 80-pin QFN package. This chip has 48 GPIO pins, many of which are used for internal functions (HDMI/DVI video, SD card interface etc). As noted above, 22 are routed to the I/O connector (CON8) on the rear panel.

The default clock rate for the RP2350B processor is 150MHz, but to generate HDMI video, we need to overclock it up to 375MHz. To support this, we use an integrated crystal oscillator to generate the base clock of 12MHz, which is multiplied in the RP2350B to give the core CPU clock.

Using a dedicated oscillator results in a more stable clock with much less jitter than using a simple crystal as used in the Raspberry Pi Pico 2 module, which helps with overclocking.

The RP2350B has eight analog inputs (pins 49 to 58), with seven of these available on CON8. To support accurate analog measurements, we have included a noise filter for the AVDD pin on the chip. AVDD is used as the reference for analog measurements and this filter, along with the PCB layout and a noise-free 3.3V supply, ensure that accurate and noise-free analog measurements can be made.

Flash & PSRAM memory

The PicoMite firmware, the BASIC program and other data is held in IC6,

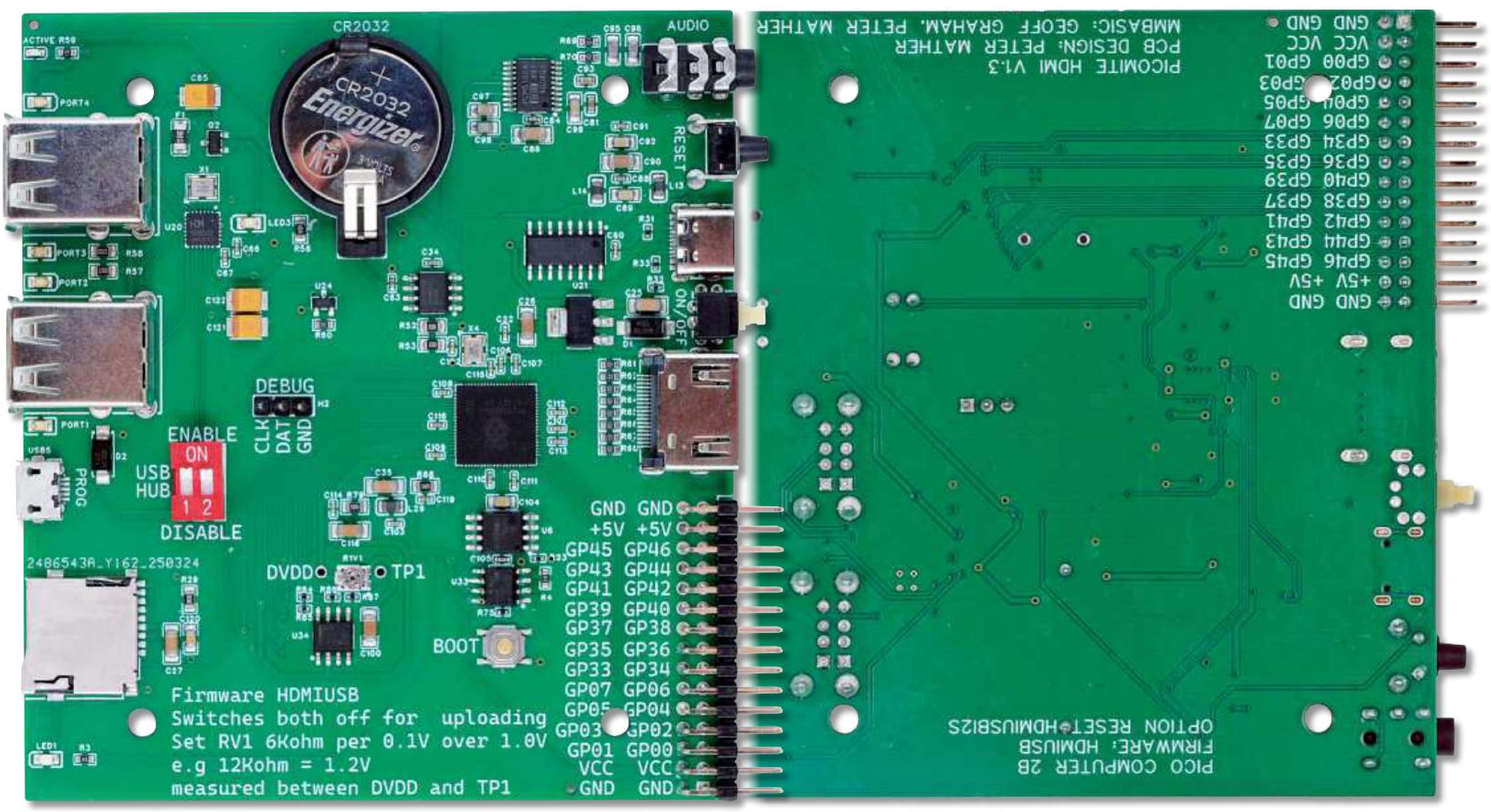

The RP2350B Computer uses a small 100 × 90mm PCB with the RP2350B processor soldered directly to the board. This is difficult to hand-solder, so we recommend either buying the board fully assembled from the Electron Publishing/*Practical Electronics* shop, or having it assembled by a company with a pick & place machine.

a Winbond W25Q128JVSIQ 128Mbit (16MiB) flash memory chip. This uses a quad SPI interface, and is designed to allow the RP2350B to execute its program directly from this chip. It can also operate with high clock speeds on the quad SPI interface (133MHz), which means that it can keep up when the RP2350B is overclocked.

Even though the SPI interface transfers data four bits at a time, and has a high clock speed, it is still quite slow compared to the RP2350B's on-chip memory. To reduce this effect, the RP2350B uses a built-in SRAM cache, and the firmware is configured to move critical sections of its code to the on-chip RAM for execution. As a result, there is very little impact on the performance from using off-chip flash memory.

On startup, the RP2350B checks if the flash memory is present and that it contains a valid program. If either are not found, it will automatically enter its firmware load mode. This involves creating a pseudo flash memory drive on the USB interface that looks like a USB drive to a Windows, Linux or macOS computer. You can use this interface to copy new firmware to the flash memory.

In our design, the BOOT switch is used to pull the chip select line low on the flash memory chip, which essentially disables it. When used on power-up, this causes the RP2350B to enter its firmware loading mode.

IC33 is an optional external PSRAM chip (APS6404L-3SQR-SN) that sits on the same quad SPI bus as the flash memory chip. This has a capacity of 64Mbits (8MiB) and is used to expand the internal RAM of the RP2350B. The PicoMite firmware will automatically add this to the general purpose RAM seen by the BASIC interpreter, allowing the BASIC program to define very large arrays.

The internal RAM of the RP2350B is more than enough for the vast majority of applications, so we have left this footprint vacant on assembled boards. Still, if you want to create truly enormous arrays in MMBasic, you can easily add the specified chip yourself. It comes in an easy-to-solder package and MMBasic will automatically recognise it once it is installed.

Be warned that PSRAM is a lot slower than the internal RAM, so there will be a performance penalty when using the extra RAM it provides.

USB interfaces

The RP2350B processor includes a USB interface and this, along with an onboard USB hub, provides four USB ports for a keyboard, mouse and gamepads. The hub function is provided by IC20, a CH334F integrated USB 2.0 four-port hub. This chip includes the USB 2.0 driver circuits (called the USB PHY) that directly drive the four USB Type-A sockets on the front panel.

The CH334F also uses an ingenious system to drive the indicator LEDs showing which USB ports are active.

Some CH334F chips on the market have a fault that causes the power protection feature of the CH334F to interfere with its operation so, in our design, we disable this feature. Resettable fuse PTC1 provides the necessary protection anyway.

To load MMBasic onto IC28, you need to disconnect the hub and directly access the USB interface on the RP2350B. This is done with two switches (S16), which isolate the hub, and an additional Type-B micro-USB connector mounted on the PCBs front edge (CON5). This is only used to load the MMBasic firmware; the procedure will be described in detail later.

Because the USB interface on the RP2350B is used for communicating with the USB hub, it cannot be used for a serial-over-USB console to communicate with a desktop or laptop computer. Having the serial console is handy for connecting to such a computer, so we use a CH340C serial-to-USB bridge chip (IC7) to provide such a console interface.

The CH340C is in a 16-pin package that includes the oscillator required to maintain the accurate timing needed for USB. It converts a TTL asynchronous serial signal from the RP2350B to a USB 2.0 signal using the CDC (communication device class) protocol over USB.

IC19 is a DS3231 real-time clock & calendar (RTCC) that provides the time and date to MMBasic. This is an extremely accurate timekeeper with an integrated temperature compensated oscillator (TCXO) and it will typically keep the time within a few seconds per month. This uses a 210mAh 3V lithium coin cell (CR2032) as the backup; the DS3231 will automatically switch to this when the 3.3V power is removed. The current drawn from this cell is very low, so the battery should last for many years.

The HDMI interface is one of the simpler parts of the circuit. The eight signal lines from the RP2350B are directly connected via 220Ω resistors to the HDMI connector (CON1), with no other components needed. The RP2350B produces a DVI signal, but HDMI transparently supports DVI so this works as the user would expect.

The SD card interface is also quite simple, with the SD card plugged into CON6 being directly driven by four sequential signal lines from the RP2350B (GPIO29 to GPIO32).

The stereo audio output is generated by the firmware running on the RP2350B as an I^{2}S data stream, which is fed to IC27, a Texas Instruments PCM5102APWR 16/24/32-bit audio DAC. Three signal lines from the RP2350B (GPIO10, GPIO11 and GPIO22) form the I^{2}S channel. The DAC generates two analog audio outputs of about 2V RMS, which are coupled to the audio output jack, CON7.

Power supply

The input power for the board is +5V supplied via the rear panel USB-C socket for power and the external console (CON2). The 5V rail powers the front-panel USB ports, but the rest of the Computer runs from 3.3V. A simple AMS1117-3.3 linear regulator, REG1, produces the 3.3V rail. Using a linear regulator avoids the electrical noise

Parts List – RP2350B Computer *(also see BOM XLS file)*

1 double-sided PCB coded 07204251, 90 × 100mm
1 Multicomp MCRM2015S or Hammond RM2015S instrument case (**optional**) ***AND***
  1 pair of black front & rear panel PCBs (07204252-3, 124 × 27mm each) ***OR***
  4 M3-tapped Nylon spacers and M3 × 6mm panhead machine screws (for feet)
1 CR2032 3V lithium coin cell (BAT1)
2 10μH 500mA 0.32Ω M2012/0805 SMD inductors (L13, L14)
  [Microgate MGFL2012F100MT-LF]
1 10μH 15mA 1.15Ω M2012/0805 SMD inductors (L29) **[Sunlord SDFL2012S100KTF]**
1 30V 750mA resettable polyfuse, M3216 size (PTC1) **[BHFuse BSMD1206-075-30V]**
1 latching right-angle PCB-mount pushbutton (S13) **[XKB Connectivity XKB5858-Z-E]**
1 right-angle tactile pushbutton switch, 6mm actuator (S15) **[HCTL TC-6615-7.5-260G]**
1 dual DIP switch (S16) **[YE DSWB02LHGET]**
1 momentary SMD tactile pushbutton switch (S17) **[XKB Connectivity TS-1187A-B-A-B]**

Connectors
1 CR2032 cell holder (BAT1) **[Myoung BS-04-A1BJ005]**
1 HDMI socket (CON1) **[HCTL HDMI-01]**
1 USB-C Socket (CON2) **[Kinghelm KH-TYPE-C-16P]**
2 right-angle horizontal stacked USB Type-A sockets (CON3, CON4)
  [Shou Han AF SS-JB17.6]
1 USB micro Type-B socket (CON5) **[Shou Han MicroXNJ]**
1 microSD card socket (CON6) **[Shou Han TF PUSH]**
1 SMD stereo audio jack socket (CON7) **[Shou Han PJ-313 5JCJ]**
1 2×15-pin right-angle 2.54mm-pitch header (CON8) **[HCTL PZ254-2-15-W-8.5]**
1 3-pin header, 2.54mm pitch (CON9) (**optional**; for serial wire debugging)
1 50kΩ 3.8 × 3.6mm SMD trimpot (VR1) **[Bourns TC33X-2-503E]**

Semiconductors
1 Raspberry Pi RP2350B microcontroller, QFN-80 (IC28)
1 128Mbit QSPI flash memory, SOIC-8 (IC6) **[Winbond W25Q128JVSIQ]**
1 CH340C serial/USB bridge, SOIC-16 (IC7)
1 DS3231MZ real-time clock & calendar, SOIC-8 (IC19)
1 CH334F quad USB hub, QFN-24 (IC20)
1 MAX809R reset supervisor IC, SOT-23-3 (IC24)
1 PCM5102APWR stereo DAC, TSSOP-20 (IC27)
1 APS6404L-3SQR-SN 64Mbit QSPI PSRAM, SOIC-8 (IC33) (**optional**)
1 12MHz crystal resonator, 3.2 × 2mm SMD-4 (X1) **[YXC X322512MSB4SI]**
1 12MHz oscillator module, 3.2 × 2mm SMD-4 (XO4)
  [TOGNJING XOS32012000LT00351005]
1 AMS1117-3.3 low-dropout 3.3V linear regulator, SOT-223-3 (REG21)
1 TPS7A7002DDAR adjustable low-dropout voltage regulator, SOIC-8 (REG34)
1 AP2317A P-channel Mosfet, SOT-23-3 (Q2)
1 red SMD LED, M2012/0805 size (LED1) **[Foshan NationStar NCD0805R1]**
1 red SMD LED, M1608/0603 size (LED2) **[Hubei KENTO Elec KT-0603R]**
5 green SMD LEDs, M1608/0603 size (LED3-LED7) **[Hubei KENTO Elec KT-0603R]**
2 SS14 40V 1A schottky diodes, SMA package (D1, D2)

Capacitors
3 100μF 6.3V B-case tantalum electrolytic **[AVX TAJB107K006RNJ]**
1 22μF 25V X7R M3216/1206 ceramic **[Samsung CL31A226KAHNNNE]**
7 10μF 50V X5R M3216/1206 ceramic **[Samsung CL31A106KBHNNNE]**
1 10μF 25V X5R M2012/0805 ceramic **[Samsung CL21A106KAYNNNE]**
2 2.2μF 16V M1608/0603 X5R ceramic **[Samsung CL10A225KO8NNNC]**
1 2.2μF 6.3V M1206/0402 X5R ceramic **[Samsung CL05A225MQ5NSNC]**
2 100nF 100V M2012/0805 X7R ceramic **[Samsung CL21B104KCFNNNE]**
2 100nF 50V M2012/0805 X7R ceramic **[Yageo CC0805KRX7R9BB104]**
1 100nF 50V M1206/0402 X7R ceramic **[Samsung CL05B104KB54PNC]**
23 100nF 16V M1206/0402 X7R ceramic **[Samsung CL05B104KO5NNNC]**
1 10nF 50V M2012/0805 X7R ceramic **[Samsung CL21B103KBANNNC]**
2 2.2nF 50V M2012/0805 NP0/C0G ceramic **[Samsung CL21C222JBFNNNE]**
1 1nF 50V M2012/0805 X7R ceramic **[Samsung CL21B102KBCNNNC]**

Resistors *(all SMD 1%)*
1 1MΩ (M1206/0402 size)
2 20kΩ (M1206/0402 size)
2 10kΩ (M2012/0805 size)
4 10kΩ (M1206/0402 size)
2 5.1kΩ (M1206/0402 size)
1 4.7kΩ (M2012/0805 size)
2 1kΩ (M1608/0603 size)
3 470Ω (M1608/0603 size)
2 220Ω (M2012/0805 size)
9 220Ω (M1608/0603 size)
2 10Ω (M2012/0805 size)
1 2.2Ω (M2012/0805 size)

created by a switching regulator, which can interfere with sensitive circuits such as analog inputs.

A system supervisor device (IC24, MAX809R) is used to monitor the 3.3V power rail and provide a reset signal to the RP2350B processor, to ensure it shuts down cleanly when the power is removed. It drives the reset pin of the RP2350B immediately when the voltage falls below a certain threshold, and will maintain it low for a short time after it has risen above the threshold.

In addition to the main 3.3V power supply, the RP2350B needs a second power supply called the Digital Core Supply (DVDD), which powers the CPU cores. Normally this is 1.1V, but for the clock speeds needed to generate HDMI video, it needs to be set higher (typically 1.3V).

In the Raspberry Pi Pico 2 module, this voltage is provided by a switching regulator that is integrated in the RP2350 chip but that causes some problems, including the need for an expensive and hard-to-source inductor. To avoid this, we use an external linear regulator, a TPS7A7002DDAR (REG34), which must be correctly adjusted before power is applied to the computer. The procedure for this is described later.

Fig.2: the overlay diagram for the RP2350B Computer. We recommend having the board pre-assembled due to the QFN-80 package RP2350B microcontroller.

Note: if you're not using the Computer with an enclosure, make sure not to leave it where children have access to it alone. Due to the risk of them swallowing the cell.

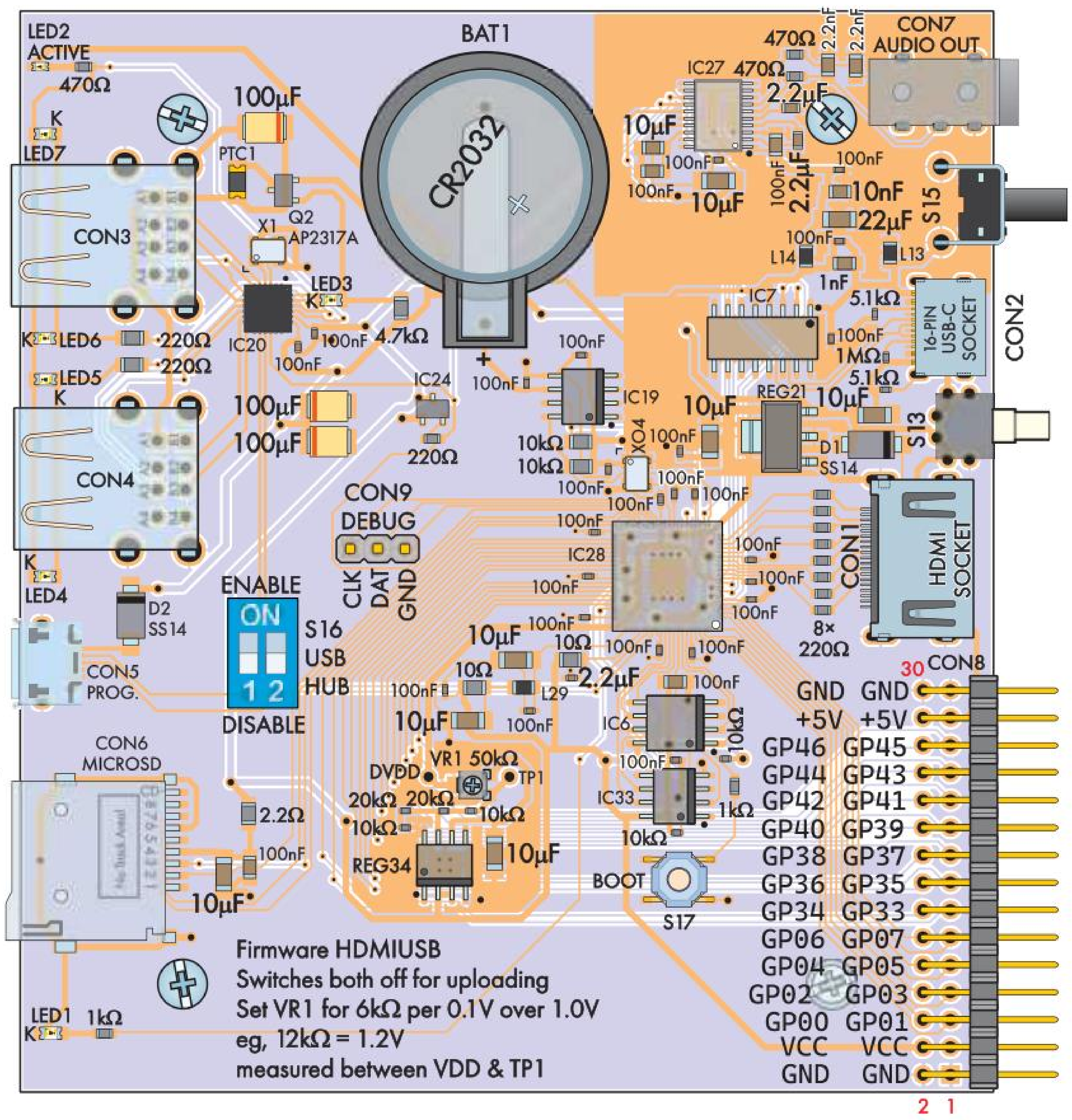
LED2
ACTIVE
470Ω
K
LED7
CON3
100µF
PTC1
X1
Q2
AP2317A
LED3
K
IC20
100nF
100nF
4.7kΩ
K LED6
220Ω
LED5
K
220Ω
100µF
100µF
CON4
IC24
220Ω
BAT1
CR2032
+
100nF
K
LED4
D2
SS14
CON5
PROG.
ENABLE
ON
1 2
S16
USB
HUB
DISABLE
CON9
DEBUG
CLK
DAT
GND
CON6
MICROSD
2.2Ω
100nF
10µF
LED1
K
1kΩ
Firmware HDMIUSB
Switches both off for uploading
Set VR1 for 6kΩ per 0.1V over 1.0V
eg, 12kΩ = 1.2V
measured between VDD & TP1
DVDD
VR1 50kΩ
TP1
20kΩ
20kΩ
10kΩ
10kΩ
REG34
10µF
10µF
10Ω
10Ω
L29
2.2µF
IC27
470Ω
470Ω
2.2nF
2.2nF
CON7
AUDIO OUT
2.2µF
10µF
100nF
100nF
10µF
100nF
2.2µF
100nF
10nF
22µF
S15
100nF
L14
L13
1nF
IC7
5.1kΩ
100nF
1MΩ
5.1kΩ
16-PIN
USB-C
SOCKET
CON2
100nF
IC19
10kΩ
10kΩ
XO4
REG21
10µF
10µF
D1
SS14
S13
IC28
CON1
HDMI
SOCKET
8×
220Ω
IC6
10kΩ
IC33
1kΩ
10kΩ
BOOT
S17
30
CON8
GND GND
+5V +5V
GP46 GP45
GP44 GP43
GP42 GP41
GP40 GP39
GP38 GP37
GP36 GP35
GP34 GP33
GP06 GP07
GP04 GP05
GP02 GP03
GP00 GP01
VCC VCC
GND GND
2 1

Building it

Fig.2 shows where all the parts go on the PCB. This design makes extensive use of surface-mounting parts. While these can all be hand-soldered, it is not easy, and can be quite time-consuming.

So, while it is possible to assemble this computer by hand, we recommend either buying it assembled from **www.electronpublishing.com/product/rp2350b-computer/** or having it assembled by a PCB fabricator.

For the latter, we recommend JLCPCB in China. The process of ordering the assembled boards from them is simple. First, download three files from the **siliconchip.au/Shop/10/3259**. These are "RP2350B Computer Gerbers.zip", which contains the design files for the PCB, "RP2350B Computer BOM.xlsx", which is the Bill of Materials (parts list), and "RP2350B Computer CPL.xlsx", which contains the component positions on the PCB.

On the JLCPCB website (**https://jlcpcb.com**), click on the "Instant Quote" button and drag the "RP2350B Computer Gerbers.zip" file onto the blue button labelled "Add Gerber File". JLCPCB will then read the files, display an image of the PCB and fill in the defaults for manufacturing options such as thickness, colour etc. You might want to select a different colour for the solder mask, but you can leave these options at the suggested defaults.

Scroll to the bottom of the page and select "PCB Assembly". This will display more options, which you can also leave at their defaults – other than selecting how many boards you want them to assemble (their minimum is two). Then click on the "Next" buttons until you reach the page requesting the BOM and CPL files. Add these files, then click on the "Process BOM and CPL" button.

The website will display a list of the parts, the quantity and their prices. All the components should be in stock but, if not, you can search for a substitute or even omit it and source it separately (which implies that you will solder it yourself). Clicking "NEXT" again will take you to the final quote detailing the total price and by clicking on "SAVE TO CART", you are done. You then need to go through the usual payment process.

Boxing it up

The RP2350B Computer's PCB is quite small, so you do not really need to mount it in a case. All you need is four rubber feet stuck to the bottom of the PCB to avoid scratching your desk (or tapped spacers in the corners, for the same reason). However, the PCB is designed to fit in a Multicomp MCRM2015S enclosure available from element14/Farnell. The same enclosure is also available as the Hammond RM2015S from Mouser, DigiKey etc.

For the front and rear panels, we have designed black PCBs with the lettering in white text. These can be ordered from the Electron Publishing shop or from a PCB fabricator (for this, download the Gerber files from **siliconchip.au/Shop/10/3259**). One nice thing about these panels is they have all the required holes, round or rectangular, neatly cut out for you!

If you are ordering the panels from JLCPCB, you should tick the option "Order Number (Specify Position)", as that instructs JLCPCB to place their tracking number on the rear of the panel. In the "PC Remark" section, you should add a note informing them that this design does not have any tracks and will be used as a front or rear panel on a box. Otherwise, they may reject the design as being incomplete.

Setting it up

When you receive the assembled boards, there are three steps that you need to take:

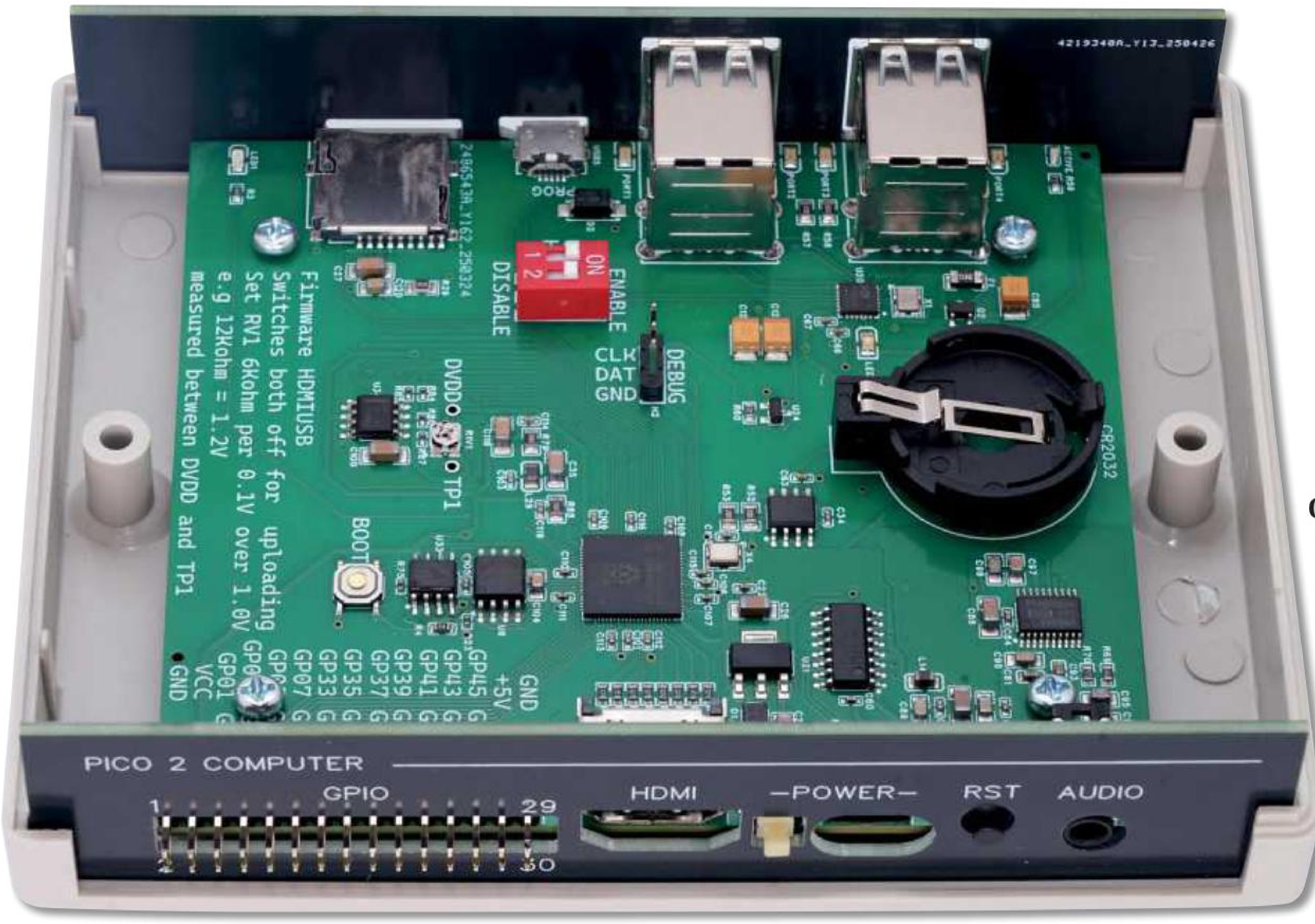

On the rear panel (from left to right) are the 30-pin external I/O connector with 22 GPIOs, the HDMI video connector, the power switch, a USB Type-C connector for power and the external console, a reset button, and the stereo jack for the audio output.

1. Adjust potentiometer VR1 to set the DVDD voltage. It is important that this is done before power is applied. Leaving the potentiometer in some random position could destroy the RP2350B processor.

2. Load the PicoMite firmware.

3. Configure the firmware.

By increasing the Digital Core Supply (DVDD) above the nominal 1.1V, we can overclock the RP2350B to reach the clock speeds (up to 375MHz) required to generate HDMI video. It is important that this is set before applying power to the board, as too high a voltage will certainly damage the RP2350B.

Set your multimeter to its resistance mode and, with the board unpowered, place the probes across the test points marked DVDD and TP1. Adjust potentiometer VR1 to give a reading of 18kΩ. This will set the DVDD voltage to 1.3V when the board is powered, and that should allow the RP2350B to correctly boot and generate a clear and stable DVI/HDMI video signal.

To load the firmware, start with no power applied and flip both switches on the PCB marked USB HUB to the DISABLE position. Then place the RP2350B into bootloading mode by holding the BOOT button down while plugging a USB cable from the front micro-USB socket into your desktop or laptop computer.

This will power up the Computer, causing the RP2350B to act like a USB memory stick and create a "disk drive" on your computer via the USB cable.

The RP2350B Computer requires MMBasic version 6.00.03 or later, as this has support for I²S audio. You can download this from siliconchip.au/Shop/6/833 or the author's website at https://geoffg.net/picomitevga.html (scroll to the bottom of the page). Extract the file PicoMiteHDMIUSBV6.00.03.uf2 (or a later version) from the ZIP.

You can then copy this file to the "disk drive" created by the RP2350B, and it will write the contents of the file to the flash memory chip. When it finishes, unplug the USB cable from the front USB socket and flip both switches on the PCB marked USB HUB to the ENABLE position. This will enable the USB hub and the front panel USB sockets.

While the virtual drive created by the RP2350B looks like a USB memory stick, it is not; the firmware file will vanish once copied, and if you try copying any other type of file, it will be ignored. If you later upgrade the firmware, note that loading the PicoMite firmware may erase all the flash memory, including the current BASIC program, any files in drive A: and all saved variables. So make sure that you backup this data first.

For the final configuration step, you need a desktop or laptop computer (or another USB serial console capable device) and use that to connect to the external console on the RP2350B Computer. This process is described in the panel overleaf. At the command prompt on the external console, enter the following command:

```
OPTION RESET HDMIUSBI2S
```

This will set up the firmware for your hardware configuration, including enabling the DVI/HDMI video output, and will save you from having to enter multiple OPTION commands for each hardware feature. After that, you can connect an HDMI monitor and keyboard/mouse, press the reset button and you should see the MMBasic startup banner on the monitor, as shown in Screen 1.

This is also a good time to set the date and time for the real-time clock. The command to do this is:

```
RTC SETTIME year, month,
  day, hour, minute, second
```

Here, "year" is two or four digits, and "hour" is in 24 hour notation. Don't forget to insert a CR2032 cell in the holder so the time will be remembered. As a final test, use the command:

```
OPTION RESOLUTION 1024
```

This will set the HDMI output to

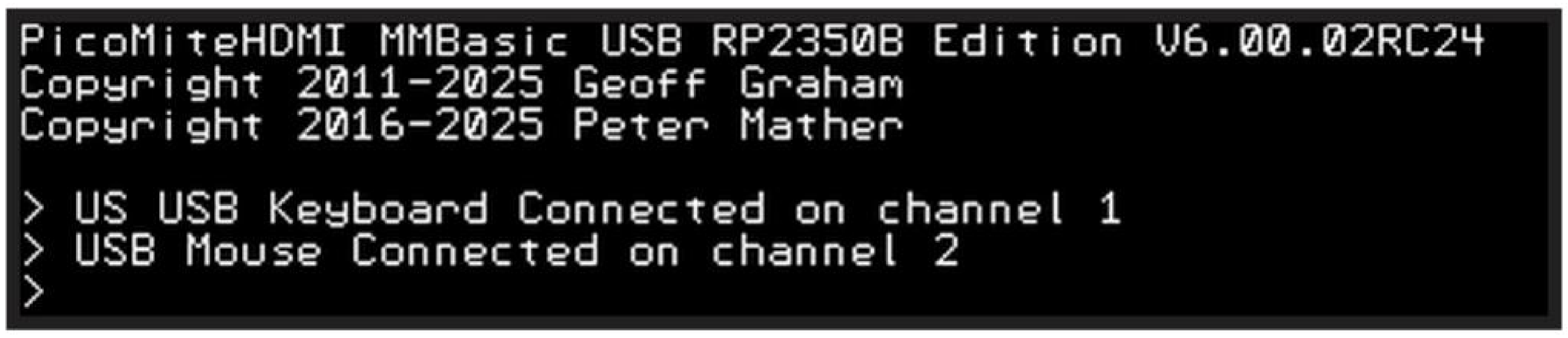

```
PicoMiteHDMI MMBasic USB RP2350B Edition V6.00.02RC24
Copyright 2011-2025 Geoff Graham
Copyright 2016-2025 Peter Mather

> US USB Keyboard Connected on channel 1
> USB Mouse Connected on channel 2
>
```

Screen 1: when you have loaded the PicoMite firmware, configured it and rebooted the computer, this is the startup screen that you should see. At this stage, you are ready to start running programs or creating your own.

its maximum resolution of 1024 × 768 pixels, and set the CPU clock speed to its maximum of 375MHz. The result should be a stable image on your monitor.

Adjusting DVDD

As described earlier, we need to increase the DVDD voltage, which powers the CPU cores, to facilitate overclocking. This is done by adjusting the onboard potentiometer as per Table 2.

By default, the RP2350B requires a DVDD of 1.1V, which is generally good for clock frequencies of up to about 220MHz. However, the firmware with HDMI capability will automatically set the clock frequency in the range of 252MHz to 375MHz, depending on the selected video resolution, so a higher voltage is needed.

We have tested many prototypes and found that a DVDD of 1.3V generally works well, which is why we recommend setting this voltage when configuring the board. However, if your Computer will not boot or shows strange behaviour, you can try DVDD voltages of 1.35V or 1.4V to see if that corrects the problem.

The absolute maximum that you should select is 1.45V. If your Computer still does not work, it is likely that overclocking is not the cause of your problem. Instead, you probably have some other fault on the board, which you should find and fix, rather than pushing the DVDD voltage even higher.

Resistance (TP1-DVDD)	DVDD
6.0kΩ	1.10V
9.0kΩ	1.15V
12.0kΩ	1.20V
15.0kΩ	1.25V
18.0kΩ	1.30V
21.0kΩ	1.35V
24.0kΩ	1.40V
27.0kΩ	1.45V
30.0kΩ	1.50V *
33.0kΩ	1.55V *
36.0kΩ	1.60V *

** not recommended due to instability*

You can set DVDD to voltages even higher than 1.4V if you wish to run the risk of damaging the RP2350B – but all processors should work correctly with 1.3V or 1.35V. You can also try DVDD voltages lower than 1.3V, and the RP2350B will run slightly cooler. However, this benefit will be limited, as raising the DVDD voltage and overclocking the processor only causes its temperature to increase by a few degrees Celsius.

Fault finding

While testing the settings for the DVDD voltage, it is possible to get the RP2350B and the firmware into a state where MMBasic will not boot or display a stable image on the monitor. If that happens, adjust the DVDD potentiometer to 6kΩ (giving a DVDD of 1.1V) and load the firmware file at: https://geoffg.net/Downloads/picomite/Clear_Flash_RP2350.uf2

This will reset the RP2350B to its factory state, allowing you to retry the setup procedure from the start.

A good test of a correctly functioning RP2350B is to load the stock PicoMite firmware without USB and HDMI support. This will run the RP2350B at its default frequency of 150MHz, and does not require any support circuitry except the 3.3V power and a DVDD of 1.1V.

To run this test, remove the power, then adjust the DVDD potentiometer to 6kΩ and set the onboard DIP switches to DISABLE. Then plug your desktop or laptop computer into the front panel USB socket while holding down the BOOT button on the PCB. You can then load the firmware file PicoMiteV6.00.03.uf2 (or later) from the firmware download ZIP file.

When this has completed, the firmware will create a serial-over-USB connection with your computer using the USB cable plugged into the front panel (leave the DIP switches in the DISABLE position). The PicoMite firmware user manual goes into detail on how to use this console connection, but with this you can load programs and test the processor as much as you like.

If this simple test does not work, check the main power to the RP2350B (3.3V) and the DVDD voltage (1.1V). If these are correct, that leaves a faulty RP2350B chip or its soldering as the main suspects.

Using MMBasic

The BASIC interpreter in the PicoMite firmware is called MMBasic. It is a modern implementation of the BASIC language that can handle large and complex programs. MMBasic includes features like long variable names, 64-bit integers, double-precision floating-point numbers and string variables. It does not need line numbers, and includes modern features such as subroutines/functions, CASE and multiline IF-THEN-ELSE statements.

On startup, MMBasic will display the command prompt (the greater-than symbol, ">") and wait for a command to be entered. It will also return to the command prompt if your program ends or generated an error message. When the command prompt is displayed, you can run a wide range of commands. For example, you can list the program held in memory (LIST) or run it (RUN).

Almost any command can be entered at the command prompt, and this can be used to test a command to see how it works. A simple example is the PRINT command, which you can test by entering PRINT "Hello World" at the command prompt.

To enter a program, you can use the EDIT command, which starts the integrated full-screen editor. This is described in detail in the PicoMite User Manual. However, if you want to give it a test, all you need to know is that anything that you type will be inserted at the cursor, the arrow keys will move the cursor and backspace will delete the character before the cursor. Finally, the F1 key will save the program and exit.

The firmware will automatically create a pseudo 14MiB 'disk drive' in the flash memory. This is called drive "A:", and can be used to store programs, images, music, configuration data, log files and much more. In addition, SD cards formatted as FAT16 or FAT32 up to 32GiB can be used for removable storage, and are referred to within MMBasic as drive "B:".

Files created in this file system can be read on Windows, Linux and macOS computers. Both file systems support long filenames, subdirectories, long file paths, random access and more.

The PicoMite User Manual is an invaluable resource that contains a detailed description of the capabilities of the firmware and the MMBasic interpreter.

One inclusion that is particularly useful is a tutorial on programming in BASIC at the rear of the manual. It is written in an easy-to-read format, with plenty of examples, and is recommended for anyone who is new to programming in BASIC.

This manual is included in the firmware download from the Silicon Chip website or the author's website at https://geoffg.net/picomite.html (scroll to the bottom of the page).

MMBasic graphics features

MMBasic has an extensive range of features that complement this computer's colourful, high-resolution video. Most are associated with the type of graphics that you would need for games, but they are also useful for business graphics and general programs. These commands and functions are described in detail in the PicoMite User manual, and in a tutorial that is included with the firmware distribution files.

Each DVI/HDMI resolution is selected with the OPTION RESOLUTION command and, for each resolution, there are a number of colour modes that can be selected with the MODE command. These modes will increase the visual size of each graphic pixel and use the memory saved to support more colours.

For example, with the resolution set to 640 × 480 pixels, you can select MODE 1 which will result in a monochrome 640 × 480 pixel display, or MODE 4, which will quadruple the size of each graphic pixel and provide more colours so that the user will see an image of 320 × 240 pixels in 32,768 colours. In both modes, the physical monitor will continue to see a video signal with a resolution of 640 × 480 pixels.

Connecting to the External Console

You communicate with MMBasic via the console, which is where you see the command prompt and type in your commands. In the RP2350B Computer, the main console is the keyboard and HDMI monitor, but you can also open an external console on your desktop or laptop computer.

This is provided via the rear-panel USB connector, which is normally used to power the computer. However, it can also provide a serial-over-USB interface for the external console.

This function is provided by the CH340C USB/serial bridge. This chip (and the similar CH341) is used in many Arduino Nano clones, and the driver for it is included by default in Windows 10/11 and Linux. Many macOS builds also include the driver. This means that you can simply plug your RP2350B Computer into your desktop computer and a connection will be automatically made.

However, if you do need a driver, help is available at **https://sparks.gogo.co.nz/ch340.html**

When you connect the RP2350B Computer, it will create a virtual serial port on your computer; you need to determine the number of this port. In Windows, this can be found in Control Panel → Device Manager → Ports (COM & LPT). The PicoMite User Manual included in the firmware download goes into more detail.

On your desktop computer, you then need to run a terminal emulator. For Windows, we recommend Tera Term, which can be downloaded from **http://tera-term.en.lo4d.com**. Within the terminal emulator, you need to set the serial port number discovered above and set the baud rate to 115,200 baud (the default speed used by the RP2350B Computer).

You should then be able to hit the Enter key in the terminal emulator and see the MMBasic command prompt (">"). When you are connected to the remote console, you can treat it the same as a keyboard/monitor combination directly connected to the RP2350B Computer. You can issue commands, edit programs and run them. You can also use the XModem protocol to transfer files to and from both computers.

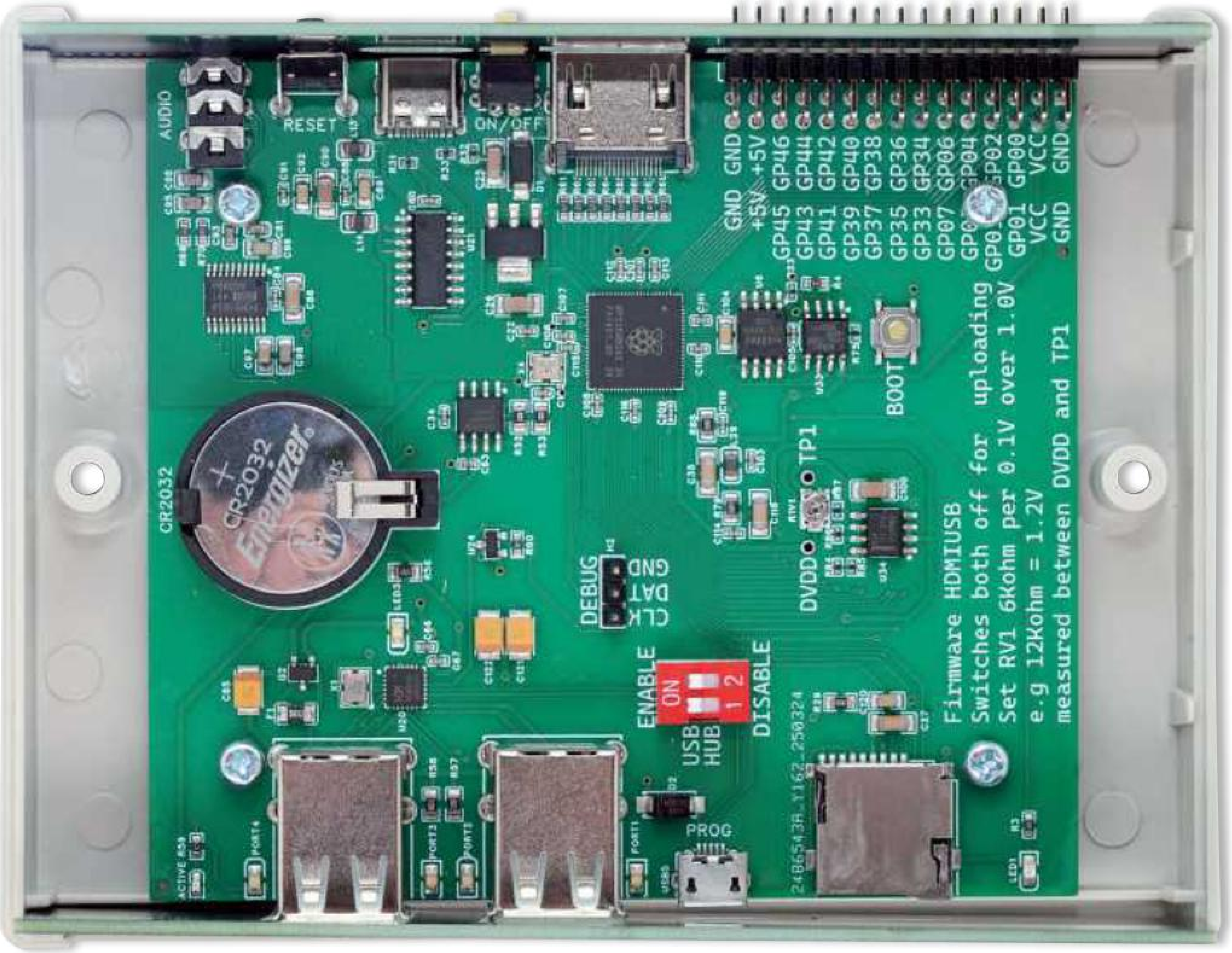

The PCB is designed to fit in a Multicomp MCRM2015S or Hammond RM2015S enclosure. At lower left are the four USB Type-A ports that can accept USB keyboards, mice and game controllers. To the right of those is a micro Type-B USB connector for loading the firmware, and finally, a microSD Card connector that will accept cards formatted in FAT16 or FAT32 with capacities up to 32GiB.

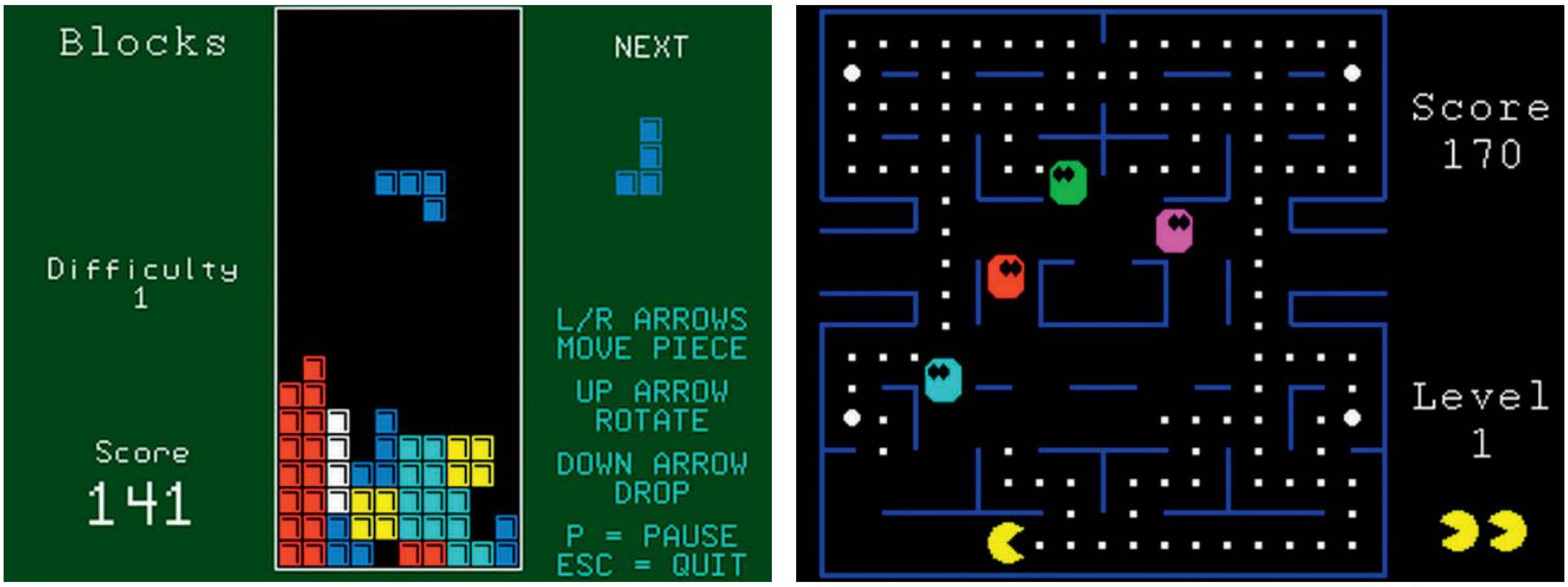

Screens 2 & 3: the software package for the RP2350B Computer includes clones of two classic games, Tetris and Pacman. They are provided so that when you get your computer running, you can immediately start having fun!

Colour is specified as a true colour 24 bit number, like on a PC. The top eight bits represent the intensity of the red colour, the middle eight bits the green intensity, and the bottom eight bits the blue. You also have at your disposal functions that give you shortcuts for selecting commonly used colours and defaults, such as the RGB() function.

There are ten basic drawing commands that you can use within MMBasic programs to draw graphics. These include drawing lines, boxes, circles and even complex polygons. The TEXT command is one of these, and is particularly powerful, allowing text to be positioned anywhere on the screen in a variety of fonts and orientations.

The RP2350B Computer includes eight built-in fonts. These range from tiny to large and most cover the full ASCII range, with some including extended graphics characters. You can also define your own fonts using the DEFINEFONT command; additional fonts are included in the PicoMite firmware download. These fonts cover a wide range of character sets, including a symbol font (Dingbats) that is handy for creating on-screen icons etc.

Framebuffers, layers & sprites

To create moving graphics like those used for games, MMBasic includes support for framebuffers and layers. These are areas of memory with the same width and height as the DVI/HDMI image, and the same colour depth.

Framebuffers can be used to construct an image that can then be rapidly copied to the physical display. Layer buffers are slightly different, and are used to create partial images that can sit on top of a background image, which can be moved over the static background.

Sprites are very useful as they allow the programmer to display elements over a background and then move them over the background without corrupting the background image. In addition, the programmer can use the sprite functions to detect collisions between sprites and between a sprite and the edges of the display.

The LOAD IMAGE and LOAD JPG commands can be used to load an image from a file and display it on the HDMI monitor. These can be used to draw a logo or add an ornate background to the graphics drawn on the screen.

The 3D Engine provided by MMBasic includes ten commands for manipulating 3D images, including setting the camera, creating, hiding, rotating etc. These are documented in a separate manual in the PicoMite firmware download, which provides a description of the 3D Engine and how to use it.

Also included in the firmware download are clones of two classic games: Tetris and Pacman (see the screenshots). So, when you get your RP2350B Computer running, you can immediately start wasting time. Have fun!

RP2350B0A2 35
PAYA01.00 24
C115

Most of the complexity is in the software loaded into the Raspberry Pi RP2350B processor. This has the same features as the RP2350A version used in the Raspberry Pi Pico 2, but comes in a larger package with more (48) I/O pins. The Raspberry Pi foundation has recently made this chip available for individual sale, so now we can use it in our own designs.

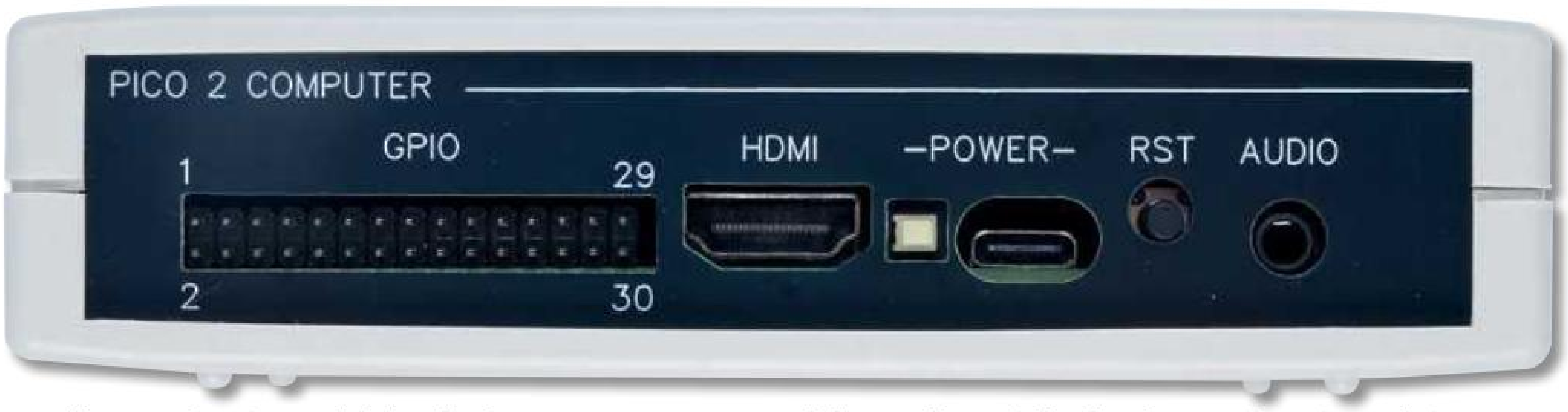

We have designed black front & rear panel boards with the lettering in white. These can be ordered from our PCB service or a PCB fabricator.

The Fox Report

Barry Fox's technology column

An opportunity for Manhattan's new Freeview box

As Sky switches customers from satellite dish reception to online streaming, there is a growing park of satellite dishes ready, willing and able to deliver free TV and radio via the Freesat service – which is roughly equivalent to terrestrial Freeview. The main difference is that Freesat has some extra free channels (100+ in all, with 35 in HD).

So now seems a very good time for the industry to sell Freesat receivers and recorders. That's what makes it so strange that Humax, one of the pioneers in satellite reception, has quit the Freesat market. But this has created a big opportunity for Humax's main rival in the "Free TV" business, Manhattan.

So it was no surprise that the 30-year-old British company recently announced a new Freesat receiver/recorder to match its existing Freeview recorders. The S4-R Freesat 4K TV Recorder is Manhattan's fourth-generation Freesat device. Conventionally, it has two tuners to record two program channels at the same time from a dish with two LNBs.

However, if the dish has a more modern wideband LNB, as used for Sky Q, the S4-R can 'tape' four channels at once. This is possible because a wideband LNB outputs all the vertically polarised signals via one dish feed and all horizontal signals via a second dish feed. A smart receiver/recorder, like the S4-R, then decodes the two feeds into four program channels.

Personally, I prefer to use the original type of LNB, but with four (Quad) or eight (Octo) F-plugs (instead of the usual two). That way, I can run separate satellite feeds to receivers and recorders in different rooms, with spare feeds to check dish alignment by testing signal strength.

As the name suggests, the new Manhattan Freesat box can also handle 4K Ultra HD, if and when 4K broadcasts are available, or when streamed.

The current Manhattan model has an onboard 500GB HDD, with 1TB and 2TB versions to follow, giving 300, 600 or 1,200 hours TV recording time. Live TV can be paused for up to two hours and rewound, too.

The user interface is clean and clear, disinguishing between live TV channels and on-demand content from streaming sources such as BBC iPlayer, ITVX, Channel 4 and 5. For copyright reasons, the streamed content cannot be recorded – just as Freely streams cannot be (legitimately) recorded.

(Tech literates will of course already be aware of the low cost HDMI-to-USB capture dongles, which are widely and openly sold online to connect a receiver to a PC running free capture software like OBS).

Pricing for the Manhattan TV S4-R 500GB model is £219.99, £249.99 for the S4-R 1TB and £279.99 for the S4-R 2TB.

The box has both Ethernet and WiFi Internet connections and an optical S/PDIF socket for digital audio output to a soundbar or hi-fi system.

There's a clear instruction book printed on good old-fashioned paper – not just a weblink to an online manual.

I found setting up the Manatattan Freesat box easy and intuitive, with no need for the manual. During the process, I discovered a valuable diagnostic tool buried in the interface.

When I plugged two dish LNB feeds into the receiver's two F-plug sockets, the set-up screen warned that there was signal from only one. This suggested a bad connection or open circuit in one feed.

But the screen also showed an "LNB Overload Detected" error message. I've not seen this before. Manhattan's helpful Help explained that this message means the LNB feed is drawing heavier than usual DC current from the box, probably because of a short circuit in the feed cable, between the signal core copper and outer braiding.

Armed with this simple clue, I tracked the cause down to a short circuit in one of the dish feeds. Once this was repaired, the error message disappeared and high-quality pictures appeared.

I also had problems connecting the box to my fibre broadband. A different error message helpfully told me that the box was connecting to my home network but not to the internet, either via an ethernet cable or by WiFi. But other equipment on the same network was working normally.

It's unclear why this happened. It could be related to the IPv6 settings on my router. I'll probably never know because the problem self-solved when I played the usual trick of shutting down and rebooting everything on the entire home network, to create a whole new stack of dynamic IP addresses.

As the *IT Crowd* always initially asked their helpline callers, "Have you tried switching it off and on again?"

Perhaps it would make sense if all error message for all equipment now routinely offered similar off-and-on-again advice.

Bottom line conclusion: Even if it weren't one of the few Freesat boxes left to buy, I'd be wholeheartedly recommending the Manhattan S4-R.

Vape-powered drones

I've previously written about the free source of lithium-ion rechargeable cells littering our streets. Every discarded single-use vape contains a good-as-new battery. As long as you use a safe charger designed for lithium-ion cells, several cells in parallel make a very useful power bank.

Since the sale of single-use vapes has been banned, there have been fewer and fewer discards to pick up. But there are obviously stockpiles of unsold vapes, and they are now finding a good home

A workshop in Ukraine is ganging batches of around fifty cells together to make a battlefield power bank, or using smaller clusters to fly drones.

The story is here to read, with some videos which (hardly surprisingly) don't reveal much about the manufacturing process: **https://pemag.au/link/accb**

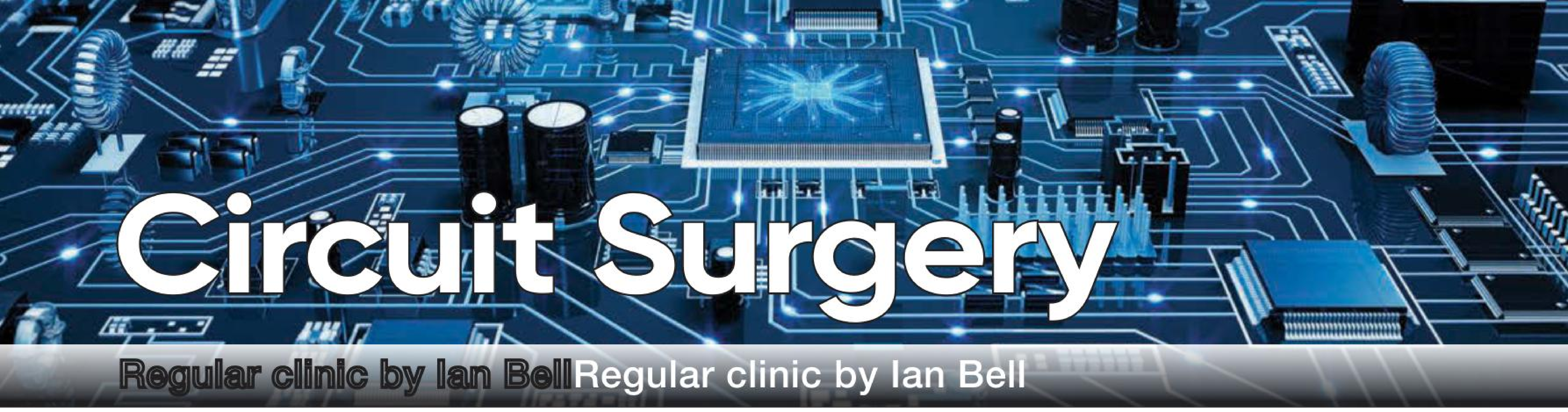

Circuit Surgery

Regular clinic by Ian Bell

Regular clinic by Ian Bell

Measuring circuit frequency response using a PC sound card, part 11: anti-aliasing & reconstruction filter circuits

Over the past few months, we have been looking at circuit frequency response, including implementing a measurement system using the 'sound card' (audio interface) of a PC or laptop together with free software called REW (Room EQ Wizard).

This was motivated by the need to measure the response of a practical implementation of an example digital filter, from our series on digital signal processing (DSP), without using advanced lab test equipment.

We have described various aspects of the signal conditioning circuitry that might be needed to interface the circuit under test to the sound card's line inputs and outputs. As noted, the inspiration for the measurement system was a DSP system, and in general, DSP circuits need analog anti-aliasing and reconstruction filters.

The requirements for these filters were discussed in depth in the DSP series, but we did not look at specific circuit designs then. Our simulations used idealised behavioural anti-aliasing and reconstruction filters where needed, as we were focusing on the digital aspects of the system.

The signal conditioning circuit for the measurement system did not include a filter, as this was considered part of the circuit under test (the digital filter system). However, an op amp based reconstruction filter was designed specifically for use in the test setup.

This month, we will look at analog filter design with this reconstruction filter as an example. First, we will quickly recap anti-aliasing and reconstruction filters, then cover some key basic analog filter circuit concepts using single op amp stages.

As with other recent articles, our discussion will have wider applicability than just the frequency response measurement and DSP systems, with the reconstruction filter used as an example.

Anti-aliasing and reconstruction filters

DSP systems often require analog filters at their inputs and outputs (see Fig.1) to prevent signal degradation due to the fundamental mathematical properties of the DSP system.

Most DSP systems take samples of their analog input signal at a fixed rate (the sampling frequency or rate, f_s) and convert these samples to digital data for processing. The system may have an adjustable sampling frequency, but generally the processing operations occur at fixed intervals once a specific rate is set.

Mathematical analysis of the process of sampling a signal shows that signals with a frequency of less than half the sampling frequency are reliably represented in the sampled data. This is known as the Nyquist sampling theorem.

The theory shows that if the input does not contain any frequency components at or beyond half the sampling frequency ($f_s/2$, known as the Nyquist frequency), it is possible to perfectly reproduce the original signal from the sampled data.

If the signal contains frequencies at or above $f_s/2$, an effect known as aliasing occurs. These frequencies become indistinguishable from other frequencies in the range up $f_s/2$, which means that the sampled signal is not an accurate representation of the original signal.

So, if the input signal contains frequencies at or above $f_s/2$, these must be removed by an anti-aliasing filter before the signal is sampled to avoid affecting the resulting samples.

How demanding this filtering is depends on how close the maximum wanted signal frequency is to $f_s/2$ and the amplitude of any unwanted signals at or just above $f_s/2$. Demanding conditions require a filter which has a very sharp cut-off close to $f_s/2$, with a gain that rapidly drops to a very low value.

The demand on the filter can be reduced by increasing the sampling frequency so that $f_s/2$ is further from the maximum wanted signal frequency. In that case, the cut-off doesn't have to be as sharp to avoid affecting the wanted signals while heavily attenuating the unwanted ones.

The DSP system under test in the frequency response measurement system did not include an anti-aliasing filter because the signal generation system was not configured to produce frequencies above the Nyquist frequency.

The spectrum (frequency content) of a sampled signal comprises images of the original signal repeated at multiples of the sampling frequency. At the top of Fig.2 is the spectrum of a signal sampled at $f_s = 50\text{kHz}$ where the original signal has a frequency content from DC up to a maximum of 20kHz. The images occur centred on 50kHz, 100kHz and other multiples of 50kHz (not shown).

When the sampled signal is converted to analog form using a DAC,

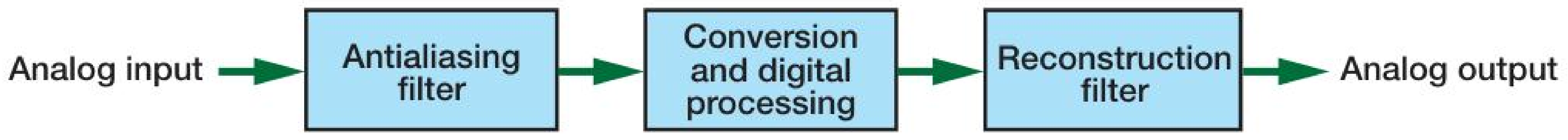

Fig.1: the role of analog filters in a DSP system.

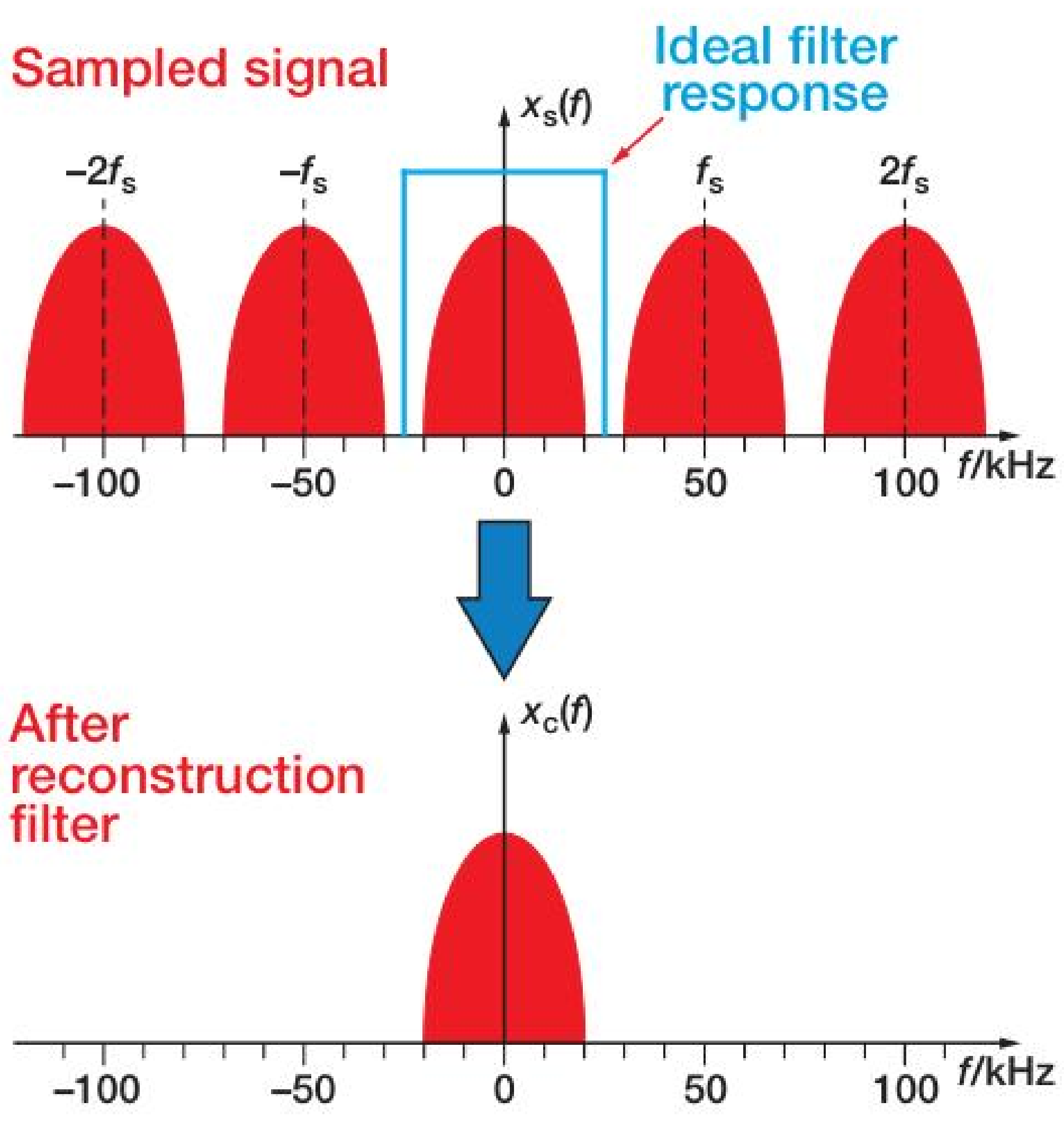

Fig.2: the action of a reconstruction filter in the frequency domain.

the image frequencies will be present in the DAC output signal. To correctly recover only the wanted signals , it is necessary to remove image frequencies using an analog reconstruction filter. An ideal filter with a cut-off of $f_s/2$ will achieve this (see Fig.2).

If the filter is able to perform this task perfectly, its output will only contain the wanted signals (the lower spectrum in Fig.2). In simple terms, you can think of this as the filter smoothing out the stepped output from the DAC.

Note that negative frequencies are also shown in Fig.2, which is usual when analysing DSP systems and related to the mathematics involved. In this case, the negative part of the spectrum is just a reflection of the positive part.

Also, the output spectrum of a DAC is not exactly the same as that of the set of samples (as shown in Fig.2) due to its frequency response, which follows the sinc mathematical function. These and other details of sampled signals, the requirements of anti-aliasing and reconstruction filters, and many other aspects of DSP were covered in depth in our series on the topic.

Our initial testing of the DSP hardware implementation used a simple RC filter, which was sufficient for basic checking but had some impact on the overall frequency response.

To prevent this influencing the results with the PC-based measurement system, it was replaced with an active filter that had a flat response in the frequency range used for testing. The filter cut-off was 20kHz and the DSP filter's Nyquist limit was 24kHz.

Bandforms and filter features

In simple terms, a filter is a circuit that passes certain frequencies (in the passband) and rejects others (in the stopband). Based on this definition, there are four basic classes of filter, referred to as bandforms, which are shown in idealised form in Fig.3. These are graphs of the filter's frequency response, plots of gain versus frequency.

Low-pass filters let low frequencies through and block high frequencies. High-pass filters let high frequencies through and block low frequencies. Bandpass filters let a specific range of frequencies through. Bandstop filters reject a specific range of frequencies.

Some other terms are used for specific cases. A notch filter is a bandstop filter with a very narrow stopband, which can be useful for rejecting a specific unwanted frequency. A comb filter has multiple, regularly spaced stopbands and passbands.

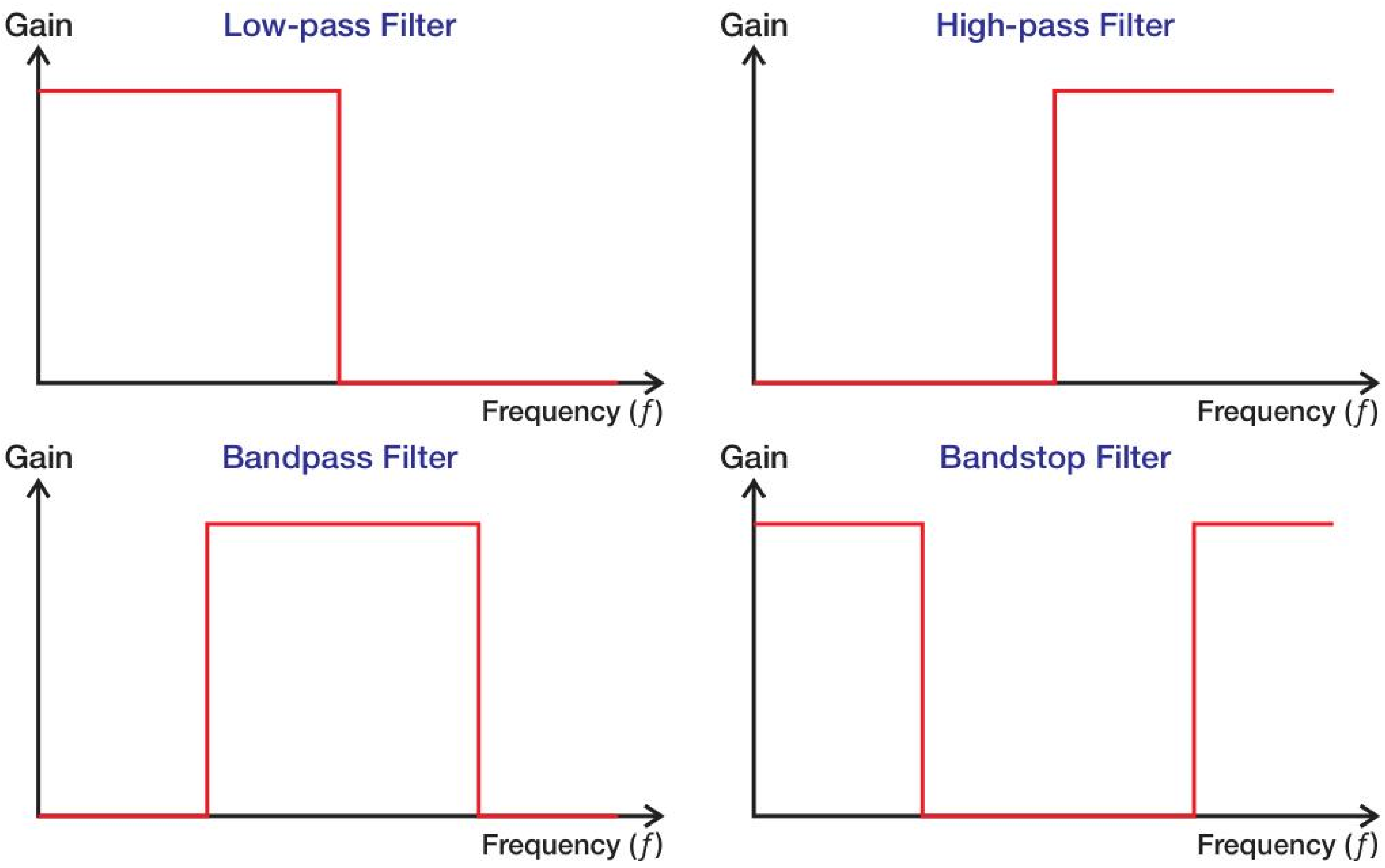

Fig.3: basic filter bandforms. Real filters don't have such steep transitions!

In addition to these frequency-dependent gain responses, there are also all-pass filters which have frequency-dependent phase shift (delay) but equal gain at all frequencies (see the recent Audio Out articles by Jake Rothman for more on these circuits).

Anti-aliasing and reconstruction filters are low-pass filters, so we'll concentrate on those in this article. However, many of the points we discuss will be relevant to other types, as are the tools which can be used to facilitate their design.

The idealised (so-called 'brick wall') filters in Fig.3 cannot be implemented. For real filters, the transition from the passband to the stopband occurs over a range of frequencies. Furthermore, the gain in the passband may not be constant (as it is implied by Fig.3) and the stopband gain will not be either zero (complete rejection) or constant at some low level.

Fig.4 shows a low-pass response with features that occur in real circuits.

Without a perfectly sharp cut-off, we need to specify exactly what we mean by the cut-off frequency. For a flat passband, the cut-off is often defined as the frequency where the filter's gain is -3dB with respect the passband gain. This is the point where the output signal has half the power it does in the passband.

For filters with passband ripple, the cut-off frequency may be defined as the frequency where the response has dropped by an amount equal to the ripple size relative to the maximum passband gain.

However, it may also be defined in terms of the gain relative to that deep in the passband (for example, very low frequencies in the case of a low-pass filter). When looking at filter specifications or design tools, take care to check how the cut-off frequency is defined.

To design a filter, we need to specify our requirements with respect to the features shown in Fig.4. By defining the cut-off frequency and gain at cut-off, the stopband frequency and gain at this frequency, and the passband gain and ripple, we effectively define a region of the response graph into which an acceptable response curve must fit (the green area in Fig.4).

Filter design tools often require these values to be entered directly, although the ripple and stopband values may be determined by other choices; for

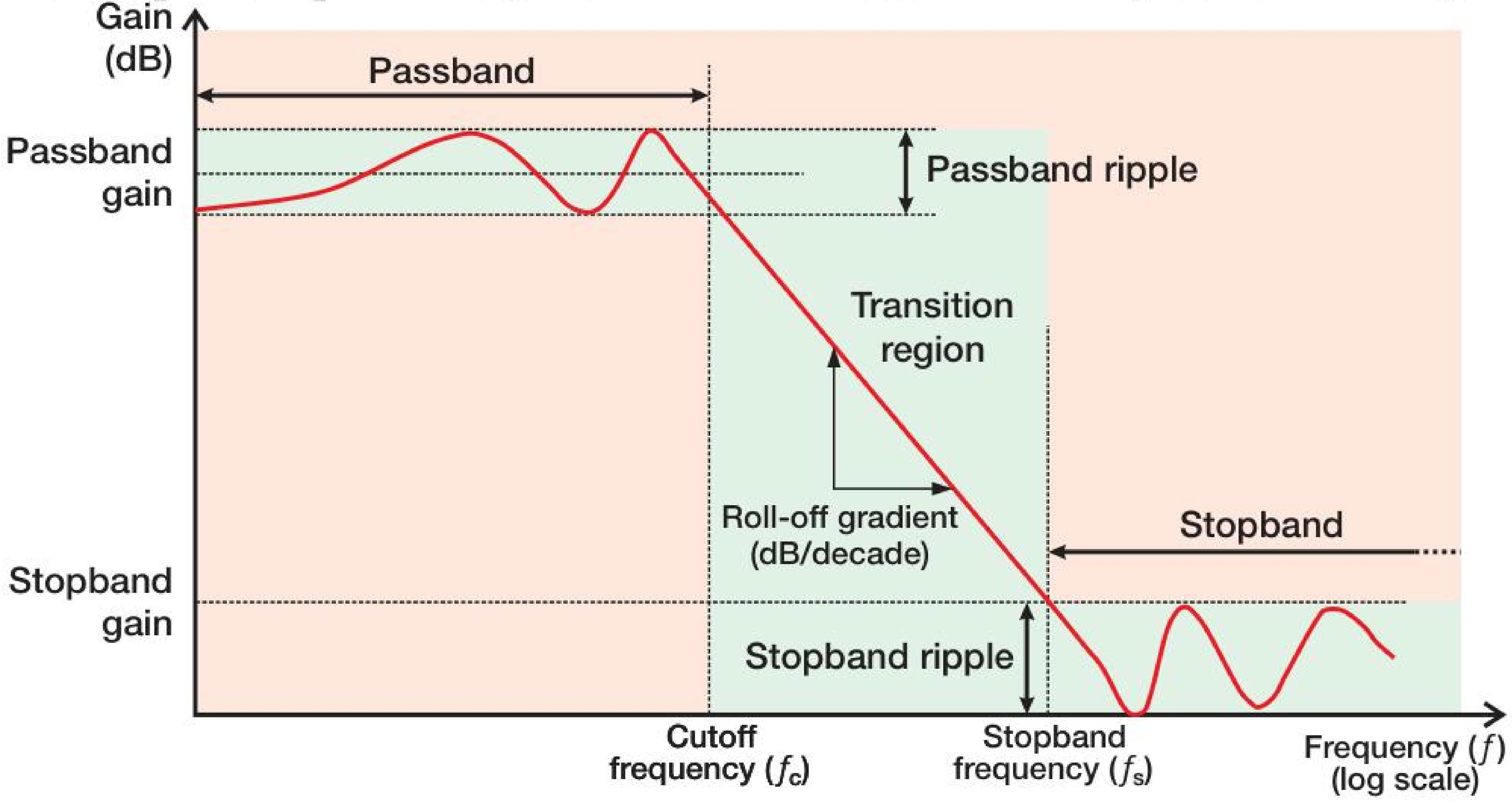

Fig.4: features of filter frequency response curves.

example, if a specific response type (see below) is selected. Some tools display graphics similar to Fig.4 to provide feedback to the user as values are entered.

On filter response plots, the gain or attenuation is usually plotted in decibels, which is a logarithmic scale. For a voltage gain A, the value in decibels is 20log10(A)dB. The frequency axis of the graph is also usually logarithmic with the scale marked in multiple-of-ten steps, referred to as decades.

However, linear scales are also used when appropriate, to emphasise specific features or when the range plotted is small (eg, for narrow band filters).

Response types

There are various standard filter response types available, named after their related mathematics. Widely used responses include Butterworth, Bessel and Chebyshev, but these are not the only ones. The features shown in Fig.4 vary with different response types, and there is a trade-off in terms of desirable features.

Various common filter responses are shown in Fig.5 and Fig.6. These all have a cut-off frequency of 20kHz, defined here as being the point the gain falls to 3dB below the low frequency gain (DC gain), which in this case is 0dB.

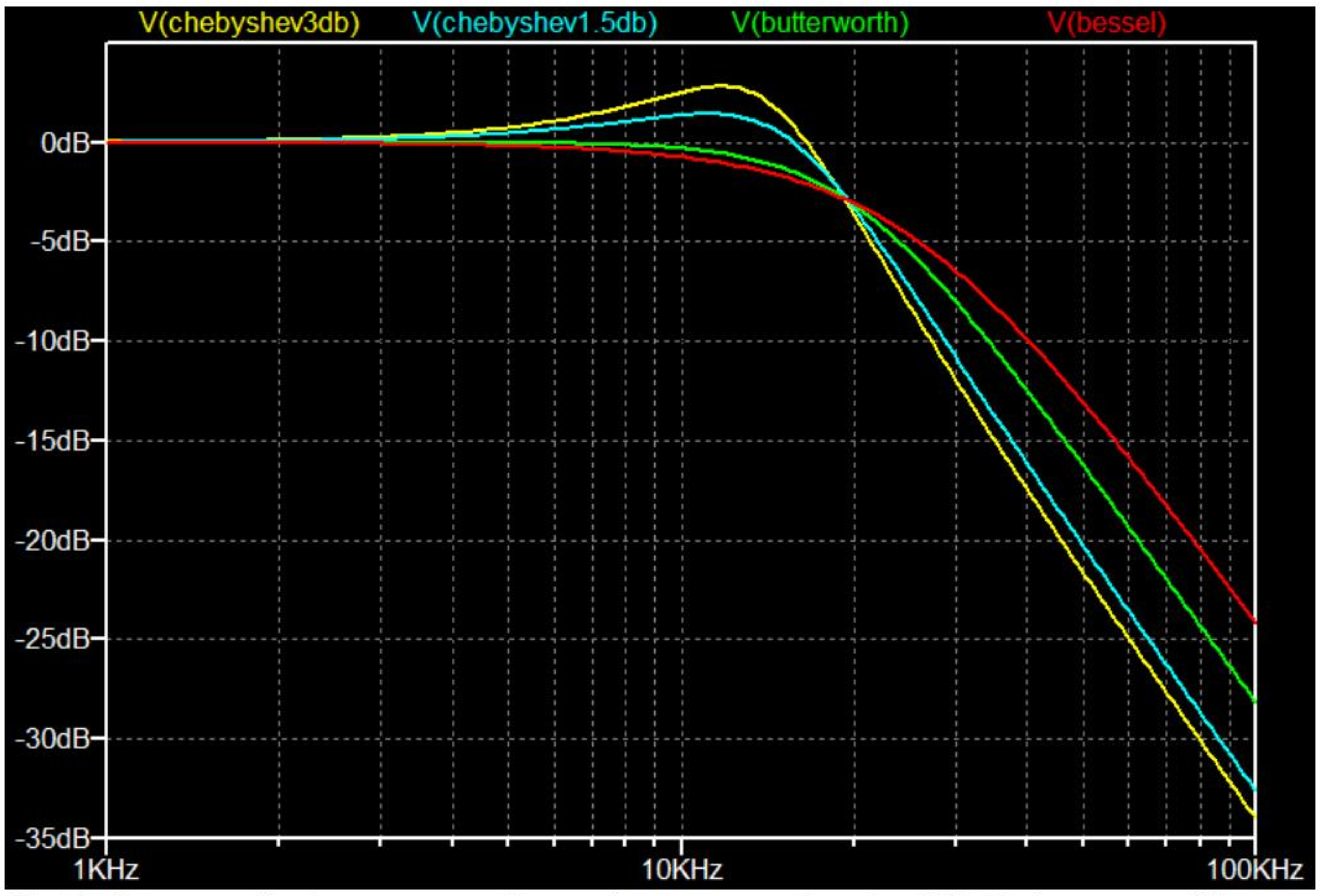

Fig.5: the magnitude response for various second-order 20kHz low-pass filters.

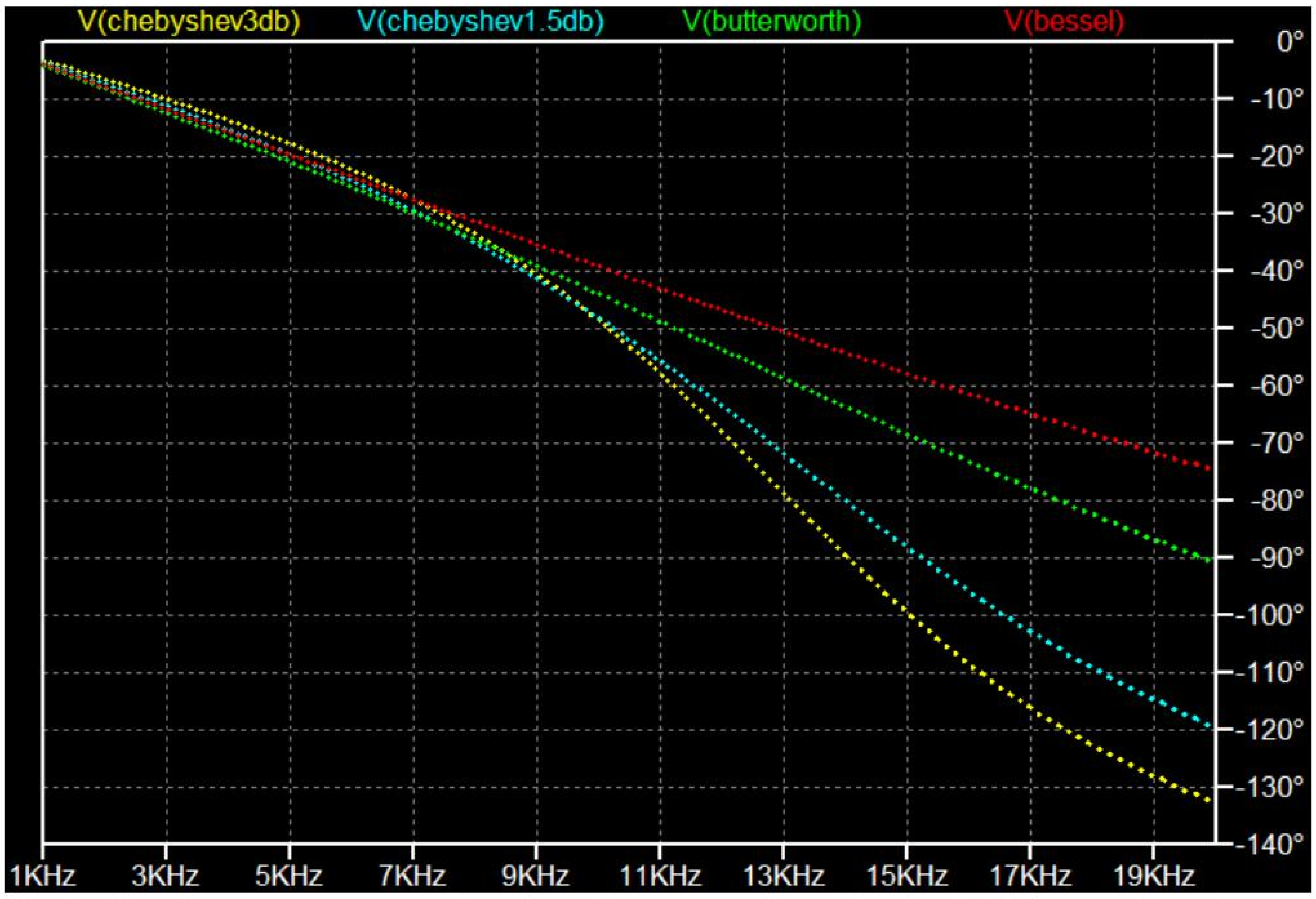

Fig.6: the phase response of various low-pass filters in the 20kHz passband, shown on a linear frequency axis.

Butterworth filters have maximally flat passbands with a relatively slow gain change near the cut-off. Chebyshev filters have passband ripple, but their gain decreases more rapidly near the cut-off. The amount of ripple can vary, with higher ripple giving faster cut-off (Fig.5, which shows examples with 3dB and 1.5dB ripple).

Bessel filters have maximally flat delay, which is equivalent to a nearly linear increase in phase shift with frequency across the passband (see Fig.6), resulting in minimal distortion. Fig.6 is plotted using a linear frequency axis so that the linearity (or otherwise) of the phase responses is clear.

Although we have named certain response types, in practice, a continuum of responses is available. Chebyshev filters with very small ripple are similar to Butterworth filters, and responses in between pure Butterworth and Bessel are available too.

The roll-off, or slope, of the frequency response in the transition region/stop band (see Fig.4) indicates how quickly the filter's gain drops as the frequency moves away from cut-off. Roll-off is usually measured in dB per decade and typically changes with frequency near the cut-off.

However, for frequencies well into the transition region/stop band, the response of many filters tends to decrease as a straight line when plotted on a graph of decibels against log frequency, as in Fig.5.

The ultimate roll-off is determined by the order of the filter; the higher the order, the faster the falloff. A single RC filter is 'first order' and rolls off at 20dB/decade. An *N*th-order filter rolls off at 20(*N*)dB/decade. The order of the filter determines the ultimate roll-off, but the response type (Butterworth, Chebyshev etc.) determines the shape of the response near the cut-off.

All the filter responses shown in Fig.5 are second-order types ($N = 2$) with an ultimate roll-off of 40dB/decade. The response curves run in parallel at higher frequencies, which is more obvious if you plot a larger frequency range than in Fig.5.

Resonance

A value called *Q*, or quality factor, of a filter determines the response type (the shape of the frequency response). For the responses shown in Fig.5, the *Q* values are 0.577 (Bessel), $0.707 = \sqrt{2} \div 2$ (Butterworth), 1.04 (Chebyshev 1.5dB ripple) and 1.3 (Chebyshev 3dB ripple).

Higher *Q* values result in larger peaks in the response. Low- and high-pass filters typically have relatively low *Q* values, while bandpass filters (particularly narrowband types) have higher *Q* values.

The properties of many filters are related to resonance. Resonance is often experienced in the tendency of some systems to respond at greater amplitude when applied oscillations match the system's natural frequency of vibration (the resonant frequency).

Often quoted real-world examples

Fig.7: an RLC second order low-pass filter.

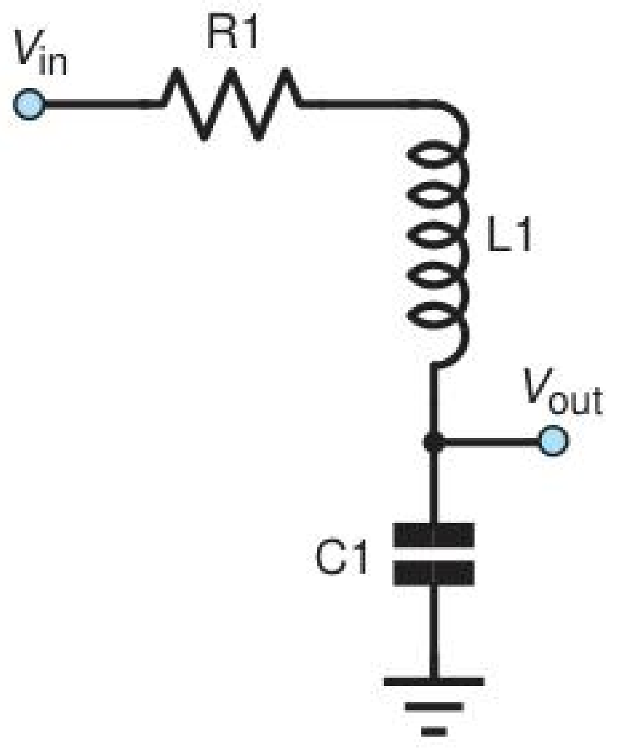

include playground swings (you have to push at the correct rate) or wine glasses shattered by singers hitting just the right note.

Resonance involves the exchange of energy between two different storage mechanisms. For mechanical examples, like the glass and swing, these are potential and kinetic energy. At the resonant frequency, the energy exchange is at its most efficient, which means that minimal energy is lost in the transfer.

This means that any energy input by a driving force (the sound waves from the singer or the person pushing the swing) produces the greatest amplitude of oscillation when it is at the resonant frequency, because relatively little energy is dissipated in each cycle.

Q is a measure of how efficient the energy exchange at resonance is. It is proportional to the energy stored divided by the energy dissipated in a cycle. A higher *Q* means lower dissipation at resonance and hence a higher amplitude peak for a given driving force or input.

RLC circuits (for example, Fig.7) are a well-known way to implement filters. They are resonant, with the energy exchange being between that stored in an electric field (in the capacitor) and a magnetic field (in the inductor). The resistance affects the *Q* – higher resistance means more energy is dissipated in each cycle, so a lower *Q*.

RC and RL circuits can also be used as filters, but are not resonant, as they only have one storage mechanism. It is possible to find a *Q* value using an energy stored to dissipated ratio, but it is low (0.5 or less) and, unlike for an (ideal) RLC circuit, varies with frequency. This means that we cannot make sharp cut-off filters with just RC or RL circuits.

Active filters built from op amps resistors and capacitors (for example, Fig.8) lack the magnetic field storage provided by inductors in RLC circuits, but they are able to behave in ways that are mathematically equivalent to RLC resonant circuits (the circuits in Fig.7 and Fig.8 can provide equal responses). They are therefore able to achieve high *Q* values if required.

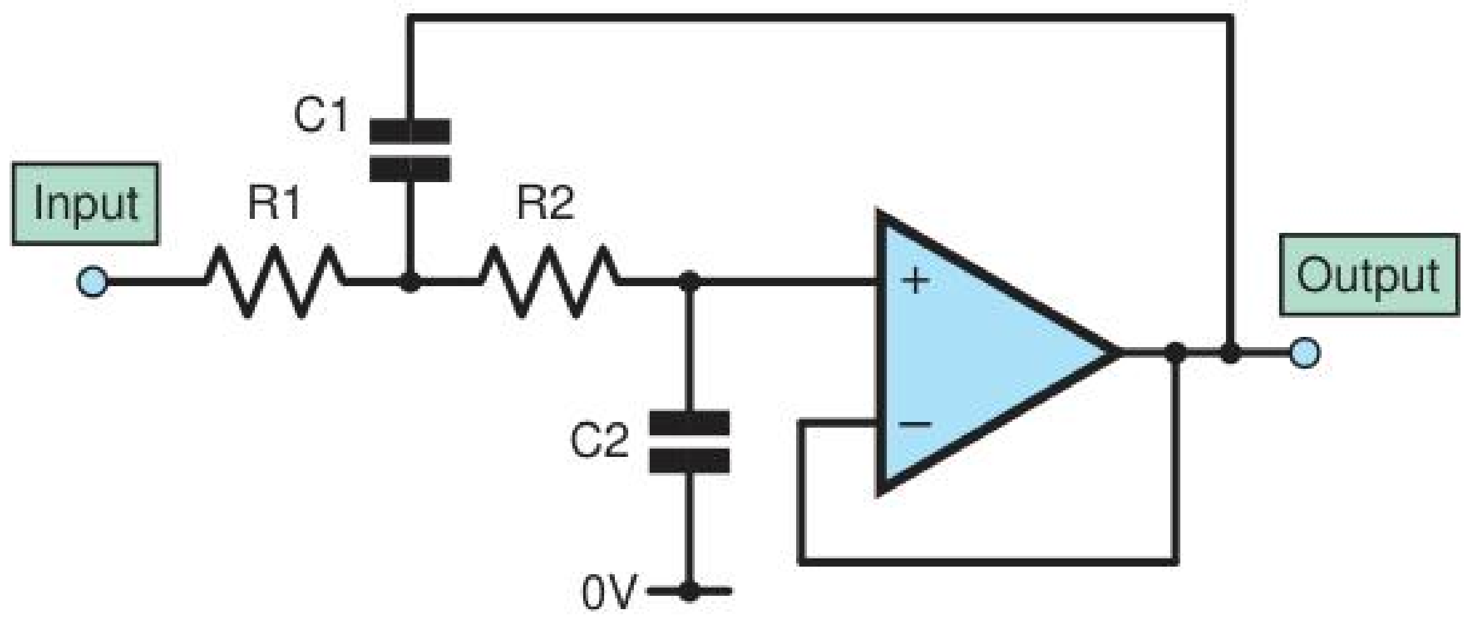

Fig.8: an active second-order low-pass filter (unity-gain Sallen-Key type).

The name 'operational amplifier' (abbreviated to 'op amp') comes from their ability to implement mathematical operations – they were widely used in analog computers to solve mathematical problems before the advent of digital computers.

For bandpass filters, *Q* is the ratio of the bandwidth relative to the centre frequency. If a band-pass filter has a centre frequency of f_0 and a -3dB bandwidth of f_b then $Q = f_0 \div f_b$. For low-pass filters, we typically require relatively low *Q* values because higher *Q* values result in a peak around the cut-off frequency (for example, the Chebyshev responses in Fig.5).

Usually, we would not want this peak to be very high. The situation is the same for high-pass filters.

For these filters, the damping factor ($\zeta = 1 \div 2Q$) is often used instead of *Q*, as it is perhaps more intuitive. Higher damping results in a slower, smoother transition from the passband to the stopband.

Resonant and cutoff frequencies

The frequency of the peaks seen in Fig.5 is related to the resonant frequency of the filter, but filters using resonant circuits (or mathematical equivalents) without peaks in their responses still have a resonant frequency. Low *Q* (high damping) produces responses without peaks, but the resonant frequency and *Q* still determine the response shape.

The resonant frequency is a fundamental property of the filter, related to the mathematics of the filter's function. The cutoff frequency is effectively arbitrarily defined, so they are not the same thing.

Fig.9 shows plots of the same filter response types as in Fig.5 (with the same scales and trace colours), but with each having the same resonant frequency (20kHz), rather than the same -3dB cut-off. The cut-off frequencies for the responses in Fig.9 are not the same as those in Fig.5, except for the Butterworth response, where both have cut-off frequencies at 20kHz (equal to the resonant frequency).

The responses in Fig.5 are the same at frequencies a long way from cut-off (both high and low), demonstrating the close mathematical relationship between filters with the same resonant frequency but different *Q* values. These responses differ around the cut-off point. The filters with higher *Q* have more peaking and a faster roll-off near their cut-off frequency.

For a particular response type, order and definition of cut-off frequency (f_c), there will be a fixed relationship between the resonant frequency (f_0) and cut-off frequency that can be expressed as a frequency scaling factor (F_s), such that $f_0 = F_s f_c$. The scaling factors are typically, but not always, in the range of 0.2 to 2.

For Butterworth filters with the cut-off defined as -3dB, the frequency scaling factor is 1; hence the equal responses in Fig.5 and Fig.9.

Analog filter circuit design

There are many different ways to implement analog filters; the best approach will depend on your requirements. As is usually the case in

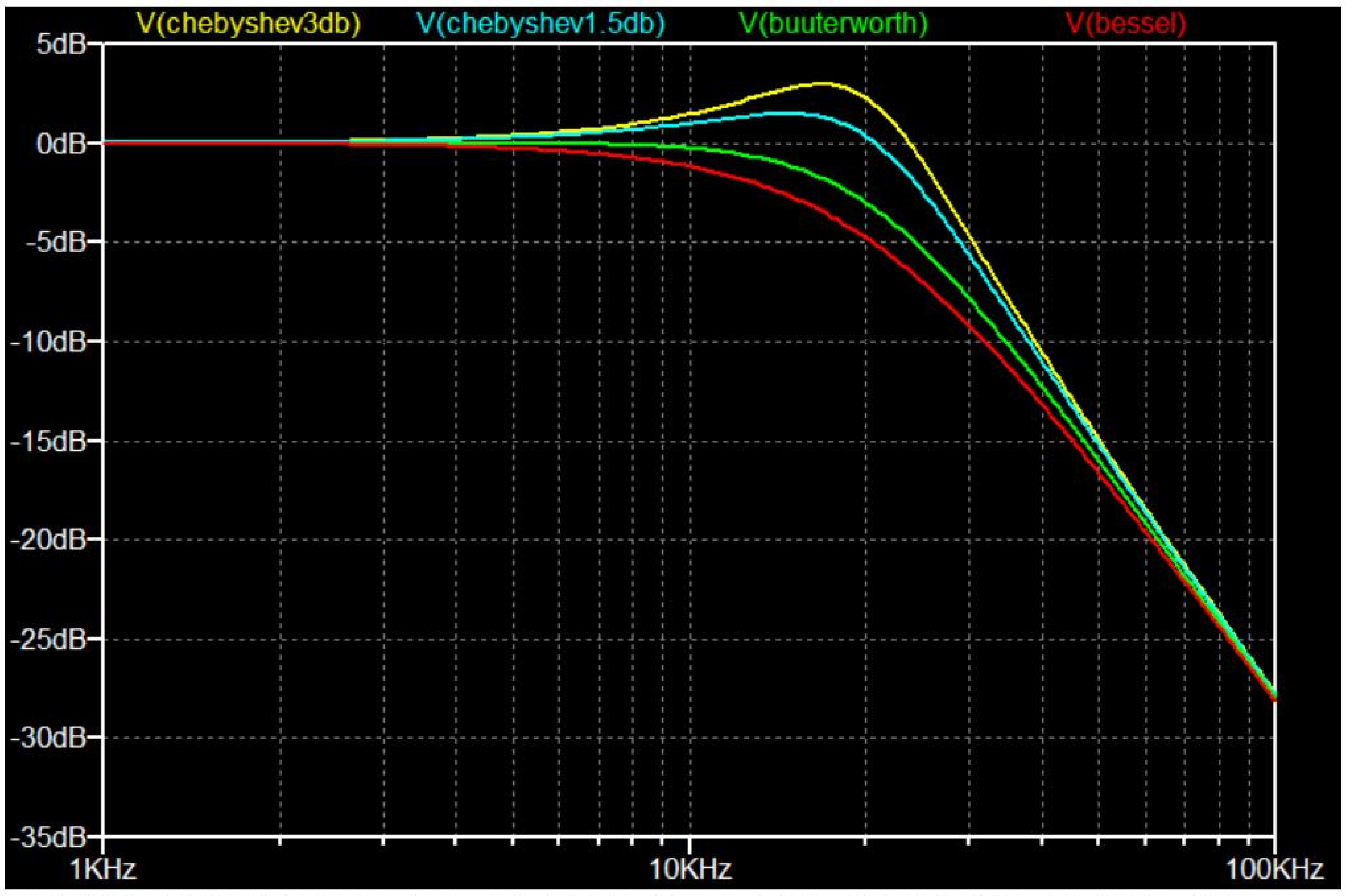

Fig.9: the magnitude response for various second-order low-pass filters with a 20kHz resonant frequency.

engineering, the better you understand and define what is needed, the more likely the outcome is to be successful.

The bandform and cut-off frequency are usually straightforward to determine from the application. The order, response type (Butterworth, Chebyshev etc) and circuit implementation choices will be based on the frequency and performance requirements. For example, how close are unwanted signals to wanted ones, how much do they need to be attenuated, and how important is flat passband gain?

One key decision is whether to use an active filter (op-amp-based) or a passive one (using just resistors, capacitors and inductors). For undemanding requirements, passive RC filters may suffice. RLC filters can deliver high performance, but at low frequencies the inductors required may be bulky and expensive.

Active filters are therefore often the best choice at lower frequencies (eg, audio), whereas at very high frequencies (RF), RLC filters may be a better choice because the inductors will be small and it could be difficult to find op amps with sufficient bandwidth.

For active filters, there are a variety of circuits that can be configured to implement a desired response; for example, Sallen-Key, multiple feedback (MFB) and state-variable filters. These have different non-ideal characteristics, which might need to be taken into consideration and balanced against factors such as cost and complexity.

Filters can be designed from first principles, based on mathematical analysis of the chosen circuit and the filter response required. This can be time-consuming and challenging if you are not already familiar with all the theory.

Fortunately, this is usually not necessary because standard filter circuits are so widely used that design formulae are readily available. There are even design tools that will do all the calculations for you.

Even before the wide availability of software tools, filter design was eased by printed tables or graphs from which relevant values (typically Q and F_s) could be looked up and used, along with the use of straightforward formulae. A good example of this is the Active Filter Cookbook by Don Lancaster, which was first published in 1975 and is described as the best-selling book on active filter design.

As well as providing design tables, the book also discussed the theory behind the circuits in detail. I have a well-used copy from the 1980s. Another useful source is the “Active Low-Pass Filter Design” application note by Jim Karki from Texas Instruments (SLOA049, see **www.ti.com/lit/pdf/sloa049**).

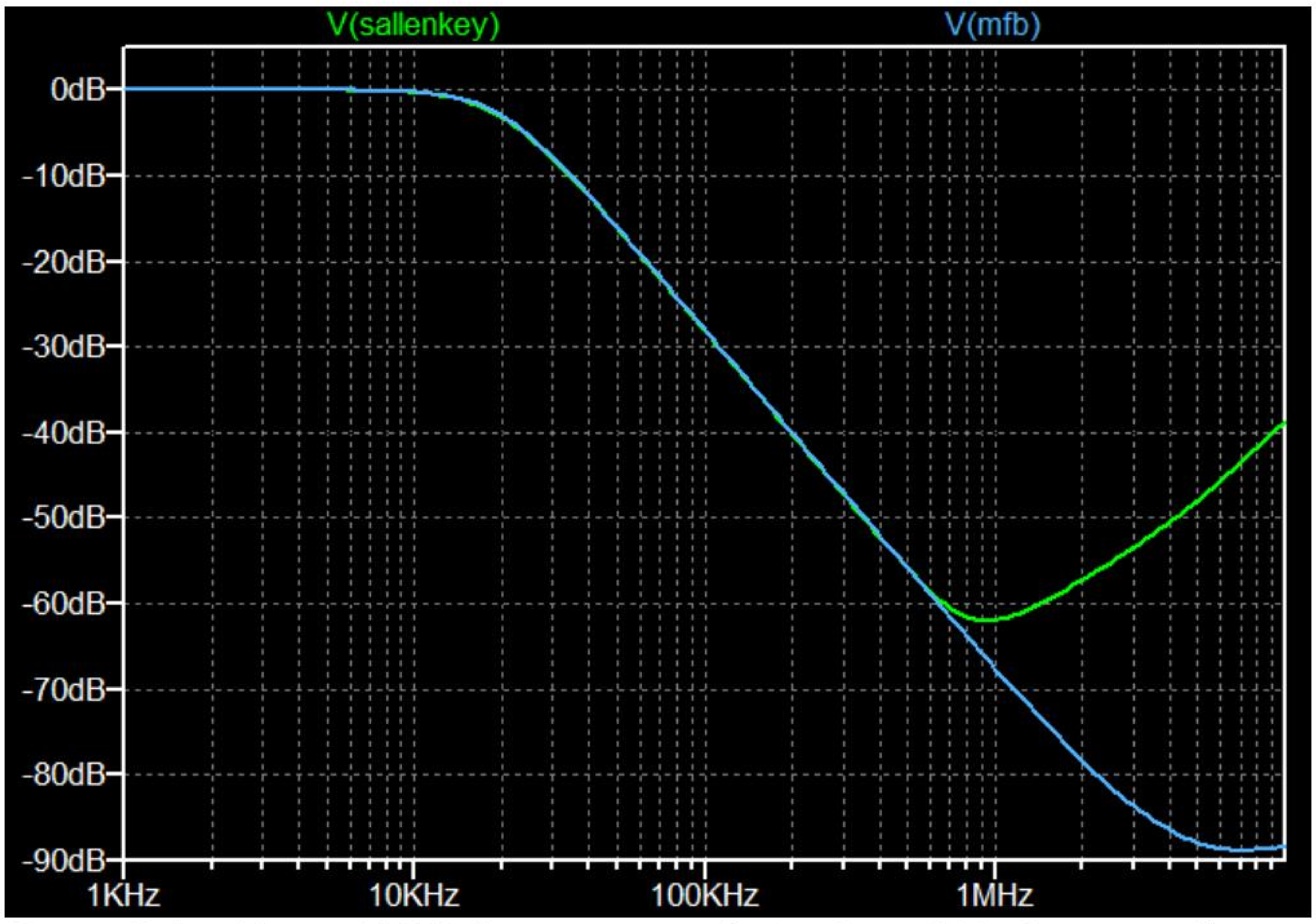

Fig.12: Sallen-Key and MFB filter responses (2nd-order, 20kHz, Butterworth).

Several semiconductor manufacturers provide online tools for active filter design. There is the Analog Filter Wizard from Analog Devices (**https://tools.analog.com/en/filterwizard/**) and FilterLab Active Filter Designer from Microchip (**https://pemag.au/link/acc3**), both of which provide low-pass, high-pass and band-pass designs.

The Filter Design Tool from Texas Instruments (**https://pemag.au/link/acc4**) also provides bandstop and all-pass designs, but unlike the other two, requires an account login.

These tools allow you to input the filter specifications (as discussed above) from which they will produce schematics with all component values calculated for you. Of course, they will use the manufacturers’ own op amps, but other similar devices can be used instead. Free online tools tend to provide a limited range of implementation and response options; still, they are very useful for many applications.

Circuit choices

Two widely used active filters are the Sallen-Key and MFB circuits. These are both second-order filters equivalent to an RLC filter (eg, Fig.7) using a single op amp. They are popular because they provide reasonable performance at relatively low complexity and component count.

We will show some low-pass versions here, but other bandforms can be obtained by switching the positions of resistors and capacitors in the circuit.

Fig.8 shows a unity-gain Sallen-Key filter, which is a simplification of the Sallen-Key filter shown in Fig.10. The frequency-dependent circuit is similar to a two-stage RC filter, but with C1 connected to positive feedback from the amplifier, rather than to ground.

This allows the circuit to have much higher Q values than can be obtained with the RC filter, which, as already noted, has a maximum Q of 0.5; it is often lower.

The version in Fig.10 is more complex but can provide gains other than unity. This circuit has an advantage for higher-Q filters, where (due to the way the maths works), the unity gain circuit can require impractical ratios between the capacitor values (this means you would need to use either an excessively large or excessively small value for one of the components).

The ability to implement non-unity gain for the Sallen-Key circuit in Fig.10 may be directly useful in some applications (eg, it can save another op amp that would be required for a separate gain stage). On the other hand, the unity-gain version has the highest gain accuracy because it does not depend on the accuracy of any gain-setting resistors (R_3 and R_4 in Fig.10).

Fig.11 shows an MFB filter – its name comes from the fact that there are two feedback paths in the frequency-setting

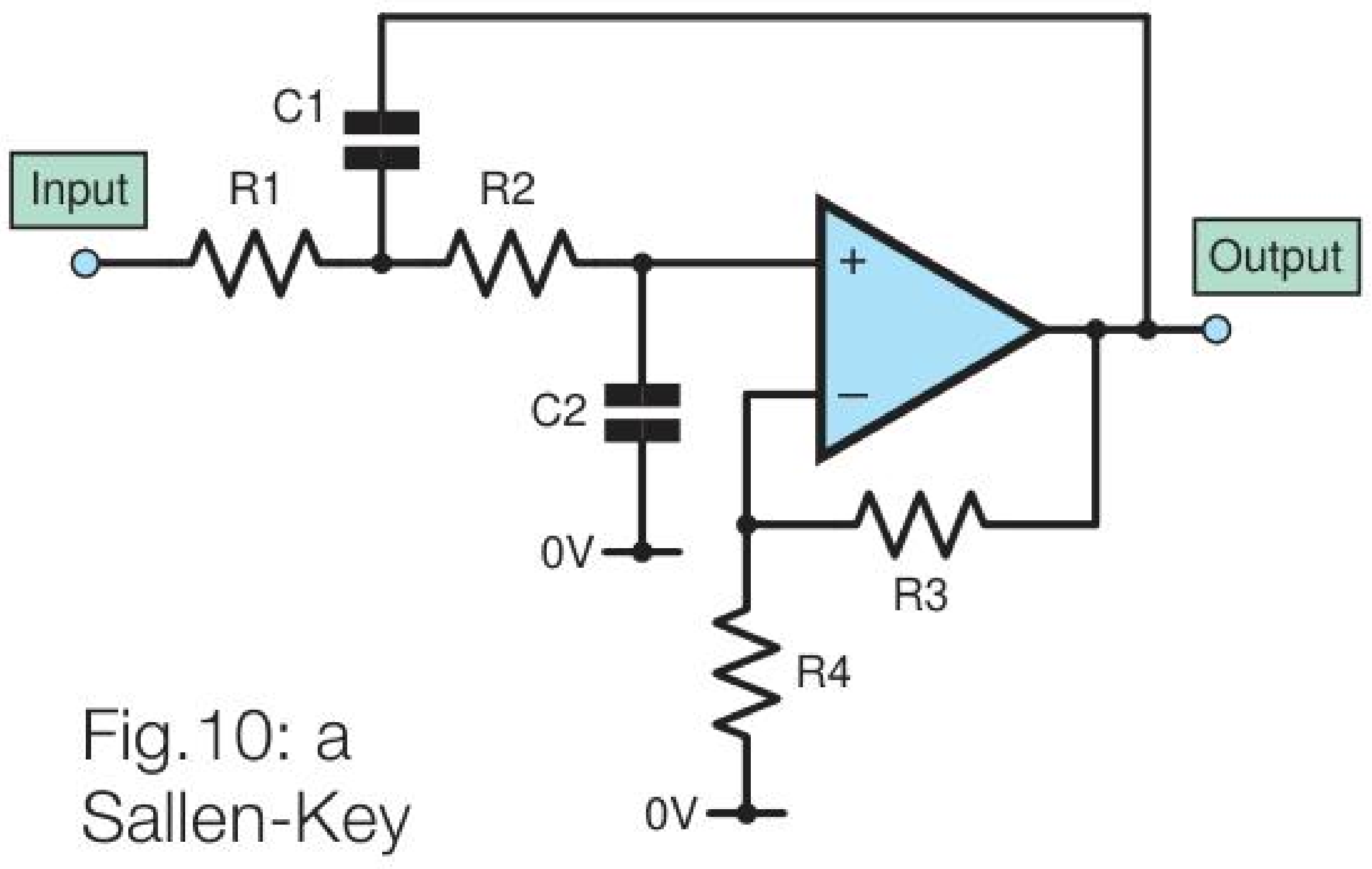

Fig.10: a Sallen-Key second-order low-pass filter.

network (R_3 and C_2 in Fig.11), whereas the Sallen-Key filter only has one (C1 in Fig.8 and Fig.10).

Sallen-Key filters tend to be easier to design (manually) than MFB filters, which accounts for their popularity. The MFB circuit has better performance at high frequencies, is better suited to higher-Q circuits, and is overall less sensitive to component variations. However, the unity-gain Sallen-Key is the least sensitive to gain variations.

If the component values in a filter circuit do not exactly match the designed values, it will deviate from the desired response. This is inevitable because components are available in limited sets of values (E12, E24 series etc), which usually do not match the required values, and individual components vary within their tolerance range and with temperature.

The degree to which a circuit deviates from its designed performance in response to a given amount of component variation is termed sensitivity and can be subjected to detailed mathematical analysis. It can also be investigated in simulation by varying components within their tolerance range and obtaining an envelope of possible responses.

Sensitivity varies with filter implementation; for higher-order and higher-Q circuits, the deviations may be very significant. Single op amp filters such as the Sallen-Key and MFB circuits do not provide the lowest possible sensitivity. If they cannot meet requirements, filters using several op amps to implement a second-order response (eg, state-variable filters) need to be used instead.

Sallen-Key circuits are non-inverting, whereas MFB filters are inverting. Sallen-Key low-pass circuits have a high input impedance at DC because the input is fed to the non-inverting input, whereas the input feeds the virtual ground at the inverting input in the MFB filter, so the input impedance is less than R1 + R2 (due to C1's finite impedance and feedback via R3).

Both filters have non-ideal performance at high frequencies, where their gain does not continue to decrease as frequency increases in line with an ideal second-order response.

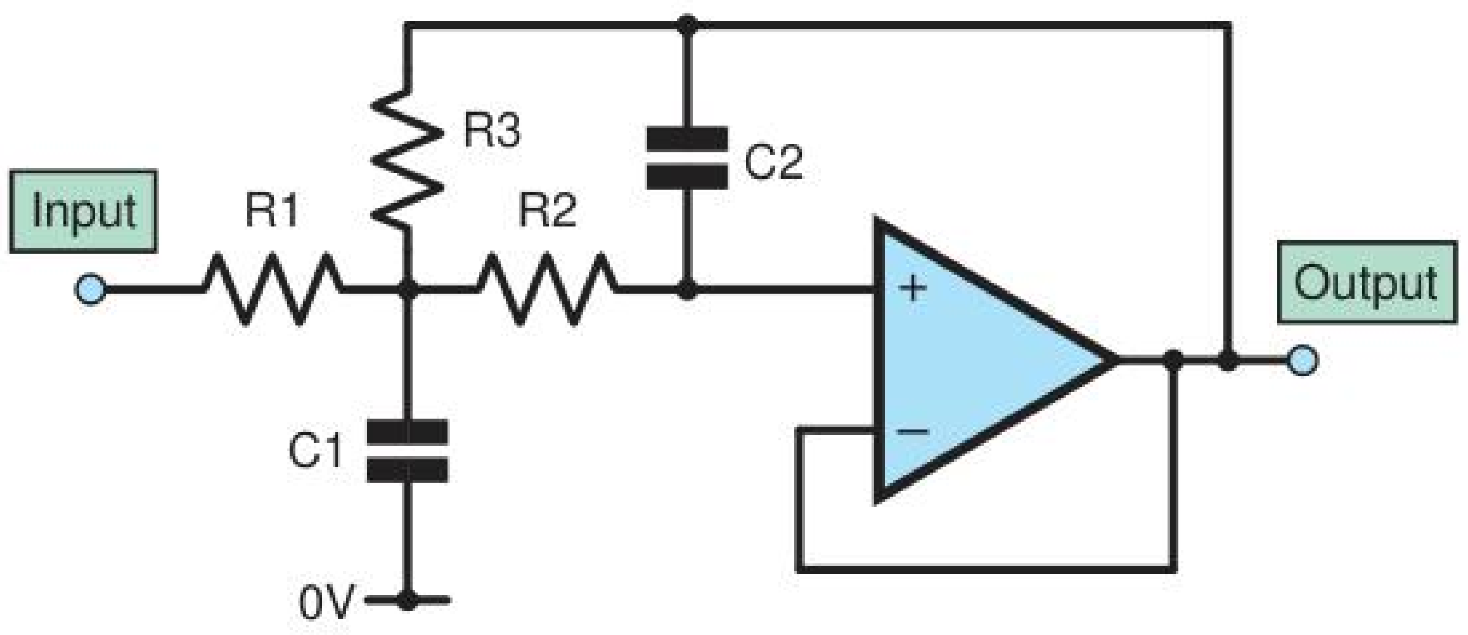

Fig.11: a multiple-feedback (MFB) second-order low-pass filter.

However, the Sallen-Key filter is significantly worse in this respect, as shown in Fig.12. This shows the responses of a 20kHz, 2nd order, low-pass Butterworth filter implemented with both Sallen-Key (green trace) and MFB (blue trace) circuits.

The gain of the Sallen-Key filter in Fig.12 increases above about 1MHz, whereas the MFB circuit's gain continues to decrease before levelling off around 5MHz. The problem is caused by the increase in output impedance as frequency increases. As the frequency increases, the op amp's open-loop gain reduces, decreasing the ability of the negative feedback to reduce the effective output impedance.

The op amp then struggles to drive the output towards 0V (which is what the output should be with high attenuation in the stop band) against the input signal feeding through to the output via the resistors and capacitors. The MFB filter has a less direct, higher impedance path from input to output, and C1 helps to shunt more input signal at higher frequencies, so it suffers less from this effect.

A large number of op amps are suitable for use in Sallen-Key and MFB circuits, but not all op amps will suit every filter. In general, the op amp should have a low input bias current to prevent DC errors, sufficient slew rate to handle the maximum amplitude required at the highest pass-band frequency required, and a low output resistance to limit the non-ideal high-frequency behaviour just described.

A key op amp characteristic is the gain-bandwidth product (GBP), which must be much larger than the filter cut-off. A rule of thumb is that $GBP > 100A_p \cdot f_C$, or $GBP > 100A_p \cdot Q^3 \cdot f_C$ for Sallen-Key filters with $Q > 1$, where A_p is the passband gain. Design tools will often assist with op amp selection.

A Sallen-Key low-pass filter

As an example of the manual approach to filter design, we will look at the Sallen-Key low-pass filter shown in Fig.10. It comprises a frequency-dependent circuit formed by R_1, R_2, C_1 and C_2, plus a non-inverting op amp configuration. The equations needed for the design are widely published. The amplifier gain (A) is set by R_3 and R_4 and is given by:

$$A = 1 + \frac{R_3}{R_4}$$

The resonant frequency, f_0, is:

$$f_0 = \frac{1}{2\pi\sqrt{R_1 R_2 C_1 C_1}}$$

The Q is:

$$Q = \frac{\sqrt{R_1 R_2 C_1 C_1}}{R_1 C_1 + R_2 C_1 + R_1 C_2 (1 - A)}$$

These equations are quite cumbersome, but simplifications can be made by placing constraints on the design, such as fixing the gain at unity (as in Fig.8). Another way Sallen-Key equations can be simplified is by using equal component values, $R = R_1 = R_2$ and $C = C_1 = C_2$, which gives:

$$F_s f_c = f_0 = \frac{1}{2\pi RC}$$

$$Q = \frac{1}{3 - A}$$

This provides very simple design equations but does not allow the overall gain of the filter to be set independently of the Q value. Still, the overall gain can be adjusted by adding a suitable gain stage.

The equal-component Sallen-Key filter circuit can be designed by choosing a required response, which sets Q and F_s (these can be looked up in filter design tables). The Q value sets the gain (A), which is set by choosing R_3 and R_4.

The frequency-setting R and C values are found by first finding f_0 from the required cut-off frequency (f_C) and F_s. Then we can either choose R and calculate C, or vice versa.

The SLOA049 application note from Texas Instruments provides four simplified approaches to Sallen-Key design and two for MFB filters, along with tables of values for Q and F_s. The Active Filter Cookbook provides a similar approach for a wider range of filters.

Multi-stage filters

Multiple second-order low-pass or high-pass Sallen-Key or MFB stages can be cascaded to form higher (even) order filters (4th, 6th etc) for faster cut-off and greater stopband attenuation. If an odd order is required (3rd, 5th etc), a first-order op amp filter can be used as one of the stages.

[Editor's note – some active filter circuits can realise a third-order response with a single op amp, but this is not possible for all topologies and may impose other restrictions.]

Fig.13 shows a unity-gain typical first-order stage, which is simply an RC filter buffered by an op amp. The circuit can be given gain using feedback resistors in the same way as an inverting amplifier.

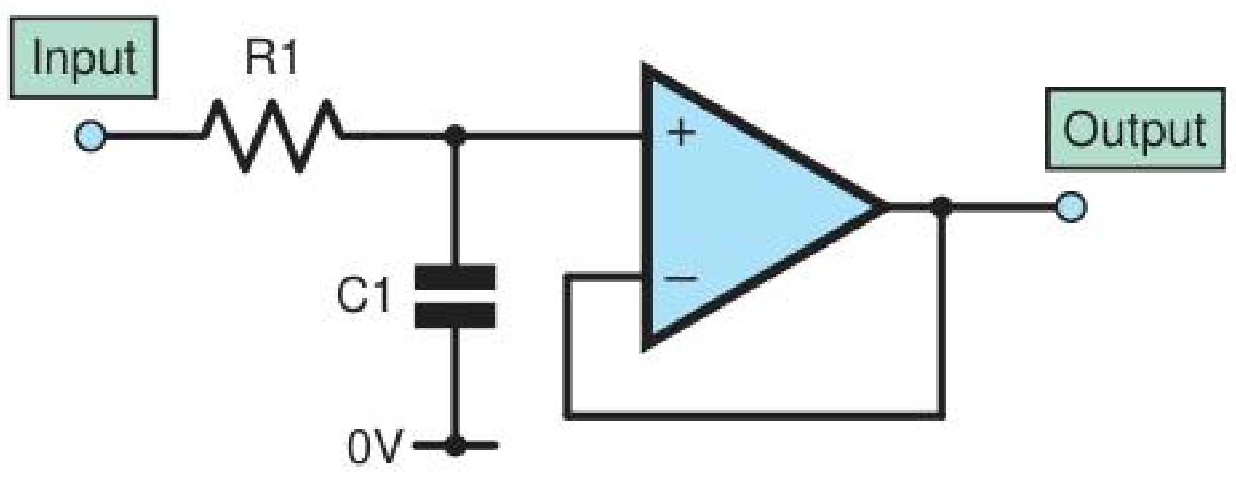

Fig.13: a unity-gain first-order stage.

The design of multi-stage filters is more complex than simply joining multiple copies of the same filter. For example, you cannot make a 4th-order 20kHz Butterworth filter by cascading two 2nd-order 20kHz Butterworth filters. With a bit of thought, this might be obvious – if both filters attenuate by 3dB at 20kHz, the two-stage filter's response will be 6dB down at 20kHz.

Unfortunately, the answer is not simply to shift the cut-off frequencies of the two stages up a bit so that the two-stage filter has a -3dB cut-off at the correct frequency. This can be done, but the response will not be a Butterworth shape – the response will have a softer cut-off and less attenuation at frequencies above cut-off.

These problems are illustrated in Fig.14. The green trace is a correctly designed 4th-order Butterworth response using two unity-gain Sallen-Key stages. The orange trace is the response from cascading two 20kHz 2nd order Butterworth stages (these both individually have the same response as shown in Fig.3 and Fig.5). This response has -3dB cut-off at around 15.8kHz.

The magenta plot is for two cascaded 24.5kHz, 2nd order Butterworth stages (24.5kHz = 20kHz × (20kHz ÷ 15.77kHz)). This has a cut-off around 20kHz, but as noted above, it has a softer cut-off than the Butterworth response.

Fig.15 shows the two individual responses (brown and grey traces) of the two stages that comprise the 4th order, 20kHz, low-pass Butterworth filter, along with the overall response (green trace), which is the same as the one as in Fig.12.

One of the individual responses shown in Fig.13 obviously has a higher *Q* than a Butterworth filter – there is a clear peak in the stage 2 (grey trace) response. Intuitively, we can think of this as compensating for the soft response obtained by simply cascading two Butterworth stages (as shown in Fig.12).

Actually obtaining the correct response requires getting the mathematical details of each stage correct which, as mentioned, may require significant effort. Fortunately, filter tables provide the numbers you need for each stage for common responses. Design tools will provide you with the entire circuit and all component values.

Mathematically, it does not matter what order the stages are in; the overall response is the same. However, there are practical considerations for real circuits.

The most common approach is to arrange the stages in order from lowest to highest *Q* because this reduces the likelihood of clipping. This optimises the filter's voltage handling, but other orders may help optimise other aspects such as noise or power consumption.

Bandpass and bandstop filters with wide differences between the cut-off frequencies can be realised using a combination of high-pass and low-pass stages. For narrower bands, where the *Q* is not too large, a single op amp filter can be used.

For higher-*Q* narrower band

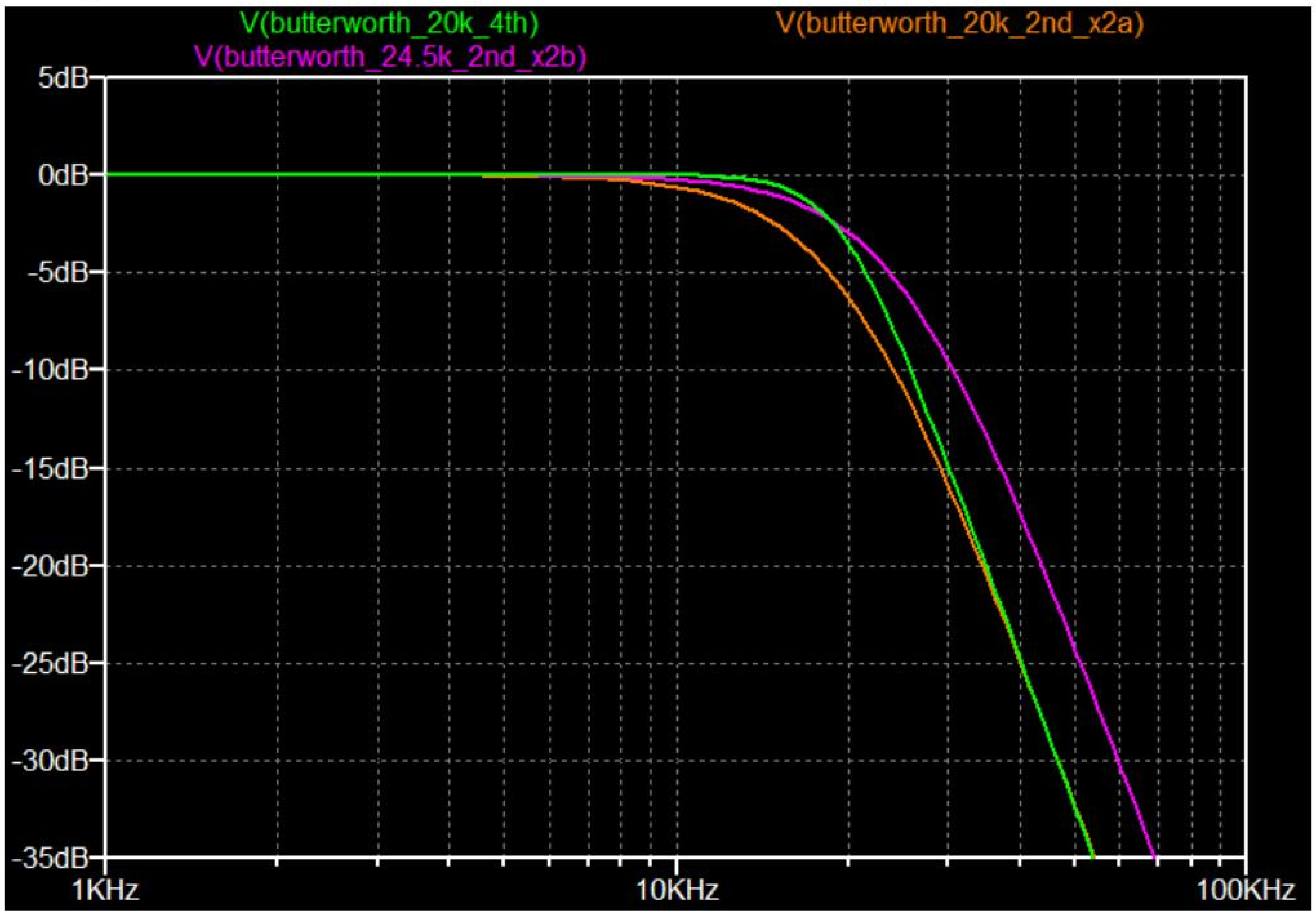

Fig.14: a comparison of 4th-order responses.

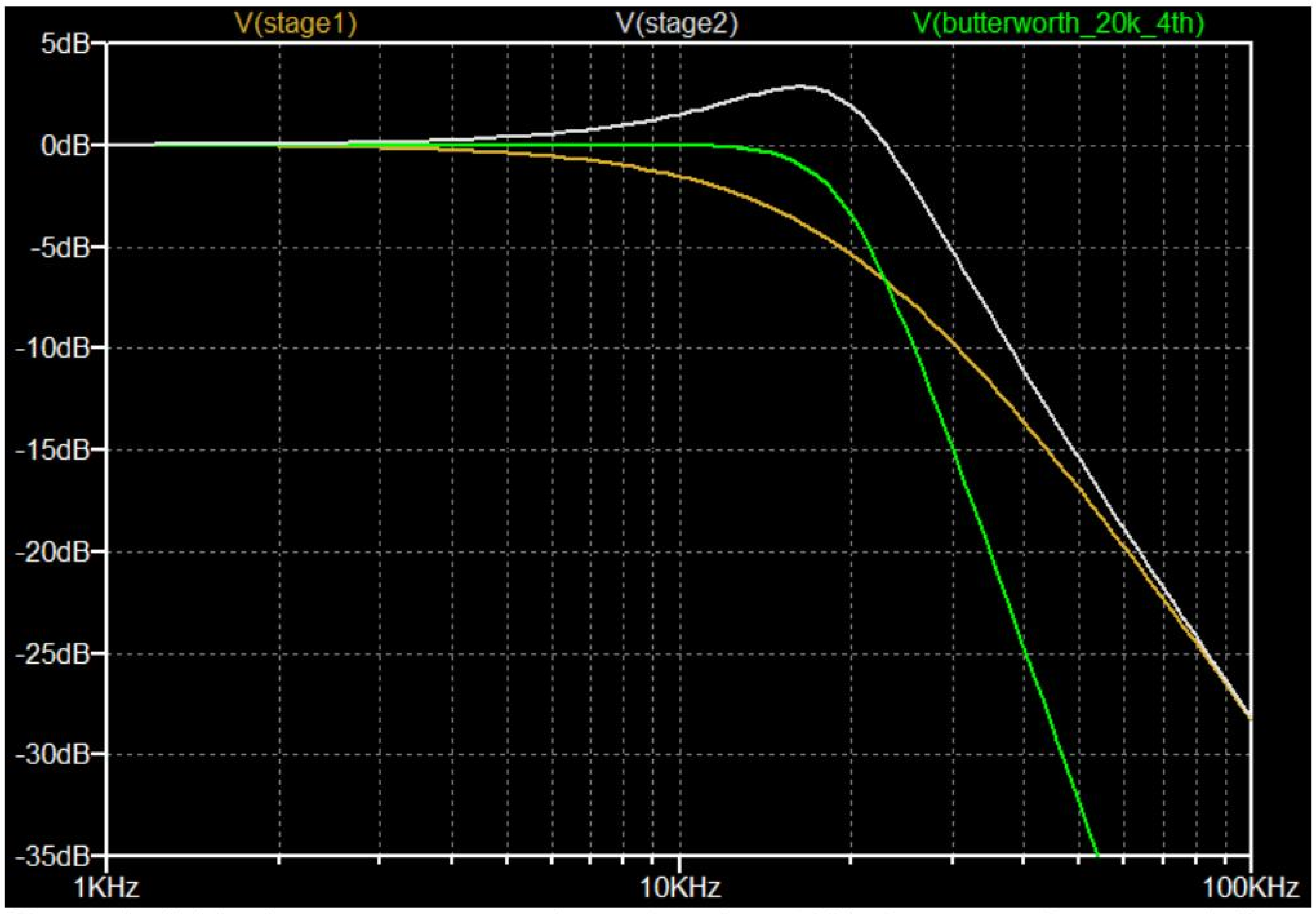

Fig.15: individual stage responses in a 4th-order 20kHz low-pass Butterworth filter.

5-year collections

2019-2023
£49.95

2018-2022
£49.95

2017-2021
£49.95

2016-2020
£44.95

Purchase and download at:
www.electronpublishing.com

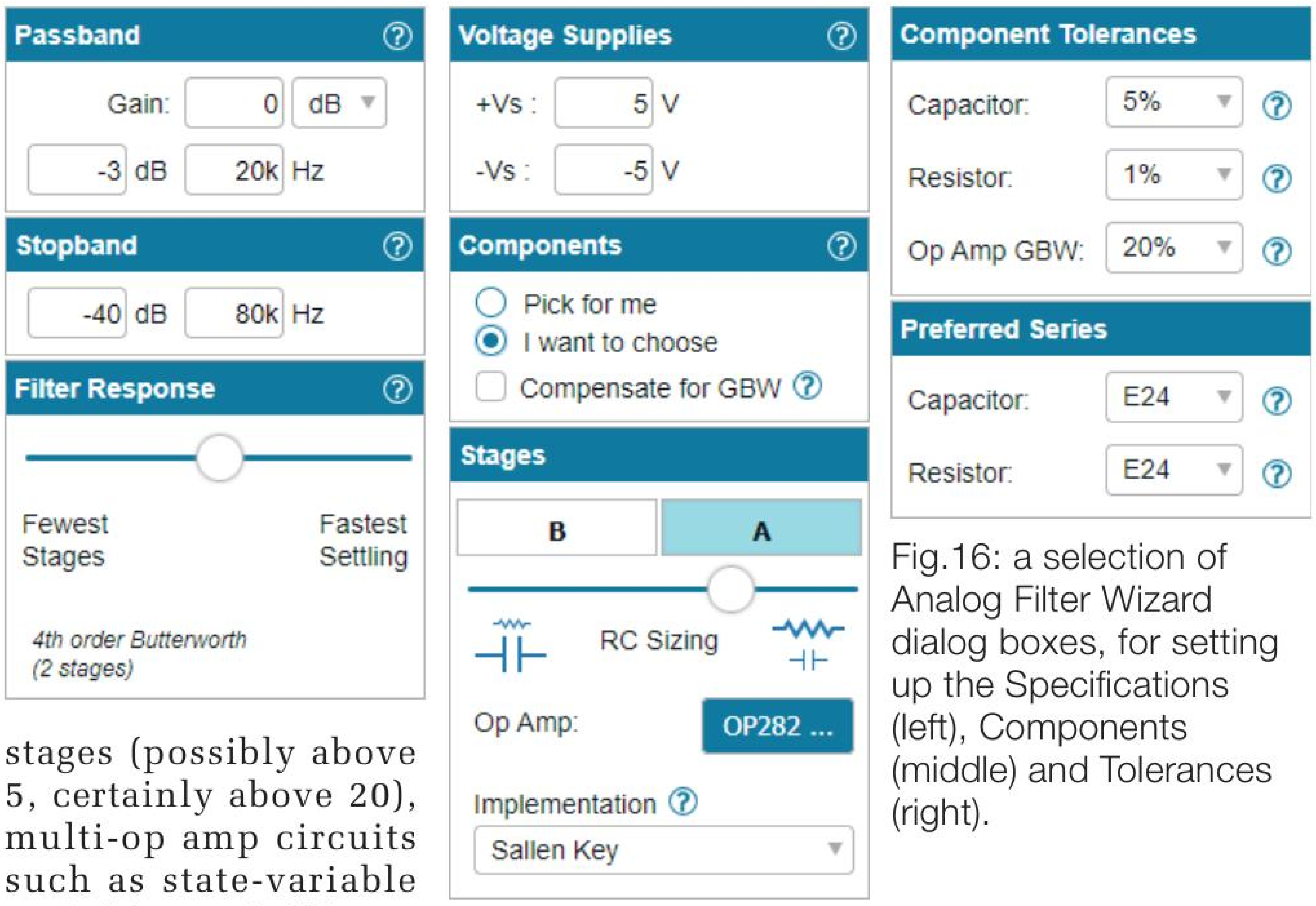

Passband

Gain: 0 dB

-3 dB 20k Hz

Stopband

-40 dB 80k Hz

Filter Response

Fewest Stages — Fastest Settling

4th order Butterworth (2 stages)

Voltage Supplies

+Vs : 5 V

-Vs : -5 V

Components

○ Pick for me

● I want to choose

☐ Compensate for GBW

Stages

B A

RC Sizing

Op Amp: OP282 ...

Implementation: Sallen Key

Component Tolerances

Capacitor: 5%

Resistor: 1%

Op Amp GBW: 20%

Preferred Series

Capacitor: E24

Resistor: E24

Fig.16: a selection of Analog Filter Wizard dialog boxes, for setting up the Specifications (left), Components (middle) and Tolerances (right).

stages (possibly above 5, certainly above 20), multi-op amp circuits such as state-variable and bi-quad filters should be used.

Using design tools

The reconstruction filter used in the DSP system-under-test by the PC sound-card-based measurement system was designed using Analog Devices' Analog Filter Wizard.

Fig.16 shows some of the on-screen dialogs encountered while using this tool, which are stepped through from left to right as the design progresses. Other tools provide similar functionality.

After selecting the filter type (bandform), low-pass in this case, the frequency and gain requirements can be entered via the Specifications dialog.

Unfortunately, the user cannot directly choose the filter order as in some other tools, but if a specific order is required, the stopband can be adjusted to achieve this.

The Filter Response slider allows the response type (Chebyshev, Butterworth, Bessel) to be selected. The frequency response and requirement limits (similar to Fig.4) are displayed to the right of the dialog (not shown here).

The next step is the Components dialog, which controls the op amp selection and calculation of RC values. The supply voltage you will be using will influence op amp selection. If you choose "Pick for me", component selection is fully automated, but it can be optimised for specific requirements like the supply voltage range, low power consumption, or low noise.

Make this choice before clicking "I want to choose" if you would like more control (as shown in Fig.16). This allows you to pick the op amp, change the relative size of the capacitors and resistors (via the slider) and select the implementation (Sallen-Key or MFB) of each stage separately.

In this case, the A and B buttons select the stage being set up by the selection controls. The order of the sections can also be changed by dragging these buttons. The Tolerances dialog is used to choose the E-series and tolerance of the resistors and capacitors.

The tool can display a range of information about the circuit, including the frequency response, step response, noise and power, the configuration and response of each stage, the schematic with all the component values and a bill of materials. The information displayed is selected via a drop-down box.

Simulation files

Most *Circuit Surgery* columns feature the use of the free circuit simulation software LTSpice. It is used to support descriptions and analysis in *Circuit Surgery*.

The examples and files for this issue are available for download: https://pemag.au/link/acby

As well as drawing the schematic diagram on-screen, the SPICE and other design files can be created and downloaded.

Fig.17 shows an LTspice schematic of the reconstruction filter used in our DSP system. This uses the OPAx134 op amps that were used throughout the system, rather than those suggested by the tool.

The simulation results in Fig.15 were obtained from this circuit. The actual implementation used E24 resistors with values of 6.2kΩ, 13kΩ and 47kΩ. Usually it's best to pick from the large range of E24- or E96-series resistor values, as they are common and inexpensive, while capacitors can become pricey if you need unusual values.

Conclusion

Filters are a large topic, so we have only looked at a small part of it. We have covered the basic concepts that are needed to understand the inputs required by design tools and discussed some of the design trade-offs related to single-IC second-order analog filter stages.

These circuits are popular; although they do not provide the best possible performance, they require relatively few components and are suited to a wide range of applications. PE

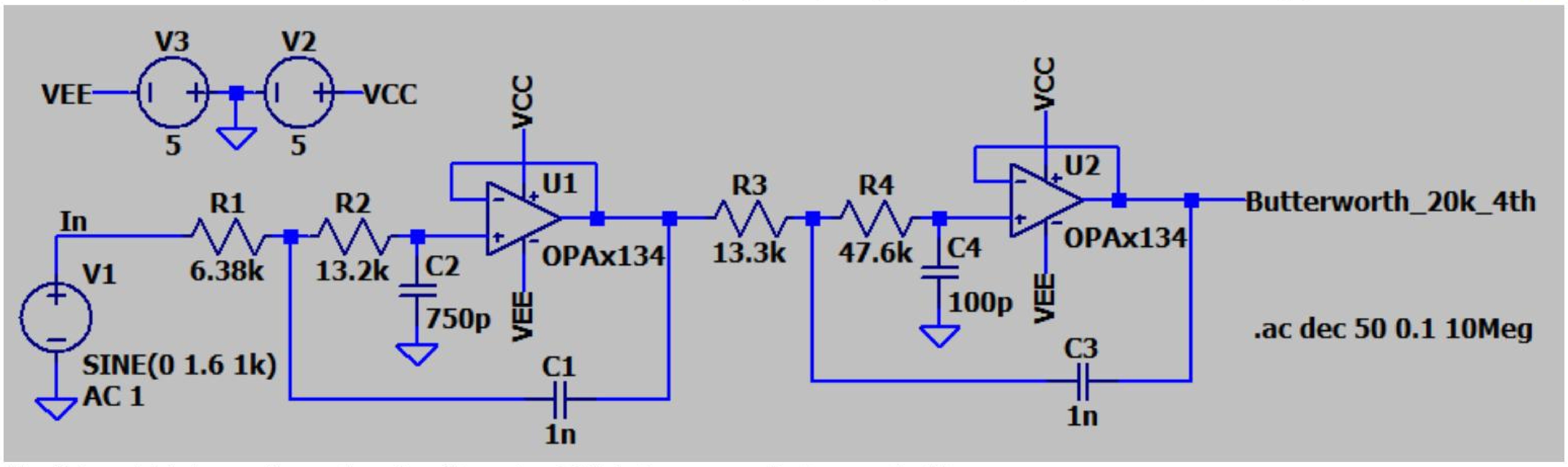

Fig.17: an LTspice schematic of a 4th-order 20kHz low-pass Butterworth filter.

By Max the Magnificent

By Max

WEIRD & WONDERFUL ARDUINO PROJECTS

Part 20: Pogo pins and pixel grins

Well, hello there. Soon, we will dive deeper into our Chronological Contraption project, whose role it will be to mark the years, months, days, hours, minutes, and seconds until the commencement of my 100th birthday celebrations, although you will be able to use yours for all sorts of things (perhaps even telling the time).

But before that, there are a couple of other topics that are rattling around in what I laughingly call my mind.

When we started our retro games console project (Photo 1), deep in the mists of time we used to call January 2025, I expected at least a few members of the *Practical Electronics* community to join me on this quest. However, I must admit to being surprised by the number of emails merrily pinging their way into my inbox.

Often, I receive a message from someone who is 'jumping ahead', saying, "I'm all up to date, so what can I do now?" Well, last month we added an inertial measurement unit (IMU) to the console. Then we used our IMU to detect whether the console was tilted to the left, right, front, or back, or any combination thereof, such as front-and-left or back-and-right.

We finished by employing this newly minted tilt information to control a virtual marble as it rolled around the display. You can find a copy of this code in the file named **CB-aug26-code-01.txt** (as usual, all files mentioned in this column are available in the August 2026 download package available from the *PE* website at https://pemag.au/link/acby).

In a crunchy nutshell, we defined a constant called `IMU_SAMPLE_TICKS` to be 200ms, or one-fifth of a second. This means we currently sample the IMU at 5Hz (five times per second). You can experiment with different delay values if you wish.

Each time we sample the IMU, we decide whether to move the virtual marble and, if so, in which direction. We move the marble only one pixel at a time, and any tilt of less than 15° is ignored.

So, the following are some ideas we (well, mostly you) might want to try:

1. We added a piezo buzzer to our console in the June 2026 issue, then we added some click, chirp, and wail sound effects to our snake game. How about if we reused these effects, like adding a click every time our virtual marble moves to a new pixel?
2. At random times, we could place 'food' pixels at random locations on the array and then add a chirp sound if our marble 'eats' (runs into) one. We could also make the food particles disappear if they aren't eaten quickly enough.
3. We currently use three of our 7-segment displays to track how many times we press the action buttons, and the other three to track how many times we press the direction buttons. We could change this to reflect how many times the marble has moved and how many food particles we've eaten.
4. We could also add random poison pixels. If we inadvertently roll our marble into one of these, we could play our wail sound, reset the counters and start again.
5. We currently have a fixed tilt angle threshold (15°) and a fixed sampling rate (5Hz), which together result in a fixed marble rolling speed. That is, once we pass 15°, it doesn't matter how steeply we tilt the console because the marble continues to travel at the same velocity. We could maintain our minimum tilt threshold of 15°, but after that, we could increase the rolling speed by increasing the sample rate (ie, decreasing the time between samples) as a function of the tilt angle.

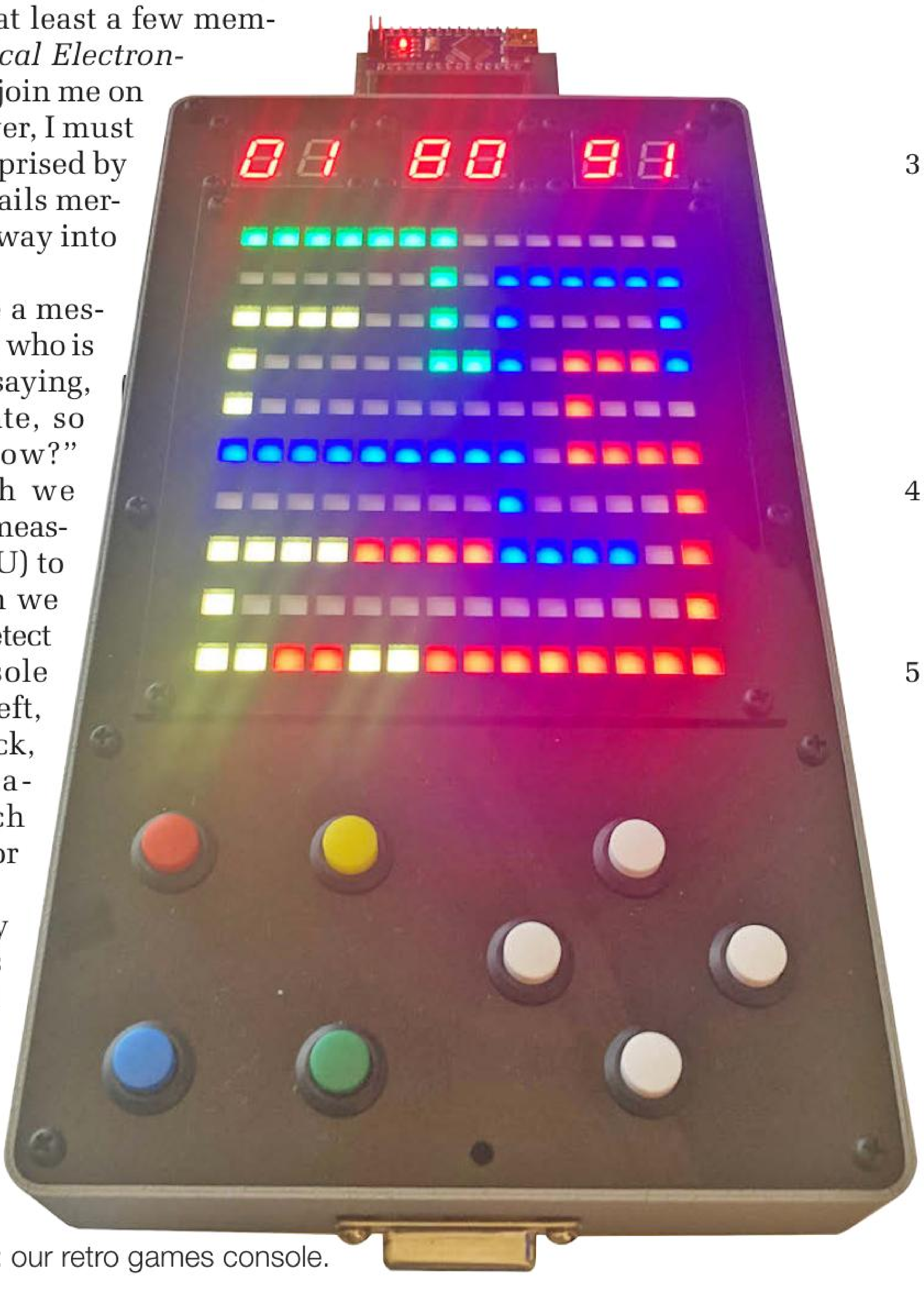

Photo 1: our retro games console.

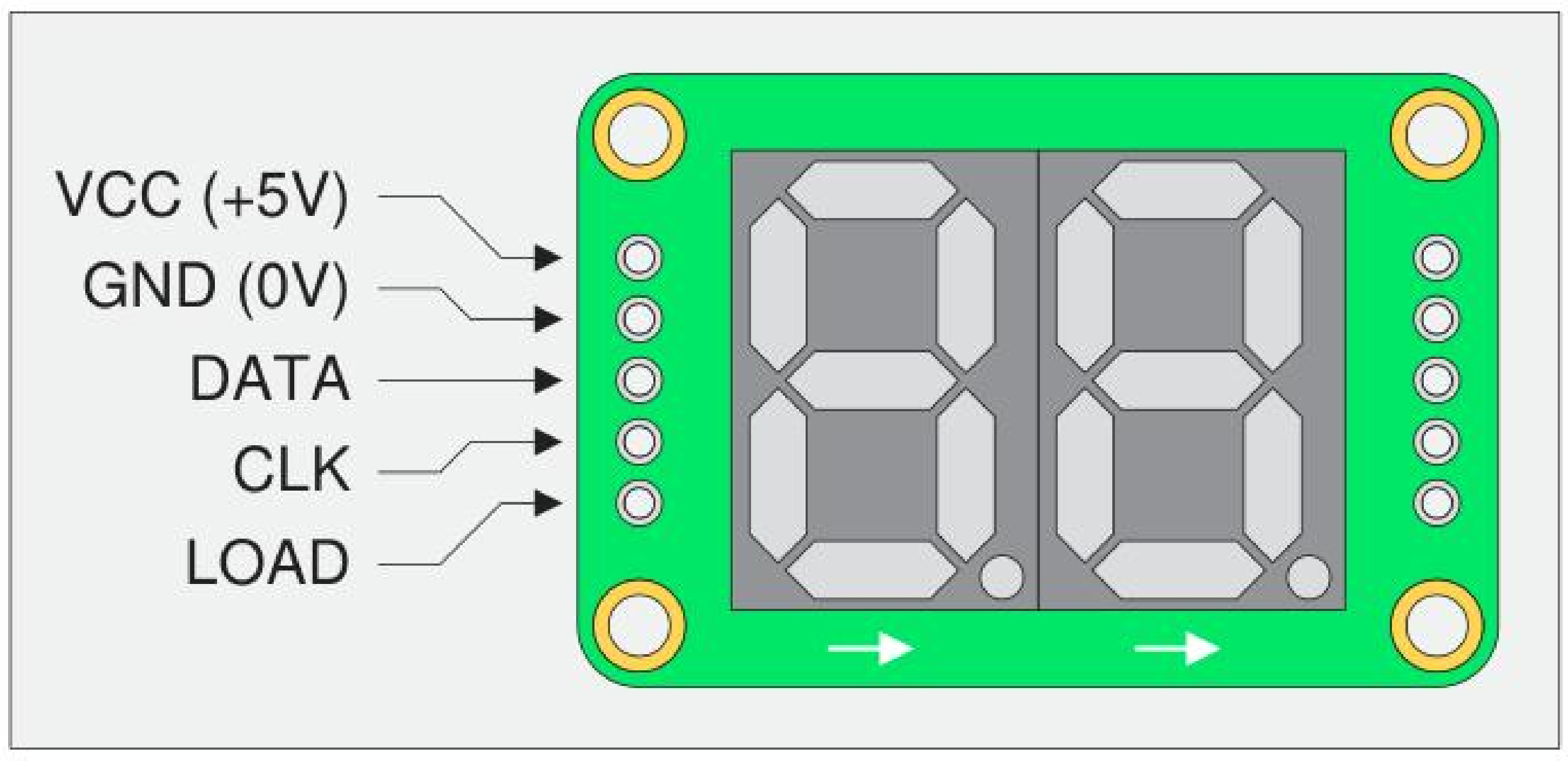

Fig.1: the pinout of our dual-digit 7-segment display.

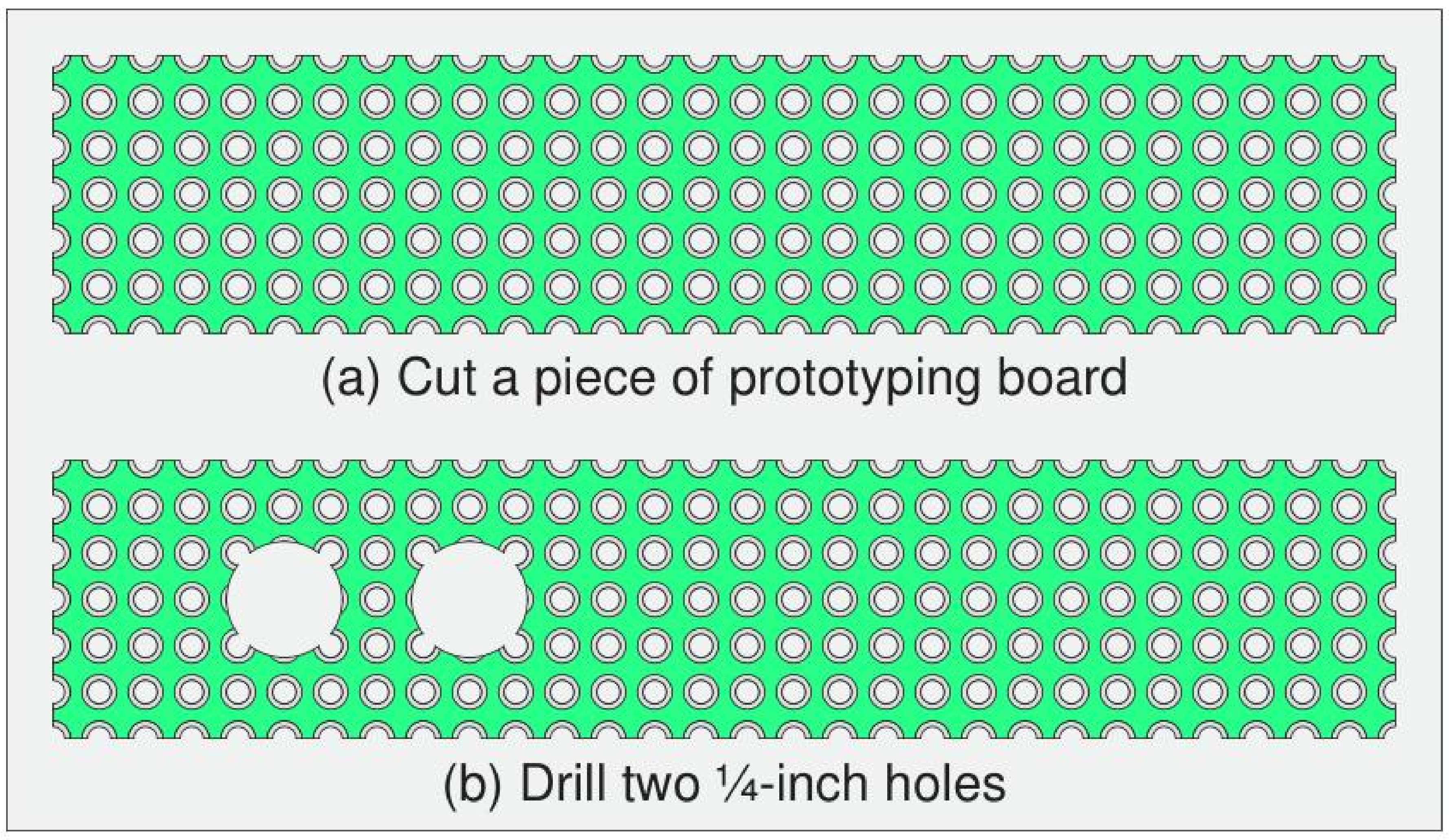
(a) Cut a piece of prototyping board
(b) Drill two ¼-inch holes

Fig.2: preparing the prototyping board for use in a test fixture.

6. We could increase the realism of our virtual marble's motion by modelling some of the physics that would be associated with a glass marble in the real world. For example, even if we keep the tilt angle constant at 20°, the speed of a real-world marble will increase over time until it reaches a limit set by factors such as friction and air resistance. Similarly, if the real-world marble is moving quickly in one direction, even if we tilt the platform the other way, inertia will cause it to continue rolling for a while before it slows, stops, and reverses direction. We could model these types of effects.

Implementing any of these ideas with our virtual marble will be a good learning experience in its own right. Furthermore, many of these tricks and techniques may be applicable to other games, such as our snake program, for example.

The jig is up

Do you recall many moons ago when we were adding the dual-digit 7-segment light-emitting diode (LED) display modules to our console (Fig.1)? At that time, I mentioned that if I ever decided to build a lot of consoles for any reason in the future, then I'd want a way to quickly test each of these display modules before any mounting or soldering took place.

This would require some sort of test fixture or test jig. Historically speaking, these aren't quite the same thing, but despite that, many people use those terms interchangeably in engineering conversations, especially in the context of electronic test systems.

I have a friend we'll call Steve (because that's his name). Steve used to be an aircraft fitter, and his work is precision personified. Whenever he wishes to create a test jig, he simply whips one up on his 3D printer. In my case, I often use a horizontal-handle hold-down toggle clamp (Photo 2).

More specifically, I usually use the GH-201-C because it's small (only six inches or about 15cm tip-to-tip when fully extended) and perfectly sized for most of the jigs I wish to create.

You can acquire these little rascals from multiple sources (just Google "GH-201-C"), and they can be surprisingly inexpensive. I currently hang my hat in the USA, and I found one supplier offering them for only $1.50 apiece.

The important mechanical feature of these clamps is their over-centre linkage. When the handle passes through the centre point, the geometry locks the clamp in place until you deliberately release it.

I must admit that I haven't always given mechanical engineering the respect it deserves, but the tactile feel of this clamp in action gives one a newfound appreciation for clever mechanical design.

For electronics hobby work, these clamps are wonderful for all sorts of things, including pogo-pin-based test and programming fixtures. "What's a pogo pin when it's at home?", I hear you cry. Don't worry, we will return to this in a moment, but first…

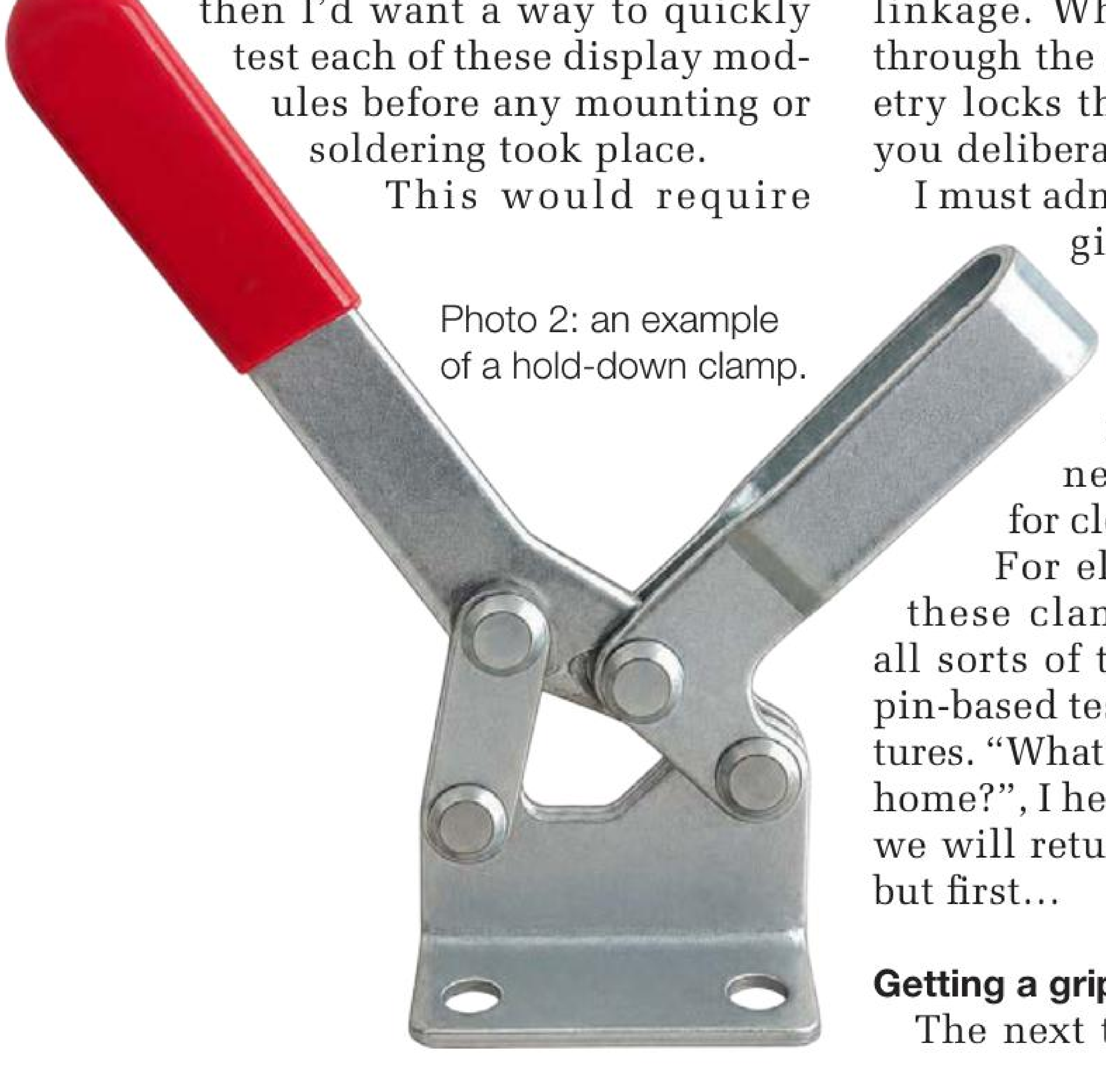

Photo 2: an example of a hold-down clamp.

Getting a grip

The next thing we're going to do is take a piece of prototyping board – the sort with plated through-holes and pads on both sides; just search Amazon for "double-sided prototyping board".

In the not-so-distant future, this will become the pogo pin carrier board (or 'test probe board') that we'll attach to our clamp.

Since our dual-digit display modules have only five holes, we can use a small strip from a kit or cut it from a larger piece, as illustrated in Fig.2(a). Next, we'll drill two ¼-inch or 6.5mm diameter holes, as illustrated in Fig.2(b).

We will need a way to attach this board to our clamp. I typically use two ¼-inch-diameter, 1-inch (25.4mm) long hex socket-head screws (aka. Allen screws), along with four washers and two nuts, of the types shown in Photo 3.

In terms of metric hardware, M6 × 25mm machine screws, washers and nuts would also be suitable.

Return to the image of the clamp (Photo 2) and observe the split forked part opposite the handle. This is usually called a "clevis", "forked clevis", "clevis arm", or "clevis mount".

In the fullness of time, we'll use our screws, washers, and nuts to attach our prototyping board to the clamp,

Photo 3: one set of the screws, nuts and washers I used.

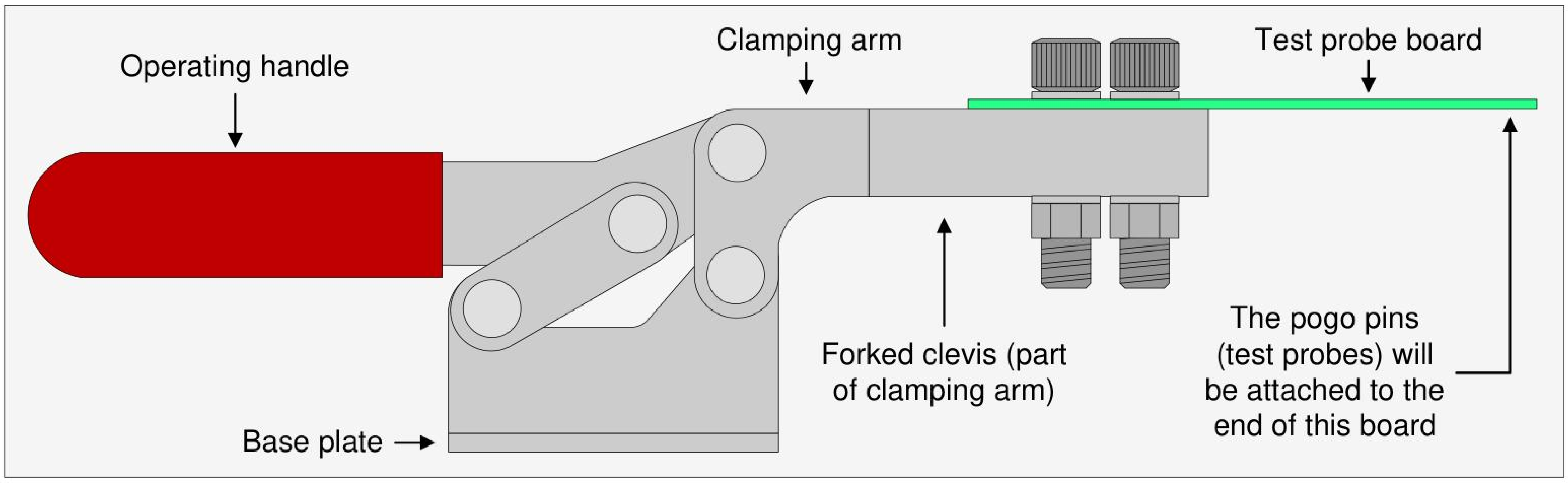
Operating handle
Clamping arm
Test probe board
Forked clevis (part of clamping arm)
The pogo pins (test probes) will be attached to the end of this board
Base plate

Fig.3: our suggested method of attaching the prototyping board to the clamp.

as illustrated in Fig.3, but first…

Springing into action

A pogo pin is a spring-loaded electrical contact used to establish quick, reliable connections between two electronic devices or circuit boards. Named after the pogo stick, it compresses to maintain constant physical and electrical contact.

The pogo pin lineup includes through-hole, double-ended, surface-mount and wire-mount styles, as well as a wide variety of pad layouts and stroke configurations. There is also a surprising diversity of tip types, two of the most common being conical (pointed) and rounded (hemispherical).

In the case of through-hole mounting, two familiar variants are collared (aka. shouldered) and uncollared (aka. straight-body).

There are hundreds (perhaps thousands) of pogo-pin styles and feature combinations, but some generic examples are illustrated in Fig.4. The plunger (or probe) is the moving part that slides in and out of the barrel. It carries the tip (conical, rounded etc) that contacts the surface under test.

The spring (not visible in this figure) pushes the plunger outward when it's unloaded. The barrel (or body) is the hollow outer tube that houses the plunger and spring and provides the fixed mechanical and electrical connection to the test probe board.

As I say, there are myriad pogo-pin offerings. The principal advantage of a collared pogo pin is that the collar serves as a mechanical stop, preventing the pin from passing through the test probe board while also ensuring a consistent mounting height.

However, uncollared pins may be preferable if the points to be probed are at different heights, such as a board with a coin-cell battery clip, where both the board and the clip need to be probed.

Professional test engineers will select specific tip geometries based on a wide range of esoteric criteria, but things are less stringent for hobbyists. Some may argue that rounded tips offer a larger contact area on pads, while others might opine that conical tips are better at penetrating surface oxidation.

In our example case of testing dual 7-segment displays, this point is moot because the points we're testing are plated-through holes, which means both tip types will make reliable contact.

In reality, most hobbyists will opt for whatever they can lay their hands on at the best price (or whatever they already have in their parts treasure chest).

I just used my micrometer to measure the ones I have, which are collared with conical tips (sadly, I no longer remember where I got them). The barrel diameter is 1mm, the plunger diameter is 0.6mm and the plunger has a 2.5mm travel (stroke).

Feeling attached

The next step is to attach our pogo pins to our test probe board. Since we are creating a test rig for our dual-digit 7-segment displays, which we will refer to as the device under test (DUT), we will need five of these pins, as illustrated in Fig.5.

We start by soldering the barrel of each pin to its associated pad, then we solder the wires to the barrels. We would also slide a small piece of heat-shrink tubing over each wire-barrel connection to provide strain relief for the joint.

The art of shim

At some stage, we will attach our clamp to a base. I typically use a small plank of timber, just a little longer and about three times as wide as the clamp itself. I also attach a small timber support block to the baseboard just under the probes. This is sized so that the tips of the probes just barely touch the wood when the clamp is in its fully lowered position (Fig.6).

The test wires aren't shown in Fig.6 to keep it simple and easy to understand.

There are all sorts of tricks you learn when you are doing this sort of thing.

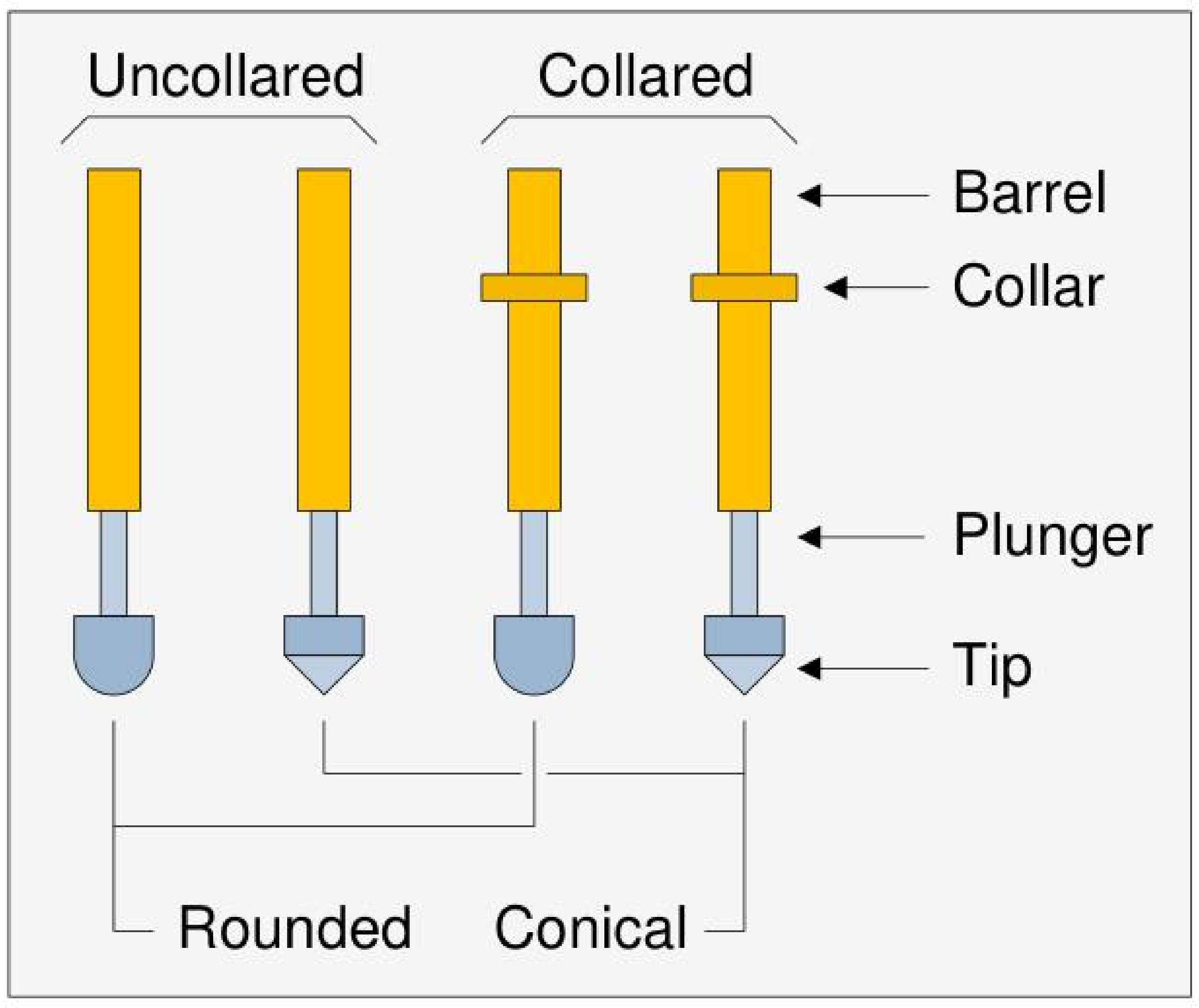

Fig.4: some common pogo pin configurations.

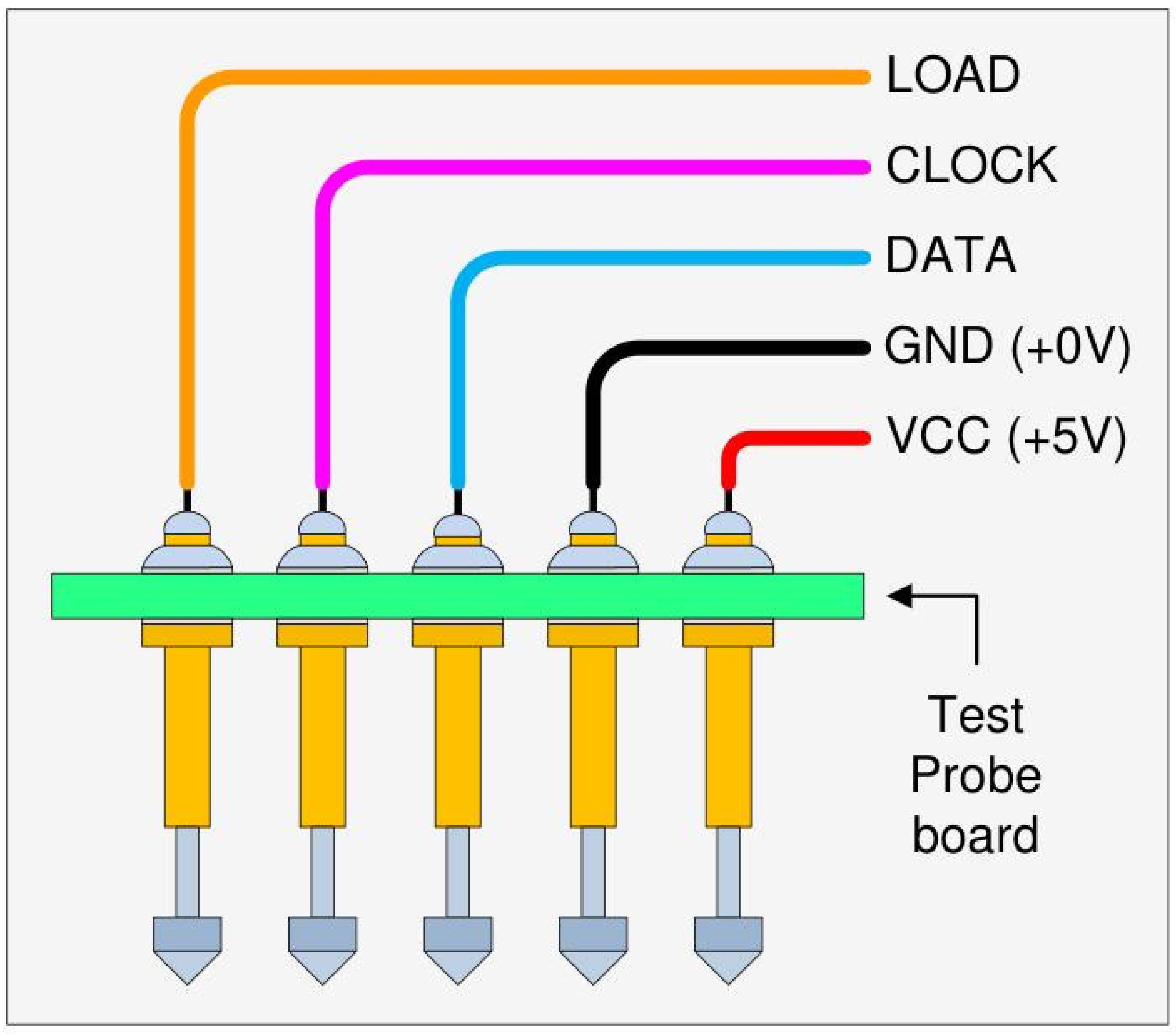

Fig.5: attaching pogo pins to the test probe board.

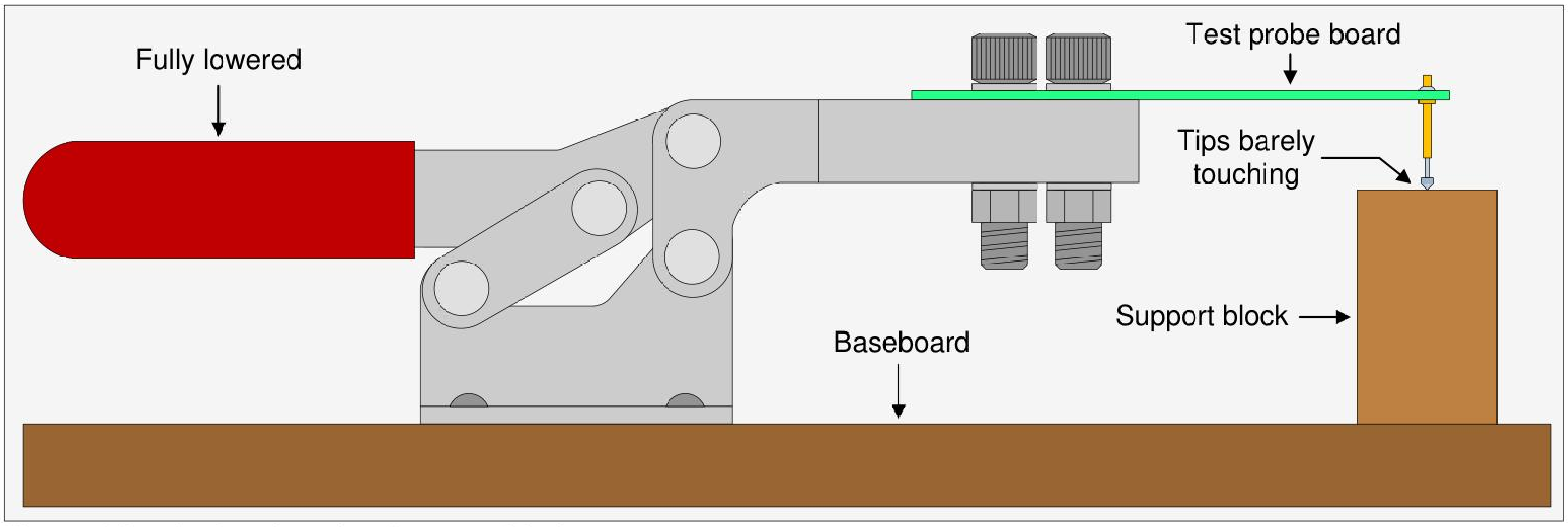
Fully lowered
Test probe board
Tips barely touching
Support block
Baseboard

Fig.6: adding the baseboard and support block.

For example, it's hard to cut the support block to the exact desired height, so it's best to go under rather than over. You can then add shims (spacers) between the baseboard and the support block to compensate. Suitable shims can be made from scraps of protoboard and cardstock, with paper used for fine adjustments.

We could simply glue the support block (and any shims) to the baseboard if we wished, but my preference is to use machine screws, nuts, and washers, as illustrated in the cutaway view in Fig.7.

This approach takes a little more time and effort upfront, but offers several advantages later. Most importantly, it allows us to tweak the arrangement by adding, removing, or changing the shims beneath the support block. It also makes the fixture easy to repair or modify, should we wish to experiment with a different block height or probe position.

Another benefit is that both the support block and test probe board can be replaced, allowing the same clamp assembly to be reused for a completely different project. Having said that, I generally prefer to keep separate fixtures for separate jobs – it's remarkable how often a jig that seemed destined for retirement suddenly proves useful again months or even years later!

Toeing the line

To ensure repeatable measurements, we need a way to locate the current DUT (device under test) in exactly the same position every time. The easiest approach is to glue a pair of guide strips, fashioned from scraps of prototyping board, to the support block.

These will serve as locating guides that register the display module relative to the pogo pins, ensuring that all five probes align with their respective plated-through holes when the clamp is lowered.

The process we use to attach these guide strips is as follows. First, we rest the end of the DUT on the support opposite the clamp, as depicted in Fig.8(a). Next, we slowly and gently close the clamp, ensuring that the tips of the probes seat in their respective plated-through holes in the DUT, as shown in Fig.8(b).

While the clamp is still engaged, attach two pieces of protoboard to the support, as illustrated in Fig.8(c). I'm showing blue protoboard pieces in this example for clarity. Try to arrange things so that their flat edges are touching the DUT.

I typically use a thin smear of two-part epoxy with a 10-minute working

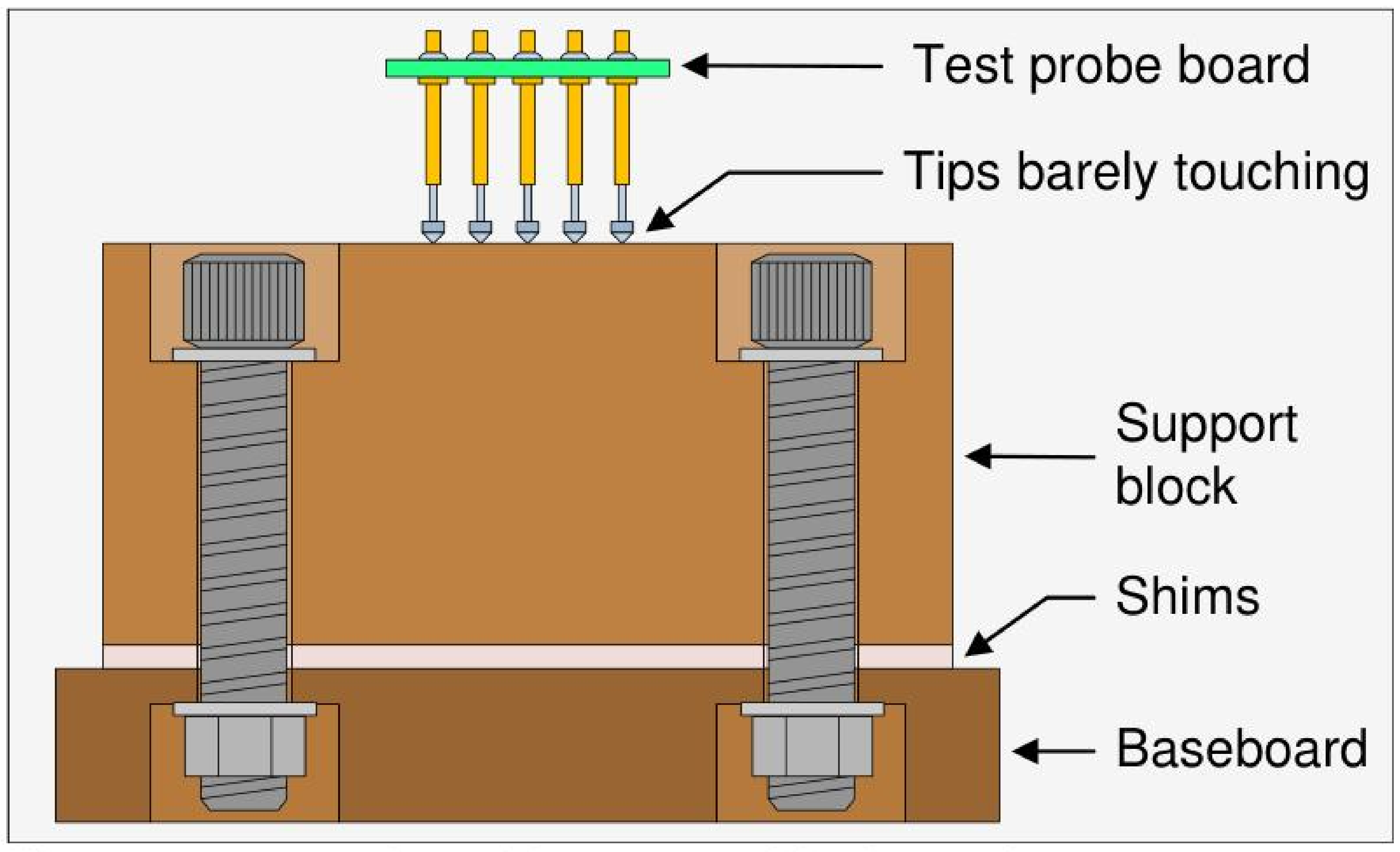
Test probe board
Tips barely touching
Support block
Shims
Baseboard

Fig.7: a cutaway view of the support block attachment.

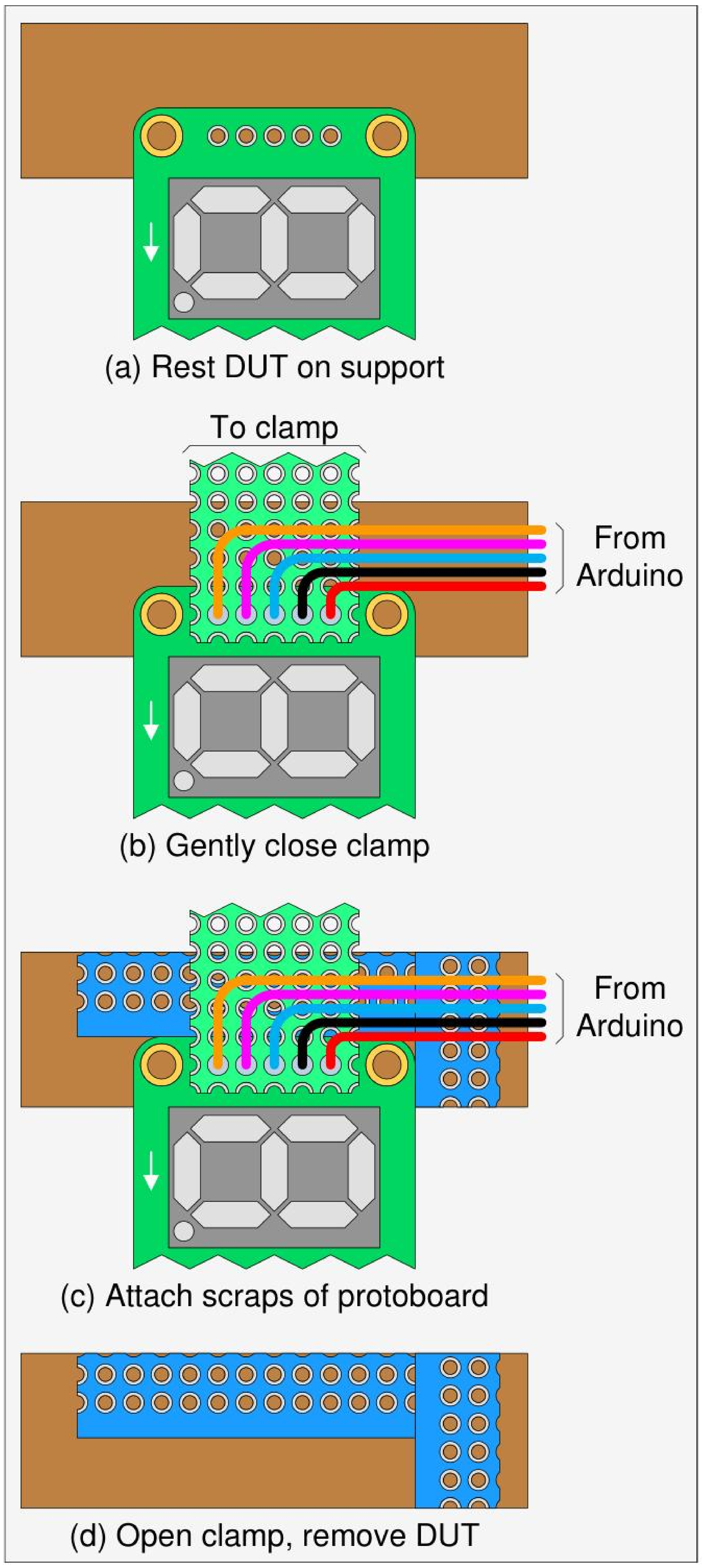
(a) Rest DUT on support
To clamp
From Arduino
(b) Gently close clamp
From Arduino
(c) Attach scraps of protoboard
(d) Open clamp, remove DUT

Fig.8: attaching the registration (guide) strips.

time (cure time) to attach these boards. Be careful not to get any on the DUT… or anything else, for that matter! Leave the clamp locked for at least 30 minutes (longer is better), then open it and remove the DUT, as shown in Fig.8(d).

In the future, you'll find that having things set up this way makes it easy-peasy lemon-squeezy to place a new DUT in precisely the same position every time.

Testing times

I typically mount at least one momentary pushbutton on the timber base, with one side connected to 0V (GND) and the other to one of the Arduino's digital input pins. I also write a test program that waits for this button to be pressed before running the test sequence.

For something as simple as our dual 7-segment display module, a visual inspection may suffice. More complex devices might benefit from multiple tests, each with an associated trigger button.

In some cases, in addition to driving the DUT's inputs, we could use Arduino to monitor its outputs and then employ the results to modify the test and/or display Pass/Fail messages (or more detailed diagnostic information) on the Serial Monitor.

Returning to the Countdown Timer…

Phew! I have to admit that our test rig discussions took longer than I expected. It may be that you don't have a use for such a device at the moment, but one day in the future you'll find yourself knee-deep in pogo pins and protoboard, and you'll say to yourself, "Good grief! Max covered exactly this situation in the August 2026 issue of PE!"

As usual, we're going to take things one step at a time. A couple of columns ago, in the June issue, we introduced the two types of boards we're working with, including the files you can use to build them. We'll start with the VFD driver board.

Look at the top of this board, as illustrated in Fig.9(a). The only silkscreen component outline on this side of the board is the white circle associated with the VFD tube itself. This is because the tube is the only component that we will be mounting on the top of the board, but that's still in our future.

Now observe the rectangular cutout in the middle of this circle. This is where we will locate the NeoPixel, which will sit beneath the tube and allow us to implement some cool lighting effects. As we discussed in an earlier column, arranging things this way will make it easier to replace the NeoPixel, should it fail, without requiring us to remove the tube first (we're thinking ahead… for a change).

I purchased a pack of 100 NeoPixels from the Led Lighting Hut (**www.ledlightinghut.com**) for $12.50. Even my poor maths tells me this works out to US 12.5¢ (~10 UK pennies) apiece, which I think is awesome, not least that I'll have lots left over for future projects.

Now observe the small silkscreened triangle associated with the upper left-hand corner of the cutout. Also observe that one corner of the upper face of the NeoPixel has a triangular embossment. Both of these features, highlighted by red circles in Fig.9(a), are used to indicate the correct orientation of the NeoPixel.

Now flip the board over, as though turning the page of a book, to reveal its underside, as illustrated in Fig.9(b). Flip the NeoPixel over in a similar fashion. Observe that the silkscreen on this side of the board contains all the remaining component and connector identifiers and outlines because, as we already noted, everything except the tube is mounted on this side of the board.

Drop the NeoPixel into the cutout, as illustrated in Fig.9(c). I inserted a small square of thin card first to ensure that the back of the NeoPixel sat flush with the underside of the board. Next, use your soldering iron to create solder bridges between the NeoPixel's pads and the corresponding pads on the board.

Add a 100nF (0.1µF) ceramic capacitor at location C3. This acts as a local decoupling capacitor; an 'energy reservoir', if you will (kind of like a tiny battery) that helps keep the supply rail steady when the NeoPixel switches its internal transistors. Mount this capacitor on the underside of the board and solder it from the top side.

Finally, add a 0.1-inch (2.54mm) pitch 2×10-pin female (socket) double-row right-angled header in the SK1 ("Socket 1") position. Also add a 2×10-pin male (plug) double-row right-angled header in the PLG1 ("Plug 1") position. As for the capacitor, mount these connectors on the underside of

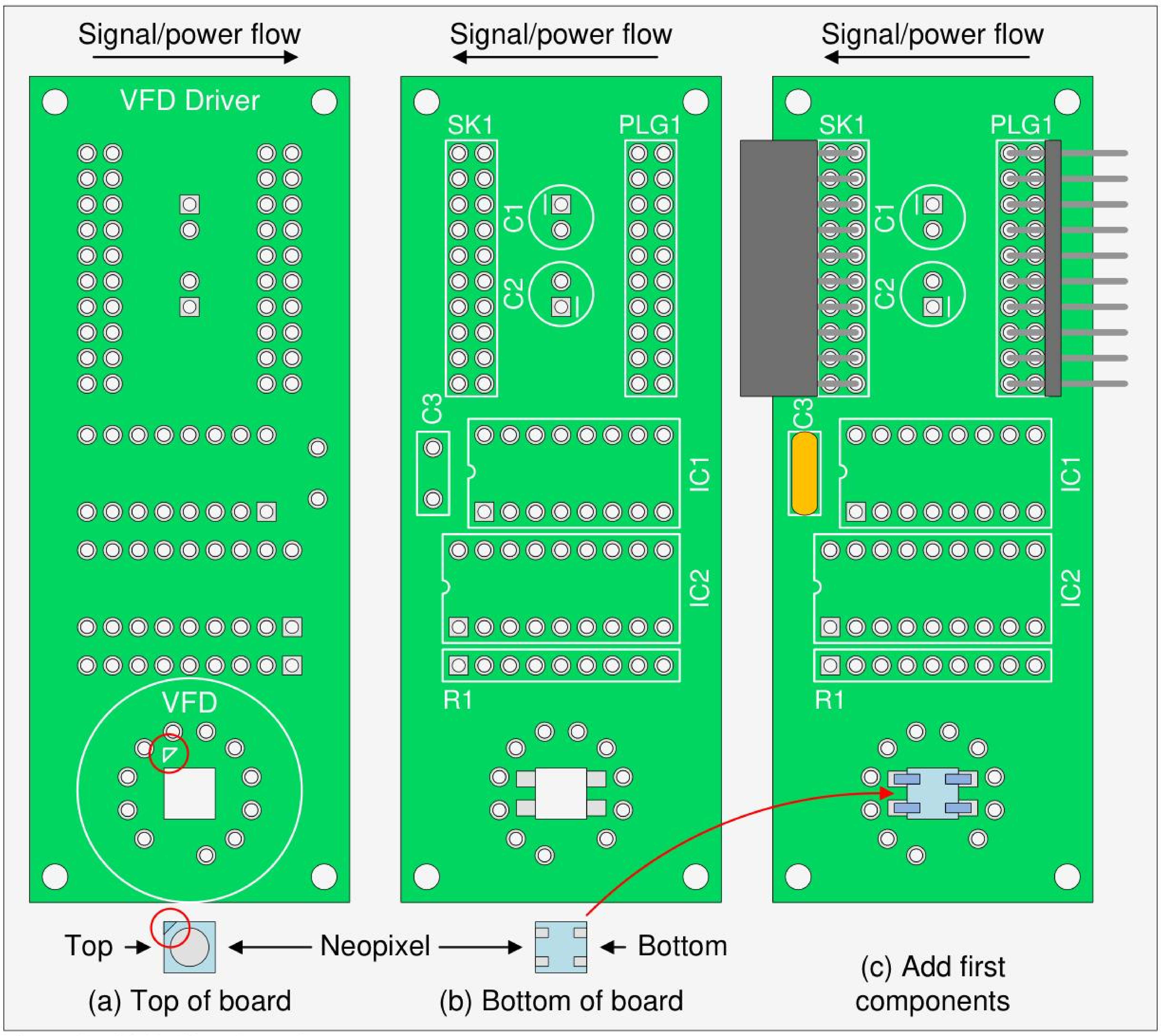

(a) Top of board

(b) Bottom of board

(c) Add first components

Fig.9: the VFD driver board.

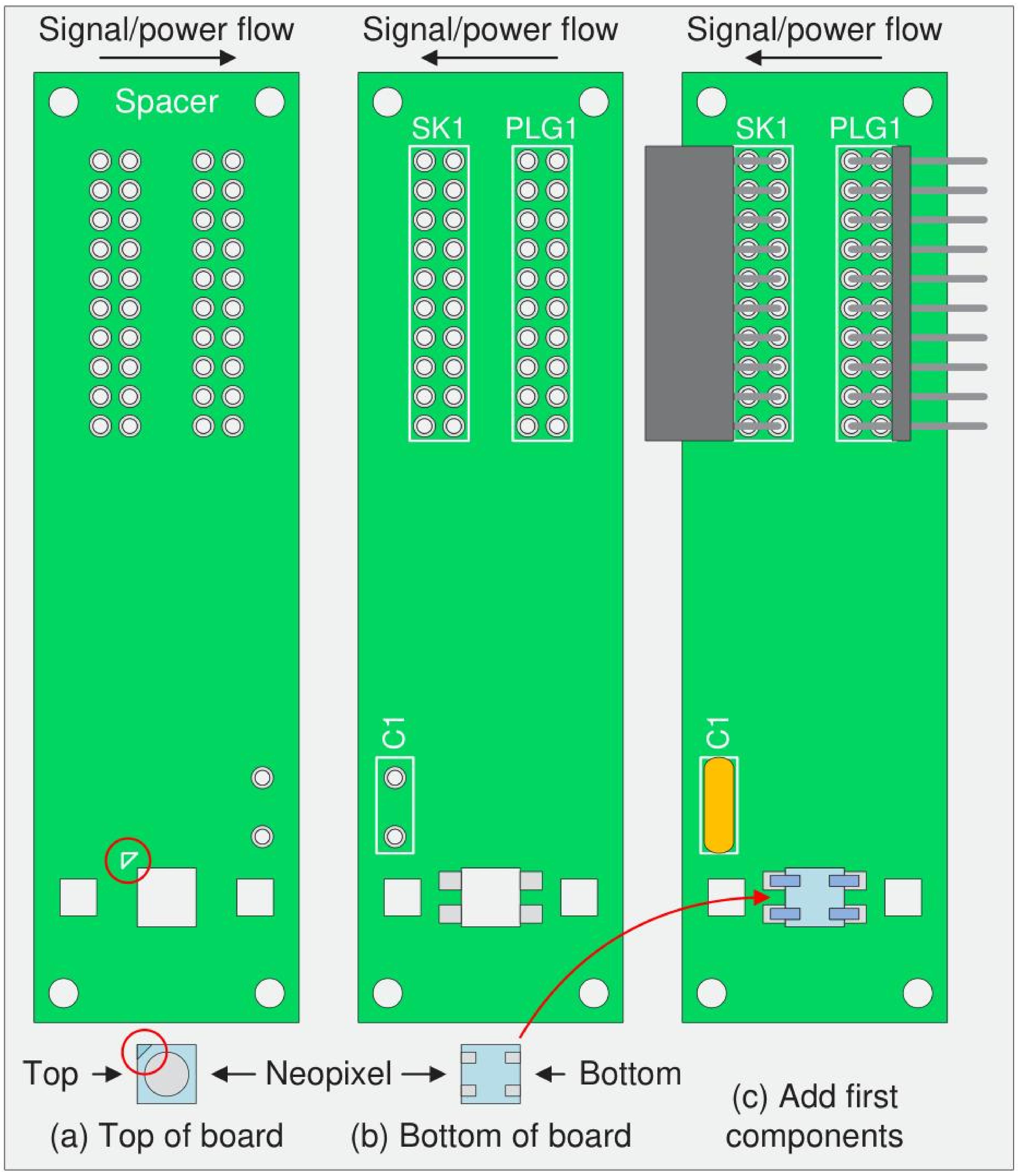

(a) Top of board (b) Bottom of board (c) Add first components

Fig.10: the spacer board has fewer parts on it.

the board and solder them from the top side.

Here is an example of where mistakes can be easily made in a PCB design – the original PCB had PLG1 on the left and SK1 on the right. Flipping the board back and forth makes one's brain wobble on its gimbals, resulting in this mistake, which has since been fixed.

In a sense, it doesn't matter which connector goes where, just so long as you're consistent with the remaining boards. Having said this (and as we discussed in a previous issue), it's generally preferable to have a socket on the last board in the chain rather than a plug, because this helps prevent any unintentional 'oopsies' involving exposed pins and short circuits.

I understand that you are awash with enthusiasm, but I would recommend that you pause after assembling your first driver board to the extent discussed thus far. I know you want to populate all of your boards (14 if you are planning on implementing a Full Monty **YYYY-MM-DD hh-mm-ss** display).

However, it's best to stick with just one board initially to make sure everything is tickety-boo – like confirming that we've got the NeoPixel the right way round, for example – before potentially making the same mistake 14 times (yes, I do speak from experience… not in this particular case, but experience nonetheless).

Adding a spacer board

Now we're going to perform a similar exercise on one of our spacer boards (Fig.10). We will use five of these boards to separate the various tube groups. In the date portion of the display, we'll have one spacer between the **YYYY** and **MM** groups, and another between the **MM** and **DD** groups.

Similarly, for the time portion, we'll have one spacer between the **hh** and **mm** groups and another between the **mm** and **ss** groups.

Each of these spacer boards has its own NeoPixel, which we will use to illuminate separator characters such as the vertical slashes in **YYYY|MM|DD** and the colons in **hh:mm:ss**. Observe the two small square cutouts on either side of the NeoPixel cutout. These can be used to attach whatever separator assembly we eventually decide to employ.

We will also have a fifth spacer board located between the date and time portions of the display. Although this board will also include a NeoPixel (allowing us to easily swap boards if necessary), we will leave it unilluminated.

Attach the NeoPixel, 100nF ceramic capacitor (annotated as C1 in this case) and connectors, as per Fig.10(c). Observe that we got the SK1 and PLG1 silkscreen legends right the first time in this case (woohoo!).

Once again, I'm sure you are itching to assemble all five spacer boards, but I recommend exercising a modicum of restraint by completing just one initially to make sure everything is hunky-dory before potentially perpetrating the same mistake multiple times.

A plethora of pins

Fig.11 presents a top-down view of the connector arrangement. The 2×10-pin plug connector is on the left, while the corresponding socket connector is on the right. The yellow-highlighted pins are associated with the shift registers that will appear on each driver board.

We don't need to concern ourselves with these signals at the moment, but we will discuss them in ~~excruciating~~ exhilarating detail next month. Similarly, we can ignore the +1.5V and +25V power connections for now.

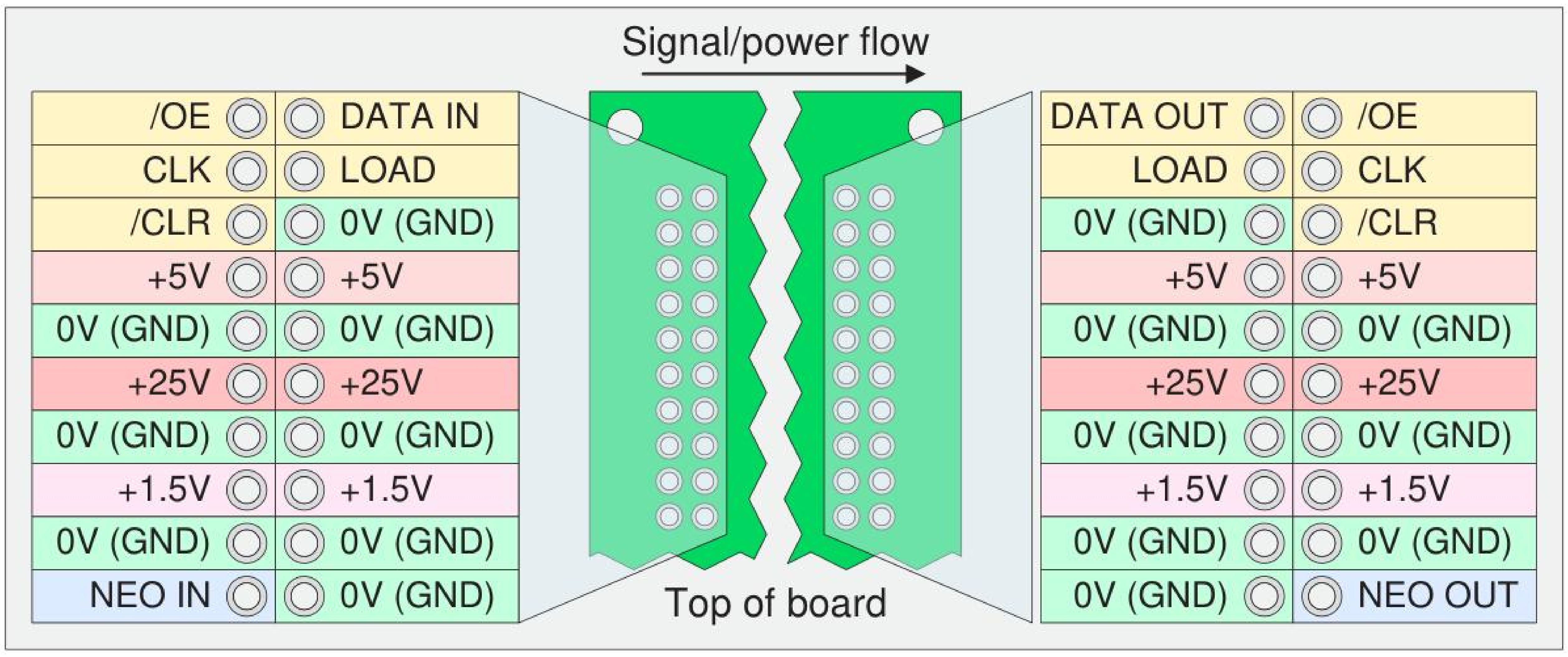

/OE	DATA IN
CLK	LOAD
/CLR	0V (GND)
+5V	+5V
0V (GND)	0V (GND)
+25V	+25V
0V (GND)	0V (GND)
+1.5V	+1.5V
0V (GND)	0V (GND)
NEO IN	0V (GND)

DATA OUT	/OE
LOAD	CLK
0V (GND)	/CLR
+5V	+5V
0V (GND)	0V (GND)
+25V	+25V
0V (GND)	0V (GND)
+1.5V	+1.5V
0V (GND)	0V (GND)
0V (GND)	NEO OUT

Fig.11: the connector pinouts, common to both board types.

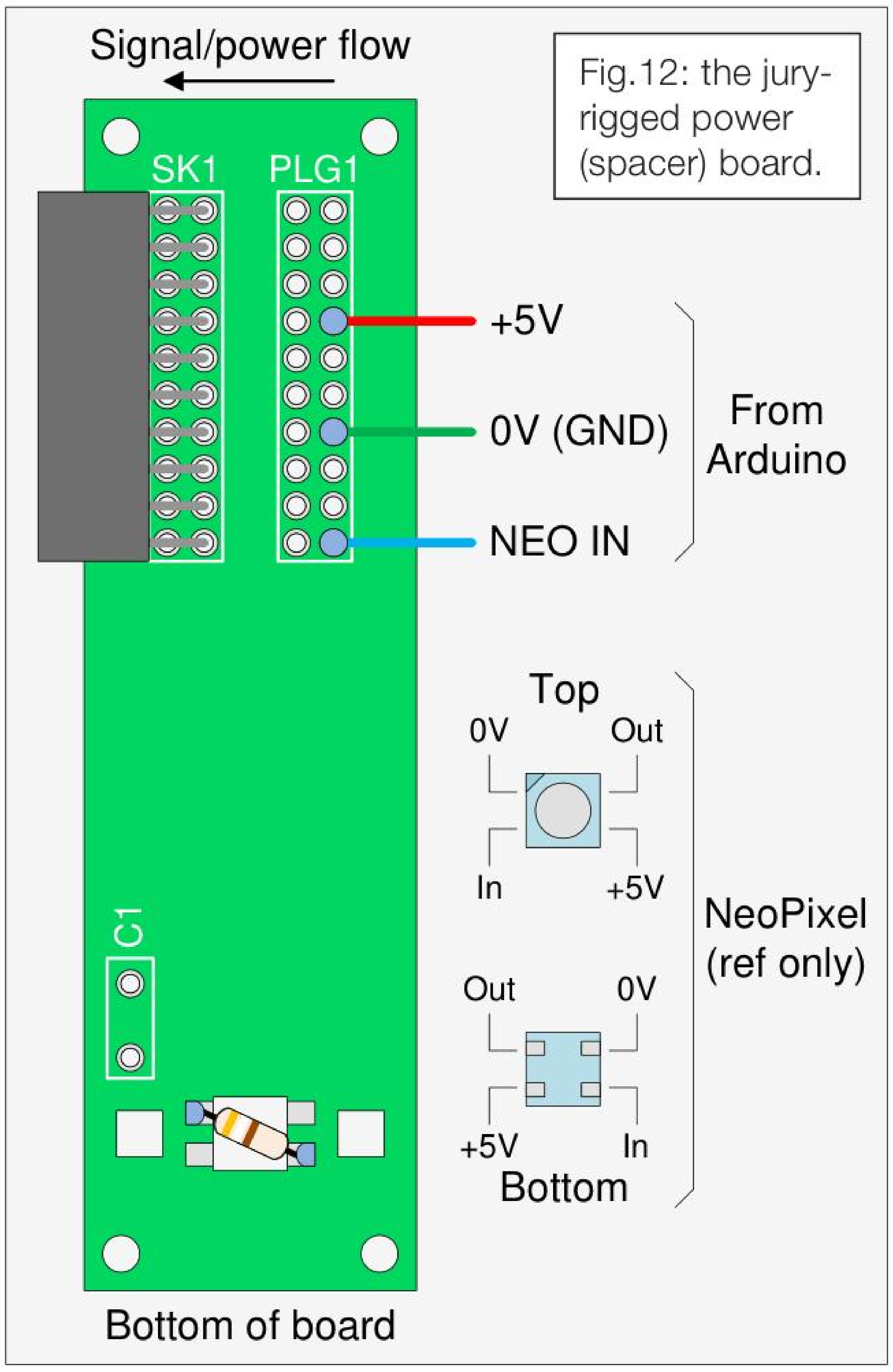

Fig.12: the jury-rigged power (spacer) board.

At this point, the only pins we really care about are the +5V and 0V (GND) power connections, along with the NeoPixel-related signals: **NEO IN** and **NEO OUT**. We'll need to drive more later once the VFDs are connected.

Introducing the power board

In the fullness of time, we're going to build an all-singing, all-dancing power board to satisfy any power-related cravings we might have. In the meantime, however, just to get the ball rolling, as it were, I've taken one of my spare spacer boards and configured it to act as a pseudo power board, as illustrated in Fig.12.

Since we're going to start off by running everything from the Arduino, I took three male-to-male flying leads, chopped one connector off each lead, bared the wire ends, and soldered them to the board.

As we've discussed multiple times before, when using a chain of NeoPixels, it's good practice to add a series resistor as close as possible to the data input pin of the first NeoPixel in the chain. This resistor helps tame the fast edges from the Arduino's output, reducing ringing and the associated overshoot and undershoot on the data line.

The value commonly recommended for this resistor lies in the range of 330Ω to 470Ω. I typically opt for a 390Ω ¼W device (coloured bands orange [3], white [9], brown [$\times 10^1$]), which sits nicely midway between these values.

We could wire this resistor inline with the **NEO IN** signal coming from the Arduino. However, since we are already using one of our spacer boards as a pseudo-power board, it's easier to attach the resistor to this board, straddling the **In** and **Out** pads associated with the NeoPixel cutout, as shown in Fig.12.

Observe that we haven't bothered to populate the C1 ceramic capacitor on this board because we won't be mounting a NeoPixel here.

All together now

We're almost there! The final step for now is to take our pseudo power board together with the driver and spacer boards we've assembled thus far and plug them all together. Fig.13 shows a top-side view of the three boards prior to assembly.

Once the boards have been assembled, we can connect the 0V (GND), +5V, and NEO IN wires to the Arduino. In this case, we're going to use digital pin 6 to drive the NeoPixel chain for no better reason than that every project needs at least one arbitrary design decision, and 6 happens to be my lucky number.

Over to you

This is the point where we write a

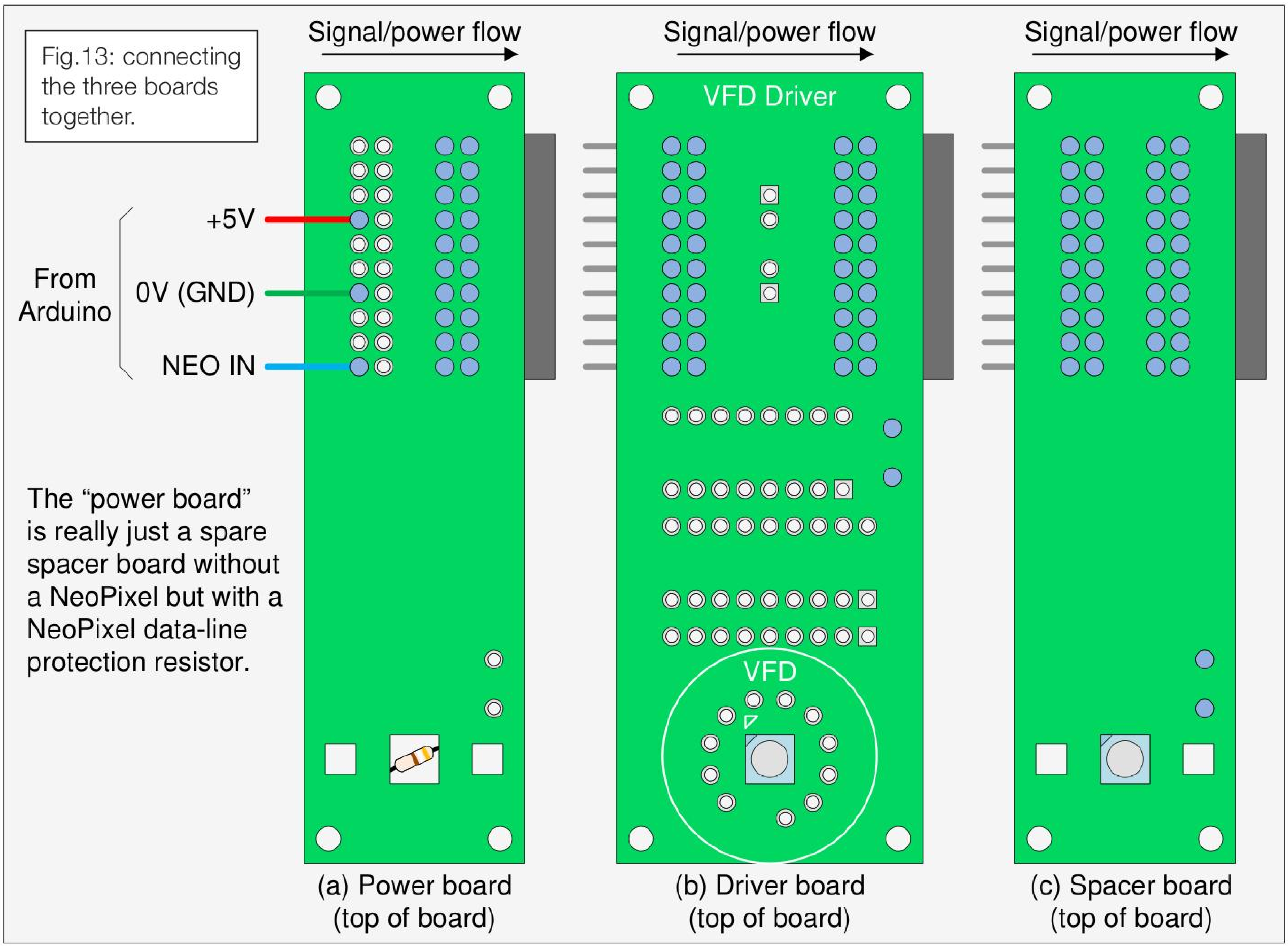

Fig.13: connecting the three boards together.

The "power board" is really just a spare spacer board without a NeoPixel but with a NeoPixel data-line protection resistor.

(a) Power board (top of board)

(b) Driver board (top of board)

(c) Spacer board (top of board)

small Arduino program to exercise our NeoPixel chain and verify that everything is working as expected before assembling the remaining boards. This will allow us to confirm things like power distribution, signal propagation, and, perhaps most importantly, that we haven't accidentally soldered any NeoPixels in the wrong way round.

Once we are happy that everything is behaving itself, we can proceed to assemble the remaining driver and spacer boards required for our chosen display configuration (whether that's a modest setup or the full-blown **YYYY|MM|DD hh:mm:ss**). We can then tweak our program to test the entire ensemble.

Now, after all the NeoPixel escapades we've enjoyed together over the past few years, including the 14×10 array on our retro games console, I'm of the opinion that you should be more than capable of writing this little test program yourselves. So, rather than me spoon-feeding you every last line of code, I'm going to throw down the gauntlet and invite you to have a go.

In its simplest form, the program needs only to initialise the NeoPixel chain and cycle the LEDs through a selection of colours and patterns to confirm that all the boards are correctly assembled and connected.

Next month, we'll revisit this topic in more detail, compare notes (and see whose version is the most elegant, the most over-engineered, or the most gloriously bonkers), and continue by adding the VFD tubes and associated circuitry.

As always, if you have any thoughts you'd care to share on anything you've read here, please feel free to email me at **max@clivemaxfield.com** **PE**

5-year collections

2019-2023
£49.95

2018-2022
£49.95

2017-2021
£49.95

2016-2020
£44.95

Purchase and download at:
www.electronpublishing.com

Devices and components used in this issue

Qty	Part	Source
19	NeoPixels (5050 WS2812B)	www.ledlightinghut.com
14	Driver boards	See *PE*, June 2026
6	Spacer boards (including power board)	See *PE*, June 2026
1	390Ω ¼W axial resistor	Any good electronics shop
19	100nF (0.1µF) ceramic capacitors	Any good electronics shop
20	2×10-pin 0.1"/2.54mm pitch right-angle headers	https://pemag.au/link/acca
20	2×10-pin 0.1"/2.54mm pitch right-angle sockets	https://pemag.au/link/acc9

ETI BUNDLE (1) Teach-In 3, 4 and 5 – all on CD-ROM – only £18.95

ELECTRONICS TEACH-IN 3 – CD-ROM
Mike & Richard Tooley

The three sections of the *Teach-In 3* CD-ROM cover a huge range of subjects that will interest everyone involved in electronics – from newcomers to the hobby and students to experienced constructors and professionals.

The first section (80 pages) is dedicated to *Circuit Surgery*, *EPE/PE's* regular clinic dealing with readers' queries on circuit design problems – from voltage regulation to using SPICE circuit simulation software.

The second section – *Practically Speaking* – covers hands-on aspects of electronics construction. Again, a whole range of subjects, from soldering to avoiding problems with static electricity and identifying components is covered. Finally, our collection of *Ingenuity Unlimited* circuits provides over 40 circuit designs submitted by readers.

The CD-ROM also contains the complete *Electronics Teach-In 1* book, which provides a broad-based introduction to electronics in PDF form, plus interactive quizzes to test your knowledge and TINA circuit simulation software (a limited version – plus a specially written TINA Tutorial). *Teach-In 1* covers everything from electric current through to microprocessors and microcontrollers, and each part includes demonstration circuits to build on breadboards or to simulate on your PC.

ELECTRONICS TEACH-IN 3

ELECTRONICS TEACH-IN 4 – CD-ROM, A BROAD INTRODUCTION TO ELECTRONICS
Mike & Richard Tooley

The *Teach-In 4* CD-ROM covers three of the most important electronics units that are currently studied in many schools and colleges. These include, Edexcel BTEC level 2 awards and the electronics units of the Diploma in Engineering, Level 2.

The CD-ROM also contains the full *Modern Electronics Manual*, worth £29.95. **The Manual** contains over 800 pages of electronics theory, projects, data, assembly instructions and web links.

It's an ideal way to learn about electronics.

ELECTRONICS TEACH-IN 4

ELECTRONICS TEACH-IN 5 – CD-ROM
JUMP START
Mike & Richard Tooley

15 design and build circuit projects for newcomers or those following courses in school and colleges.

The projects are: ■ Moisture Detector ■ Quiz Machine ■ Battery Voltage Checker ■ Solar-Powered Charger ■ Versatile Theft Alarm ■ Spooky Circuits ■ Frost Alarm ■ Mini Christmas Lights ■ iPod Speaker ■ Logic Probe ■ DC Motor Controller ■ Egg Timer ■ Signal Injector Probe ■ Simple Radio Receiver ■ Temperature Alarm.

PLUS

PIC'n' Mix – starting out with the popular range of PIC microcontrollers and *Practically Speaking* – tips and techniques for project construction.

The CD-ROM also contains:
■ Complete *Teach-In 2* book, a practical introduction to PIC microprocessors
■ MikroElektronika, Microchip and L-Tek PoScope software.

ELECTRONICS TEACH-IN 5

Three Teach-ins for the great price of £18.95

PLUS you also get the contents of the free CD-ROM from each issue...

... so that's another TWO Teach-Ins and The Full Modern Electronics Manual!

By Andrew Levido

Power Electronics

Part 5: power factor correction & EMI filtering

In last month's article, we mentioned the importance of power factor for an efficient electrical grid. This time, we will look at some active techniques that can help in this regard. We will also cover EMI filtering, which is related in the sense that it is also concerned with the mitigation of unwanted current harmonics.

Electromagnetic interference (EMI) is a general term for any disturbance caused by an electromagnetic field that negatively impacts the performance of electrical or electronic equipment. EMI can be radiated through space or conducted from one device to another through signal or power cables.

While you can (and should) take steps to make sure your designs are not susceptible to EMI produced by other devices, your main focus should be on making sure your designs are not producing unacceptable levels of EMI that could affect other equipment.

EMI standards such as EN55032 require radiated emissions in the 30MHz to 1GHz range to be below certain field strength thresholds when tested with a standard antenna at a distance of 10m. Mitigating radiated EMI requires close attention to shielding of enclosures, grounding, minimising conductor loop areas, optimising PCB layout, the use of ground planes and controlling the slew rate of signals.

Conducted EMI

We will focus on conducted EMI, specifically signals that are conducted back into the power source by switching converters. The standards are generally concerned with frequencies in the 150kHz to 30MHz range, and require the level of signals within to fall below specified thresholds over different parts of the band, typically measured using a spectrum analyser.

To give you an idea of what is required, conducted EMI for a Class A device must be below 79dBμV from 150kHz to 500kHz and below 73dBμV from 500kHz to 30MHz when measured with a 'quasi-peak' detector. The dBμV units describe the amplitude of the conducted emissions with respect to a 1μV reference. 79dBμV is therefore about 9mV RMS and 73dBμV is about 4.5mV RMS.

Requirements for Class B devices are considerably lower.

EMI is usually managed by the addition of filters on the lines. The switching frequency of many modern converters is higher than 150kHz, so the converter's input filter plays a critical role in meeting conducted EMI specifications. Fig.1 shows a standard buck converter with a simple capacitive input filter C_f and with source impedance Z_S.

Our task is to analyse this filter and ensure that the voltage amplitude of the switching-frequency ripple (and its harmonics) is below the required threshold.

So far in this series, we have used average value analysis to understand the converter's periodic steady-state (PSS) operation and complex frequency analysis to determine the converter's dynamic performance. Neither of these will help us now, so we will revert to good old AC time-domain analysis.

This is a technique which, as its name suggests, ignores the DC component of the signal and focuses on the AC component. For example, the PSS model shows us that the input current (i_x) of the converter in Fig.1 has a rectangular shape with a duty cycle D and an amplitude of I_L as shown in the upper chart there.

If we remove the DC component of the input current, we get the alternative picture shown in the lower chart. I have shown the current here with a duty cycle of 0.5, which gives the highest AC RMS current. If the duty cycle moves away from 0.5 in either direction, the RMS current decreases,

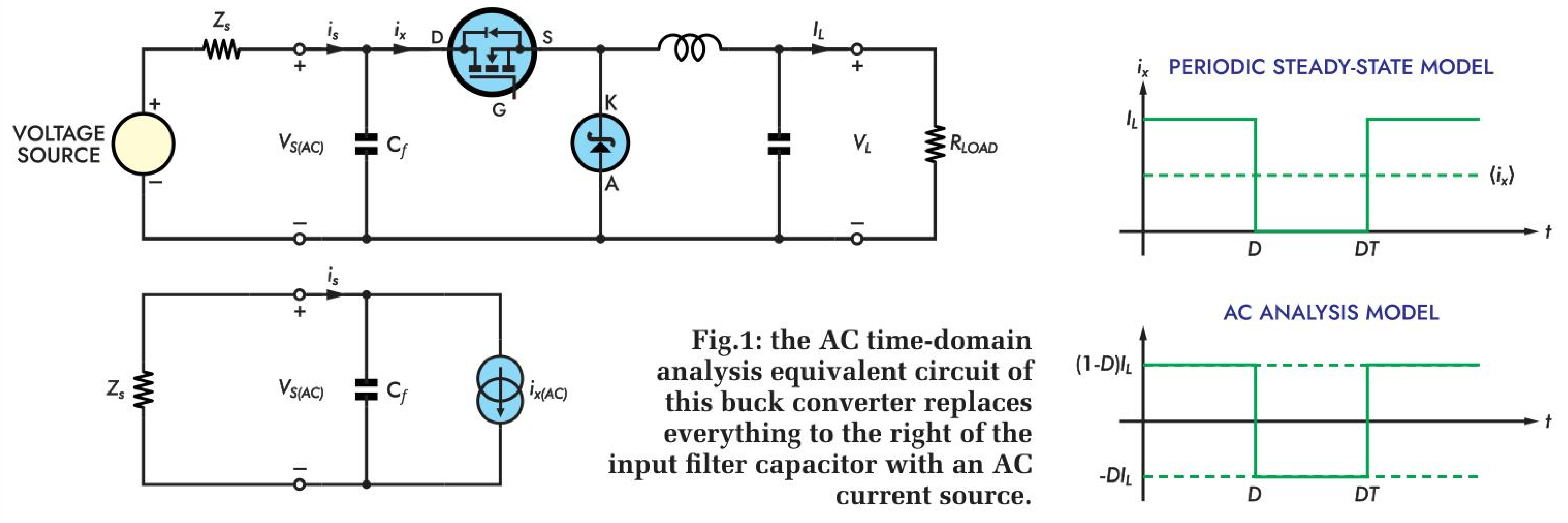

Fig.1: the AC time-domain analysis equivalent circuit of this buck converter replaces everything to the right of the input filter capacitor with an AC current source.

reaching zero at the extremes when D = 0 or D = 1.

This is a common approximation because we usually want to design EMI filters for the worst-case situation. It is also easiest to calculate the harmonics of the AC waveform if it is a true square wave.

The lower circuit in Fig.1 shows the AC analysis model of the buck converter. Everything to the right of the input filter capacitor is replaced with an AC current source $i_{x(AC)}$, and the DC voltage source is eliminated altogether. In this case, the current source will be a variable duty cycle rectangular wave with a peak-to-peak amplitude of I_L.

We will use this model to design a suitable input filter in a moment. First, we should think about how we are going to measure the conducted EMI in this circuit.

The voltage that our spectrum analyser would see, $v_{S(AC)}$, is obviously highly dependent on the source impedance, Z_S. We can assume this is quite low at DC, but who knows what it will look like over the 150kHz to 30MHz band of interest.

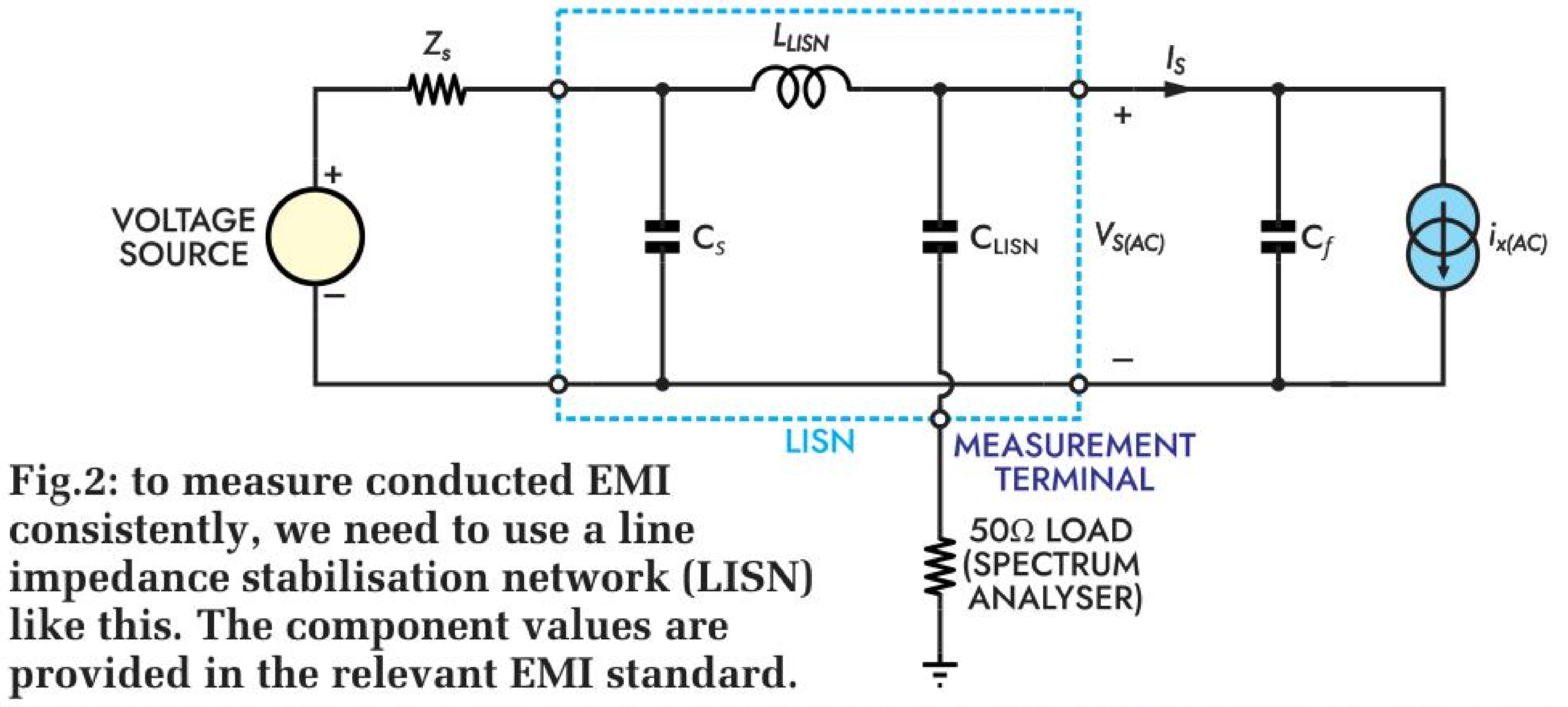

Fig.2: to measure conducted EMI consistently, we need to use a line impedance stabilisation network (LISN) like this. The component values are provided in the relevant EMI standard.

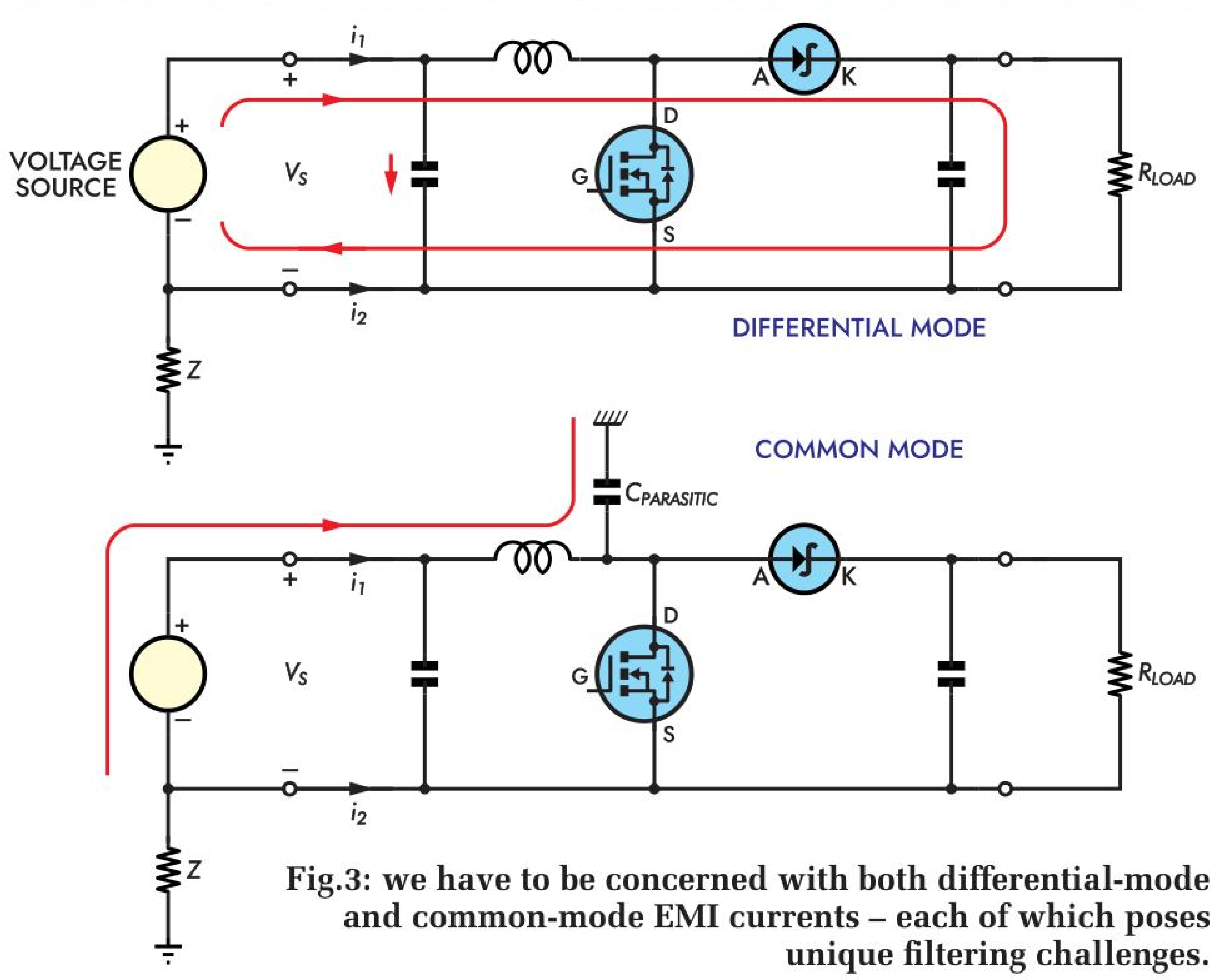

Fig.3: we have to be concerned with both differential-mode and common-mode EMI currents – each of which poses unique filtering challenges.

The LISN

To make meaningful and repeatable EMI measurements, we have to specify a standard source impedance at the frequency of interest. For this reason we use a line impedance stabilisation network (LISN) when making conducted EMI measurements. LISNs are used with both DC and AC sources.

Fig.2 shows the AC model connected to a voltage source with impedance Z_S via a LISN inside the dotted box. I have reinstated the source voltage to indicate that the converter is powered through the LISN, which has a low impedance at DC or mains frequency but presents a load of 50Ω to the converter input at the frequencies of interest.

The LISN's inductor and capacitor values are chosen so that C_S is effectively a short circuit and L_{LISN} is effectively open-circuit at the measurement frequencies. The impedance at the converter's input is therefore the 50Ω input impedance of the spectrum analyser. C_{LISN} blocks any DC or mains-frequency AC from reaching the analyser, since the converter has to be powered up to make the measurements.

The LISN's component values are specified in the relevant EMI standard, but typical values might be C_S = 1μF, L_{LISN} = 50μH and C_{LISN} = 100nF. Most LISNs use air-cored inductors to keep stray capacitances low, and there may be a resistor in series with C_S to damp resonances (more on this below).

There will probably also be a high-value resistor (≥1kΩ) between the measurement terminal and common so that the measurement terminal does not float when no spectrum analyser is connected.

Commercial LISNs may also include additional filter stage(s) on the source side to limit the influence that EMI entering from the source has on the measurement.

The LISN network shown in Fig.2 is repeated on the positive and negative lines in a DC LISN, and on each phase and the Neutral conductor of an AC LISN so that common-mode and differential-mode measurements can be made.

Common mode versus differential mode

So far we have been analysing converters and their input filters using a huge assumption: we have assumed that all current flowing into one input terminal flows out of the other one as per the upper diagram in Fig.3. This has been a reasonable thing to do for everything we have done so far, but it does not stand up when we are looking at higher frequencies.

The lower diagram represents an alternative high-frequency current path where there is some parasitic capacitance to Earth, for example between the drain tab of a TO-220 Mosfet and an Earthed heatsink. This current enters via the positive input terminal but returns to the source via Earth – there is no corresponding current coming out of the negative input terminal.

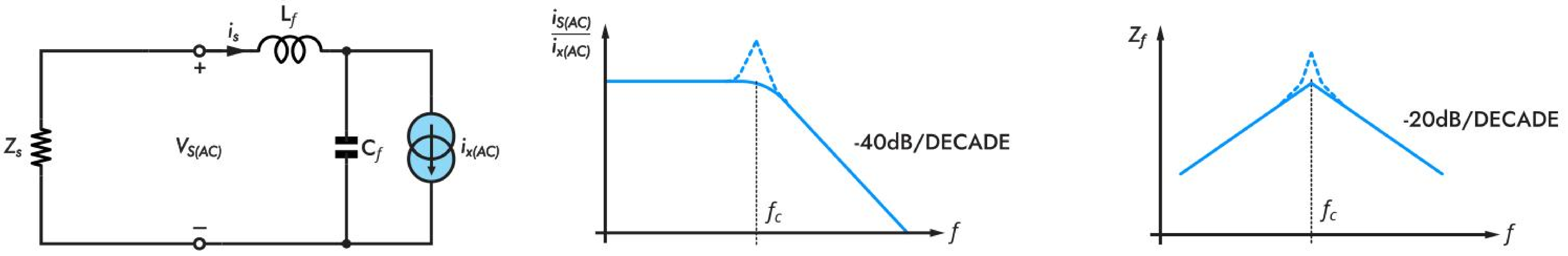

Fig.4: an LC differential-mode filter like this one may require damping to eliminate oscillations caused by gain peaking at the LC resonant frequency.

This is just one possible alternative path for current to flow; there will be many in a real converter, including some related to the negative terminal.

In reality, both types of current flow will be happening at the same time, so the currents labelled i_1 and i_2 will be the sum of the two. The current that flows into one terminal and out the other is termed the differential-mode current (i_{DM}), and the current that only flows into one terminal is the common-mode current, i_{CM}.

The differential-mode current includes the normal operating current of the converter, including all of its harmonics, while the common-mode current is related to leakage paths.

Mathematically, i_{DM} is defined to be $\frac{1}{2}(i_1 - i_2)$ and i_{CM} is $i_1 + i_2$. Note that both i_1 and i_2 flow into the converter in this model. These definitions give a clue to the names; differential-mode current is related to the difference in currents flowing into the converter, while common-mode currents are related to the total current flowing into both terminals.

It is perhaps more intuitive to look at these equations from the other direction – in terms of the currents into the positive terminal and that coming out of the negative one, ie, i_1 and $-i_2$, respectively.

In this case, $i_1 = i_{DM} + \frac{1}{2}i_{CM}$ and $-i_2 = i_{DM} - \frac{1}{2}i_{CM}$. In other words, differential-mode current flows into one terminal and out the other, while common-mode current flows equally into both terminals and out somewhere else.

Differential-mode input filter

EMI standards put limits on both differential-mode and common-mode interference, so both have to be filtered. These two filtering problems are different in nature and have different challenges and solutions. We'll start with the differential-mode filter.

To do this, we will go back to the AC analysis model we created in Fig.1. The input filter was a simple capacitor, and we saw that its effectiveness was dependent on the source impedance. For EMI measurements, we can use a LISN to standardise the source impedance, but for everyday operation, we are stuck with an unknown impedance.

We can reduce this dependence by employing an LC filter like that shown in the AC equivalent circuit of Fig.4.

I have drawn this filter as it appears in the converter, with its input on the right and its output on the left. You might be wondering why, if this is the case, the inductor is on the output side of the filter and not on the input side, as is usual for LC filters. This is a current-sourced filter, so the source has a much higher impedance than the load (Z_S).

In a typical voltage-sourced filter, the source has a lower impedance than the load. In both cases, the filter works most effectively if the inductor is on the low-impedance side, since its impedance increases with frequency.

The graphs to the right of the schematic show the current transfer function of the filter (ratio of output current i_s to input current i_x), which looks like that of any typical LC low-pass filter. The cutoff frequency is $1 \div (2\pi\sqrt{L_f C_f})$, and the roll-off is -40dB per decade. To the right of that is the filter's impedance characteristic.

At frequencies well below f_c, the impedance is dominated by the inductance; at frequencies above f_c, it is dominated by the capacitance.

With ideal components, as we approach the cutoff frequency, the magnitude of the transfer function and impedance are theoretically infinite. With real components, there will always be some degree of natural damping, but LC filters often exhibit significant peaking at the resonant frequency, as shown dotted in the diagrams.

LC filters tend to oscillate because of this peaking, especially if excited by a harmonic-rich square wave. This problem is compounded in power electronics because switching converters often have a negative input resistance. This negative resistance provides 'negative damping' and increases the likelihood of oscillation.

To understand how a switching converter can exhibit negative input resistance, consider a DC-DC converter with a fixed output voltage and load. Under these circumstances, some amount of power is being delivered to the load and consequently drawn from the input source.

If the input voltage were to rise a little bit, the control loop would adjust the duty cycle to keep the output voltage constant. The output power remains constant, so therefore does the input power, causing the input current to drop slightly.

Ohm's Law dictates that the input resistance is the change in voltage (positive in our example) divided by the change in current (negative), so the incremental input resistance must be negative.

Damping

For these reasons, it is quite common to require some form of damping on the input LC filter of a switching converter. Fig.5 shows one common way to do this. The damping capacitor C_d is larger than the filter capacitor, so it appears close to a short circuit at the undamped filter's resonant frequency. This puts R_d effectively in parallel with C_f, providing the necessary damping. This series resistor/capacitor combination is often referred to as a 'snubber'.

Selecting the damping resistor value is an optimisation problem. If it is too small, the damping capacitor appears in parallel with C_f, shifting the cutoff frequency but not contributing much damping. If it is too large, it also does not provide much damping. The optimum resistor value depends on the ratio of C_d to C_f, which is usually denoted by the Greek letter xi (ξ).

Their derivation is a bit complicated, but you can use the expressions to the right of Fig.5 to calculate the optimum value of the damping resistor and the resulting maximum impedance of the filter. The latter is important because we need to keep it low to reduce the impact of the converter's negative input impedance.

A realistic example

It is probably easier to follow if we work through a simple example. Let's assume we have a 60W buck converter with a 12V input and 6V/10A output operating at a frequency of 500kHz. The worst-case duty cycle is 0.5, so the AC input current will be a square wave with a peak-to-peak amplitude of 10A.

Let us suppose that we want to design an input filter that reduces this current ripple by a factor of 100, to no more than 100mA peak-to-peak.

We first have to work out the cutoff frequency of an undamped LC filter that will give us the required attenuation. We do this by initially assuming that most of the energy in the square wave occurs at the fundamental frequency. We know a square wave only has odd harmonics, and that their amplitude is given by $I_{n(pk\text{-}pk)} = 2I_{(pk\text{-}pk)} \div n\pi$, where n is the harmonic number.

The peak-to-peak amplitude of the fundamental component of current will therefore be 6.37A. Just as a check, the next harmonic (the third) would have an amplitude ⅓ of that, or 2.12A, and each subsequent harmonic will have a proportionally lower amplitude.

The desired attenuation factor of 100 means we require the peak-to-peak amplitude of the fundamental component of the filter's output to be 63.7mA or lower. We will use a lower value, say 25mA, to account for the fact that we have only considered the fundamental component.

We can now calculate the required cut-off frequency to achieve this level of attenuation from the relationship $i_s \div i_x = f_c^2 \div f_{sw}^2$. Rearranging and substituting in the switching frequency and currents gives us a filter cut-off frequency of 31.3kHz. We can use this to choose the filter components using the equation $f_c = 1 \div 2\pi\sqrt{L_f C_f}$.

However, we can't just chose any values for L and C, because we also want to make sure that the filter's impedance $Z_f = \sqrt{L_f \div C_f}$ is significantly smaller in magnitude that the converter's (negative) input impedance to minimise the probability of unwanted behaviour.

The converter's input impedance is easily calculated by Ohm's law to be -2.4Ω (-12V ÷ 5A). If we therefore choose Z_f to be 0.2Ω and use both equations, we end up with a value for L_f of 1.01µH and for C_f of 25.4µF. We can safely round these to 1µH and 25µF, respectively.

Just out of interest, I simulated the circuit with these values and without any damping. I used a simple square wave current source (no negative impedance) and set the source impedance to zero, as per Fig.6(a). The result is shown in Fig.6(b).

The switching frequency is certainly attenuated significantly (you can't really see it), but the filter oscillates with a peak-to-peak amplitude of 12A at the resonant frequency. Clearly, we do need to add the damping capacitor and resistor.

Given the filter capacitance C_f is 25µF, would be convenient to set ξ to 4, making C_d a nice round 100µF. The formulae in Fig.5 give us an optimum value for R_d of 0.14Ω and a maximum filter impedance of 0.17Ω.

This is not a huge amount of damping resistance, so it is possible that some or all of it can come from the damping capacitor's ESR if you were to use an electrolytic here – for once, the ESR of a capacitor comes in handy!

I simulated the damped filter, with the results as shown in Fig.7. Note the difference in scales between the damped and undamped responses. You can see that the switching frequency ripple has been reduced to about 50mA peak-to-peak, inline with our design criteria, but there is some

Fig.5: the addition of a damping resistor and capacitor, as shown here, is often necessary to minimise the oscillation in an LC filter. The optimum values can be determined from the equations on the right.

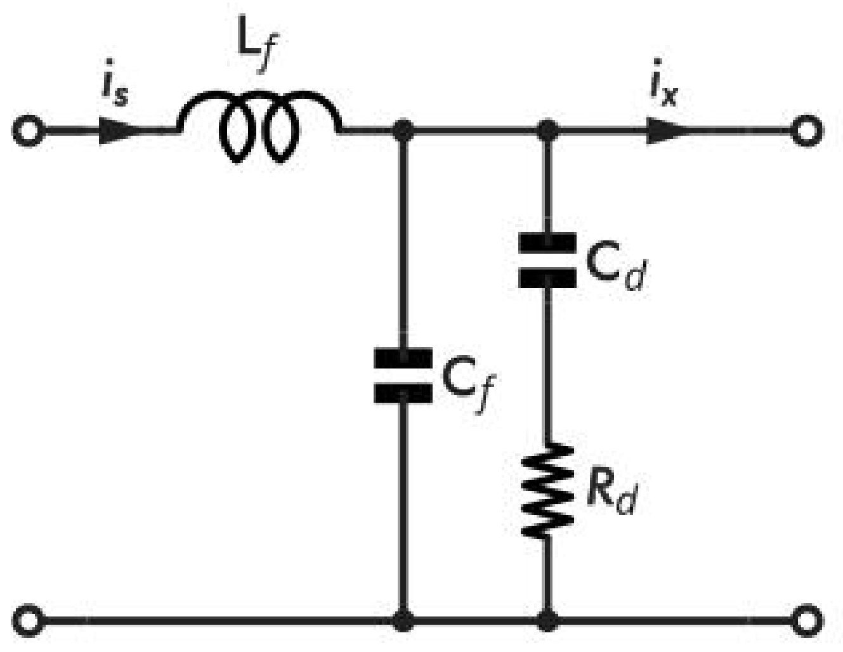

$$\xi = \frac{C_d}{C_f} \qquad Z_f = \sqrt{\frac{L_f}{C_f}}$$

$$R_{d(opt)} = Z_f \sqrt{\frac{(2+\xi)(4+3\xi)}{2\xi^2(4+\xi)}}$$

$$Z_{max} = \frac{Z_f \sqrt{2(2+\xi)}}{\xi}$$

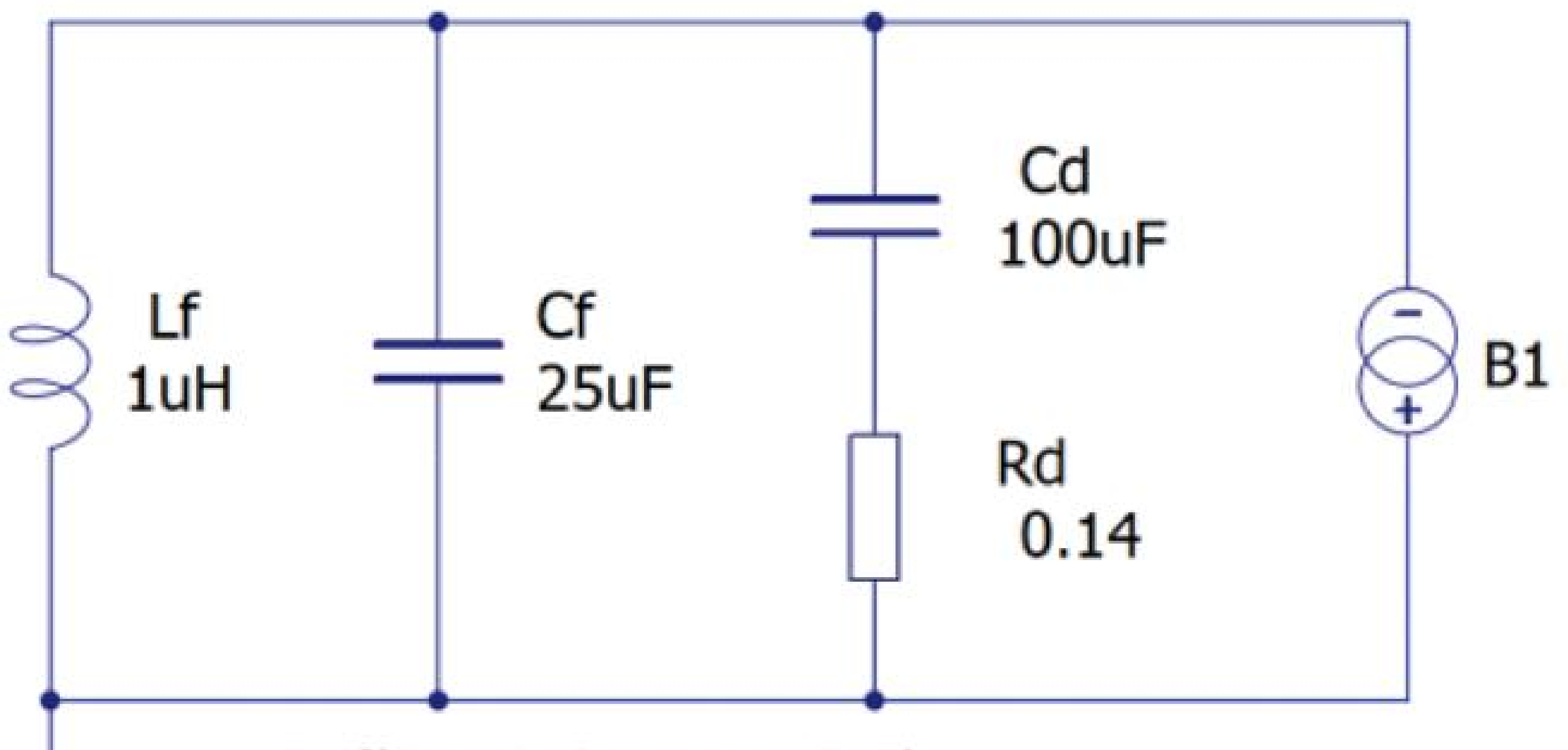

```
I=if(time % 2µ > 1µ, -5, 5)
.tran 0 500µ 400µ
```

Fig.6: the simulation circuit (left) to check the oscillation of an LC filter. Without damping (C_d and R_d omitted), the filter oscillates at its resonant frequency and with an amplitude of 12A peak-to-peak (below).

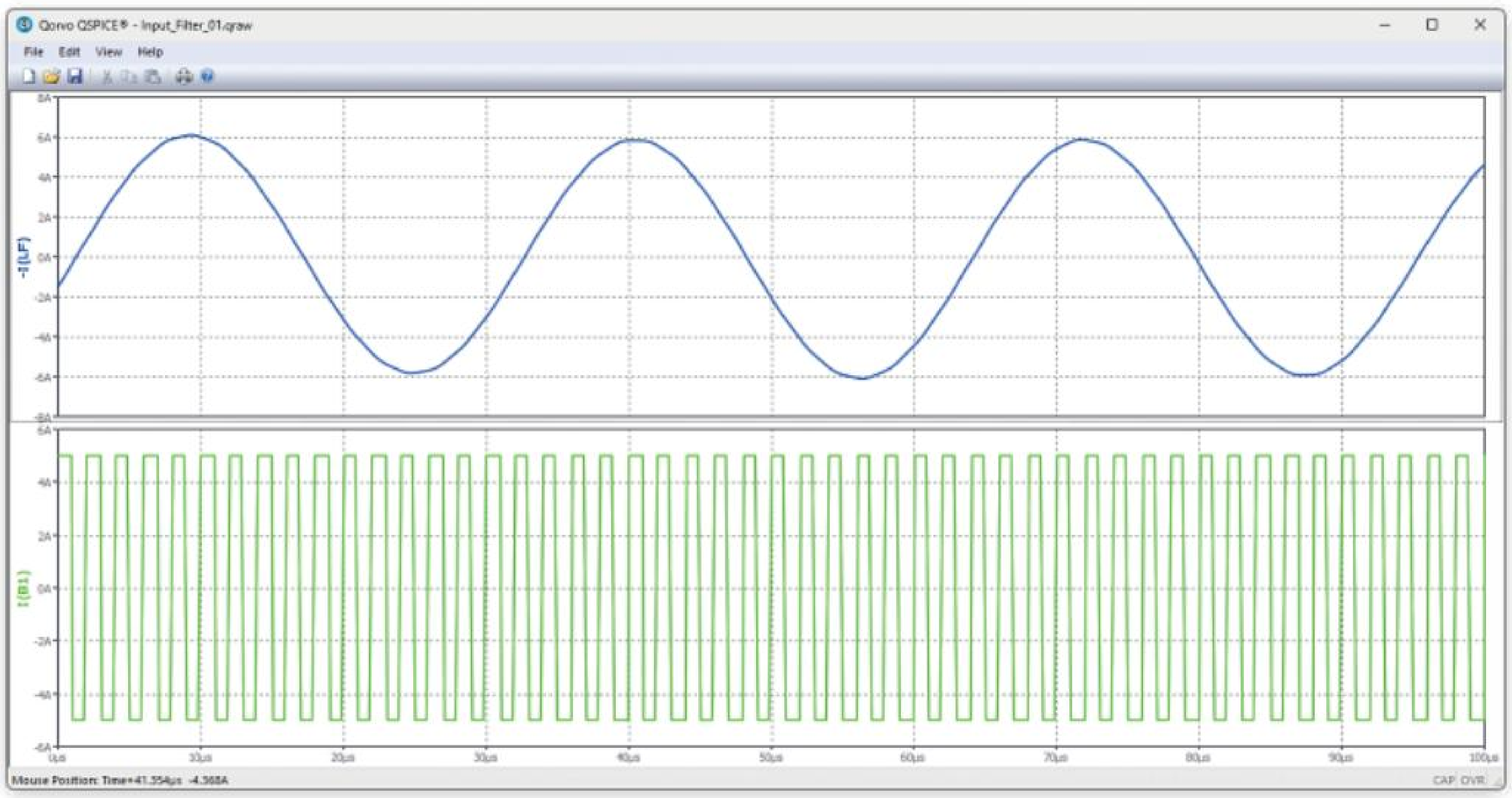

Mouse Position: Time=41.354µs -4.368A

residual ripple (200mA peak-to-peak) at the filter's resonant frequency.

Fortunately, this is well below the bottom end of the EMI frequency range, so it might be something we could live with.

Common-mode input filters

A differential mode filter like this will have no effect on common-mode signals because there is a low impedance path for common-mode signals through it via the 'ground' line. A common-mode filter therefore has to be effective on both conductors. This is often achieved with the use of coupled inductors, as shown in Fig.8. These are also often called common-mode inductors or common-mode chokes.

The windings are arranged such that the flux produced by differential-mode current cancels out, as shown at the left of the figure, while that due to common-mode currents adds up.

When there is perfect coupling, the differential-mode current, which includes the relatively high operating current, does not produce any flux in the core. No flux means no differential-mode inductance and no flux density, so the core can be much smaller than it would otherwise have to be.

With perfect coupling, common-mode inductors present an inductance to common-mode signals but appear 'invisible' to differential-mode signals.

Because the windings on these inductors are often at high voltages with respect to each other, they tend to be wound on opposite sides of a toroidal core, which means there will be some leakage inductance, so in reality there will be some meaningful level of differential-mode inductance, although lower than the common-mode inductance.

You can see the common-mode inductor with the blue core in Fig.14 towards the top of the picture. The two windings and the spacing between them are clearly visible.

Although it only produces a small amount of flux, the differential-mode current still flows through the windings, so they must be dimensioned appropriately. Common-mode chokes are not restricted to two windings; three-winding common-mode chokes are used to build filters for three-phase systems, for example.

When we designed the differential-mode filter above, we started with a clear model of the source current i_x and worked from there. The source of the common-mode currents is leakage through circuit parasitics, so developing such a model is not really feasible.

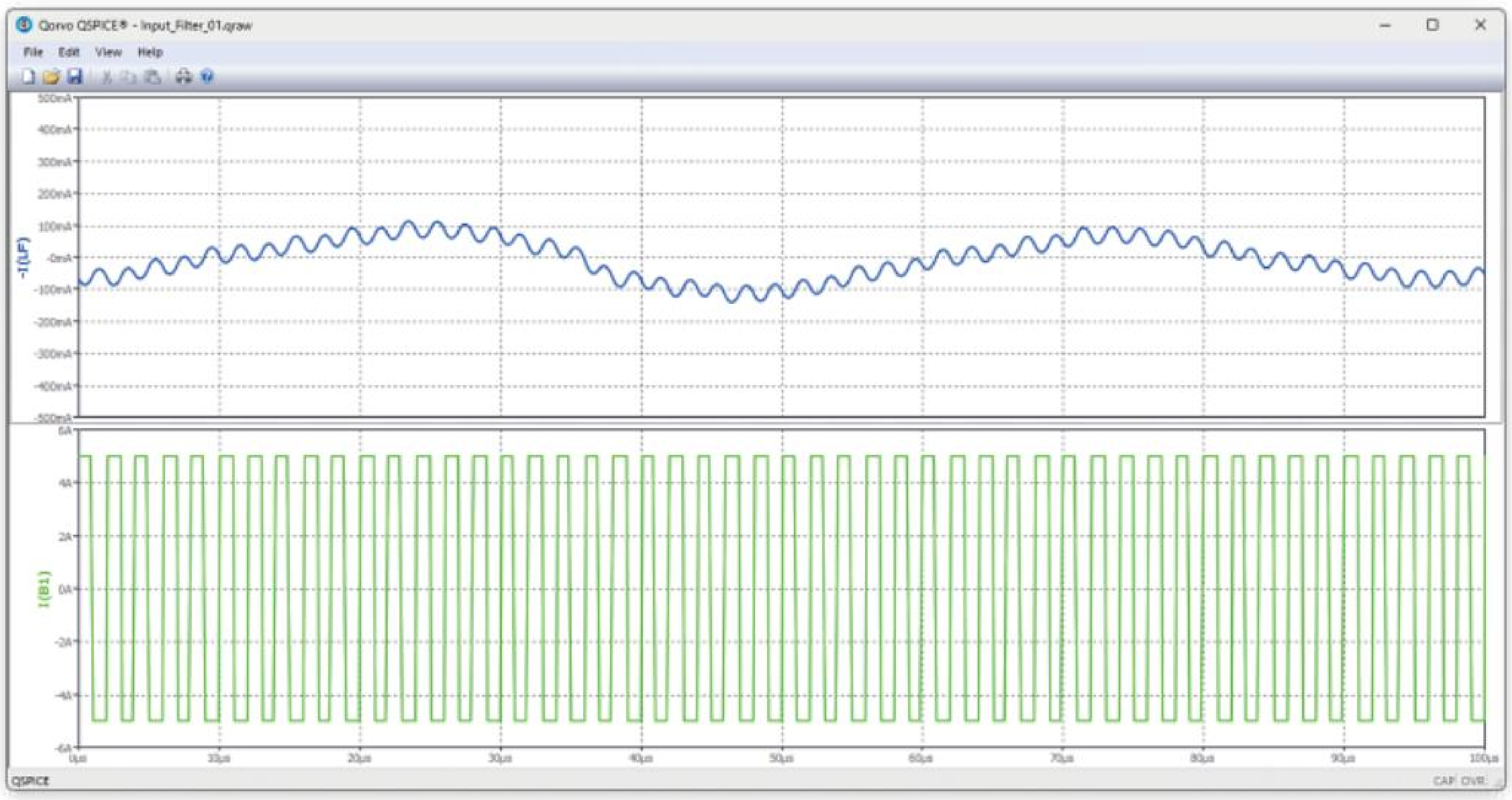

Fig.7: adding the damping components reduced the ripple to 100mA peak-to-peak. The 500kHz switching ripple is attenuated to approximately half of that.

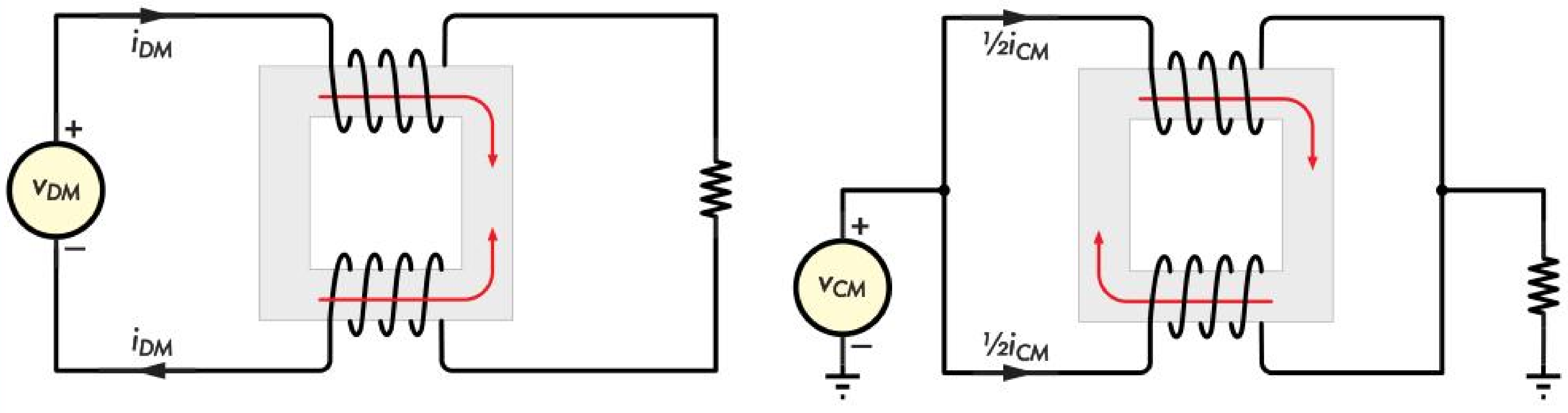

Fig.8: a common-mode inductor has two windings arranged so that the fluxes produced by differential-mode currents cancel and those due to common-mode currents add.

The 'right' way to start the design is to build the circuit without a filter and measure the raw common-mode noise across the spectrum of interest. We could then use the limits in the appropriate EMI standard to determine the required filter characteristic and proceed from there.

Most of the time, this is not practical, and there are some practical limitations on the design of mains common-mode filters that mean that many decisions are made for you. You can usually therefore do a good enough job by selecting 'reasonable' component values and validating through testing.

Fig.9 shows a typical example of a single-stage common-mode filter designed for mains use, with the supply on the left and the converter (the source of the common-mode noise current) on the right. The common-mode inductance of L and the two C_Y capacitors forms the common-mode filter. The leakage inductance of L and the capacitor labelled C_{X2} form a differential-mode filter.

Capacitor C_{X1} (not always present) provides some filtering of noise coming into the converter and reduces the input source impedance at higher frequencies. The resistor is there to discharge the capacitors when the mains is removed so the mains plug does not pose a shock hazard.

Class-X & Class-Y capacitors

It is no accident that I have labelled the capacitors X and Y. It is mandatory to use safety-certified "Class X" capacitors across the mains and "Class Y" capacitors from Live (or Line) to Earth. Apart from having appropriate voltage ratings, these capacitors are designed to fail safely.

Class Y capacitors have the most stringent requirements; they are required to fail open-circuit so that the mains is never shorted to the device enclosure, endangering the user. Class X capacitors, on the other hand, are often designed to fail short-circuit. You can use an appropriately rated Class Y capacitor across the mains, but you should never ever use a Class X capacitor between Live/Line (or Neutral) and Earth.

Safety-rated capacitors come in various sub-classes that denote the peak voltage they can tolerate. Lower subclass numbers mean higher voltage capability. For the 230V mains voltage in the UK and Europe, you should use the X2 and Y2 subclasses as a minimum. The higher-rated X1 and Y1 subclasses are also OK, but not strictly necessary.

Never use lower-subclass components or ones without the proper certification. You can easily recognise safety-rated capacitors because their cases are usually smothered in logos from certification bodies.

The Class Y capacitors in a common-mode filter provide a leakage path from Live to Earth, so their maximum value is dictated by the acceptable leakage current at mains frequency. Industrial products can usually have a leakage current of no more than 0.5mA (at 250V AC), limiting C_Y to a maximum value of about 6nF. This is why you will often see 2.2nF or 4.7nF ceramic Class Y caps in these filters.

Class X capacitors can be larger; 220nF, 470nF or even 1µF values are not unusual. Much larger than this, and you run into problems discharging them fast enough. You can decrease the value of the discharge resistor only so far before its power dissipation becomes a problem.

The higher Class X capacitance means that these filters can provide appreciable differential-mode filtering, even though the differential mode inductance is lower. Typical filters use common-mode inductors in the 0.33mH to 10mH range. If more attenuation is required, it is common to add a second or even third stage in series, rather than using larger inductors.

Fig.9: a typical common-mode filter includes safety-rated Y-Class capacitors from Active to Earth and X-Class between Active and Neutral. It is really important to use the correct parts in these critical locations.

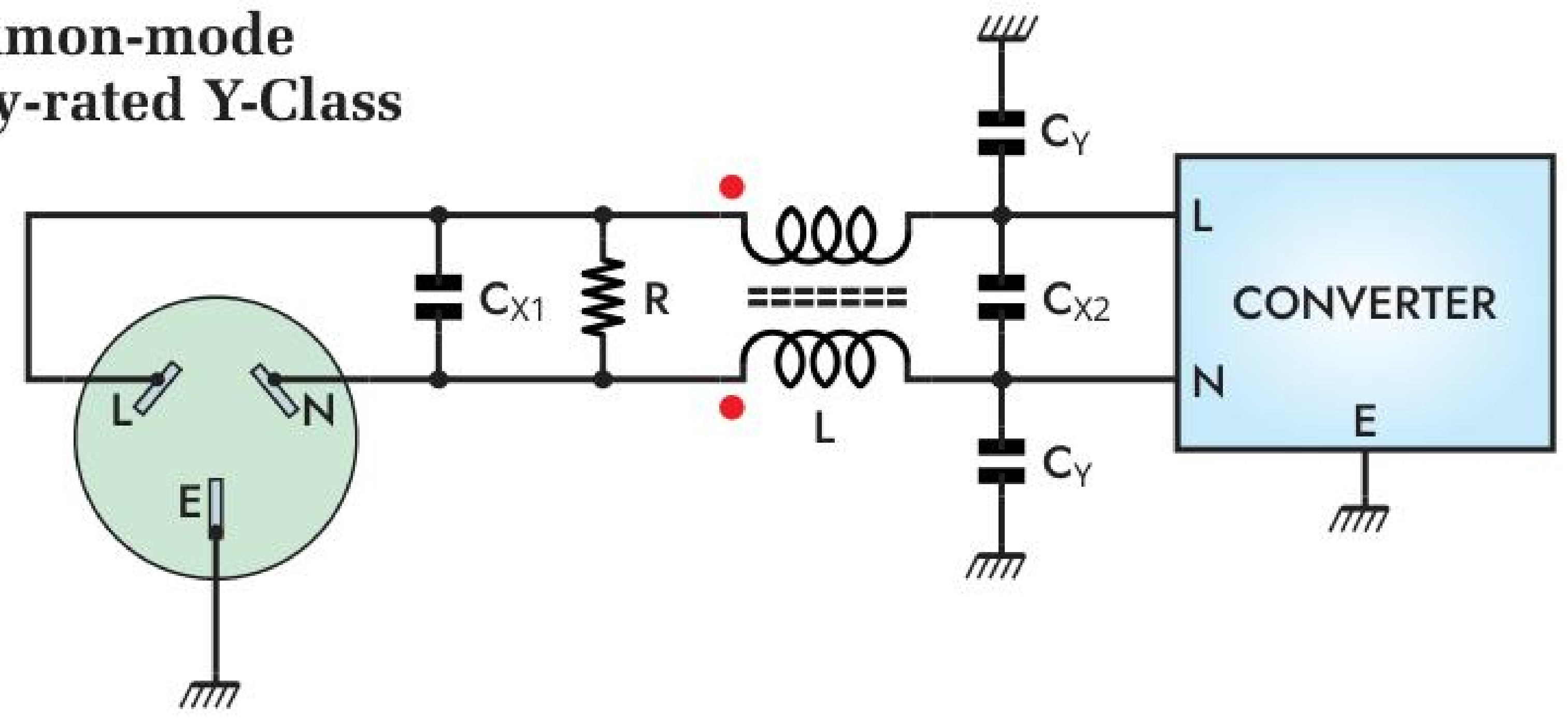

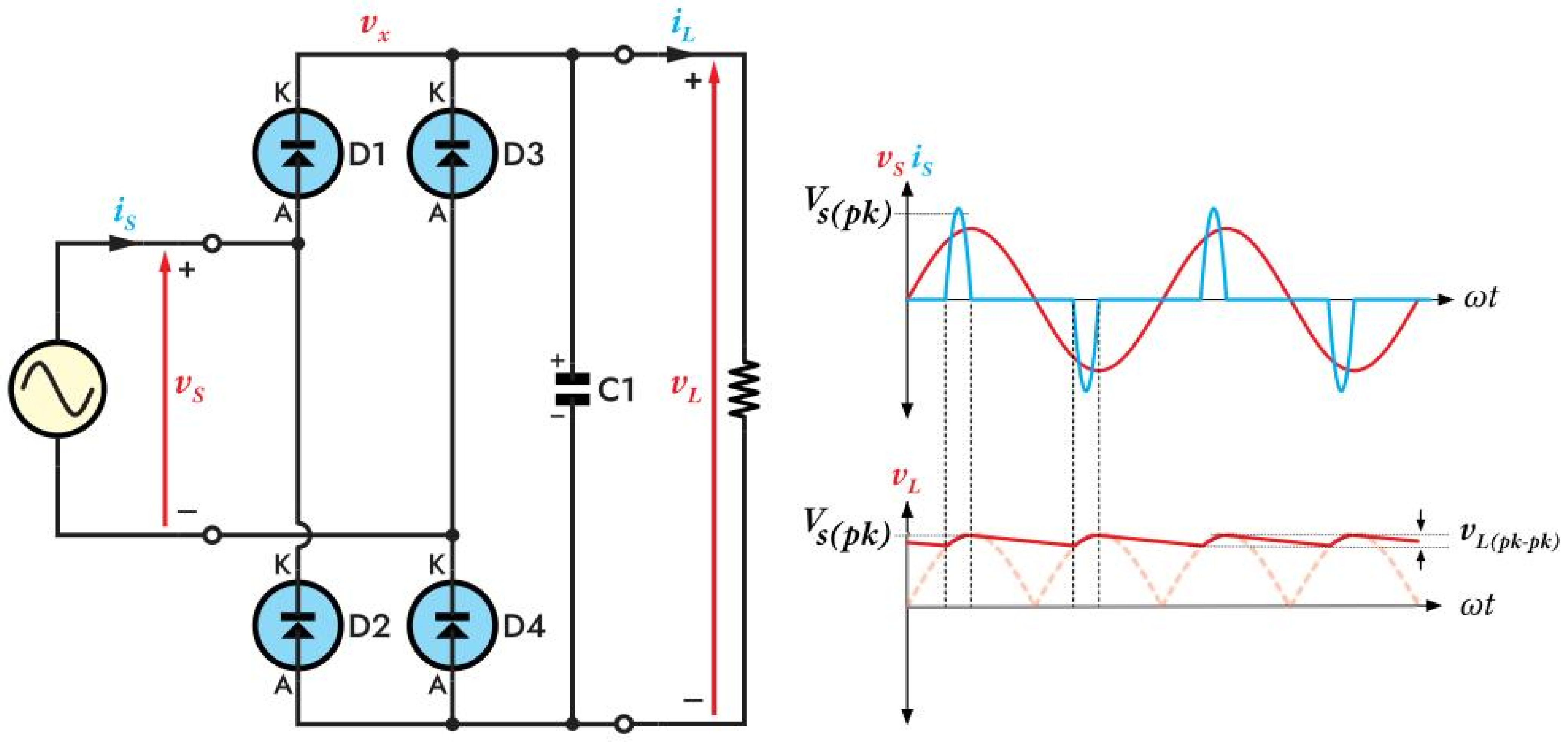

Fig.10: a power factor correction circuit ‘spreads out’ the spiky current waveform produced when the capacitor charges at the peak of the mains.

Power factor correction (PFC)

EMI filtering is concerned with high-frequency harmonics, but you will recall from the last article that with a sinusoidal voltage source, only the fundamental component of the source current contributes usable power (real power), designated ‹*p*›, with units of watts.

The higher harmonic components of current do however contribute to the RMS value of current and therefore to the ‘apparent power’, S, defined as the product of RMS voltage and RMS current and having units of volt-amperes (VA). The ratio of real power to apparent power, ‹*p*› ÷ S, is the definition of power factor.

For unity power factor, the current must not only have a purely sinusoidal shape; it also has to be in phase with the voltage. For example, an inductive load such as a motor will not have unity power factor even though the current is sinusoidal, because of the phase shift between voltage and current.

In this case, correcting the power factor can be as simple as adding a capacitor of appropriate value across the load to bring the phase shift between voltage and current back to zero. This is known as passive power factor correction.

Things are not this simple with AC-DC converters, as we saw last time. The most common arrangement of a full bridge followed by a capacitive filter results in a current waveform with narrow spikes near the voltage peaks, corresponding to the period in which the capacitor is charged. This is illustrated in Fig.10.

Active power factor correction aims to spread these peaks and make the overall source current waveform more sinusoidal in shape. Pushing current into the filter capacitor while the input voltage (shown dotted in red) is lower than the DC voltage implies that the PFC circuit must be capable of producing an output voltage higher than its input. The obvious candidate is a boost converter.

Fig.11 shows the typical circuit of an active power factor corrector. A boost converter is interposed between the rectified mains input and the load (often another DC-DC converter). The boost converter is driven by a current-mode modulator, as shown in the diagram at the bottom of Fig.11. Crucially, its input reference current is forced into a ‘rectified sine’ shape.

Thus, the boost converter produces a steady DC voltage across C1, but draws a roughly rectified-sinewave-shaped current through L1, and thus a near-sinewave-shaped current from the source.

The current-mode modulator monitors the inductor current and controls the Mosfet’s on-time to make the current track the reference current, which is the output of the error amplifier/compensator multiplied by the rectified sine signal. This latter is derived from the mains so that the input current is in phase with the voltage, resulting in a very good power factor.

The load voltage must be higher than the peak of the mains, so it is normally set to about 400V. This allows for a wide range of AC input voltages – say, from 90V AC to 280V AC.

You don’t have to use a boost converter, although this is by far the most popular topology due to its simplicity.

Fig.11: the PFC converter uses a current-mode boost converter to generate the output voltage. The reference current is modulated to shape the inductor current into a 'rectified sinewave' shape so the input current is sinusoidal.

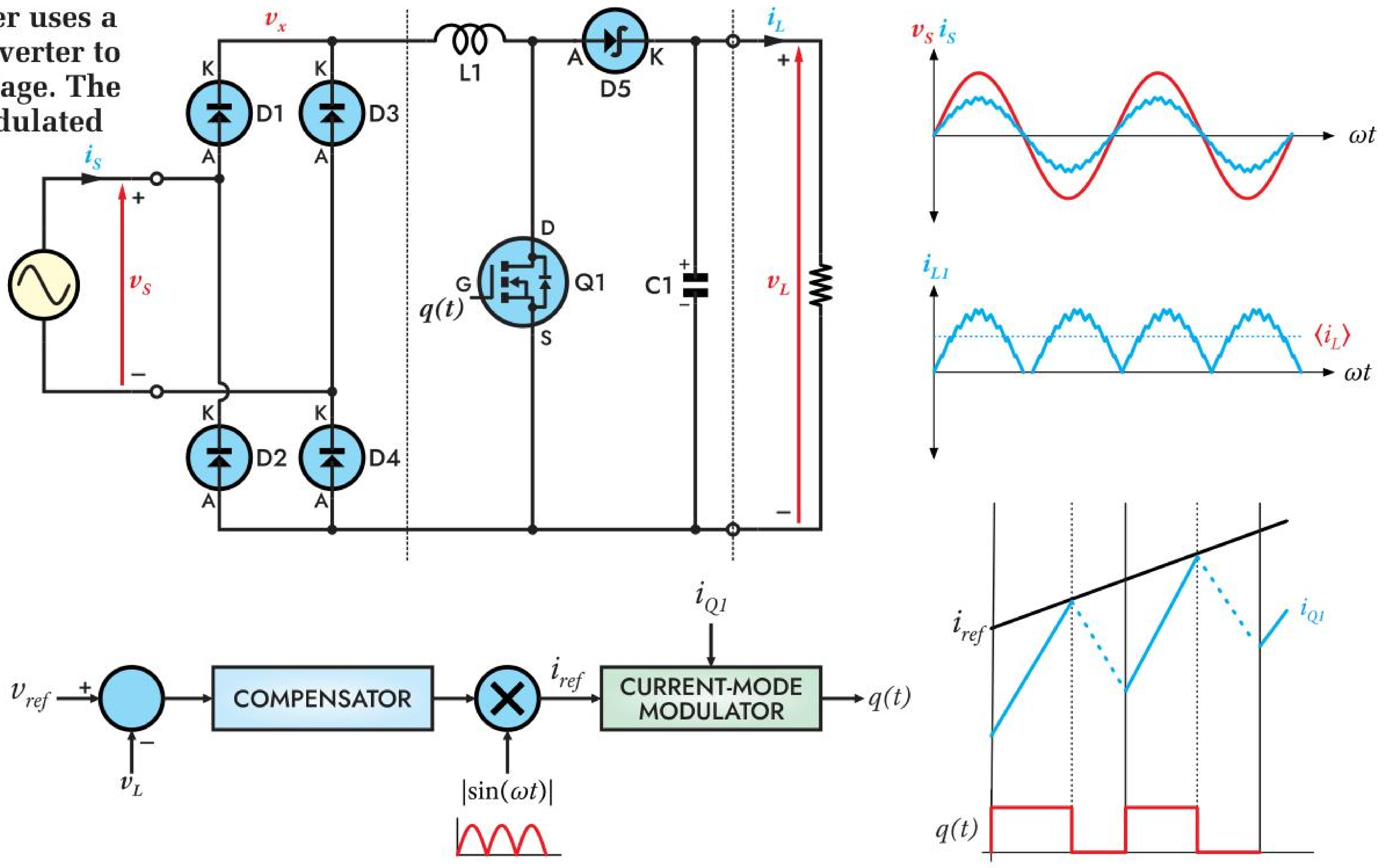

Fig.12: there are several alternative PFC topologies like these, but they all work on the same basic principle as that shown in Fig.11.

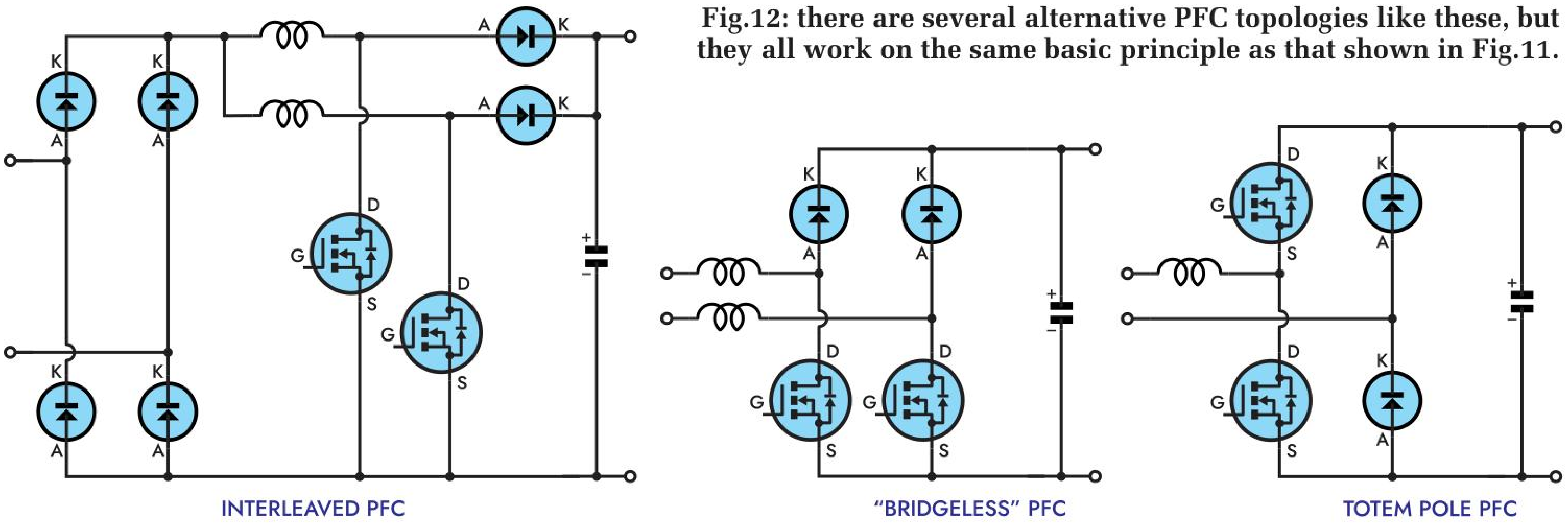

INTERLEAVED PFC

"BRIDGELESS" PFC

TOTEM POLE PFC

You obviously can't use a buck converter because it does not work when its input voltage is lower than its output, a state that will occur near every zero crossing.

PFC variants

There are of course many variations on this theme, several of which I have shown in Fig.12. On the left is the interleaved power factor correction circuit. You can see that this is really two parallel boost converters, which are normally driven 180° out of phase with each other, feeding a common filter capacitor.

This has the advantage of higher output power and effectively doubles the switching frequency as seen at the input, simplifying the input filtering.

The next variant is described a "bridgeless" PFC converter, but this is a bit of a misnomer since the upper two diodes plus Mosfets and their body diodes clearly form a bridge rectifier. The functions of the rectifier and boost converter are integrated, providing better efficiency since several diode drops are eliminated.

It can also be thought of as two boost converters in parallel, although this time each one is operating on alternate half-cycles. In theory, you can get away with a single inductor in one leg, but at the cost of increased common-mode EMI.

An even more efficient variant is the so-called "totem-pole" architecture. Here, one Mosfet acts as a synchronous rectifier each half-cycle while the other is switching. This is more efficient than the bridgeless PFC because a Mosfet can have a much lower voltage drop than a diode.

An even more efficient version uses four Mosfets, eliminating diodes altogether. There is a penalty to pay in terms of complexity with totem-pole PFC converters because they require a high-side driver.

A practical PFC converter

It is a bit beyond the scope of this article to run through the complete design of a PFC converter, but we can do the next best thing and take a look at a real example from an evaluation board; in this case, an EVL-4986-350W from ST Microelectronics (Fig.14).

This is a 350W boost-converter type PFC based on the L4986 IC, a very typical example of the type of chip that is readily available these days. The circuit, redrawn from the EVL-4986-350W data brief, is reproduced in Fig.13.

The mains input on the left is fused

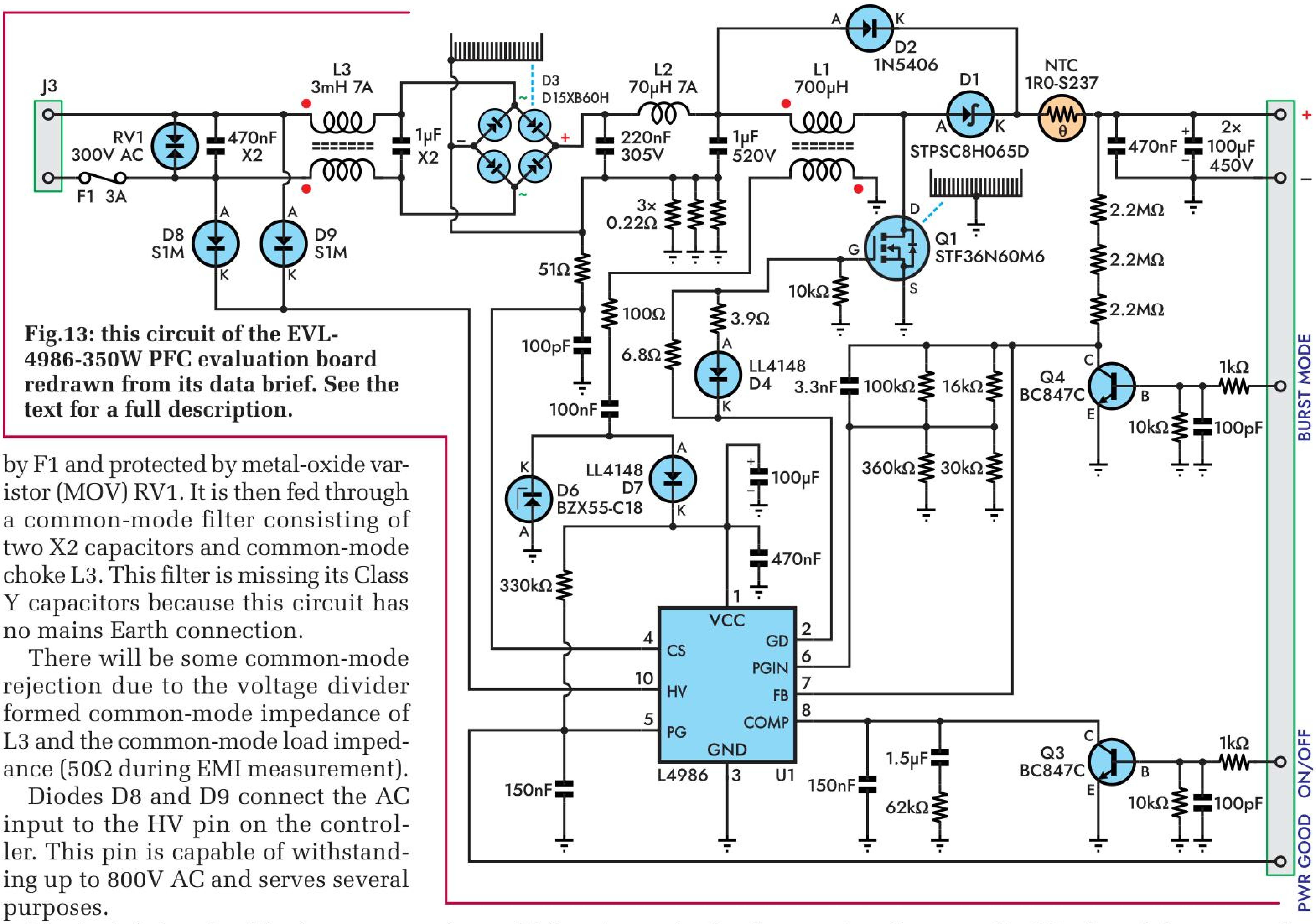
J3
RV1
300V AC
470nF
X2
F1 3A
L3
3mH 7A
1μF
X2
D8
S1M
D9
S1M
A
K
D3
D15XB60H
L2
70μH 7A
220nF
305V
1μF
520V
3×
0.22Ω
L1
700μH
D2
1N5406
D1
STPSC8H065D
NTC
1R0-S237
θ
470nF
2×
100μF
450V
+
–
Q1
STF36N60M6
G
D
S
10kΩ
2.2MΩ
2.2MΩ
2.2MΩ
51Ω
100Ω
3.9Ω
100pF
6.8Ω
LL4148
D4
3.3nF
100kΩ
16kΩ
Q4
BC847C
C
B
E
1kΩ
10kΩ
100pF
BURST MODE
100nF
LL4148
D7
D6
BZX55-C18
100μF
360kΩ
30kΩ
470nF
330kΩ
VCC
CS
HV
PG
GND
GD
PGIN
FB
COMP
1
2
3
4
5
6
7
8
10
L4986
U1
150nF
1.5μF
62kΩ
150nF
Q3
BC847C
1kΩ
10kΩ
100pF
ON/OFF
PWR GOOD

Fig.13: this circuit of the EVL-4986-350W PFC evaluation board redrawn from its data brief. See the text for a full description.

by F1 and protected by metal-oxide varistor (MOV) RV1. It is then fed through a common-mode filter consisting of two X2 capacitors and common-mode choke L3. This filter is missing its Class Y capacitors because this circuit has no mains Earth connection.

There will be some common-mode rejection due to the voltage divider formed common-mode impedance of L3 and the common-mode load impedance (50Ω during EMI measurement).

Diodes D8 and D9 connect the AC input to the HV pin on the controller. This pin is capable of withstanding up to 800V AC and serves several purposes.

Firstly, it is involved in the startup of the controller. If a voltage exceeding about 29V is sensed on this pin, the capacitors on the V_{CC} pin are charged from it via an internal current limiter until it reaches a voltage sufficient for the control chip to start.

Once the PFC converter is up and running, the V_{CC} pin is supplied by the auxiliary winding on the boost inductor L1, via a 100Ω series resistor, 100nF AC-coupling capacitor and diode D7. Zener diode D6 limits the V_{CC} voltage to a maximum of about 18V.

The HV pin is also used to sense the AC voltage for the undervoltage/brownout protection circuit and to provide the modulation required to shape the input current. The HV pin can also detect when the mains is removed and switch in a current sink to discharge the X-capacitors, obviating the need for a discharge resistor and its associated power dissipation. That's a lot of functions for one pin!

The AC input is rectified by a 15A 600V bridge rectifier (D3) mounted on one of the two heatsinks. The rectifier is followed by a differential-mode filter comprising L2 and a 1μF capacitor, which reduces the fundamental of the 65kHz switching noise at the input by a factor of around eight and the higher harmonics by a proportionally greater factor.

The boost converter consists of the inductor L1, Mosfet Q1 and diode D1, with one 470nF and two 100μF capacitors forming its output filter. Diode D2 precharges these capacitors when the mains is first applied so that the boost converter can start up much faster than it would if it had to charge them from zero.

The 1Ω cold resistance of the NTC thermistor limits the capacitor inrush current, but as current flows through it in operation, the resistance drops by a couple of orders of magnitude and it can be more-or-less ignored.

The Mosfet current is sensed across the three parallel 0.22Ω shunt resistors below L2. The resulting (negative) shunt voltage is fed via a 51Ω resistor to the controller IC, where it is compared to the current reference to determine the Mosfet switch-off instant. If the CS pin voltage falls below -0.49V, an internal overcurrent comparator overrides the modulator, limiting the peak current to about 6.7A.

The Mosfet gate is driven via 3.9Ω and 6.8Ω resistors, plus diode D4. This network allows for separate control of the Mosfet's switch-on and switch-off times. Q1's gate is charged (to switch it on) via just the 6.8Ω resistor but is discharged via both resistors in parallel, compensating for the fact that the STF36N60M6

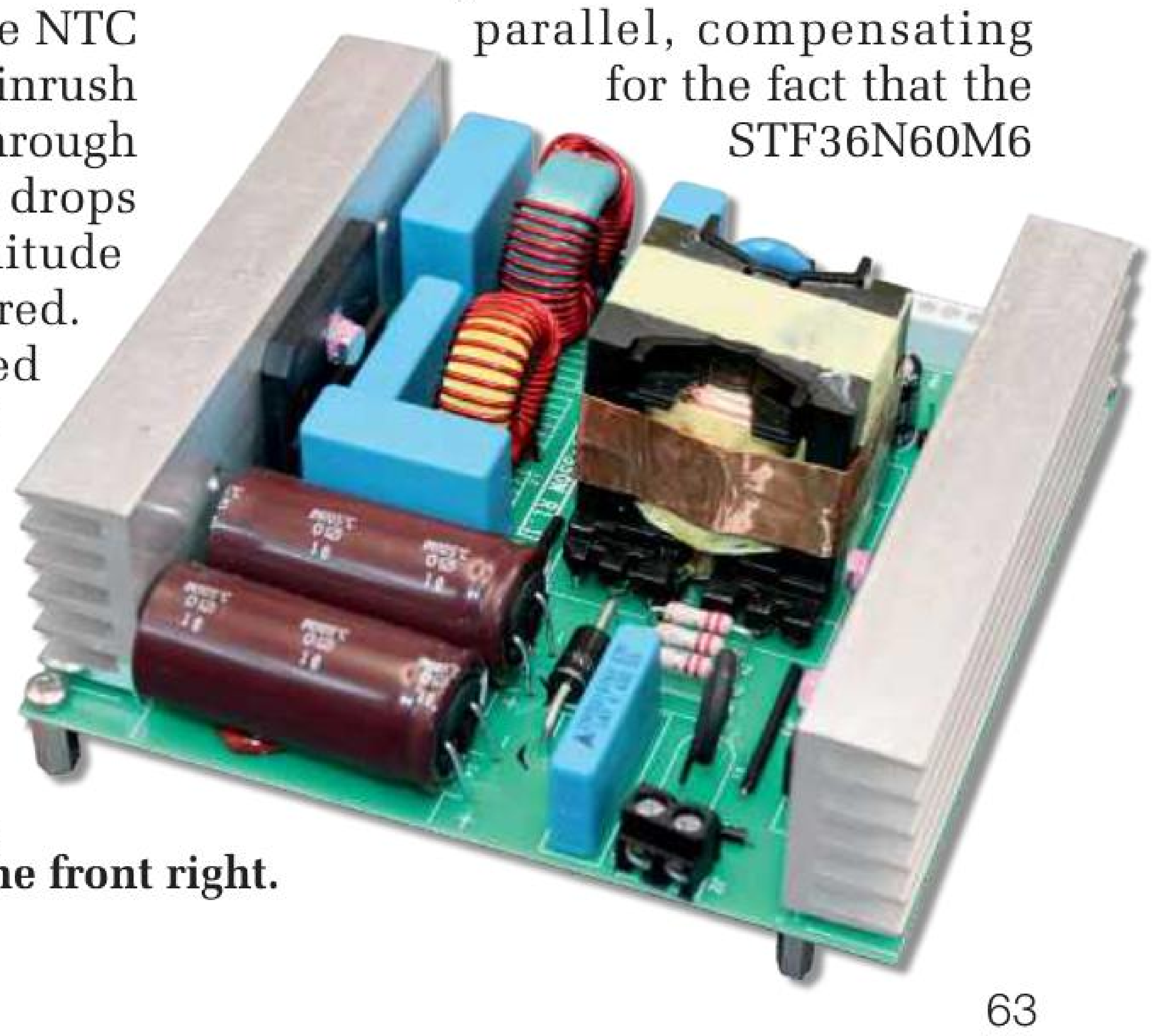

Fig.14: the PFC evaluation board described in the text. The input connector is hidden behind the large boost inductor, and the output connector is at the front right.

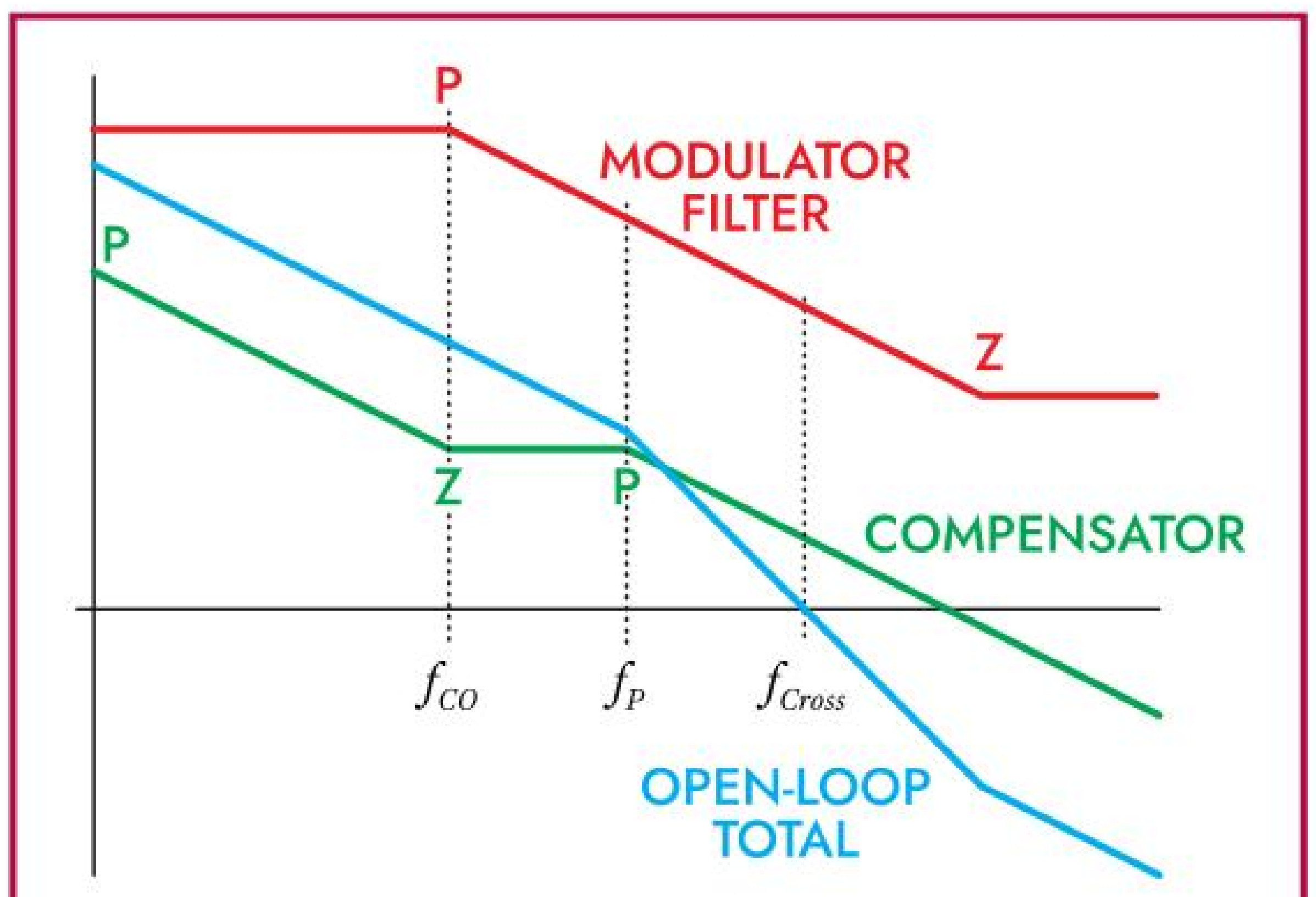

Fig.15: the compensator for the PFC converter is similar to that for a conventional DC-DC converter. The crossover frequency must be lower than 100Hz or the control loop will try to eliminate the modulation we need to shape the input current.

has a much slower inherent switch-off time (50ns) than its switch-on time (15ns).

Output voltage feedback is provided to the FB pin on the controller IC (U1) by the divider formed by the three 2.2MΩ resistors, together with the series/parallel combination of four different-value resistors to ground (16kΩ, 100kΩ, 30kΩ & 360kΩ).

This feedback voltage is internally compared to a 2.5V reference to create the error signal. Like the current sense input, an independent comparator shuts the boost converter off if the feedback voltage exceeds the reference by more than about 7%.

If the voltage at the feedback pin falls below about 0.5V, the controller enters 'external burst mode', in which switching is inhibited. This prevents the output voltage from rising uncontrollably in the case that the voltage sense resistors become open-circuit and also allows an external controller to switch the converter off via Q4.

This feature might be used to reduce power when a following converter was disabled or had a very light load. Disabling and enabling the PFC in this way is fast because the control chip does not go through the whole start-up procedure each time.

The voltage feedback divider doubles as an input for the controller's power-good comparator. If the voltage at the PGIN terminal exceeds 2.375V, the open collector 'power good' (PG) pin is asserted low.

Compensation

The internal error amplifier's compensation is set by the network hanging off its pin 8. This forms a classic Type II compensator, which has two poles and one zero. For more details, see the second article in this series, published in the May 2026 issue of *Practical Electronics*. The compensator poles and zeroes are positioned to provide dominant-pole compensation to the overall open-loop gain.

The red line in Fig.15 shows the frequency response of the PFC's modulator and output filter. This has a single pole at f_{CO}, determined by the converter's output capacitance and its load resistance, and a zero formed by the output capacitance and its ESR. The output capacitance is 200µF and the minimum load resistance is 457Ω ($400V^2 \div 350W$), so the pole occurs at about 1.74Hz.

We don't need to worry about the frequency of the zero formed by the output capacitance and its ESR for reasons that will become apparent soon.

The cyan/blue line shows the desired open-loop gain required for stability, rolling off at a steady -20dB per decade from the origin (effectively DC), then taking a turn down to -40dB per decade at frequency f_P.

In a normal converter, we would position this pole to cancel the filter's ESR zero to maximise the bandwidth of the control loop. However, for PFC converters, we have to limit the loop bandwidth so the crossover frequency (the frequency where loop gain falls to 0dB) is below twice the mains frequency.

We have to do this so the control loop does not respond to the 100Hz ripple on the output and try to counteract the very modulation we are relying on to shape the current.

The compensator's second pole (the first is at the origin) is therefore typically placed at some frequency, f_P, that forces the crossover frequency to be less than 100Hz. The filter zero caused by the output capacitance and its ESR is therefore more-or-less irrelevant since the control loop is not effective at this frequency.

The evaluation board's compensator has its zero set by the 62kΩ resistor and 1.5µF capacitor near to 1.71Hz – pretty much bang on the output capacitance/load resistance pole. The upper pole is set to 17.1Hz by the 62kΩ resistor and 150nF capacitor, well below the 100Hz ripple frequency.

I have not mentioned transistor Q3 and its associated base drive components yet. The controller chip has a threshold detector on the COMP pin that shuts down the PFC converter if the voltage is below about 0.5V. This can be used to stop and start the converter, but unlike Burst Mode control, the converter goes through a full soft-start cycle when enabled.

Testing

I tested the PFC evaluation board on my bench with a 500Ω load. The current and voltage waveforms are shown in Fig.16. The current (green trace) is certainly close to a sinusoid, but has some visible vestiges of switching ripple. Its shape tracks the input voltage (yellow trace) almost exactly, including its slightly flat top caused by all those non-PFC converters on my line.

The RMS current and voltage measurements on the right must each be scaled by a factor of 10 for 243V and 1.33A respectively, giving an apparent power of 323W. The average DC voltage and current in the load measured 396.7V and 0.785A, respectively, for a real power of 311.4W. The resulting power factor is 0.96, which is about as good as we could expect.

We have now covered DC-DC converters and AC-DC converters in a fair bit of depth. Next time, we will dive into the interesting world of DC-AC converters. **PE**

Fig.16; the upper trace shows the PFC converter's input current at near full load. The current is similar in shape to the input voltage shown below. The measured power factor was 0.96.

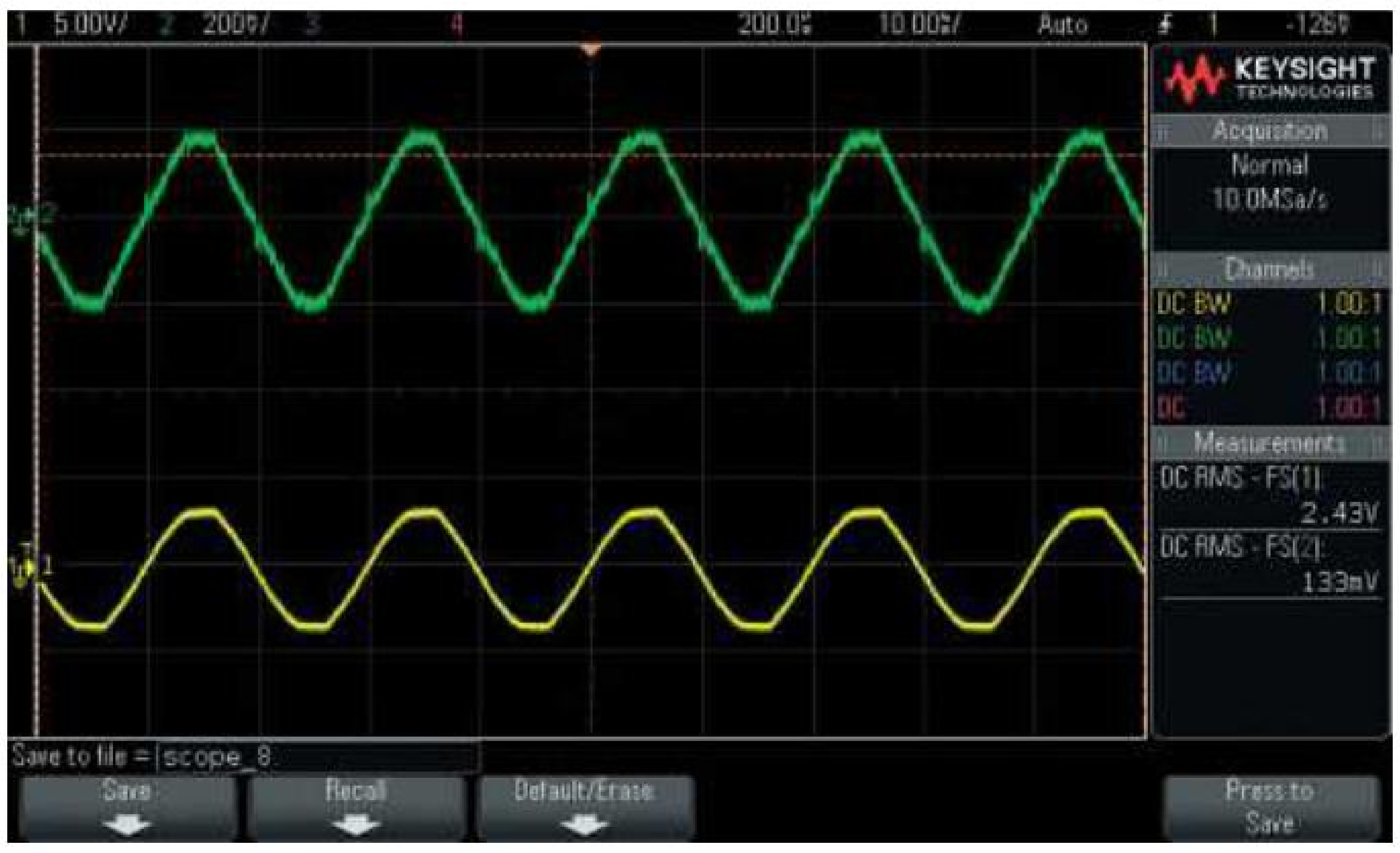

DC RMS - FS(1): 2.43V
DC RMS - FS(2): 133mV
Save to file = scope_8

DOWNLOAD YOUR PE/EPE BACK ISSUES

COMPLETE-YEAR collections – all 12 issues for each year!

From just £5.95 each

VOL 28 – January to December 1999 – **£5.95**
VOL 29 – January to December 2000 – **£6.95**
VOL 30 – January to December 2001 – **£7.95**
VOL 31 – January to December 2002 – **£7.95**
VOL 32 – January to December 2003 – **£7.95**
VOL 33 – January to December 2004 – **£7.95**
VOL 34 – January to December 2005 – **£8.95**
VOL 35 – January to December 2006 – **£8.95**
VOL 36 – January to December 2007 – **£8.95**
VOL 37 – January to December 2008 – **£8.95**
VOL 38 – January to December 2009 – **£10.95**
VOL 39 – January to December 2010 – **£11.95**
VOL 40 – January to December 2011 – **£12.95**
VOL 41 – January to December 2012 – **£14.95**
VOL 42 – January to December 2013 – **£15.95**
VOL 43 – January to December 2014 – **£16.95**
VOL 44 – January to December 2015 – **£17.95**
VOL 45 – January to December 2016 – **£19.95**
VOL 46 – January to December 2017 – **£22.95**
VOL 47 – January to December 2018 – **£27.95**
VOL 48 – January to December 2019 – **£27.95**
VOL 49 – January to December 2020 – **£29.95**
VOL 50 – January to December 2021 – **£32.95**
VOL 51 – January to December 2022 – **£34.95**
VOL 52 – January to December 2023 – **£34.95 – NEW!**
VOL 53 – January to December 2024 – **£34.95 – NEW!**

FIVE-YEAR collections – 60 issues!

From just £14.95 each

PE2832: Jan 99 to Dec 03 – £14.95
PE2933: Jan 00 to Dec 04 – £14.95
PE3034: Jan 01 to Dec 05 – £14.95
PE3135: Jan 02 to Dec 06 – £14.95
PE3236: Jan 03 to Dec 07 – £14.95
PE3337: Jan 04 to Dec 08 – £14.95
PE3438: Jan 05 to Dec 09 – £19.95
PE3539: Jan 06 to Dec 10 – £25.95
PE3640: Jan 07 to Dec 11 – £25.95
PE3741: Jan 08 to Dec 12 – £25.95
PE3842: Jan 09 to Dec 13 – £33.95
PE3943: Jan 10 to Dec 14 – £33.95
PE4044: Jan 11 to Dec 15 – £33.95
PE4145: Jan 12 to Dec 16 – £35.95
PE4246: Jan 13 to Dec 17 – £37.95
PE4347: Jan 14 to Dec 18 – £38.95
PE4448: Jan 15 to Dec 19 – £39.95
PE4549: Jan 16 to Dec 20 – £42.95
PE4650: Jan 17 to Dec 21 – £44.95
PE4751: Jan 18 to Dec 22 – £44.95 – NEW!
PE4852: Jan 19 to Dec 23 – £44.95 – NEW!

20 YEARS OF PE!

AMAZING BUNDLE OFFER
Every issue from 1999 – 2018

240 magazines for just

£69.95

PE2832: Jan 99 to Dec 03
PLUS!
PE3337: Jan 04 to Dec 08
PLUS!
PE3842: Jan 09 to Dec 13
PLUS!
PE4347: Jan 14 to Dec 18

Download your collections at: www.electronpublishing.com

AUDIO OUT

By Jake Rothman

All-pass filters, part 5 – phase-linear crossover and more

Over the last few issues, we've been looking into all-pass filters, ie, those that affect the phase response but not the frequency response of a signal. We've even presented multiple circuit boards to implement practical all-pass filters for practical purposes, like loudspeaker crossover time alignment and making audio signals more symmetrical so they can be recorded or transmitted at a higher level (louder).

Phase-linear crossover board

As promised, I have now had a board made for the subtractive phase-linear crossover circuit (Fig.33) described in part three of the all-pass series, in the June 2026 issue. I've added a few stability components (resistors R17 & R18, plus capacitors C9, C10 & C12) as well as decoupling capacitors C14, C15, C16, C17 & C18 to the original design.

There was one spare op amp (IC3b) in a dual package left over, so this was used for a polarity inversion circuit. The new, complete circuit is given in Fig.52. The curve is that of a classic fourth-order Linkwitz-Riley (LR) crossover with a -6dB dip at the crossover point of 500Hz, as shown in Fig.53.

Incidentally, I find it odd that someone can have a circuit that is simply two cascaded Butterworth filters named after them. I guess it's the analysis that followed that was so significant. *[Editor's note: consider that the response of two cascaded Butterworth filters is not the same as a second-order Butterworth filter response.]*

Elektor magazine published the first home constructor's design for a phase-linear crossover in 1987, which was a three-way design fixed at 500Hz and 5kHz. It had a sizable impact at the time. The idea was that the relative phase between the outputs did not shift with frequency. The result is supposed to be a small, constant delay across the whole audio band.

In the *Elektor* tradition of "form before function", the design had a difficult PCB layout with thin tracks that fell off during soldering. It also had an onboard power supply using an unobtainable LM325 dual-voltage regulator. The critical capacitors were weird Dutch Philips polystyrene types with diagonally placed pins. I later discovered that LCR in Wales makes a compatible type.

Despite the difficulties, of course, I had to build one (shown in Photo

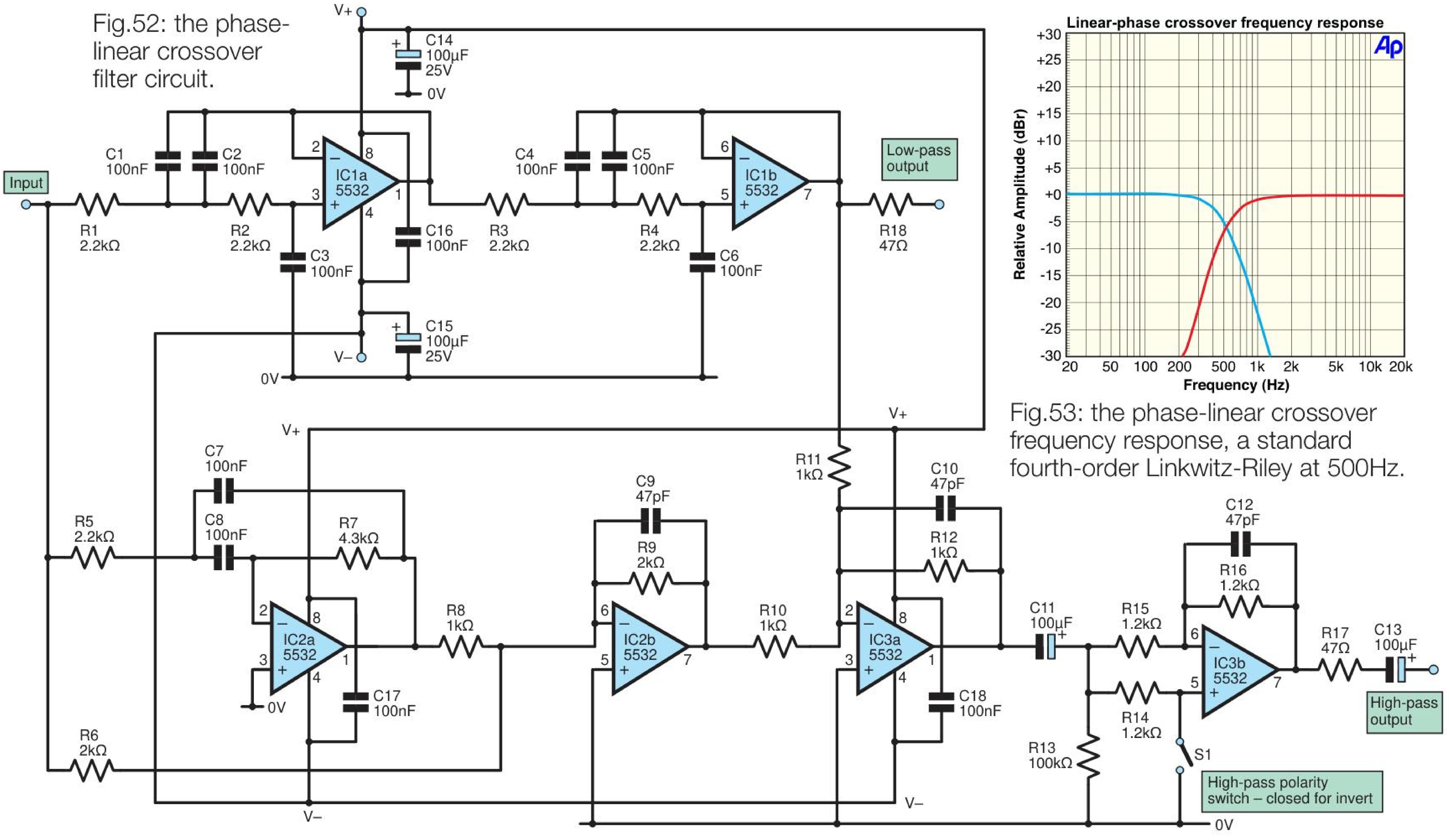
Input
C1 100nF
C2 100nF
R1 2.2kΩ
R2 2.2kΩ
C3 100nF
IC1a 5532
V+
C14 100µF 25V
0V
C16 100nF
C15 100µF 25V
V–
0V
R3 2.2kΩ
C4 100nF
C5 100nF
R4 2.2kΩ
C6 100nF
IC1b 5532
Low-pass output
R18 47Ω
V+
R5 2.2kΩ
C7 100nF
C8 100nF
R7 4.3kΩ
IC2a 5532
0V
C17 100nF
R6 2kΩ
V–
R8 1kΩ
C9 47pF
R9 2kΩ
IC2b 5532
R10 1kΩ
V+
R11 1kΩ
C10 47pF
R12 1kΩ
IC3a 5532
C18 100nF
V–
C11 100µF
R13 100kΩ
R15 1.2kΩ
R14 1.2kΩ
C12 47pF
R16 1.2kΩ
IC3b 5532
S1
R17 47Ω
C13 100µF
High-pass output
High-pass polarity switch – closed for invert
0V

Fig.52: the phase-linear crossover filter circuit.

Linear-phase crossover frequency response
Ap
Relative Amplitude (dBr)
+30
+25
+20
+15
+10
+5
+0
-5
-10
-15
-20
-25
-30
20
50
100
200
500
1k
2k
5k
10k
20k
Frequency (Hz)

Fig.53: the phase-linear crossover frequency response, a standard fourth-order Linkwitz-Riley at 500Hz.

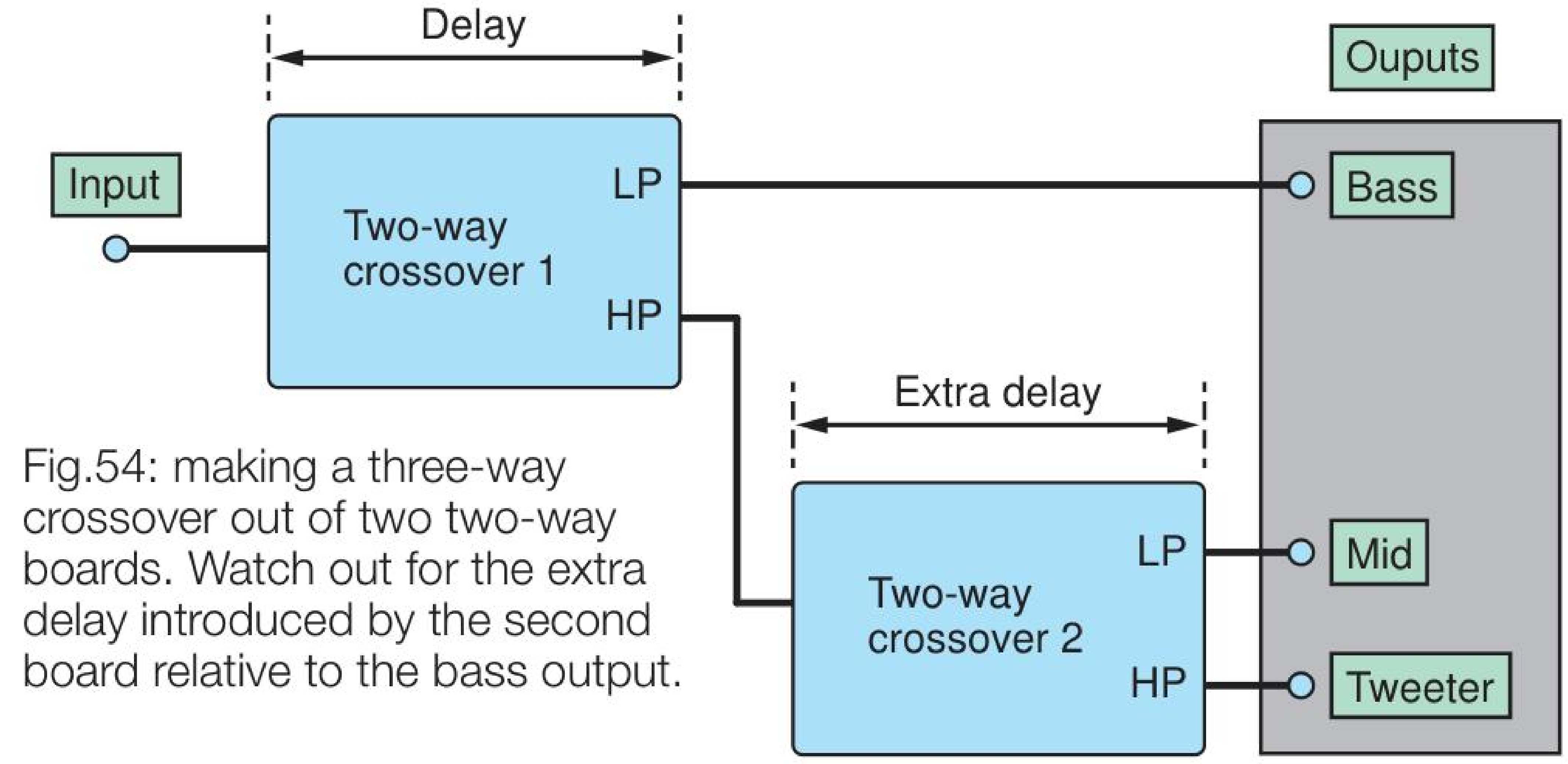
Delay
Ouputs
Input
Two-way crossover 1
LP
HP
Bass
Extra delay
Two-way crossover 2
LP
HP
Mid
Tweeter

Fig.54: making a three-way crossover out of two two-way boards. Watch out for the extra delay introduced by the second board relative to the bass output.

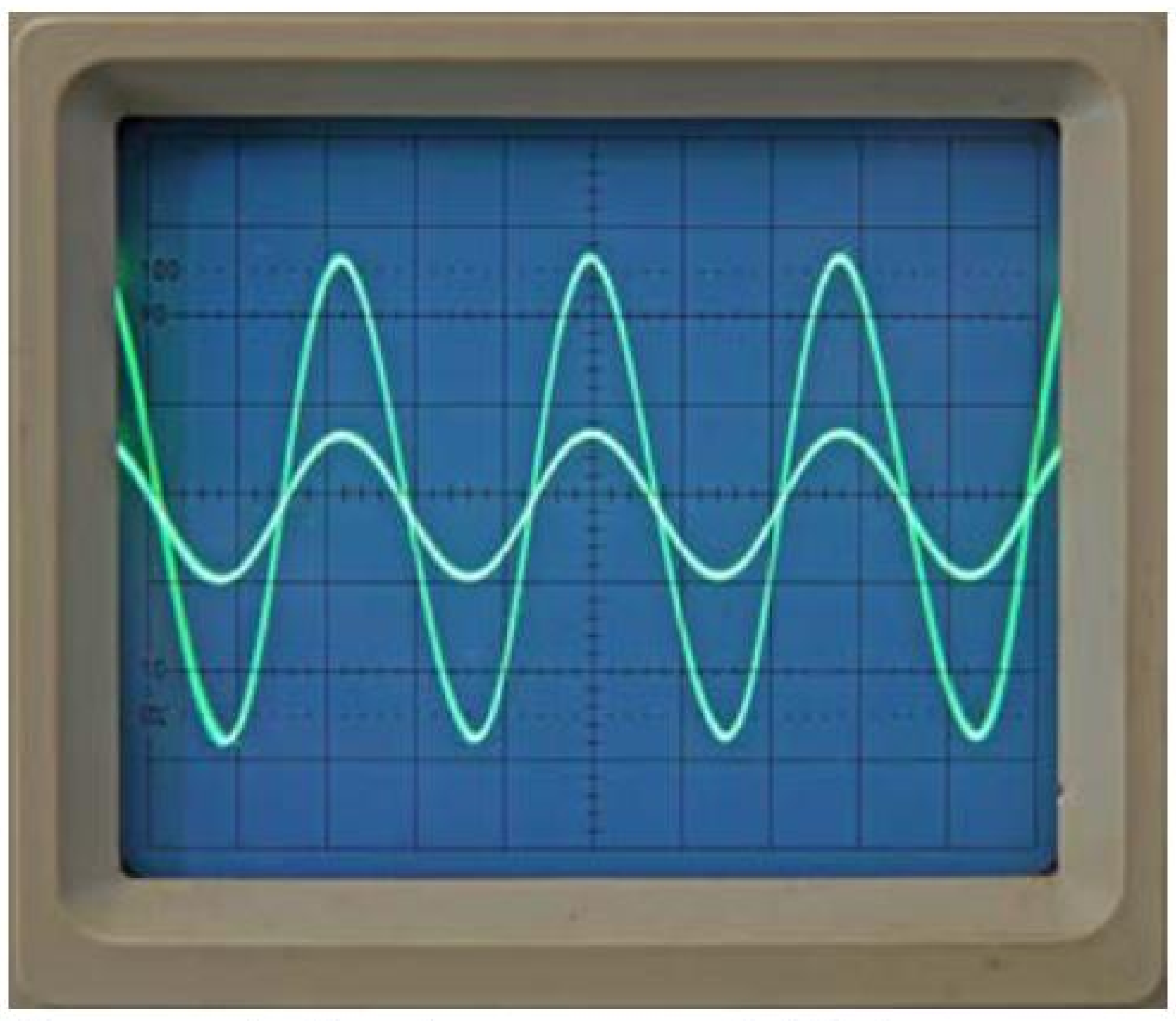

Scope 1: the low-pass & high-pass signals remain in phase during a sweep through the crossover region.

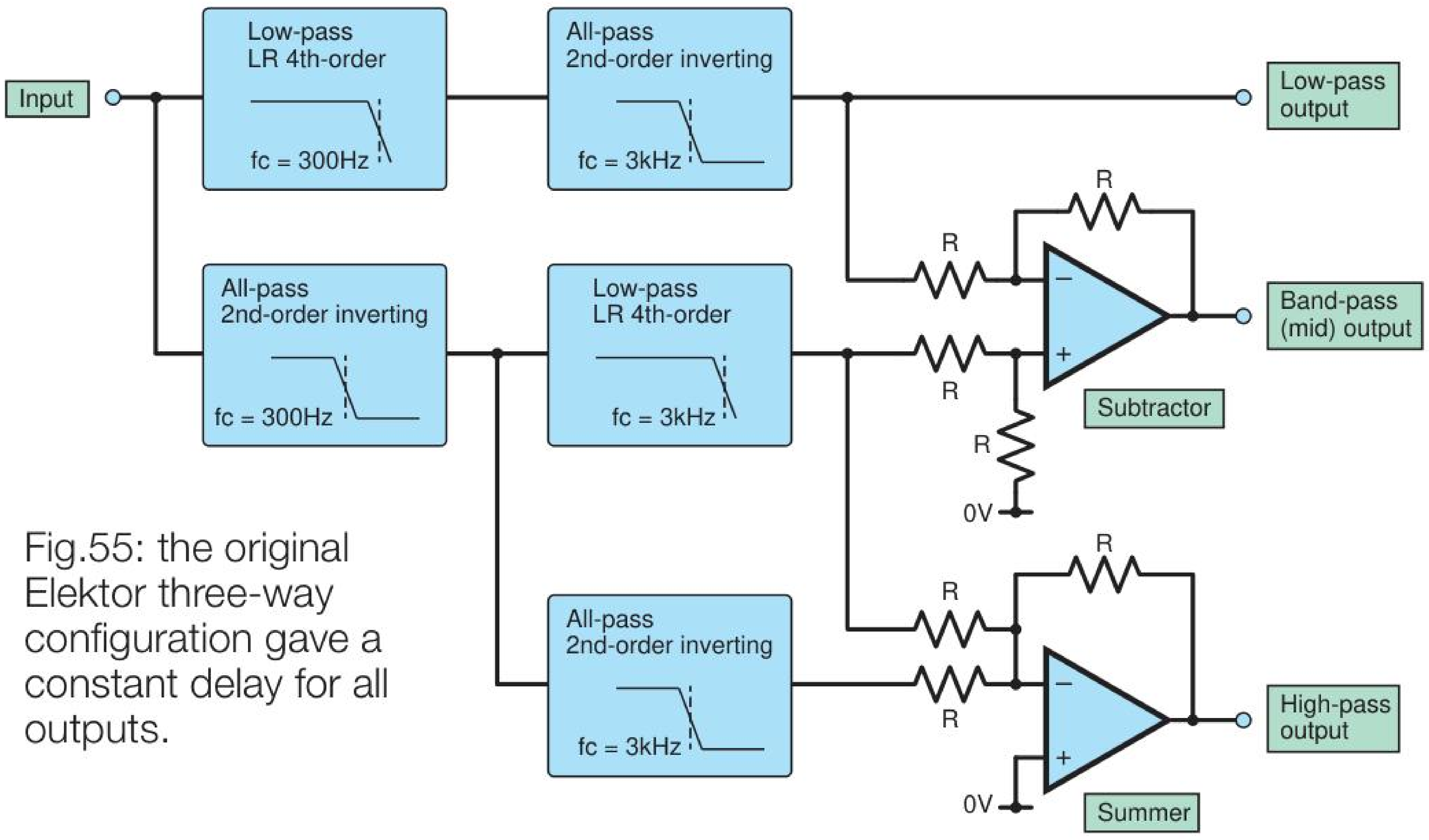
Input
Low-pass LR 4th-order
fc = 300Hz
All-pass 2nd-order inverting
fc = 3kHz
Low-pass output
All-pass 2nd-order inverting
fc = 300Hz
Low-pass LR 4th-order
fc = 3kHz
R
R
R
R
Band-pass (mid) output
Subtractor
0V
All-pass 2nd-order inverting
fc = 3kHz
R
R
R
High-pass output
0V
Summer

Fig.55: the original Elektor three-way configuration gave a constant delay for all outputs.

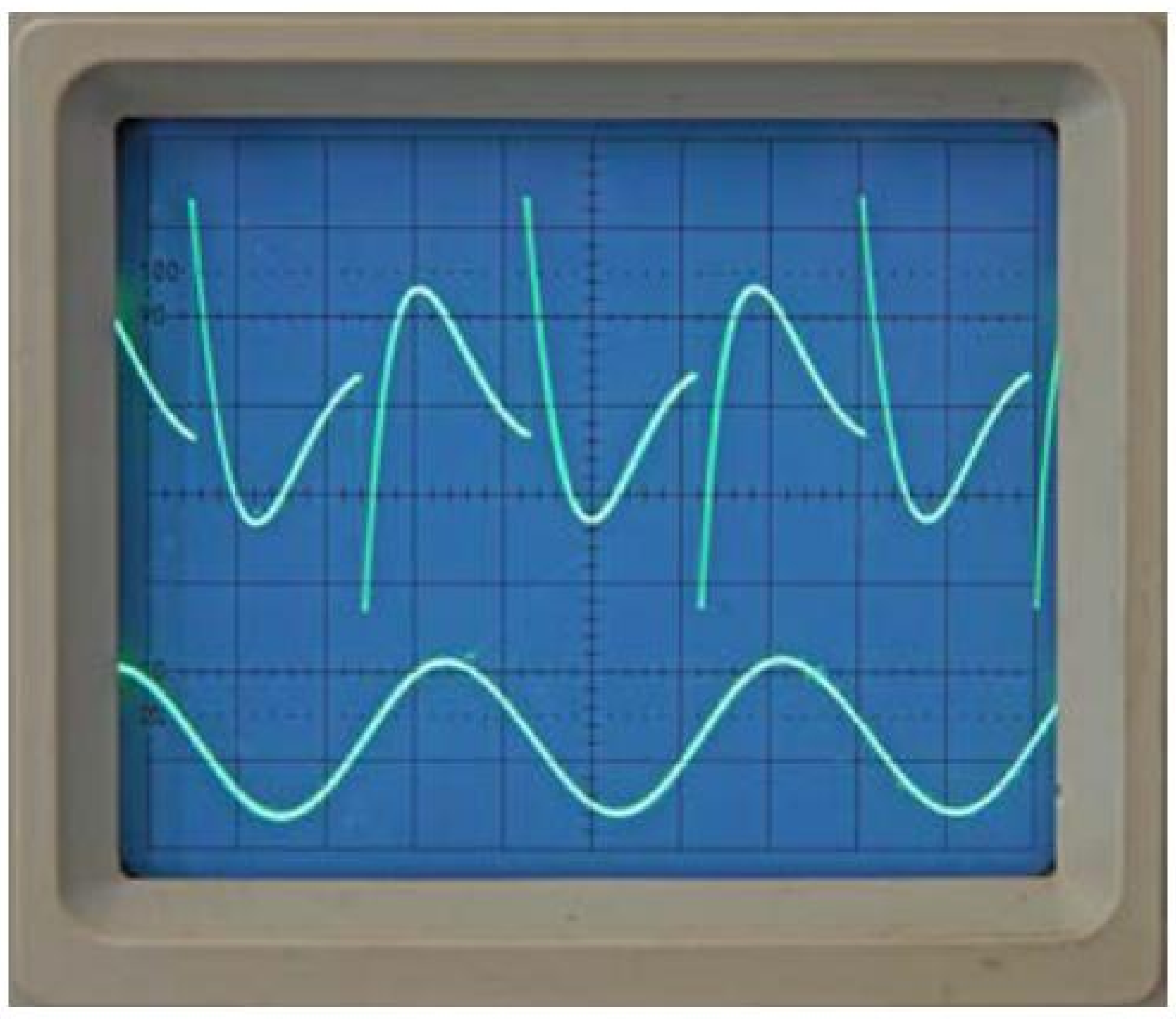

Scope 2: the effect of a high-pass filter on a 500Hz square wave. The state variable gave the same result.

42) and found it worked well with a Philips 50mm hard-paper dome midrange driver, a 10-inch (250mm) bass unit and a one-inch (25mm) Mylar dome tweeter.

The use of high-value resistors, LF353 op amps, and the delay and subtraction stages all made it very hissy, especially the tweeter output. I tried running it at +6dBu while attenuating the output to the power amps, but it was still bad. I ended up binning it after the umpteenth track breakage.

Obviously, a board redesign was called for. I thought a two-way board would be the simplest to start with. I did think another could be cascaded if a three-way design was needed, as shown in Fig.54, but the mid/tweeter would then be delayed relative to the bass. However, with a physically displaced woofer, this could be a good thing.

For a proper three-way crossover with a consistent delay, a new three-way board will have to be designed using the block diagram shown in Fig.55, along the lines of the original *Elektor* circuit.

However, I won't bother doing that now, for reasons given below.

Relative phase

In theory, the high-pass and low-pass outputs should remain relatively in-phase as the frequency is swept through the crossover point. Using a dual-trace oscilloscope showed this to be the case – see Scope 1. This is not like using separate high-pass and low-pass filters, where there is a phase difference between the two outputs.

I then tested a state-variable filter, which also employs subtraction. Interestingly, it had the same lack of relative phase shift between the high-pass and low-pass outputs. This makes it a viable competitor to the phase-linear filter. I thought maybe the group delay would be more variable with frequency; the phase-linear filter is meant to be constant.

I looked at the output waveforms with square waves and found both filters to give the same resulting waveshapes, shown in Scope 2. This suggests that the phase response and therefore the group

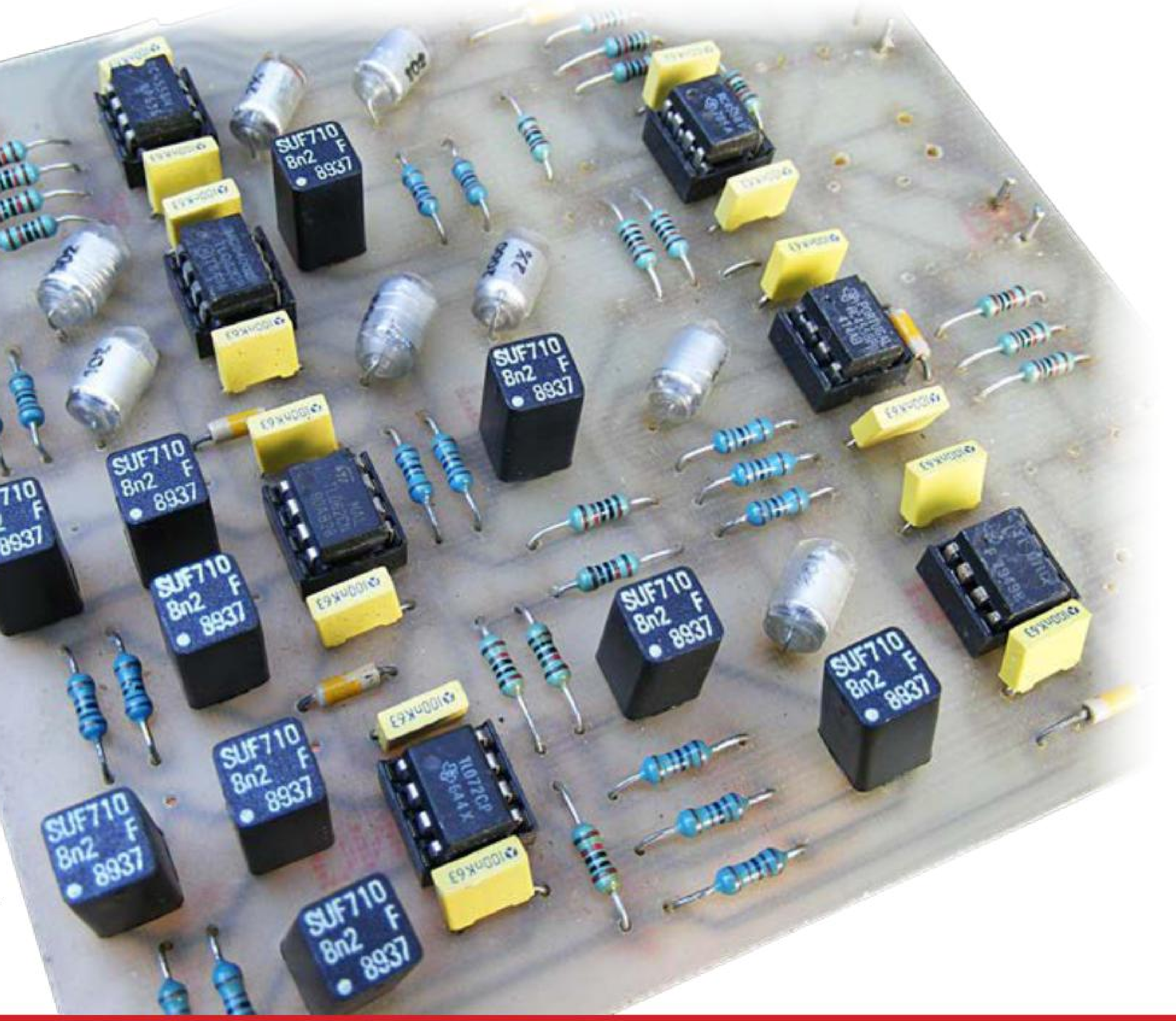

Photo 42: the Elektor phase-linear crossover board. Its tracks were too thin for a single-sided board.

delay were the same for both filters.

For a fourth-order filter, the state-variable uses four frequency-determining capacitors, whereas the phase-linear uses six, which makes it slightly more expensive to do the same job. It is also more susceptible to component tolerances.

As is sometimes the case, when I try a new wonderful circuit trick based on papers in the *Journal of the Audio Engineering Society*, full of complex (in both senses of the word) mathematics, I find there is little to be gained compared to standard textbook stuff being knocked out by Chinese manufacturers, such as the £150 Behringer state-variable based crossover filter I compared it to.

A photo of that unit was shown in Photo 12 in part two of this series, in the May 2026 issue, on page 55. Marketing and technical hype must always be personally tested. With a true phase-linear filter, the outputs would sum to the original input waveform. For both filters, the output is an all-pass function.

Still, I had 30 boards made, so they will have to make themselves useful; they just need two more capacitors. They will also provide an experimental platform for investigating subtraction techniques, and the second-order all-pass network could be useful for something like an EQ dip.

Tweaks

Going back to separate high-pass and low-pass filters based on the Sallen and Key configuration would need eight capacitors. However, this offers a great advantage which the state-variable and phase-linear circuits lack: control of the overlap at the crossover point.

Table 1 – frequency-determining crossover capacitor selection

Frequency	Capacitor value
5kHz	10nF
4kHz	12nF
3kHz	15nF
2kHz	27nF
1kHz	47nF
700Hz	68nF
600Hz	75nF
500Hz	100nF
300Hz	150nF
250Hz	220nF
125Hz	390nF
100Hz	470nF

Yes, there are phase problems, but the final acoustic result is superior to the hole-in-the-middle effect invariably produced by the classic Linkwitz-Riley state-variable filter (a result of its -6dB dip) using real drivers with natural roll-offs.

[Editor's note: In theory, a Linkwitz-Riley crossover gives ideal on-axis summing, although the off-axis response may not be perfect. Still, real drivers rarely behave like textbook sources. Other alignments may sacrifice some on-axis perfection while improving the perceived integration or off-axis balance. It will depend on the drivers, layout and listener preference.]

Frequency scaling

For the 500Hz crossover frequency, all the frequency-determining capacitors are 100nF. Some of the filter capacitors are doubled up, such as the feedback capacitors C1/C2 and C4/C5. This is because sometimes the doubled values, such as 200nF, are from the E24 series and so harder to obtain.

There's also the advantage that if all the 100nF capacitors are from the same batch, they're likely to be much closer in value to each other than their tolerances might suggest.

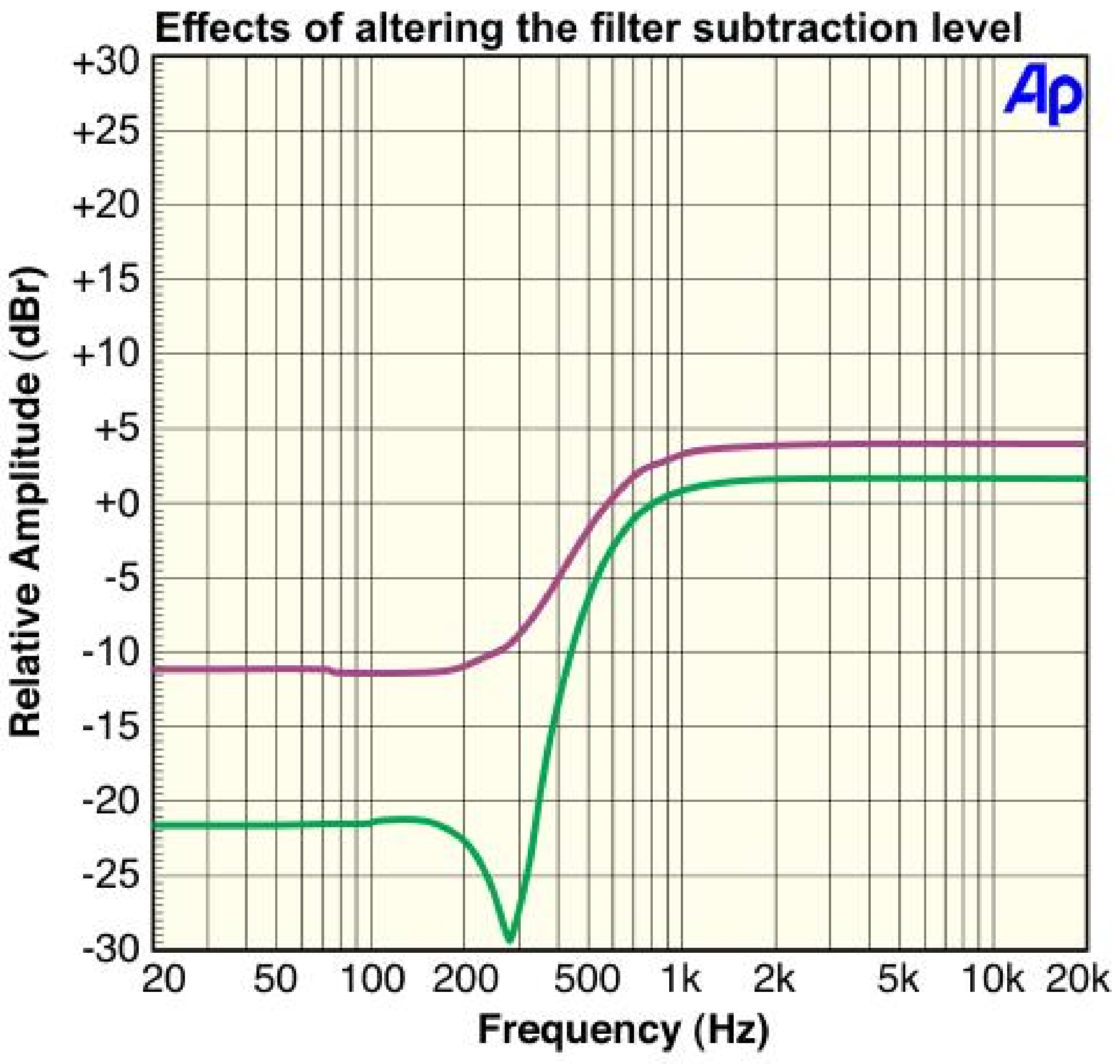

Fig.56: the effect of altering the subtraction level in the filter.

The equal-value Sallen and Key circuit is not used because it has gain in the passband, increasing the noise level. The resistors are all kept the same and as low in value as possible for minimum Johnson (thermal) noise. To change the frequency, scale the capacitors accordingly – see Table 1. These are all rounded off to the nearest E12 value, so the frequencies are somewhat approximate.

Nice curves

R9, the subtraction mixing resistor, is the most critical component. Fig.56 shows the effect of using 1.8kΩ and 2.4kΩ values for R9. If not enough signal is subtracted (1.8kΩ), the high-pass action just stops and it flattens off. Too much (2.4kΩ) and a notch develops, with the signal coming back with a polarity reversal.

Tweaking R9 can produce a useful curve akin to that used in the KEF 104aB speaker for the

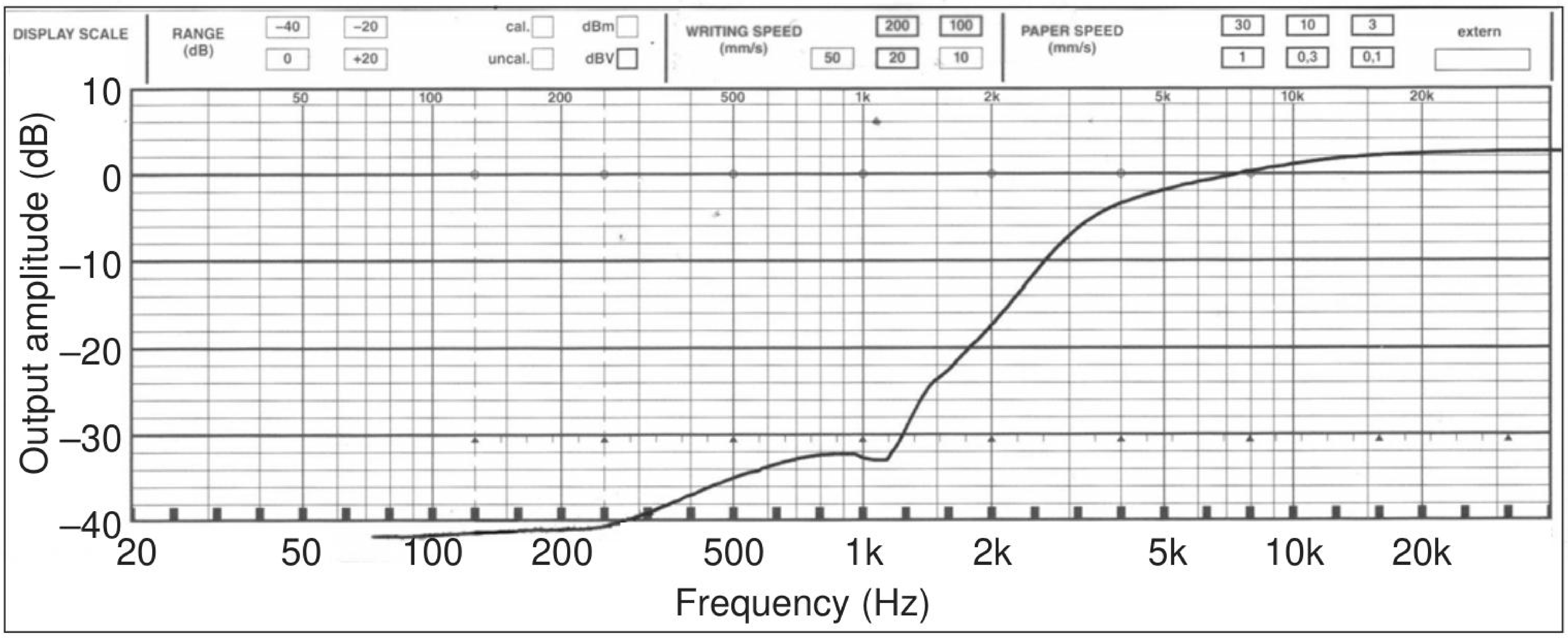

Fig.57: KEF's 104aB tweeter high-pass filter. Notice the anti-resonance notch and the reversion of the third-order slope to first-order afterwards.

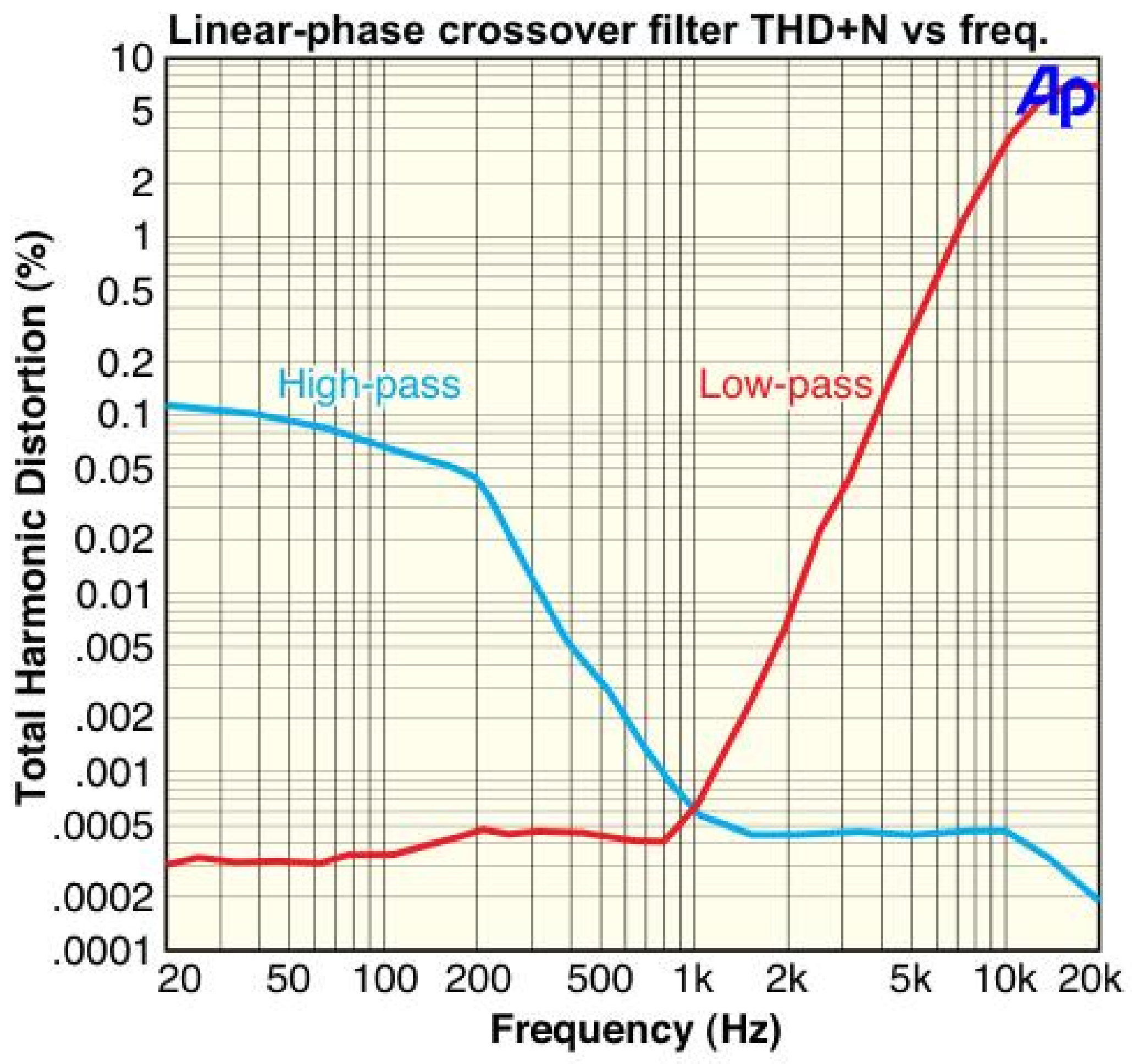

Fig.58: the artificially high distortion for the crossover filter at 8V RMS.

tweeter described in Audio Out, June 2026. The response of this third-order high-pass filter is shown in Fig.57. This takes into account the second-order high-pass slope that the T27 tweeter exhibits after resonance, making the total electroacoustic output a smooth third-order.

The dip to suppress the tweeter's fundamental resonance at 1.2kHz can be seen, after which the curve slope reduces to -6dB/octave. These types of filters work well with satellite speakers with a pronounced bass resonant hump, such as the LS3/5a, in subwoofer applications. Also, dome-type mid-range drivers often have high-Q resonances around 350Hz, such as the ATC 3-inch dome and some Philips units.

Some dome tweeters with skimpy neodymium magnets, such as the DT28, often roll off with a peak at 2kHz. They will also benefit from a bit of a notch. Remember that the reduced stop-band attenuation will reduce power handling and increase distortion.

Distortion measurements

I have tried measuring the distortion of filters with the THD+N (total harmonic distortion plus noise) measurement macro supplied with the Audio Precision system, but it gave rather strange results. The main problem is that as the filtering action takes place, there is less and less signal for the distortion analyser to work on.

This gives the false impression that the distortion is rising excessively rapidly as the analyser ramps up the gain to compensate. The effective result is a boosted noise component of the residual signal, giving falsely high reading. This test is designed for amplifiers, which have a flat response. It helps if the filter is driven at a high level and a bit of inverse pre-filtering is applied to flatten it out.

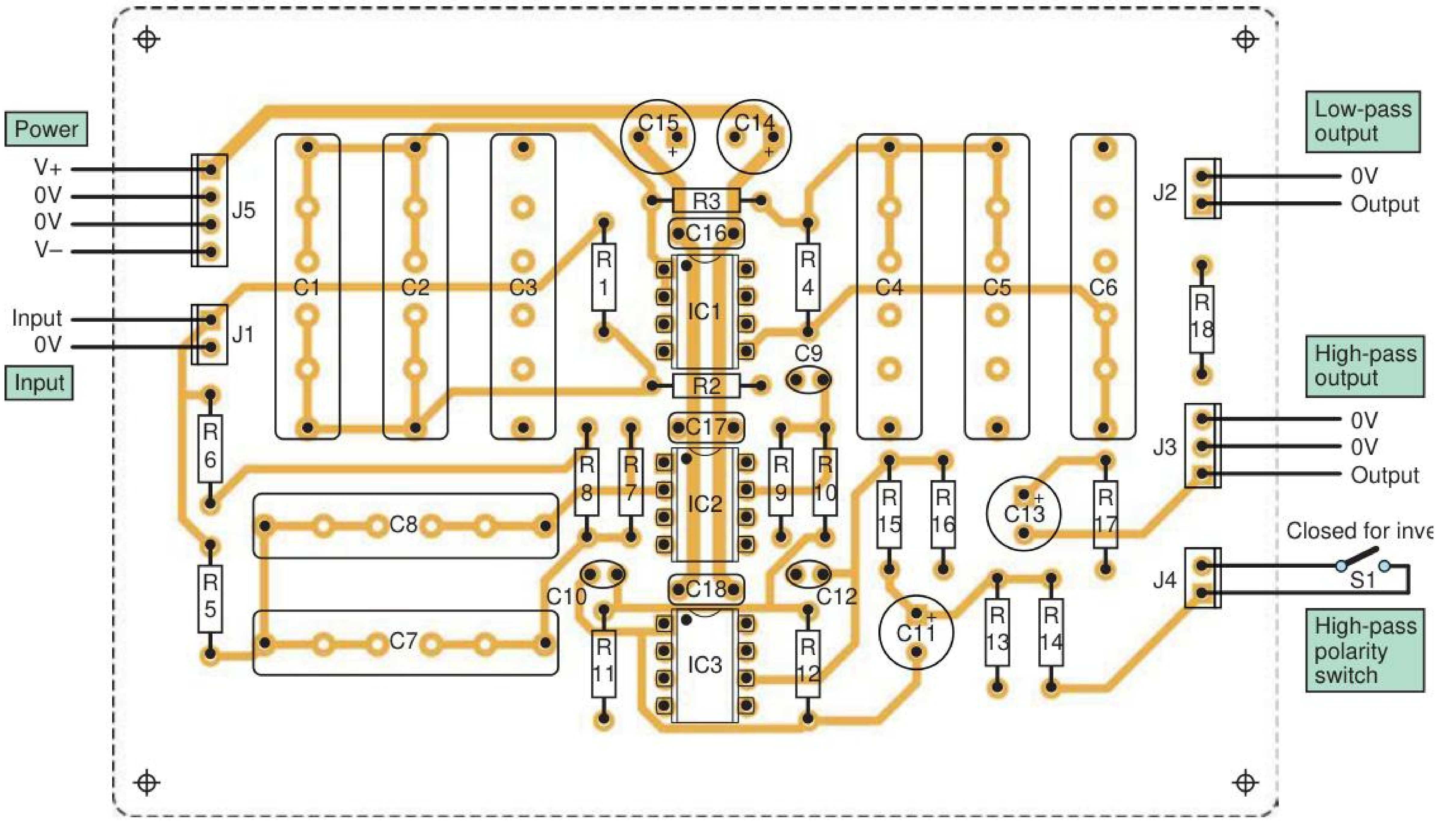

Fig.59: the PCB overlay for the phase-linear crossover. Note the multiple outlines available for the frequency-determining capacitors.

Of course, all filters do have a real rise in distortion in the turnover region, where the main filter slope takes place between the passband and the stopband. This is because there is voltage developed across the capacitors, a higher common-mode voltage on the op amp input pins, and positive feedback to compensate for resistive losses.

The question is how to measure the filter THD accurately, which I can't do at the moment. The result is shown in Fig.58, using NE5532 op amps and polystyrene capacitors. When I look at the residual on the scope or do an averaged FFT, the distortion is much lower than indicated in the graph. The distortion in the passband is very low; almost that of the op amps alone.

Taking the same measurements at 1V RMS gave higher distortion readings, showing it is a noise effect.

Assembly

This is a conventional, mature 1980s audio technology design with no fiddly surface-mount resistors, just proper blue thin-film axial types. There is plenty of space for different shapes and sizes of frequency-determining capacitors; six mounting holes are provided for each. The PCB overlay is shown in Fig.59 and the completed assembly in Photo 43.

One of my friends had bags of 16nF Suflex polystyrene capacitors, which are very large for their value, and they fitted fine.

Using the board

It should go without saying that the filter should be driven from a low impedance source, since its

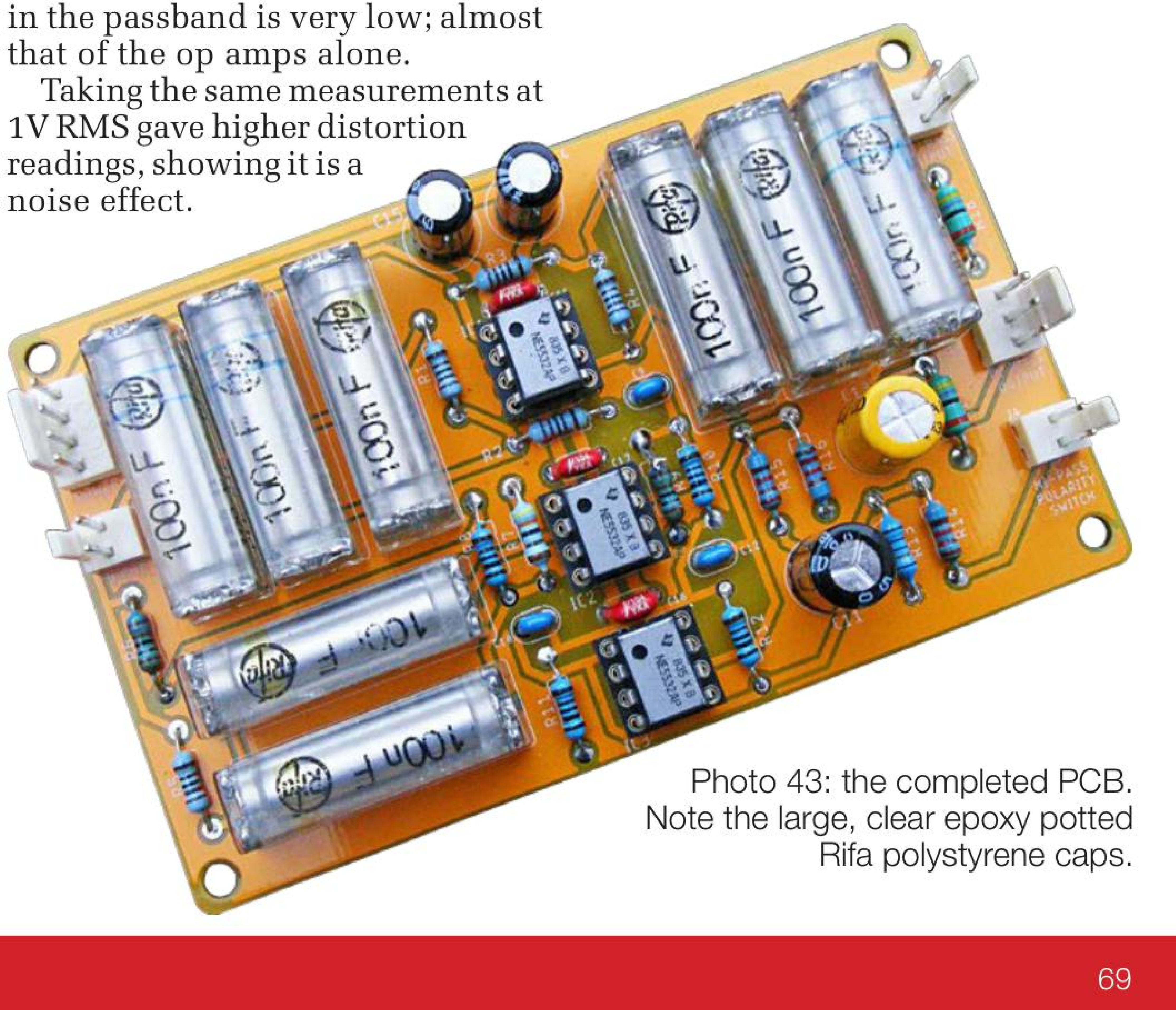

Photo 43: the completed PCB. Note the large, clear epoxy potted Rifa polystyrene caps.

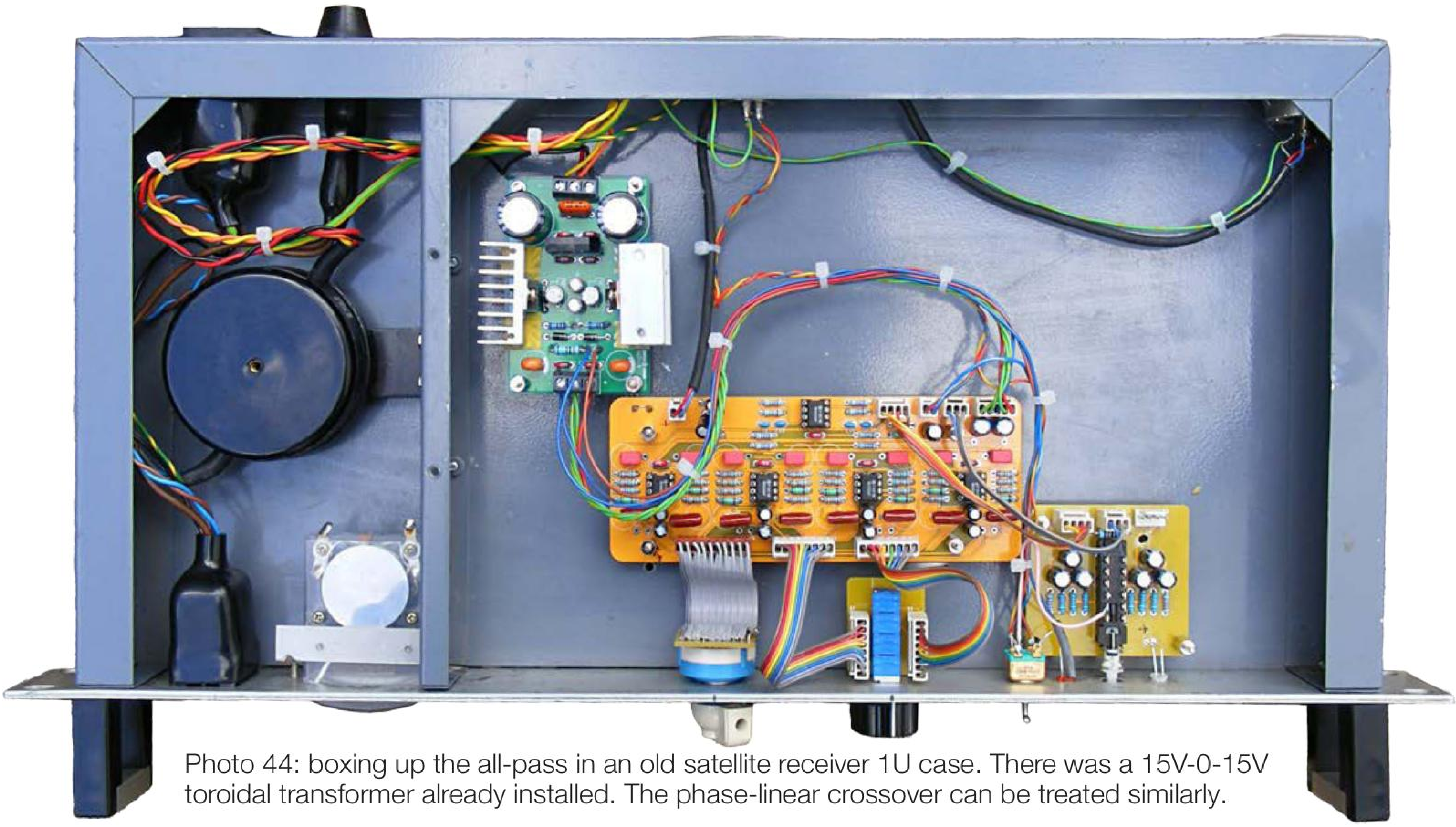

Photo 44: boxing up the all-pass in an old satellite receiver 1U case. There was a 15V-0-15V toroidal transformer already installed. The phase-linear crossover can be treated similarly.

input impedance is around 800Ω. This driver can be a voltage follower or a differential amplifier for input balancing.

For minimum noise, drive the board as hard as possible, making sure the power amps it feeds clip first. The output of the board will often need considerable attenuation to achieve this, since most power amps are fully driven at 775mV RMS or thereabouts.

Active speaker systems often suffer from multiple Earth loops. Earth isolation can be obtained by using balancing transformers at the outputs. I used 3:1 step-down transformers to get lower current drive requirements and attenuation at the same time.

When selecting the crossover frequency, the drivers should be flat to about an octave away from the crossover frequency to avoid frequency response dips.

The only way to get crossovers right is to actually measure the combined acoustic output, which is a lot of work.

Boxing clever

I will now get back to the project we described last month, the adjustable all-pass filter using an eight-gang pot. We finished the article last month without having put it in a case. This advice will also apply to the phase-linear crossover, since its case requirements are much the same.

Fox boxing up the all-pass system, I used a 1U case from an old satellite receiver, as shown in Photo 44. There was a 15-0-15V toroidal transformer already installed and an edgewise signal level meter (sadly broken). Its slot will have to be filled by an illuminated logo in Quad style.

This is another bit of audio electronics that drives me mad. Like all studio engineers, I prefer my gear in 19-inch (483mm) rack cases, but they are becoming expensive and difficult to get.

For some reason, 1U high (44.45mm, 1¾-inch) cases are easier to find, but they have insufficient internal headroom for things like toroidal transformers, heatsinks and old-format XLR sockets. As shown in Photo 45, the XLRs have to go on their side because there is usually a lip from the lid and base. One way around it is to use Neutrik PCB-mount connectors.

Q-max punches (Photo 46) are excellent for enlarging existing holes. The old format XLR sizes are 25mm for female sockets and 19mm for the male types. New format panel-mount sockets (Photo 47) are all 23mm. Always drill the 3mm mounting holes after the socket has been placed in the hole so that they line up.

2U cases are vastly superior for audio circuits, being 2.5 inches (63.5mm) tall, giving good front panel space for proper ‘human-sized’ knobs. You will have to give £87 to RS for a good aluminium one though. I balk at the cost; it’s often more than the electronics inside!

I’m going to join forces with Grindle and other engineers to get a load made based on extruded

Photo 45: I was disappointed that traditional XLR sockets wouldn’t fit normally on this 1U case; they had to go sideways. Still, it only cost £3.00!

Photo 46: “Q-max” punches give a much cleaner result than drilling. Old guys have big collections from the valve era, so they’re cheaper at rallies.

Photo 47: the new XLRs introduced by Neutrik take up less room and require identical holes. The trouble is I still have hundreds of the old types!

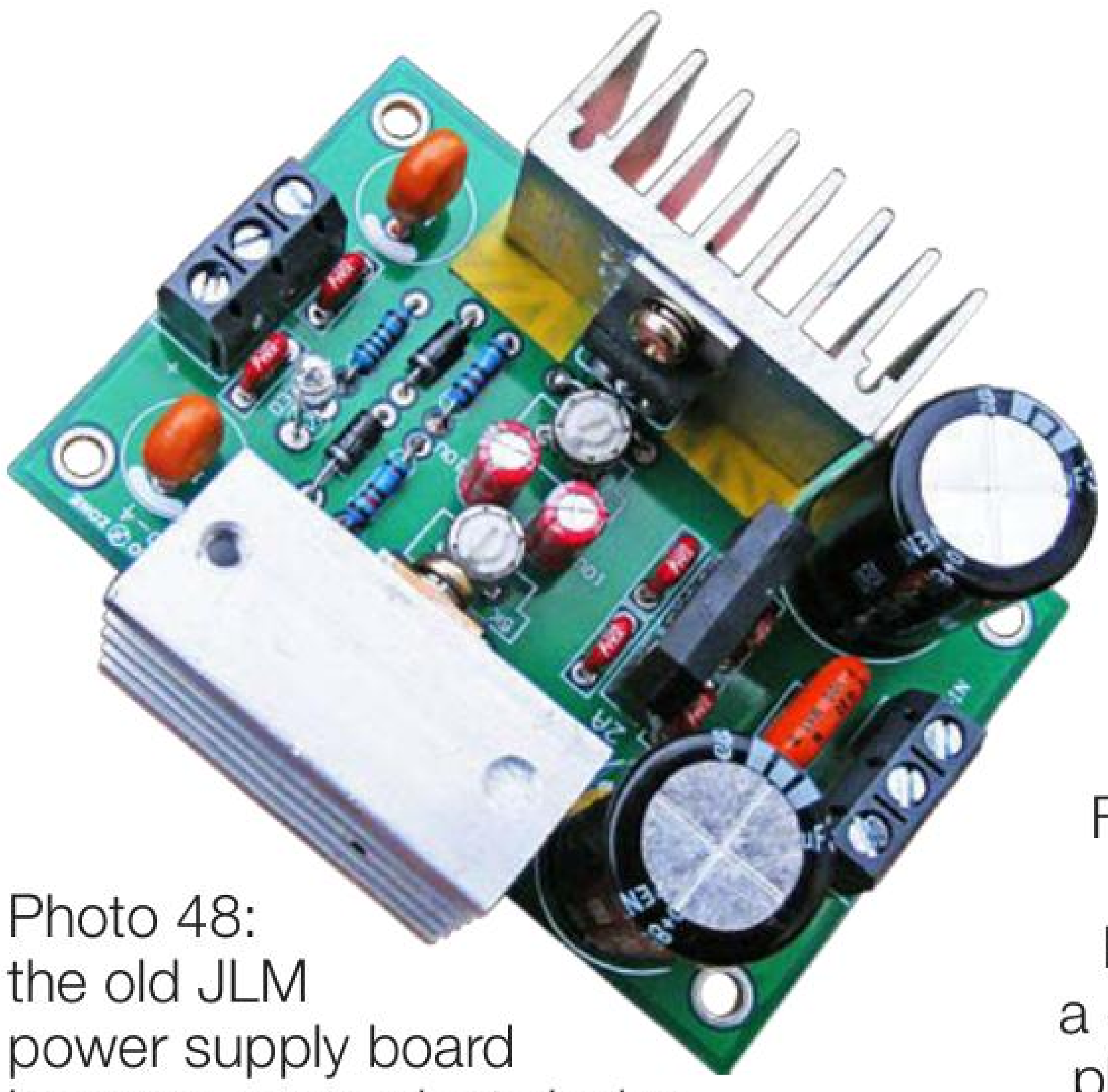

Photo 48: the old JLM power supply board is a very convenient design. I'll design my own soon.

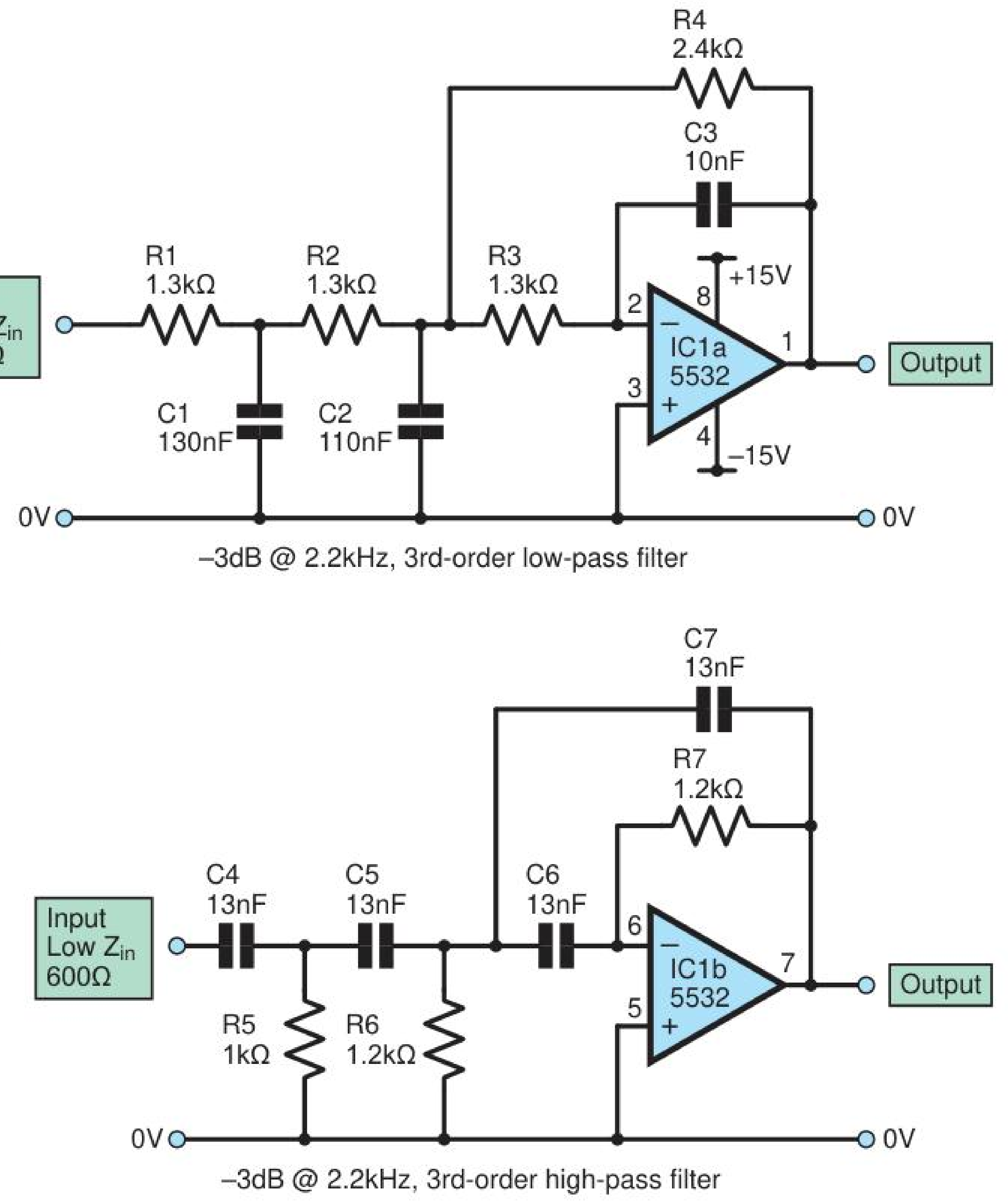

Fig.60: the interesting inverting third-order Rauch crossover has a -3dB dip at 2.2kHz. I plan to investigate this configuration further.

aluminium corner pieces. It's always worthwhile scouring radio rallies for old equipment with nice metal cases. Often, only a new front panel is required and a bit of hole punching at the back. I got the case I used for this project at a radio rally for just £3!

Aluminium boxes are best if you are having the mains transformer in the case, since steel can spread its magnetic field around, increasing the risk of hum. Conversely, steel cases can minimise hum by their magnetic screening effect if the transformer is outside.

In studios, we always try to have equipment with internal power supplies, though, because multiple plugpacks make an awful mess with the cabling and degrade overall system reliability. For the power supply in Photo 48, I used an old kit board from the Australian company JLM Audio, with a standard LM317/LM337-based circuit.

Not again!

As usual, doing this one measurement has opened a whole new area of investigation. Apparently, the most popular filter configuration, the Sallen and Key used here, is one of the worst for distortion. Ton Giesberts, *Elektor*'s chief audio designer, found that the inverting multiple-feedback type or Rauch filter is almost 10× better (*Summer Circuits*, July-August 2005).

These filters are not used much because it's hard to calculate the component values, although this process is described in the National Semiconductor Audio/Radio handbook (section 5, page 2). They were used in the *ETI* Active Speaker by Barry Hughes and Paul Hynes years back in September 1982, and a crossover based on this is shown in Fig.60.

[Editor's note: I prefer multiple-feedback filters over Sallen-Key as they provide more effective attenuation at HF. Coincidentally, this is explained in Circuit Surgery *this month – see page 44].*

I thought the *ETI* Active Speaker was one of the best magazine active speakers I've built and I learnt a lot. Op amps in inverting configurations can give lower distortion because there is no common-mode voltage signal on the two input pins.

They do suffer higher noise and lower input impedance in this configuration, though. I'm going to use a Rauch configuration in an all-pass filter to form a subtractive crossover to see how that works out.

Phased out?

Yes there's more all-pass filter stuff we could do, obviously including a guitar phaser pedal, but I need to give it a rest for a while. Later on, we'll use all-pass filters in column speakers, multiple tweeter arrays and the D'Appolito dual-midrange system with the tweeter in the middle. The Quad ELS63 electrostatic speaker used concentric rings fed by a tapped series of all-pass filters.

Some public address speaker systems even use phased-array steering, a technique borrowed from radar and antenna design. I'm looking to use modulated all-pass filters to make a 'rotating' Leslie loudspeaker!

There's scope for employing all-pass filter delay lines for 'look-ahead' control in limiters, de-essers and pop filters, where the processing comes in before the audio peak arrives. The BBC created some interesting designs in the 1960s using this technique.

Possibly the weirdest all-pass filter music applications of all are frequency shifters. The Barberpole Phaser uses a constant frequency shift resulting in an infinitely ascending or descending sweep, is perhaps the most exciting thing. It's based on the auditory illusion of Shepard tones.

Photo 49 shows one made by Harold Bode sold by Synth-Werk;

BARBERPOLE PHASER™
BODE SOUND CO.
MODEL NO. 8101
BY SYNTH-WERK
FREQUENCY SHIFTER

Photo 49: a Barberpole phaser from Synth-Werk.

I will have to do one. You never know, it might lead to a new song, which has been the original drive for this electronic audio design path I've been on since 1979.

Parts List – Linear-phase crossover

1 double-sided PCB coded AO-AUG-26, 108 × 75mm
3 NE5532 dual low-noise op amps, DIP-8 (IC1-IC3)
3 2-pin, 0.1"/2.54mm Molex-type polarised headers, housings and pins (J1, J2 & J4)
1 3-pin, 0.1"/2.54mm Molex-type polarised header, housing and pins (J3)
1 4-pin, 0.1"/2.54mm Molex-type polarised header, housing and pins (J5)

Capacitors
8 100nF close-tolerance frequency-determining capacitors* (C1-C8)
2 100µF 25V radial electrolytic (non-polarised preferred) (C11 & C13)
2 10-100µF 25V electrolytic (C14 & C15)
3 100nF 50V X7R ceramic, 5mm pitch (C16, C17 & C18)
3 47pF C0G/NP0 ceramic, 2.5mm pitch (C9, C10 & C12)

* select the appropriate value from Table 1. I used 100nF ±2% RIFA polystyrene (see AOShop). Polypropylene and 250V high-voltage polyester will also work well. All should be matched within 2% of each other.

Resistors (all ¼W axial thin-film ±1%)
1 4.3kΩ (E24) or 4.42kΩ (E96) (R7)**
5 2.2kΩ (R1-R5)
2 2kΩ (R6 & R9)
3 1.2kΩ (R14, R15 & R16)
4 1kΩ (R8, R10-R12)
2 47Ω (R17 & R18)

** two 2.2kΩ (E12) resistors in series gives closer to the optimum 4.4kΩ

The NE5532's decline continued

I was interested in why the all-pass filter seemed to be a distortion stress test for the op amps in our discussion of new vs old NE5532s last month. Ben Duncan suggested that the impedance of the all-pass stage may dip below 600Ω at some point. I measured it and found it was 940Ω at low frequencies, dropping to 600Ω above 8kHz.

I needed to check this, since it is possible for the impedance to drop lower than expected with configurations based on the op amp differential amplifier. There is a situation where the resistor feeding the inverting input pin can have anti-phase signals on both ends, making the resistor appear lower than it is. I covered this phenomenon in the discrete differential buffer described in the April 2024 issue (see Fig.32 on page 64).

I mentioned that the maximum output swing had been deleted from the datasheet for the new version of the Texas Instruments NE5532. An omission is always a bad sign, and it turns out my suspicion was valid. The output swing has dropped by a volt.

Measured using ±15V rails with no load, the new device gave 27V peak-to-peak, or 22.5V peak-to-peak into 600Ω. There was a touch of oscillation on the negative rail at clip as well. Using the old NE5532, it was 28V and 23.5V, respectively, with clean clipping.

As the Editor wrote in last month's editorial, the new design changes the input transistors from NPN to PNP. This reverses the direction of the DC bias currents. This means that careful orientation of electrolytic capacitors to agree with the resulting small negative offsets introduced would now have to be reversed.

This was a technique we employed at Calrec in Hebden Bridge, which I don't think made any audible difference, but it may have made the capacitors last longer. Also, all those fancy mic-pre and phono circuits that paralleled extra input transistors with the internal transistors for lower noise won't work with these new devices.

Two good things (silver linings?) are that the bias current with the new design is half that of the old version, and the noise level also measures the same when used in a standard RIAA preamplifier circuit.

These things are a clue as to the identity of the 'new design'. I suspect it is a re-engineered version of the RC4558. There was a special low-noise (4nV/$\sqrt{\text{Hz}}$) version of this, the obsolete JRC NJM2041 used in Philips/Marantz amplifiers and Fostex tape machines. It was specified to run from ±22V rails maximum, so I suspect it was an RC4558 made on the same process as the NE5532.

Conclusion

That's it regarding all-pass filters, at least for now.

I recently attended Retrotech and I will have a report on that shortly, including some photos of interesting devices.

I am increasingly yearning for retro technology, if only because devices made in the past were intended to be repairable.

Many products made since about 2015 (including cars and washing machines) are intended to be disposable – use it until it breaks, then throw it away and buy a new one. Not me. PE

power
ALL-PASS FILTER
POLES
EIGHT
FREQUENCY
OUT
IN
POLARITY
RED INVERTED

Photo 50: the front panel of the finished all-pass filter we built last month.

AO*Shop*

The home for specialist audio, analogue and historic components – provided by Jake Rothman, *PE's Audio Out* columnist. The AOShop is your best bet for classic analogue 'NOS' (new old stock) components, including all parts for *Audio Out* projects and designs.

Ge semiconductors

Small-signal PNP transistors

NKT214F, OC57, OC59, 2N1377, 2N525	**£1.00**

Low-noise PNP transistors

GET106	**£2.50**

Small power PNP transistors

AC153, AC153K, AC188K	**£1.50**

Small power NPN transistors

AC176, AC141K	**£2.00**

High-voltage PNP transistors

OC77, CV7001	**£1.50**

TO3 PNP power transistors

AD149, AD161, AD162	**£2.00**
AD140	**£3.50**
AD149, AD161/2 matched pair	**£5.00**

RF PNP transistors

OC41, OC42, 2SA12, 2SA53, AF124, AF178, GET872A	**£1.50**

NPN transistors

OC139, OC140, ASY73	**£2.00**

Diodes

CV7049 (OA10), CG92 (OA91)	**£0.50**

Si semiconductors

Diodes

ZC5800 RF Schottky	**£0.20**

Low-noise silicon transistors

BFW16A, 2SC3071, 2SC3068, 2SA1016K, 2SC2362K, 2SA970BL	**£1.50**
2SC2204, 2SD655, BC550C	**£0.50**
ZTX651	**£0.30**
ZTX751	**£0.50**

RF transistors (suitable for Theremin)

BF180	**£0.40**
BF199	**£0.50**

Audio power MOSFETs

Exicon 10N20, 10P20	**£6.50**
Hitachi 2SJ99, 2SK343	**£3.50**
Hitachi 2SJ56, 2SK176	**£8.50**

JFETs

BFW11, BFW10, TIS73L, J177, J113, U1994, U1898, 2SJ176, J201	**£1.00**
J175, J176, J112, J111, 2N3820, 2N5457, BF244, 2N5460, J230	**£0.60**

Small power output/driver transistors

2SB649A, D669A, 2SA1208, 2SC2910, MJE253G, MJE243G, 2SA1725, 2SC4511	**£1.20**
BD139,BD140, BD135, BD136, BD435, BD436, MPSA63, BCV46	**£0.50**

MOSFETs

ZVP2106A	**£0.30**
Dual-gate 3SK45, BFS28	**£1.50**

Metal-cased transistors

BCY71	**£0.30**

Amplifiers

LM318 high-speed op amp	**£0.35**
µA709 metal-cased op amp	**£2.00**
5534H metal-cased op amp	**£3.00**
LM384, TDA2030A, TDA2050V	**£1.50**
TL082 (ceramic pack)	**£1.00**
TAA435 (Mullard power amp driver for AD161/AD162)	**£1.20**

ICs

That/dbx 2180 VCA/VCF	**£6.00**
CA3080 VCA/VCF (vocoder)	**£2.80**
CA3280 VCA/VCF	**£4.00**
LM13600/ LM13700 VCA/VCF	**£2.00**
PT2399 echo/delay	**£1.50**
Original TI 44V NE5532	**75p**
Nisshimbo 44V NE5532DD	**£1.00**
SMT version	**50p**
New 36V TI NE5532	**50p**
Original TI NE5534A	**£1.40**

Dual transistors

2N2639, 2N2223, 2N2910 (NPN)	**£4.00**
E401 (JFET Moog)	**£4.00**
2SK2145-Y dual JFET	**£0.80**
2N5564 JFET	**£8.00**
HN3C51F, HN3A51F	**£1.00**
DMMT3904/6, HN1A01F, HN1C01F	**£0.50**

Loudspeakers

PE Mini-Monitor

Volt PE165 6.5-inch woofer (each)	**£85**
Morel MDT29 tweeter (each)	**£25**
Kit *pair* of PE165/MDT29 plus Volt crossover parts and PCBs	**£299**
Monacor DT-28N tweeter (each)	**£35**
Vifa 19mm BC20SC15-04 tweeter (each)	**£15**

Volt crossover inductors

1.2mH, 1.5mH, 2mH, 2.7mH, 0.5mH (tapped at 0.3mH) (each)	**£5.85**

Fully tested reclaimed speakers

Vifa BC14 5-inch woofer (each)	**£10**
Vifa TC26 1-inch tweeter (each)	**£10**

Low-price speakers

Philips 4-inch 4070	**£2.00**
EMI 10x6-inch, 30Ω Alnico	**£7**
64mm 64Ω neodymium	**£1.20**

Capacitors

Note '10/63' denotes '10µF 63V'.

Polyester

3.3/100, 4.7/250, 4.7/63	**£1.00**
5.6/63, 8.2/63, 10/63	**£2.00**
Mullard 'Mustard' C296 0.22/400	**£2.00**

Polycarbonate

Axial 2.2/63 1%, 4.7/160, 6.8/63	**£1.00**

Radial

6.8/160V, 10/63	**£2.00**
Reclaimed 22/63	**£2.00**

Polystyrene

Philips 1% 4.7nF/160, 6.2nF/500, 12nF/63, 22nF/63, 110nF/63, 24nF, 2nF	**£1.00**
RIFA 2% 100nF for active xov.	**£1.00**
Suflex 90.9nF 0.5%	**£2.00**
Suflex 2.5% 10nF/63 (rad. or ax.)	**£0.50**

Radiation resistant

Siemens cellulose acetate MKL 2.2/25	**£0.80**

Electrolytic – Mullard blue 017 series

10/25, 22/25, 100/10	**£0.50**
150/40, 470/40, 1000/25	**£1.00**

Tantalum – axial metal cased

22/50, 47/35, 68/25, 100/20, 120/10, 150/16, 220/10, 330/6	**£2.00**
22/35, 33/35, 47/20, 68/15, 100/10, 150/6	**£1.25**
4.7/50, 6.8/35, 10/25, 10/35, 22/15	**£1.00**

Axial moulded-case tantalum

Kemet axial 6.8/10	**£0.30**
Kemet radial 33/10	**£0.40**
STC radial 100/20	**£1.50**

Tantalum bead

22/50	**£1.00**
470/3	**£2.00**
680/6.3	**£3.00**

Wet tantalum

220/25 axial	**£3.20**
Castanet button 140/30, 470/3	**£3.20**
Hughes 540/10	**£3.20**

Bipolar

Hermetic bipolar tantalum 16/35	**£3.20**
Elcap axial 10/50	**£0.50**
Generic radial 100/16, 470/35, 100/ 63, 22/35, 4.7/35, 220/16	**£0.50**

Philips solid-aluminium (axial) 121/123

47/16	**£1.00**
330/6.3	**£2.00**
100/35	**£4.00**

Philips Pearl 122 series (radial)

10/16	**£0.30**

Silvered mica (radial)

1nF/500 1%	**£1.00**

Trimmer capacitors

Vishay plastic-film 4-40pF	**£0.80**
Vishay plastic-film 5.5-45pF	**£1.00**
Vishay plastic-film 5-80pF	**£1.20**
Vishay plastic-film 10-250pF	**£2.00**
Mica 1-12pF, 2-40pF	**£1.00**

Audio transformers and inductors

Eagle transformers

LT44, LT722 driver, LT700, LT723 500Ω output	**£2.50**
LT30 500mW output	**£3.50**
5:1 interstage (fuzz box)	**£1.50**

Repanco

T/T3 splitter transformer	**£4.00**
CH2 5mH RFC	**£2.00**

Balanced output transformer

Vigortronix 600Ω VTX-101-007	**£10**
Vigortronix 600Ω VTX-101-3001	**£10**
Vigortronix 600Ω VTX-101-3002	**£15**
Gardners 150Ω	**£10**
Reclaimed BBC LL74/MPC nickel core 600Ω	**£12**
Low-level 1:1 600Ω (modem)	**£2**
Reclaimed mic input transformer	**£15**

Inductors

82µH, 4.7mH, 100µH, 270µH, 10µH, 14µH (low Z)	**£0.50**
4-inch ferrite rod with MW and LW windings	**£3.00**

Special resistors

Bourns wire-wound trimmer 5kΩ 3059 JM panel-mount	**£2.00**
Thermistor RA53, R13	**£4.00**
A13	**£2.00**
Thermistor CZ1, CZ6	**£1.50**
Holco H2 2.2MΩ 1W, 1%	**£1.00**
Welwyn 1GΩ 2W	**£1.00**
5k Bourns 3321H cermet trimmer	**£0.50**

Potentiometers

Bourns 81

25kΩ lin cermet	**£2.00**
25kΩ lin, 5kΩ lin cond. plastic	**£3.00**

Bourns 91

10k dual-gang lin or log	**£10.00**

Plessey moulded-track

5kΩ log with switch	**£3.00**
50kΩ A/log	**£3.00**
Mil 250kΩ lin dual	**£5.00**

Bourns

8-gang 50k A/log	**£7.50**
ALPs 4-gang 100k A/log	**£3.00**

Alpha

16mm 4.7kΩ A/log	**£0.80**
220kΩ A/log	**£0.80**
10kΩ lin centre-detent dual-gang	**£1.50**

Allen Bradley J series/Honeywell

10kΩ lin 1 million cycles	**£5.00**
Blore Edwards AB 45 dual 5kΩ A/log with switch	**£3.50**
Alps RK9 dual-gang 5kΩ RD law	**£4.00**
Alps 50k log tapped motor. stereo	**£5.00**
BI P260 500kΩ log conductive plastic 1 million cycles	**£2.00**
Colvern wire-wound 100kΩ or 50kΩ dual-gang 3W	**£5.00**
Mil Spec hermetic 10Ω	**£8.00**

Miscellaneous

PCBs

Phase-linear crossover PCB	**£3.00**
8-gang All-pass Filter PCB	**£3.00**
8-gang Pot PCB	**£1.50**
Polarity Inversion PCB (Alps)	**£1.50**
Polarity Inversion PCB (alt.)	**£1.50**
All-pass Filter PCBs (three)	**£4.00**
.. Rotary Switch (AO0626ROT)	**£1.50**
.. Pot Board (AO0626POT)	**£1.50**
Silent Stomp Switch (pair)	**£4.00**
Penta-fuzz Bender (*PE*, Feb26)	**£3.00**
Pre-driver (*PE*, Jan26)	**£3.00**
Pre-driver jack bd (*PE*, Jan26)	**£1.50**
Fuzz Box (*PE*, Nov25)	**£3.00**
Fuzz Box jack bd (*PE*, Dec25)	**£1.50**
Dual JFET Buffer (*PE*, Oct25)	**£2.00**
Mosfet Buffer (*PE*, Oct 2025)	**£2.00**
Dual Mosfet Buffer (*PE*, Oct25)	**£2.00**
Cascode Amp/PS (Sep 2025)	**£2.00**
Pocket Theremin (*EPE*, 1996)	**£2.00**
Elysian Theremin (*EPE*, 1996)	**£6.00**
Synth VCF, VCO (*EPE*, 2017)	**£3.00**
48V PSU (*EPE*, 2019)	**£3.00**
SMT dual transistor adapter	**£0.40**

Switches Blore Edwards/Plessey/etc

ALPs 4-pole push switch	**£1.50**
MH1 4-pole 3-way	**£3.00**
Elma 01 2-pole 6-way	**£6.00**
3PDT guitar pedal stomp switch	**£3.50**

Valves

EC88, PCL84	**£3.00**

Contact

Jake Rothman
Manchester House
Market Street, Craven Arms
Shropshire SY7 9NN
(visit by appointment)
+44 (0)1597 829102
jrothman1962@gmail.com

Payment

PayPal, bank transfer, cheques (payable to "J Rothman", UK pounds only). No VAT payable

Postage

Small Jiffy bag £2.99
Small package £4.99

Scan me!

Max the Magnificent

From Dr McCormick's mercury thermometer to AI-powered diagnostics, I take a look at how yesterday's science fiction is quietly becoming today's reality

I'm constantly amazed at the pace of medical progress. When I was about five years old, in the early 1960s, I had some trouble breathing. My mum took me to our family doctor, Dr McCormick. He said that I needed to have my tonsils removed. He also moaned a bit about the fact that the rules had changed and he would have to refer me to the hospital.

In the good old days, he said, he would have performed the operation himself in his surgery. I can only say that I'm glad I wasn't born in the good old days!

All I can remember about his surgery was a height-measuring rod attached to a weighing scale, a blood pressure cuff, and a wall chart showing parts of the human body (in case he forgot where they were).

The only other medical equipment I remember seeing was the stethoscope hanging around his neck, the wooden tongue depressors he used to make me gag, and a big mercury thermometer he stuck in my mouth while instructing me not to talk and then asking me questions.

Then there's now

Anything else in the early 1960s required a referral to a specialist or the hospital. By comparison, during a visit to my doctor's surgery several years ago, I noticed the outer door to their reception area was making an annoying squeak, so I returned the next day with a can of WD-40 (I guess WD-1 through WD-39 didn't quite do the trick), which addressed the problem.

That squeak must've been annoying the receptionist too. Ever since then, if I ask, "Is there any chance you can squeeze me in", I usually manage to get an appointment within a couple of hours.

By some strange quirk of fate, this happened just yesterday. For the past couple of days, I've had a cough that's been making my eyes water and my chest ache. The pain in my chest was so intense I started to worry that I was having a heart attack! Happily(?), it turns out that my coughing was so bad that I'd pulled a muscle.

The reason I'm waffling on about this is that the doctor (well, one of her minions) gave me a chest X-ray and an EKG. They also took a nasal swab to rule out the flu and COVID, and they drew some blood and ran a batch of tests in real time in their on-site lab. Although they didn't use it in this case, they also have an ultrasound machine and goodness knows what else in the surgery.

All of which makes me wonder what doctors in the early 1960s would have thought if they could see a modern family doctor's surgery. I suspect they would have assumed they'd inadvertently wandered onto the set of a sci-fi film.

The knee bone's connected to…

When my dear old dad had a hip replacement operation in the 1970s, he was confined (physically restrained) to his hospital bed for weeks before they let him start walking.

By comparison, one of my friends who is in his mid-70s had a hip replacement just a couple of months ago. He went into the hospital early one Tuesday morning. I called him in the evening to see how he was doing. He was already back home. I'd caught him climbing the stairs to his bedroom!

Starting about ten years ago, several of my contemporaries began to need knee replacement operations. My eyes are watering just thinking about this. They all said that the first couple of weeks after the operation were extremely painful, but after a couple of months, they felt like they'd been given a new lease on life.

Once again, by comparison, two more of my friends have had knee replacement operations recently. Apparently, there is a new nerve-blocker technique, because both were walking the day after the operation using nothing more than over-the-counter pain medication.

Scan me!

Many of the technologies that were the stuff of science fiction when I was a kid don't even raise a quizzical eyebrow today. This makes me wonder what we might expect in the not-too-distant future.

Dare we hope that one day we'll each have handy-dandy little AI-powered diagnostic machines in our homes? I'm envisaging being able to insert my finger to have a drop of blood taken and receive a diagnosis of any common ailments just a few seconds or minutes later.

I'm also looking forward to the day when my doctor has a full-body scanner in her office. I imagine stepping into a booth, standing still for a few seconds, and then watching a detailed 3D model of my innards appear on a screen, all displayed in glorious colour.

Of course, the real magic wouldn't be the pictures themselves. It would be the AI systems working behind the scenes, comparing my scan with millions of others, spotting tiny abnormalities that no human physician could reasonably be expected to notice and highlighting potential problems long before they started causing symptoms.

The best part would be catching things early. Instead of waiting until something hurts, breaks, leaks, swells, or otherwise announces its presence in an unpleasant fashion, doctors could identify many problems while they were still small, simple and easy to treat.

Futuristic technologies

Traditional industrial robots are astonishingly precise, but they are also remarkably clueless. Put a car door in exactly the right place, and a robot can weld it all day long. Move the door a couple of inches or centimetres, however, and the robot may suddenly find itself having an existential crisis.

One company working to change this is CynLr (www.cynlr.com). Its goal is to give robots something approaching human-like object intelligence. Instead of relying solely on pre-programmed instructions, these systems learn by interacting with objects, observing the results of their actions and gradually building an understanding of how things behave.

Imagine a robot encountering an unfamiliar object. Rather than simply seeing a collection of pixels, it begins to recognise concepts such as shape,

weight, balance, movement and purpose. It learns that a cup can be picked up by the handle, a drawer can be opened by pulling, and that some objects are fragile while others are not.

This may sound like a small step, but it represents a profound shift. Robots that can understand the world through experience could eventually work safely alongside humans, adapt to unfamiliar situations and perform tasks that are currently beyond the reach of conventional automation. As the folks at CynLr said, "We are teaching machines not just to see the world, but also to understand it."

Itera's liquid circuit board concept.

Where are my keys?

Speaking of things that would have sounded like science fiction not so very long ago, consider AI-powered glasses that remember where you left your keys.

One company exploring this idea is Brilliant Labs (**https://brilliant.xyz**), with its Halo smart glasses and Noa AI assistant. Halo looks remarkably like an ordinary pair of spectacles. However, hidden inside are cameras, microphones, bone-conduction speakers, a tiny display and enough computing power to make me squeal in delight.

According to Bobak Tavangar, the company's CEO, the system can see what you see, hear what you hear, and engage in real-time conversations about the world around you.

What really caught my attention is Noa's memory capability. Rather than simply answering questions, it builds a personalised knowledge base based on the wearer's experiences. This means you could ask questions like, "Where did I leave my keys?" or "What was the name of the bald guy I met at last week's conference?" and have a reasonable expectation of receiving a useful answer.

As Bobak told me, the goal is not merely to create smarter glasses, but to create a kind of memory assistant that helps you keep track of your life. As someone who spends an inordinate amount of time at my workbench looking for tools and components that 'were here just a minute ago', I can definitely see the appeal!

A circuit board that rewires itself

Once traditional PCBs (printed circuit boards) have been designed and manufactured, their electrical connections are fixed forever (well, unless you wield a scalpel, a reel of wire and a soldering iron). If you want to make more than minor modifications to the circuit, you usually need to spin a new board.

Itera (**www.itera.co**) is working on a radically different approach. Its technology is based on multiple layers of ultra-thin glass containing microscopic channels through which liquid metal can flow. By controlling where the metal moves, the system can create, remove and reroute electrical connections on demand.

The result is a circuit board that can effectively rewire itself. Need to connect two signals? Create a path. Need to disconnect them? Remove the path. Need to route a signal somewhere completely different? Reconfigure the board.

This may sound like Terminator-2-level technology, but Itera has already demonstrated working hardware and attracted significant interest from industries ranging from automotive and defence to hyperscale computing and semiconductor development.

As Itera's CEO AJ Cooper explained to me, the long-term vision is to make hardware development dramatically faster and more flexible. If successful, engineers could one day modify physical circuitry almost as easily as updating software. As someone who has spent countless hours redesigning and respinning circuit boards, I find this to be a remarkably appealing prospect!

A blast from the past

Sometimes, we become so fixated on what is to come that we inadvertently overlook what has already been. While most companies are focusing on ever-larger artificial neural networks (ANNs), the answer to running AI on low-power edge devices may lie in a remarkably different approach with roots tracing back to research conducted in the Soviet Union in the 1960s.

One company championing this idea is Literal Labs (**www.literal-labs.ai**), whose technology is based on Tsetlin Machines. Unlike neural networks, which learn by adjusting vast numbers of numerical weights, Tsetlin Machines learn using collections of simple logical rules. The result can be AI models that are dramatically smaller, faster and more energy-efficient than their neural-network counterparts.

This is particularly important at 'the edge', where devices often have only a few kilobytes of memory and must run for years on tiny batteries. In demonstrations presented by Literal Labs, Tsetlin Machine implementations have achieved comparable accuracy to neural network solutions while consuming a fraction of the memory, processing power and energy.

While much of the AI world is racing toward ever-larger models containing billions or trillions of parameters, the future of edge AI may emerge from an elegant idea that has been hiding in plain sight for more than 50 years. **PE**

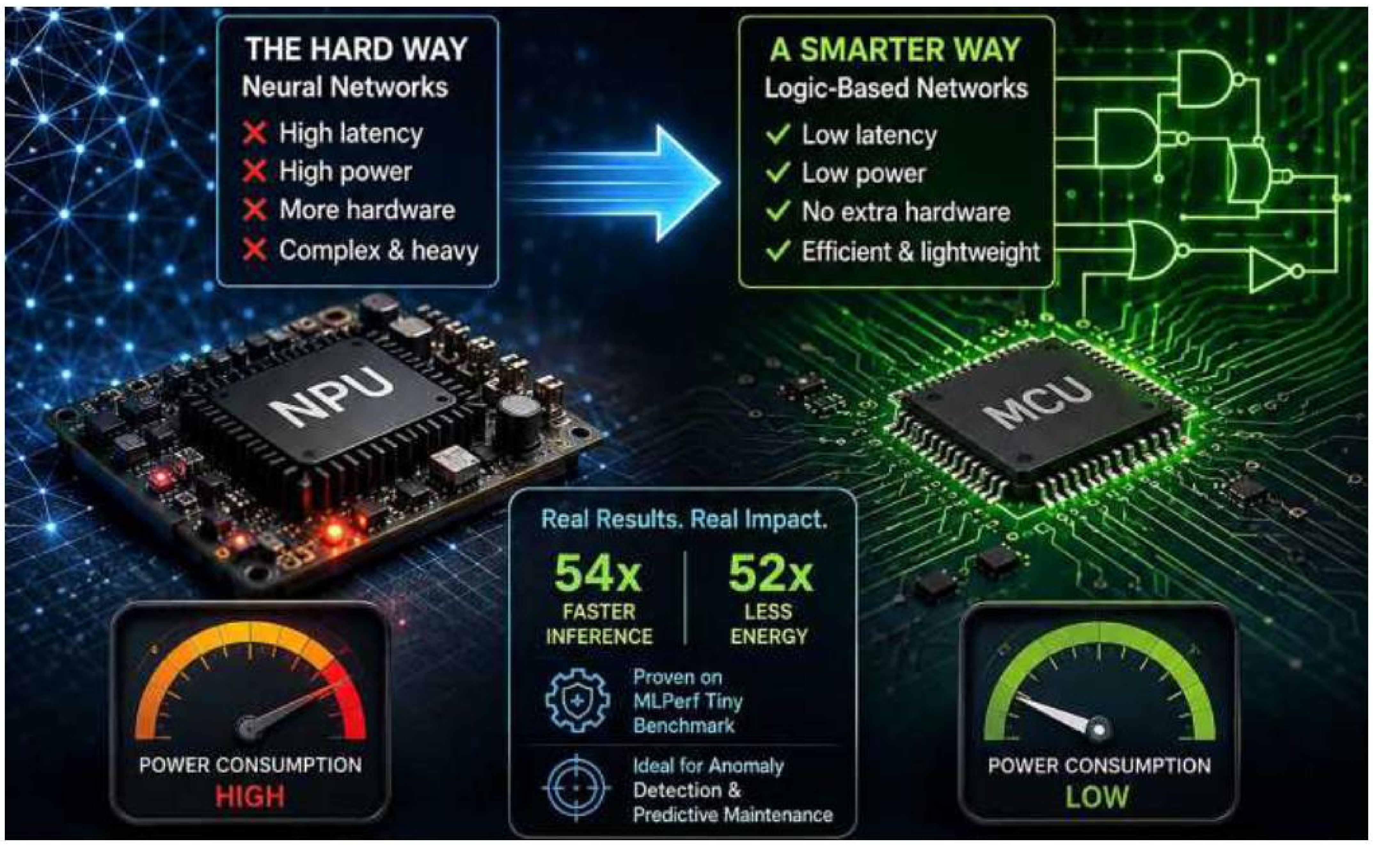

Practical Electronics PCB SERVICE

PROJECT	CODE	PRICE
AUGUST 2026		
RP2350B Computer (assembled)	07204251A	£54.99
USB-C Power Monitor PCB set (including flex cable)	04102251-3	£6.99
Audio Out Phase-Linear Crossover PCB	AO-AUG-26	£4.99
VFD Chronometer digit board	CBAUG26-1	£2.99
VFD Chronometer spacer board	CBAUG26-2	£2.99
JULY 2026		
RP2350B Development Board (assembled)	07107251A	£24.99
SmartProbe PCB	P9054-04	£4.99
SWD Adaptor board for the SmartProbe	P9045-A	£2.99
Audio Out New All-Pass Filter PCB	AOJUL26-1	£4.99
Audio Out Alps Polarity Switch PCB	AOJUL26-2	£2.99
Audio Out E-switch Polarity Switch PCB	AOJUL26-3	£2.99
JUNE 2026		
RGB LED 'Analog' Clock PCB (black)	19101251	£7.99
USB Power Adaptor PCB (set of two)	18101251	£2.99
433MHz Receiver Module PCB	15103252	£2.99
Audio Out All-Pass Filter PCB set (three PCBs)	AO-JUN-26	£6.99
MAY 2026		
SSB Shortwave Receiver three PCB set	CSE250202-4	£15
Tool Safety Timer PCB	10104251	£3.99
433MHz Transmitter Module PCB	15103251	£2.99
APRIL 2026		
Versatile Battery Checker PCB	11104251	£3.99
Versatile Battery Checker front panel (black, 0.8mm)	11104252	£4.99
Power Rail Probe PCB	P9058-1-C	£3.99
Pico 2 Audio Analyser PCB/panel (black)	04107231	£3.99
MARCH 2026		
USB-Programmable Frequency Divider PCB (blue)	04108241	£3.99
Rotating Light PCB (black)	09101251	£2.99
433MHz Transmitter PCB	15103251	£2.99
Arduino Uno Game Cartridge PCB (Cool Beans)	CBmar26uno	£3.99
Arduino Nano Game Cartridge PCB (Cool Beans)	CBmar26nano	£2.99
Silent Stomp Switch PCB pair (Audio Out)	AO-MAR26-*	£3.99
FEBRUARY 2026		
Power LCR Meter PCB	04103251	£7.99
Versatile Waveform Generator PCB	04104251	£5.99
JANUARY 2026		
High-Bandwidth Differential Probe	9015-D	£5.99
NFC-Programmable IR Remote Keyfob	15109231	£2.99
Pre-driver Overdrive Pedal main PCB	AO-JAN26-1	£4.99
Updated jack PCB for the Pre-driver	AO-JAN26-2	£3.99
DECEMBER 2025		
Variable Speed Drive (black)	11111241	£11.99
Digital Capacitance Meter	04111241	£5.99
Battery-Powered Model Train transmitter	09110241	£3.99
Battery-Powered Model Train through-hole receiver	09110242	£3.99
Battery-Powered Model Train SMD receiver	09110243	£3.99
Battery-Powered Model Train battery charger	09110244	£3.99
Transmanium Fuzz Box jack PCB	AO-DEC-25	£3.99
NOVEMBER 2025		
Capacitor Discharger	9047-01	£4.99
5MHz, 40A Current Probe	9049-01	£5.99
Transmanium Fuzz Box main PCB	AO-NOV-25	£4.99

PROJECT	CODE	PRICE
OCTOBER 2025		
Seaside Sound Simulator PCB (blue)	01111241	£7.99
Fender Jazz Bass pickguard	23109241	£5.99
J&D Luthiers T-Style pickguard	23109242	£5.99
Music Man Stingray pickguard	23109243	£5.99
Fender Telecaster pickguard	23109244	£4.99
3D Printer Filament Dryer control PCB	28110241	£4.99
SEPTEMBER 2025		
Automatic LQ Meter PCB	CSE240203A	£5.99
Automatic LQ Meter front panel (black)	CSE240204A	£5.99
Compact Hi-Fi Headphone Amplifier PCB (blue)	01103241	£4.99
Discrete Ideal Bridge Rectifier TH or SMD PCB	18108241/2	£2.99
Dual Rail Supply Protector PCB	18109241	£3.99
Audio Out Cascode Amplifier PCB	CASCODEA	£4.99
Audio Out Cascode Amplifier Power Supply PCB	CASCODEP	£4.99
AUGUST 2025		
Micromite Explore-40 PCB	07106241	£2.99
Micromite Explore-40 Audio Breakout PCB	07101222	£2.99
8-Channel Learning IR Remote Receiver PCB	15108241	£5.99
FlexiDice PCB set	08107241-2	£4.99
JULY 2025		
Compact OLED Clock & Timer PCB	19101231	£4.99
180-230V DC Motor Speed Controller PCB	11104241	£9.99
Mains Power-Up Sequencer PCB (same as Feb '25)	10108231	£11.99
JUNE 2025		
Styloclone (case version)	23106241	£6.99
Styloclone (standalone version)	23106242	£7.99
Dual Mini LED Dice (TH LEDs, white solder mask)	08103241W	£2.99
Dual Mini LED Dice (TH LEDs, black solder mask)	08103241B	£2.99
Dual Mini LED Dice (SMD LEDs, white solder mask)	08103242W	£2.99
Dual Mini LED Dice (SMD LEDs, black solder mask)	08103242B	£2.99
Dual Hybrid Supply regulator board	18107211	£5.99
Dual Hybrid Supply front panel control board	18107212	£2.99
Dual Hybrid Supply CPU board	01106193	£3.99
Dual Hybrid Supply LCD adaptor	01106196	£2.99
MAY 2025		
Skill Tester 9000	08101241	£9.99
USB-C Serial Adaptor (black solder mask)	24106241	£2.99
DC Supply Protector (SMD adjustable version)	08106241	£3.99
DC Supply Protector (TH adjustable version)	08106242	£3.99
DC Supply Protector (TH fixed version)	08106243	£3.99
APRIL 2025		
ESR Test Tweezers PCB set	04105241+	£5.99
Fan Speed Controller Mk2	10104241	£4.99
Calibrated Microphone (SMD version)	01108231	£3.99
Calibrated Microphone (TH version)	01108232	£3.99
MARCH 2025		
Pico Gamer	08104241	£9.99
Compact Frequency Divider	04112231	£4.99
FEBRUARY 2025		
Laser Communicator transmitter	16102241	£3.99
Laser Communicator receiver	16102242	£3.99
Model Railway Points Controller transmitter	09101241	£3.99
Model Railway Points Controller receiver	09101242	£2.99
Mains Power-Up Sequencer	10108231	£11.99

PCBs for most recent *PE/EPE* constructional projects are available. From the July 2013 issue onwards, PCBs with eight-digit codes have silk screen overlays and, where applicable, are double-sided, have plated-through holes, and solder mask. They are similar to photos in the project articles. Earlier PCBs are likely to be more basic and may not include silk screen overlay, be single-sided, lack plated-through holes and solder mask.

Always check price and availability in the latest issue or online. A large number of older boards are listed for ordering on our website.

In most cases we do not supply kits or components for our projects. For older projects it is important to check the availability of all components before purchasing PCBs.

Magazine back issues are available – see https://www.electronpublishing.com/product-category/pe-back-issues-print-and-digital/

Double-sided | plated-through holes | solder mask

PROJECT	CODE	PRICE
JANUARY 2025		
USB to PS/2 Converter for VGA PicoMite	07111231	£3.99
ps2x2pico USB to PS/2 Converter	07111232	£3.99
Compact Microphone Preamplifier (case version)	01110231	£5.99
Compact Microphone Preamplifier (integrated version)	01110232	£5.99
DECEMBER 2024		
Raspberry Pi Clock Radio PCB pair	19101241/2	£12.99
VGA PicoMite (blue)	07107221	£5.99
Secure Remote Switch receiver	10109231	£4.99
Secure Remote Switch transmitter (module version)	10109232	£2.99
Secure Remote Switch transmitter (discrete version)	10109233	£2.99
NOVEMBER 2024		
Ideal Diode Bridge Rectifiers (28mm square)	18101241	£3.99
Ideal Diode Bridge Rectifiers (22mm square)	18101242	£3.99
Ideal Diode Bridge Rectifiers (4-pin SIL)	18101243	£3.99
Ideal Diode Bridge Rectifiers (tiny SOT-23)	18101244	£3.99
Ideal Diode Bridge Rectifiers (standalone SMD)	18101245	£4.99
Ideal Diode Bridge Rectifiers (standalone TH; 2oz copper)	18101246	£6.99
Multi-channel Volume Control (volume PCB)	01111221	£4.99
Multi-channel Volume Control (control PCB)	01111222	£4.99
Multi-channel Volume Control (OLED PCB, black)	01111223	£4.99
Coin Cell Emulator (black)	18101231	£3.99
OCTOBER 2024		
TQFP-32 Programming Adaptor	24108231	£4.99
TQFP-44 Programming Adaptor	24108232	£4.99
TQFP-48 Programming Adaptor	24108233	£4.99
TQFP-64 Programming Adaptor	24108234	£4.99
2m VHF FM Test Signal Generator	06107231	£4.99
SEPTEMBER 2024		
PIC Programming Adaptor	24105231	£4.99
Salad Bowl Speaker crossover	01109231	£7.99
AUGUST 2024		
Arduino ESR Meter combined L/C-ESR	04106182	£9.99
Arduino ESR Meter separate ESR	04106183	£7.99
Watering System Controller	15110231	£11.99
JULY 2024		
Dynamic NFC Tag (22 × 31mm)	06101231	£5.95
Dynamic NFC Tag (86 × 54mm)	06101232	£7.95
Reciprocal Frequency Counter	CSE230101C	£8.95
Reciprocal Frequency Counter front panel (black mask)	CSE230102	£7.95
Pi Pico-based Thermal Camera	04105231	£6.95
JUNE 2024		
Loudspeaker Test Jig	04106231	£12.95
MAY 2024		
GPS-Disciplined Oscillator	04103231	£12.95
Dual RF Amplifier	CSE220602A	£5.95
Songbird	08103231	£7.95
APRIL 2024		
Basic RF Signal Generator	CSE221001	£8.99
Basic RF Signal Generator front panel (black solder mask)	CSE220902B	£9.99
Silicon Chirp Cricket	08101231	£7.99
Test Bench 'Swiss Army Knife'	04110221	£9.99
MARCH 2024		
Digital Volume Control Potentiometer SMD version	01101231	£8.95
Digital Volume Control Potentiometer through-hole version	01101232	£9.95
Advanced SMD Test Tweezers body	04106221	£6.95
Advanced SMD Test Tweezers legs (pair)	04106212	£7.95

PROJECT	CODE	PRICE
FEBRUARY 2024		
Active Mains Soft Starter	10110221	£10.95
JANUARY 2024		
Q Meter	CSE220701	£8.95
Q Meter front panel (black solder mask)	CSE220704	£7.95
Raspberry Pi Pico W BackPack	07101221	£8.95
DECEMBER 2023		
Digital Boost Regulator	24110224	£8.95
Dual-Channel Power Supply for Breadboards	04112221	£11.95
Display Adaptor for the Breadboard PSU	04112222	£9.95
NOVEMBER 2023		
LC Meter Mk3	CSE220503C	£9.95
DC Supply Filter for vehicles	08108221	£8.95
Discrete Audio Op Amp PCB	AO1-JUL23	£9.95
Discrete Audio Op Amp PCB + essential components	AO2-JUL23	£17.95
OCTOBER 2023		
Buck/Boost Charger Adaptor	14108221	£9.95
PIC Breakout Board for SOIC parts	24110225	£5.95
PIC Breakout Board for DIP parts	24110222	£5.95
AVR64DD32 Breakout board	24110223	£5.95
Automatic Train Controller	09109221	£6.95
Chuff Sound module	09109222	£6.95
SEPTEMBER 2023		
Mini LED Driver	16106221	£7.95
New GPS-Synchronised Clock	19109221	£9.95
AUGUST 2023		
110dB RF Attenuator	CSE211003	£9.95
Universal Battery Charge Controller (2023 update)	14107192	£9.95
Wide-Range OhmMeter	04109221	£12.95
JULY 2023		
Multimeter Checker/Calibrator	04107221	£10.95
JUNE 2023		
Arduino Programmable Load	04105221	£8.95
Buck-Boost LED Driver	16103221	£8.95
MAY 2023		
Precision AM-FM DDS Signal Generator	CSE211002	£14.95
Improved SMD Test Tweezers programmed PIC	0410621PIC	£12.95
AO 2x-dual-to-quad through-hole (pack of five)	AO1-MAY23	£6.95
AO 2x-dual-to-quad SMD (pack of five)	AO2-MAY23	£6.95
AO 2x-single-to-dual through-hole (pack of five)	AO3-MAY23	£6.95
AO 2x-single-to-dual SMD (pack of five)	AO4-MAY23	£6.95
APRIL 2023		
500W Amplifier Module	see p.22, April 2023	
Clipping Indicator (per channel)	01112211	£7.95
CD Welder Power Supply (one needed)	29103221	£9.95
CD Welder Controller (one needed)	29103222	£9.95
CD Welder Energy Storage module (several needed)	29103223	£7.95
AO Universal Dual Op Amp Board	AO1-APR23	£9.95
AO Stereo RIAA precision passives kit for dual op amp	AO2-APR23	£8.95
MARCH 2023		
Pico BackPack	07101221	£9.95
Semaphore Signal (controller)	09103221	£7.95
Semaphore Signal (blade)	09103222	£5.95

All prices include VAT and UK p&p. Add £4 per *project* for post to Europe; £5 per *project* outside Europe.

Orders and payment should be sent to:

Practical Electronics, Electron Publishing Ltd
113 Lynwood Drive, Merley, Wimborne, Dorset BH21 1UU
Tel 07918 614662   Email: pe@pemag.au
Online Shop: www.electronpublishing.com

Sorry, cheques cannot be accepted as we are based in Australia and our UK bank account does not allow cheque deposits.

NOTE: Most boards are in stock and sent within seven days of order receipt. Please allow up to 28 days delivery if we need to restock.

Double-sided | plated-through holes | solder mask

PROJECT	CODE	PRICE
FEBRUARY 2023		
Tesla Coil driver board	26102221	£9.95
Tesla Coil potentiometer board	26102222	£5.95
Cooling Fan Controller & Loudspeaker Protector	01102221	£8.95
Remote Gate Controller	11009121	£12.95
JANUARY 2023		
Classic LED Metronome – 8-LED	23111211	£7.95
Classic LED Metronome – 10-LED	23111212	£8.95
Multi-Channel Speaker Protector – 6 channel	01101221	£9.95
Multi-Channel Speaker Protector – 4 channel	01101222	£7.95
Remote Control Range Extender – IR-to-UHF	15109212	£5.95
Remote Control Range Extender – UHF-to-IR	15109211	£7.95
AO Universal Single Op Amp Board	AO1-JAN23	£7.95
DECEMBER 2022		
Hummingbird Amplifier	01111211	£9.95
SMD Trainer PCB	29106211A	£8.95
NOVEMBER 2022		
USB Cable tester – main PCB	04108211	£12.95
USB Cable tester – front panel	04108212	£5.95
USB Cable tester – optional panel	SC5970	£5.95
Model Railway Carriage Lights – PCB	09109211	£6.95
AO trnsfmr PCB – standard VTX-A range	VTX-101-007	£6.95
AO trnsfmr PCB – dual-outline VTX102-3001/101-3002	VTX-Dual	£6.95
OCTOBER 2022		
SMD Test Tweezers – PCB and pair of tweezer arms	04106211-2	£11.95
SMD Test Tweezers – programmed PIC12F1572-I/SN	0410621A	£7.95
Tele-com	12110211	£12.95
SEPTEMBER 2022		
Touchscreen Digital Preamp – main board	01103191	£12.95
Touchscreen Digital Preamp – adaptor board pair	01103192	£5.95
20A DC Motor Speed Controller	11006211	£9.95
AUGUST 2022		
Multi-purpose Battery Manager – I/O Expander	11104212	£5.95
Multi-purpose Battery Manager – Switch Module	11104211	£8.95
Simple MIDI Music Keyboard (for 8 switches)	23101213	£6.95
Nano Pong	08105212	£7.95
JULY 2022		
Silicon Labs AM/FM/SW Radio	CSE210301C	£10.95
Level Crossing Controller	09108211	£6.95
JUNE 2022		
Full-wave Motor Speed Controller	1010221	£8.95
PIC Programming Helper for 8-pin PICs only	24106211	£7.95
PIC Programming Helper for 8, 14 or 20-pin PICs	24106212	£10.95
Advanced GPS Computer	05102211	£9.95
MAY 2022		
Bus board PCB for Analogue Vocoder	AO1-MAY22	£10.95
Complete set of 14 PCBs for Analogue Vocoder	AO2-MAY22	£97.95
Programmed EEPROM for Digital FX Unit	FX1-MAY22	£10.95
Programmed PIC for Digital FX Unit w/ potentiometer	FX2-MAY22	£8.95
APRIL 2022		
64-key MIDI Matrix shield	23101211	£8.95
64-key MIDI Matrix switch board	23101212	£11.95
High-current Battery Balancer	14102211	£10.95
Digital FX Unit – using potentiometer	01102211	£9.95
Digital FX Unit – using BCD switch	01102212	£9.95
Universal Audio PSU	AO1-APR22	£11.95

PROJECT	CODE	PRICE
MARCH 2022		
Mini Isolated Serial Link	24102211	£5.95
Busy Loo Indicator	16112201	£5.95
Analogue Vocoder – Band-pass filter board	AO1-MAR22	£9.95
Analogue Vocoder – HP/LP filter board	AO2-MAR22	£9.95
FEBRUARY 2022		
Arduino-based Power Supply	18106201	£9.95
Battery Monitor Logger	11106201	£10.95
Electronic Wind Chimes	23011201	£10.95
Analogue Vocoder – Driver Amplifier	AO-FEB22	£8.95
JANUARY 2022		
Vintage battery Radio Li-ion Power Supply	11111201	£9.95
MiniHeart: A Miniature Heartbeat Simulator	01109201	£8.95
DECEMBER 2021		
AM/FM/SW Digital Receiver	CSE200902A	£13.95
Balanced Input and Attenuator for USB CODEC	01106202	£11.95
NOVEMBER 2021		
Dual Battery Lifesaver	11111202	£6.95
OCTOBER 2021		
Mini Wi-Fi LCD BackPack	24106201	£8.95

For the many earlier PCBs that we stock please see the PE website: www.electronpublishing.com

PE/EPE PCB SERVICE

Order Code	Project	Quantity	Price

Name ....
Address ....
....
Tel ....
Email ....
Card No ....
Valid From ....Expiry Date ....
Card Security No ....

You can also order PCBs by phone, email or via the shop on our website: www.electronpublishing.com
No need to cut your issue – a copy of this form is just as good!

Kits and pre-programmed microcontrollers are available from the Silicon Chip shop in Australia for many of the projects published in *Practical Electronics*. Kits relevant to article in this issue:

USB-C Power Monitor short-form kit (includes everything but case, battery & glue)	https://siliconchip.au/Shop/20/7489	AU$72 (~£38) + P&P

To see a complete list of the kits available, visit: https://siliconchip.au/Shop/20
Pre-programmed microcontrollers are listed here: https://siliconchip.au/Shop/9
In many cases, you can also order printed circuit board(s) for the same projects: https://siliconchip.au/Shop/8

VAT is charged to UK customers at check-out from the Silicon Chip shop and currently, orders under £85 should not attract any extra duties.
Please allow 1-2 weeks for delivery (longer in some cases).

CLASSIFIED ADVERTISING

Practical Electronics

If you want your advertisements to be seen by the largest readership at the most economical price then our classified page offers excellent value.

The rate for semi-display space is £10 per centimetre high, with a minimum height of 2·5cm. All semi-display advertisements have a width of 5.5cm. The prepaid rate for classified adverts is 40p per word (minimum 12 words).

For rates, further information on display and classified advertising or to book an ad, please email us at pe@pemag.au

Practical Electronics reaches more UK readers than any other UK monthly hobby electronics magazine. Our sales figures prove it.

We have been the leading monthly magazine in this market for more than thirty years.

W5SWL Electronics

Technical Products and Small Component Parts, RF and Audio Connectors, Hobby Electronics, Ham Radio to Microwave Products, General Hobby Supplies, Technical Books, Tools, and More. **Located in the United States.**

Visit **www.W5SWL.com**

BOWOOD ELECTRONICS LTD

Suppliers of Electronic Components

www.bowood-electronics.co.uk

Unit 10, Boythorpe Business Park, Dock Walk, Chesterfield, Derbyshire S40 2QR. Sales: 01246 200 222

Send large letter stamp for Catalogue

COAST ELECTRONICS

BREAKOUTS-COMPONENTS-CONTRACT DESIGN-3D PRINTER PARTS-MUSICAL-MICROCONTROLLERS

WWW.COASTELECTRONICS.CO.UK

MISCELLANEOUS

VALVES AND ALLIED COMPONENTS? For free stock list and/or advice, please contact me: geoffdavies337@gmail.com Telephone: 01788 574774

PIC DEVELOPMENT KITS, DTMF kits and modules, CTCSS Encoder and Decoder/Display kits. Visit www.cstech.co.uk

Electrical Industries Charity (EIC)

We help people working in the electrical, electronics and energy community as well as their family members and retirees.

We use workplace programmes that give the industry access to financial grants and a comprehensive range of free and confidential services.

www.electricalcharity.org

electrical industries charity

ADVERTISING INDEX

AOSHOP	73
ENIGMA COMPONENT SHOP	17
HAMMOND MANUFACTURING	26
MICROCHIP TECHNOLOGY	Outer back cover
PCBWAY	Inner front cover
PDF BACK ISSUE DOWNLOADS	46, 55, 65
TEACH-IN BUNDLES & DVDS	55

Advertising mailing address

Electron Publishing Australia
PO Box 194
Matraville NSW 2036
Australia

Email pe@pemag.au

Web www.electronpublishing.com

For editorial contact details, see page 2.

Coming Up – in the Sep/Oct issues

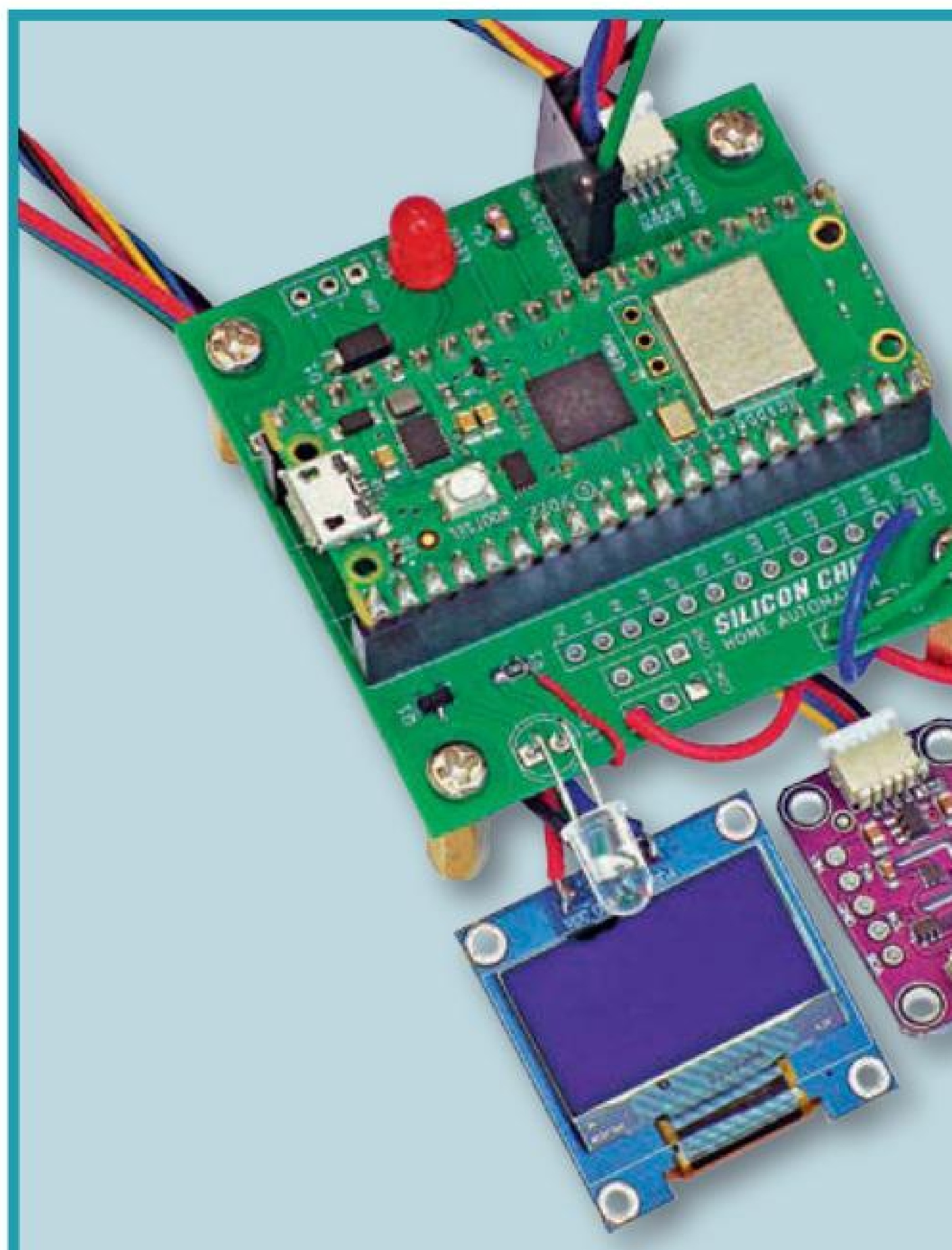

Home Automation Satellite

We explain how to set up a HomeAssistant hub, then connect sensors and displays

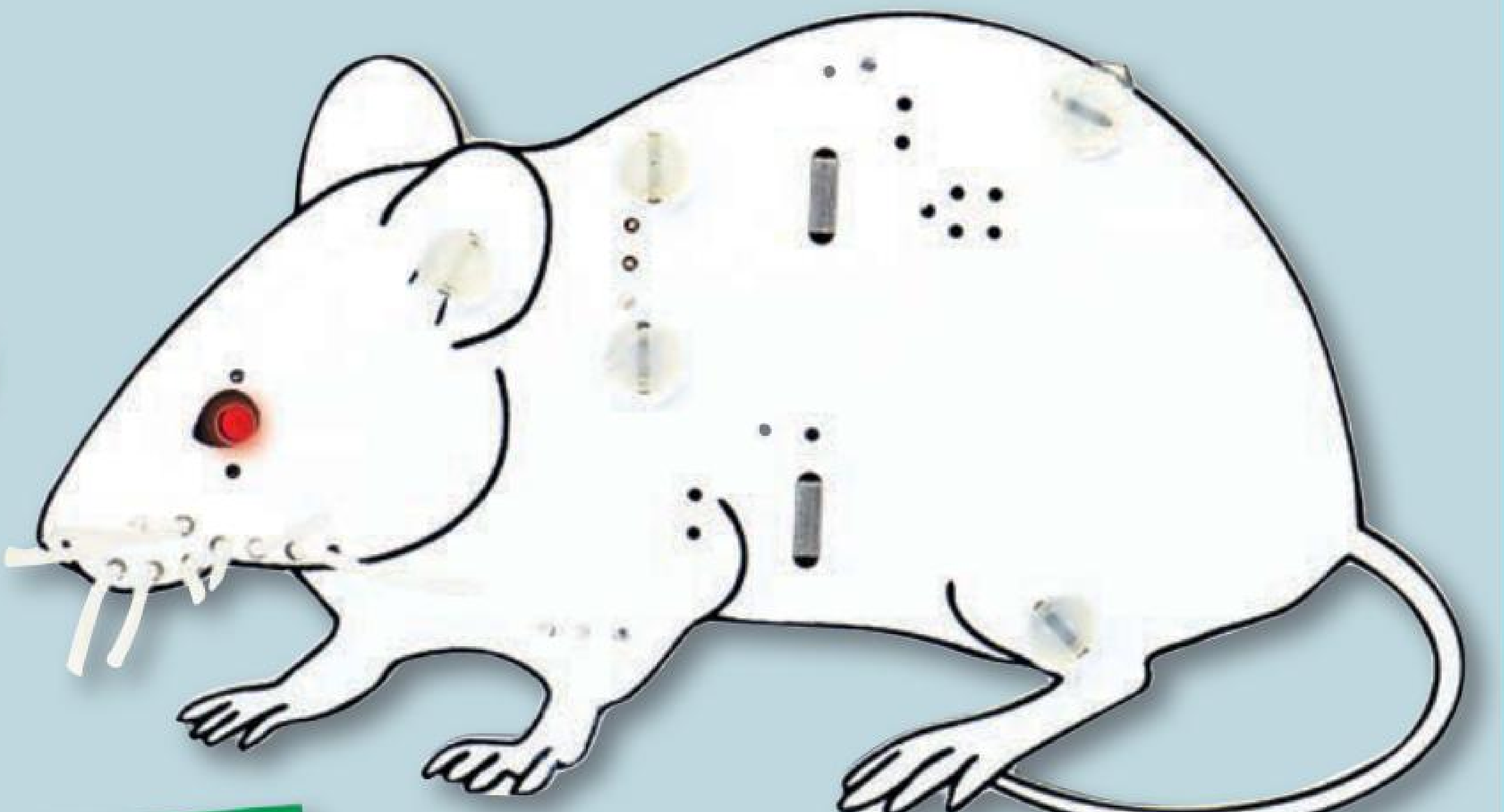

Mic the Mouse

Mic doesn't eat much - just the occasional coin cell. Mic is a bit shy and only squeaks, with flashing eyes, when it's dead quiet!

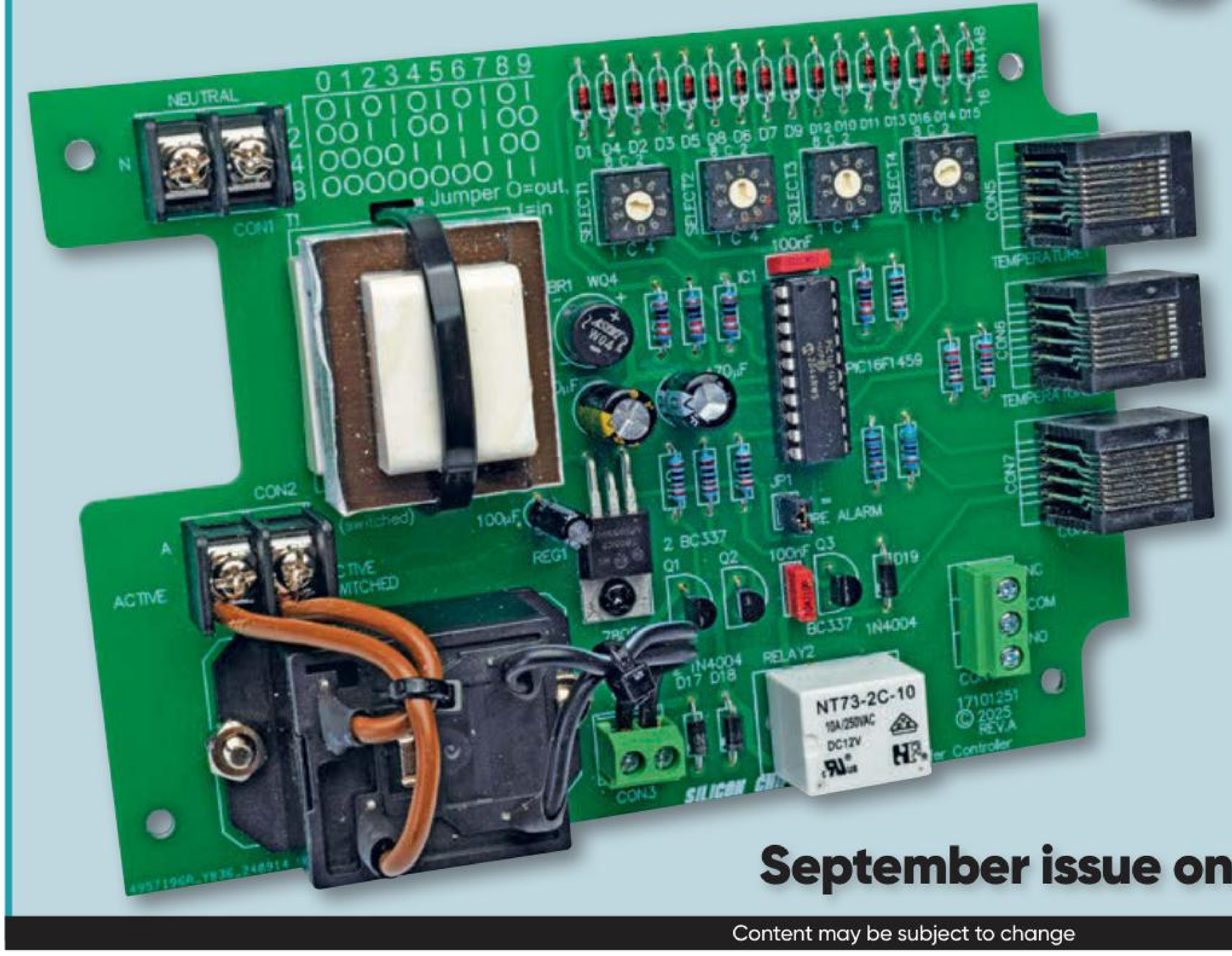

Ducted Heat Transfer Controller

It senses the difference in temperature between rooms and automatically switches on a fan to transfer warm/cool air when required. It's highly configurable.

September issue on sale: 5th of August, 2026

Content may be subject to change

Practical Electronics

Subscriptions hotline

To subscribe or renew online, paying by credit/debit card or PayPal, please visit our shop at: www.electronpublishing.com

For those wishing to pay by direct debit, cheque or over the telephone, please call 'Select Publisher Services' on 01202 087631, or send a cheque (payable to: '**Select Publisher Services Ltd**') with your details to:

Practical Electronics Subscriptions, PO Box 6337, Bournemouth BH1 9EH, United Kingdom

Remember, we print the date of the last issue of your current subscription in a box on the address sheet that comes with your copy.

Digital subscribers, please call 07918 614662 or visit: www.electronpublishing.com

Published on approximately the first Thursday of each month by Silicon Chip Publications, PO Box 194 Matraville NSW 2036 Australia. Printed in England by The Manson Group, Reynolds House, 8 Porters Wood, Valley Road Industrial Estate, St Albans AL3 6PZ. Distributed by Seymour, 86 Newman St, London W1T 3EX. Subscriptions UK: £33.99 (6mo); £59.99 (12mo.); £114.99 (2yrs). EUROPE: airmail service, £38.99 (6mo); £69.99 (12mo); £129.99 (2yrs). REST OF THE WORLD: airmail service, £46.99 (6mo); £84.99 (12mo); £164.99 (2yrs). Make payments to 'Practical Electronics', Practical Electronics Subscriptions, PO Box 6337, Bournemouth BH1 9EH United Kingdom. Email: pesubs@selectps.com. PRACTICAL ELECTRONICS is sold subject to the conditions that it shall not, without the written consent of the Publishers first having been given, be lent, resold, hired out or otherwise disposed of by way of Trade at more than the recommended selling price on the cover, and that it shall not be lent, resold, hired out or otherwise disposed of in a mutilated condition or in any unauthorised cover by way of Trade or affixed to or as part of any publication or advertising, literary or pictorial matter.

Did you know our online shop now sells the current issue of *PE* for £5.99 inc. p&p?

Practical Electronics
The UK's premier electronics, computing and maker magazine
Max's Cool Beans
Making test fixtures & building the VFD clock
Teach-In 12
Part 10: short-range RF devices, including LoRa
Audio Out
Linear-phase crossovers
Circuit Surgery
Anti-aliasing and reconstruction filters
Measure USB voltage, current & power up to 60V/±5A
USB-C Power Monitor
RP2350B Computer:
Overclockable
HDMI video output
Stereo audio
Up to four USB keyboards, mice or game controllers
microSD card socket
Internal flash & RAM
USB-C power input
Compatible with the MMBasic interpreter
PLUS!
Techno Talk – Self-learning robots and reconfigurable PCBs
The Fox Report – Manhattan's new Freeview receiver box
Feature – How USB-C Power Delivery works
Aug 2026 £5.99
www.electronpublishing.com
@practicalelec
practicalelectronics
Practical Electronics
Audio Out
How symmetricisers boost radio volume
Circuit Surgery
Sending & receiving balanced audio
RP2350B Dev Board: A more powerful Pico 2
Jul 2026 £5.99

You read that right! We now sell the current issue of your favourite electronics magazine for exactly the same price as in the High Street, but we deliver it straight to your door – and for UK addresses we pay the postage. No need to journey into town to queue outside the newsagent. Just go to our website, set up an account in 30 seconds, order your magazine and we'll do the rest.

www.electronpublishing.com

Powering Innovation, Driving Performance

Dependable, High-Voltage Solutions for Every Application

Our broad portfolio of high-voltage products and solutions deliver the performance, scalability and reliability needed to power innovation across industries. From electric vehicles and renewable energy systems to industrial automation and aerospace applications, our solutions are designed to meet the demands of industrial, automotive, aerospace and other critical applications.

Key Features

- **Extensive and Scaleable Portfolio** High-voltage silicon, IGBT, and SiC technologies available in discrete and module configurations tailored to your power needs
- **Superior Efficiency** Proprietary technology for optimized thermal management and reduced power losses
- **Field-Proven Reliability** Hi-Rel and automotive-qualified with HV-H3TRB capability for harsh environments
- **Accelerated Development Workflow** Comprehensive tools, software and technical support to simplify design and speed up your time-to-market

Whether you're designing for automotive, industrial or energy systems, Microchip is your trusted partner for high-voltage solutions that drive success. Explore our portfolio today and take your designs to the next level.

MICROCHIP

microchip.com/PickYourPower

The Microchip name and logo and the Microchip logo
are registered trademarks of Microchip Technology
Incorporated in the U.S.A. and other countries. All other
trademarks are the property of their registered owners.
© 2026 Microchip Technology Inc. All rights reserved.
MEC2651A-UK-05-26